Examination of the factors affecting quality on continuous annealing processing lines.

Saunders, Paul

Engineering Doctorate in Steel Technology

Examination of the Factors Affecting Quality on Continuous Annealing Processing Lines

Paul Saunders

Submitted to the University of Wales in fulfilment of the requirements for the Degree of Doctor of Engineering

Civil and Computational Engineering Centre
School of Engineering
Swansea University
November 2008

SUMMARY

The Continuous Annealing Processing Line (CAPL) of the Corus Strip Products UK integrated works in South Wales, United Kingdom, is one of the most modern lines of its type in the world. It produces thin and wide carbon strip steels of the highest quality in terms of metallurgical consistency, surface quality and dimensional tolerances.

Tensioned strip can travel at a velocity of up to 600m/min at temperatures in excess of 750°C. The yield point of the strip is naturally reduced at these annealing temperatures; therefore the contact interaction that develops between the transport roll and the strip steel it is transporting is critical. The primary focus of research is on maintaining the elasticity of the strip steel as it passes through the furnace section of the continuous annealing processing line. In particular focusing on the heating and adjacent soaking sections of the CAPL, where the temperatures are at their highest.

The thesis is concerned with the roll-strip interaction and its many different parameters - roll geometry, strip dimensions, strip tension and strip temperature. Research concentrated on the initial contact plane, where the strip first comes into contact with the transport roll. Results indicate that the strip's elastic stress-state is most affected by the fillet that circumnavigates the transport roll, especially where the fillet intersects the initial contact plane.

The parameters chosen took into consideration the future operational commitments of the CAPL, because continual demand is always increasing the threshold. To perform the task assigned the author made use of extensive computational finite element method models.

A second aspect of the research was to consider acceptable temperature differentials between the transport roll and the strip steel at initial contact. The strip has a low yield stress at its annealing temperature, thus an excessively high temperature differential will create a buckle risk. Therefore, an experimental programme was developed in conjunction with industrial partners Stein Heurtey to investigate acceptable temperature differentials for initial contact conditions.

DECLARATIONS AND STATEMENTS

DECLARATION

This work has not previously been accepted in substance for any degree and is not being concurrently submitted in candidature for any degree.

Signed (candidate)

Date 26/11/08

STATEMENT 1

This thesis is the result of my own investigations, except where otherwise stated. Where correction services have been used, the extent and nature of the correction is clearly marked in a footnote(s).

Other sources are acknowledged by footnotes giving explicit references. A bibliography is appended.

Signed (candidate)

Date 26/11/08

STATEMENT 2

I hereby give consent for my thesis, if accepted, to be available for photocopying and for inter-library loan, and for the title and summary to be made available to outside organisations.

Signed (candidate)

Date 26/11/08

CONTENTS

ACKNOWLEDGEMENTS

This project has been carried out at Corus Port Talbot and at the School of Engineering, Swansea University. This project forms part of the research programme of the Engineering Doctorate Centre - Wales, under the auspices of the Engineering and Physical Research Council. My thanks go to both Corus Group PLC and the Engineering and Physical Research Council for providing funding for this project.

I would like to thank Professor Arthur Lees (Academic Supervisor, Swansea University) and Dr Darryl Lewis (Industrial Supervisor, Corus Group PLC) for their advice and guidance throughout.

I would also like to thank my industrial partners and co-sponsors Stein Heurtey, who provided me with invaluable technical information on the Port Talbot Continuous Annealing Processing Line. I must also thank Stein Heurtey for providing me with access to their Bar-Le-Duc experimental testing facilities.

I would like to thank Martin Hardy for tirelessly reading and correcting the grammar.

My final thoughts and thanks go to my parents Brian and Christine who have given me the most support over the years.

LIST OF FIGURES

LIST OF TABLES

1. INTRODUCTION

Opening Remarks

This chapter represents a general overview of the work undertaken and also describes the motivation for the present study of Continuous Annealing Processing Line (CAPL) quality issues, in particular, the interaction between the furnace transport roll and the moving strip.

1.1 GENERAL PROJECT OVERVIEW

This research project is based on the thin sheet sector, of which the automotive sector and tinned products constitute most of the custom. Demands in particular from the automotive industry require the utilisation of ultra low carbon interstitial free products, which have stringent property requirements. Automotive design in the future will require products to be wider, lighter, and of a high strength, all of which will push CAPL technology to the limit with ever-higher annealing temperatures. The development of newer grades of steel product is never ending, as are the production problems that go with these initiatives, such as the struggle to produce steels that are clean of metallic inclusions[1]. A full understanding of the processing mechanisms, with a strong interaction from French CAPL furnace suppliers Stein Heurtey, will contribute to the future strategy of CAPL processing conditions and operational set-up.

1.2 PORT TALBOT INTEGRATED WORKS

The Corus site in South Wales at Port Talbot is dedicated to the production of strip products for many varied industries. The importance of strip production to the future viability of the company cannot be underestimated; the continuous annealing processing line is an integral part of the production line. The illustration of the works process flow diagram is shown in *Figure 1.1* below.

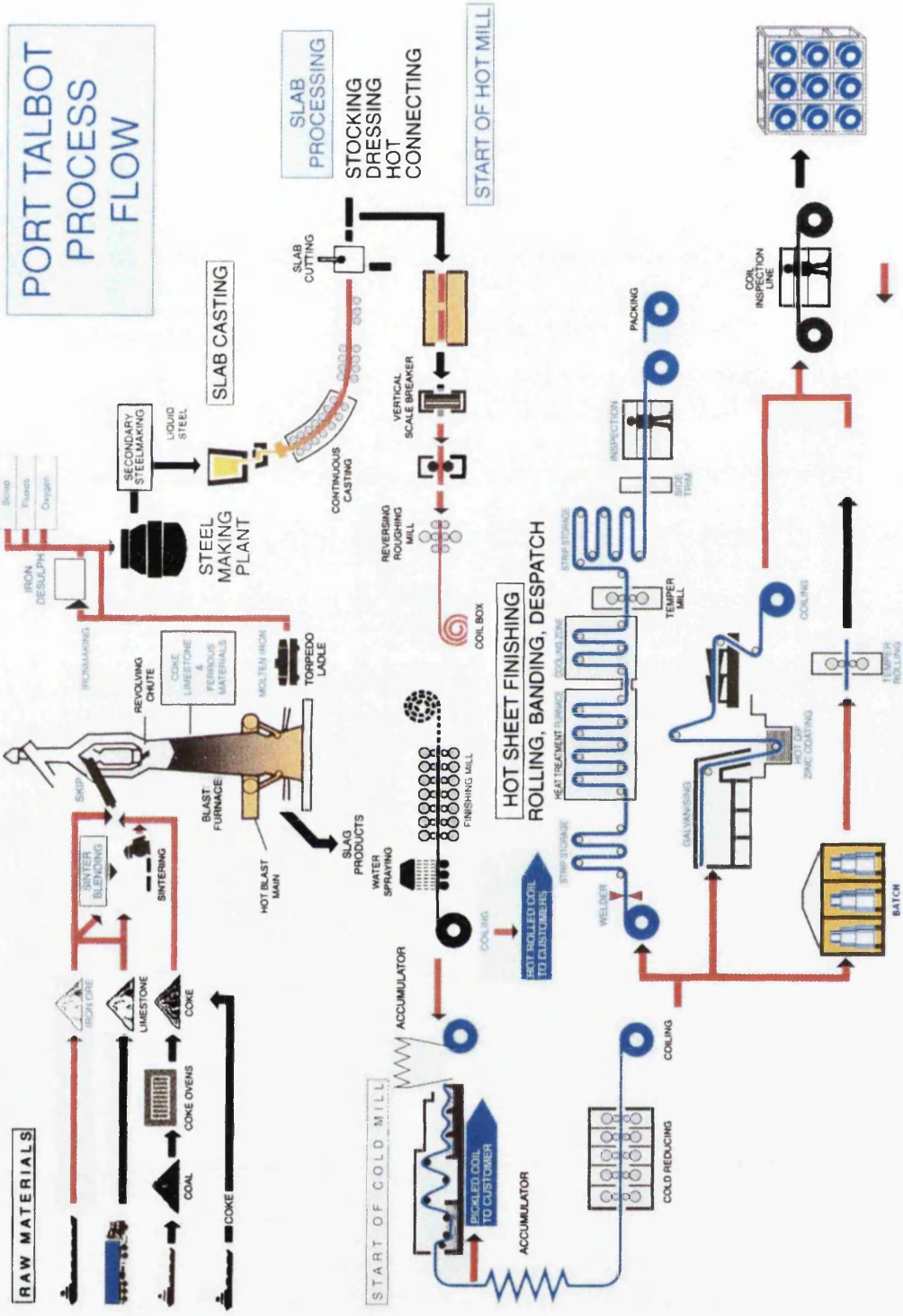

Figure 1.1 Process Flow Diagrams of the Port Talbot Steelworks

In Corus Port Talbot Steelworks, molten steel is continually cast, referred to as Concast to form slabs of nominal thickness 234mm, with the width up to 1875mm, dependent on the strand used at the Concast. The length of the slab can also vary between 7-10m, dependent on the application of the slab itself, set by the customer. After the slab is stored for some time and then reheated, it is hot rolled to reduce thickness or gauge from a cast gauge of 234mm to a hot reduced gauge of between 1.2 and 17.5mm, to produce what is commonly known as Hot Rolled Coil. This product can be dispatched and sold directly to the customer or can be further processed. The material is then coiled, since now it has a length in kilometres.

The product is then pickled to remove surface scale built up during the hot rolling process and, again, can be sold to the customer at this stage as Pickled (and Oiled) coil. The pickled coil is then further reduced at the cold rolling mills, where the gauge is reduced to a minimum of 0.3mm or a maximum of 2.0mm; again, the gauge will depend on the customer's requirements.

After receiving the heavy reduction, the material has been considerably work hardened and requires a further operation in order to make the material workable once more. This process is known as annealing, which can be either batch or continuous. Since the installation of the CAPL in June 1998 at the Port Talbot works, the process has been continuous and takes a matter of seconds to perform the annealing operation. In contrast, the batch annealing process, using either single (Ebner) or multi-stack arrangements, can take between 48 and 72 hours to complete the operation. Once the process is complete, the material is then passed to the Temper Mills (in the case of the CAPL, this process is continuous), where a slight reduction in the gauge is given (known as a skin pass) in order to eradicate the yield point elongation phenomenon and suppress the formation of so-called Lüders lines on further processing. The material is now directed to the coil inspection lines (CIL) before packaging and final dispatch to the customer[2].

1.3 THE CONTINUOUS ANNEALING PROCESSING LINE (CAPL)

Technologically, the process is complicated therefore the greater the understanding of some of the basic mechanisms during processing, the greater the scope for effective development of products in the future. Corus have plenty of experience of running continuous annealing lines at their Trostre tin coat line in Llanelli. A transfer of knowledge and experience was forthcoming from Trostre to Port Talbot. It was hoped that the continuous annealing operation at Port Talbot would run effortlessly without any major strip quality issues after commissioning. However, the problem that Corus soon realised is that no two CAPL's behave the same; even CAPL's, which run identical carbon-steel grades to the Port Talbot CAPL, suffer from different operational problems which affect productivity. Therefore, the standard CAPL configuration that was bought on licence from Stein Heurtey using patented Nippon Steel technology is only an ideal operational set-up.

Once the decision to use a continuous annealing line was made, there would be no going back to the batch annealing process, with a unit cost investment of nearly 200 million pounds; the CAPL represented the future of the Port Talbot integrated steelworks. A limited batch annealing process would still be available at the Llanwern steelworks for the more specialist steels, however, the bulk of the South Wales steel operations with its concentration on the more commercial carbon-steel grades would be, in the future, continuously annealed.

The overwhelming advantages of the continuous annealing process over the batch annealing process, has accordingly led to a far greater effort being applied to its development in recent times. Most of Corus' principal niche product range of deep drawable, low-carbon sheet steel can only be satisfactorily processed on the continuous annealing processing line (CAPL) at Port Talbot. This product range, which encompasses drawable quality (DQ), deep-drawable quality (DDQ) and extra-deep-drawable quality (EDDQ) grades, requires extremely low carbon and niobium chemistries (i.e. <0.002% & 0.001% wt respectively[1, 3, 4]), optimised heating cycles and rapid cooling capability. Such requirements combine to impose extremely stringent demands and tolerances on the processing line and its components. The major benefit between continuous or batch process routes is that in the former, far higher production rates and heating control can be attained due to the continuous, high-speed transport of steel through various heat cycles.

Conversely, problems that impact on production quality or delay during this process will incur a far higher penalty.

Deep drawable steels require minimum recrystallisation conditions of 720-800°C for over 40 seconds. During this stage, the strip will have approached the latter zones of the heating furnace section and will continue to travel through the soaking furnace section, representing the most critical phase of transport control, as illustrated in *Figure 1.2* below.

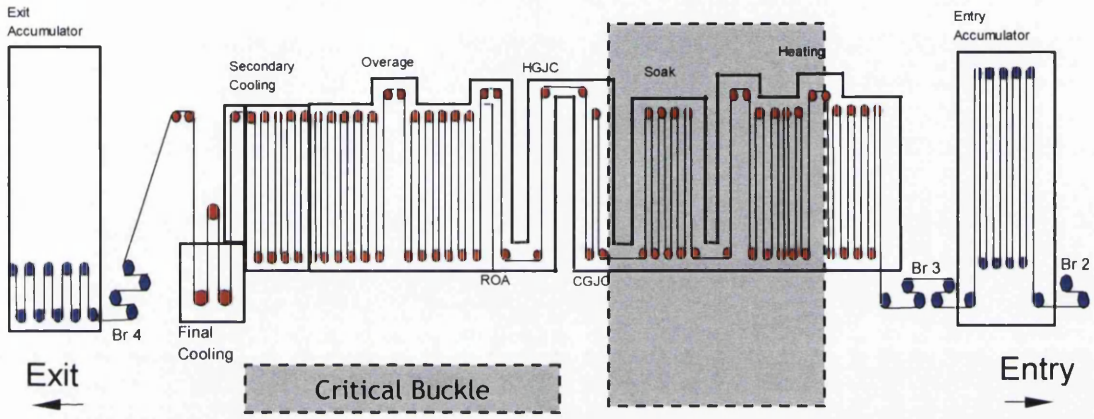

Figure 1.2 Schematic of the Process Line, Identifying the Zones and the Rolls where Recrystallisation Occurs

Furnace transport rolls enable the strip to follow a desired path through the many different zones that make up the furnace section of the continuous annealing processing line. Transport rolls only provide a limited motive force to drive the strip along; the majority of the motive force comes from the bridal rolls. Even so, the hard contact that is generated between the transport rolls surface and the strip surface is sufficient to impart considerable stress onto to the strip. This stress can come from a number of factors apart from the initial contact friction; including strip wrap angle and in-line tension. While it is desirable to have strip tensioning focussed towards the roll centre for maximum steering capability, any stresses must be limited from approaching yield stress conditions during any steady state or transient line condition.

Much literature[5-7] is evident on CAPL roll design, particularly by the Japanese steel makers over the past 20 years. However, the simple fact that all major

producers continue to report strip buckling serves to illustrate the complexity behind achieving a single optimum solution for all conditions.

The area of CAPL research, which requires the most attention in Port Talbot and is the most widely researched topic in the steelmaking world for continuously annealed products - is the effect of in-line buckle. Defined as a roll-strip interaction problem, it has two major interacting components: the roll taper (the most important part of the roll geometry) and in-line strip tension. These two components vary significantly as the strip moves through the furnace, due to the different zonal temperatures and therefore changing strip yield behaviour that comes into affect at different stages of the continuous annealing cycle.

1.4 THE IMPORTANCE OF HOMOGENOUS TEMPERATURE WITHIN THE FURNACE

Temperatures importance to CAPL modelling cannot be underestimated. The strip as it travels through the different furnace zones will have to endure many rapid changes in operational zonal temperature. This is further exacerbated by the fact that the roll-strip temperature is not always uniform, in some zones the roll is hotter than the strip, and in others it is the reverse. However, the affect on strip quality is always the same. If a sufficiently large temperature differential is developed between the strip and the roll then strip shape will be affected due the effects of expansion and contraction, which can lead to buckle if the strip is close enough to its yield point (at elevated temperatures the strip is often near its yield point operationally). An added complication is that often the temperature distribution across the rolls surface is not equal, whereas the temperature distribution across the strips surface is rarely an issue unless there is a poor interaction contact - this is because the strip is never processed above a gauge of 2mm. Even though thermal contact is an important research topic in its own right, the issue as far as computational simulations is concerned is not, the strip can remain isothermal - this is because variations to the strips temperature can be performed by the use of temperature dependent mechanical properties. Fundamentally, and as far as research is concerned the most important factors, which have come to light, are those operational parameters such as line tension, roll crown and roll crown fillet. These parameters and others like them are more readily controllable, whereas the high operating temperatures required for the recrystallisation process are simply essential. Corus have managed to control

differential contact temperatures effectively; unacceptable temperature differentials between the strip and the roll do not occur very often.

1.5 INTRODUCTION TO BUCKLE

The four main ongoing concerns that affect production potential are heat buckle, cool buckle, snakey buckle and strip tracking. Any of these could have an effect on the steel's productivity. The mechanism for all types of buckle are fundamentally the same, it is where the buckle occurs that dictates what it is named. It must be noted that any unit cost improvement to CAPL operational effectiveness has to be firmly justified to the Corus management, as cost of production downtime is so severe. This policy is encapsulated into any future CAPL operational and production changes, which makes small operational benefits hard to see through to fruition.

1.6 PROJECT OBJECTIVES

After extensive discussions between Corus, the industrial partners (Stein Heurtey) and the academic Supervisor, the project objectives were set as:

- To perform an extensive literature review of all relevant aspects of the continuous annealing processing line (CAPL) - an investigation into the history, development and current advances in CAPL technology. Review of high temperature contact modelling, both analytical and computational. Review of Corus RD&T reports into buckle incidents and analysis of Corus computational FEM modelling to date. Review of metallurgical aspects that are directly relevant to roll-strip contact interactions.
- To develop, plan and execute an experimental programme that considers the impact of excessive contact temperature differentials - to review, modify and then make use of an experimental pilot facility that represents the furnace section of the CAPL. To develop a fully-coupled computational model of the pilot facility for validation purposes.
- Investigate hot tensile test results for a range of elastic and plastic mechanical properties.
- Analyse the current CAPL operational parameters to develop a matrix of variables - consider all pertinent operational and design parameters that are associated with the roll-strip contact interaction.
- Develop computational FEM simulations to analyse all relevant aspects of the roll-strip contact model. This is to include the development of uncoupled

static, uncoupled dynamic and uncoupled heat transfer roll-strip contact models.

- Take a matrix of CAPL variables and develop it further to consider the variables of the future. The simulations to include, but not exclusively, changes to: strip dimensions, roll geometries, strip mechanical properties, furnace operating temperatures, in-line strip tension, roll speed and roll frictional coefficients.
- Analyse computational results and discuss. Highlight the deficiencies and areas of where improvements can be made.
- Validation of computational models with the Matoba equation and other pertinent literature.
- Further computational simulations as and where required.

1.7 LAYOUT OF THESIS

The thesis consists of eight chapters and an appendix, the present chapter forming an introduction to the thesis and providing the motivation for the research. The following chapters consider general literature, elasticity and plasticity, pilot test facility investigations and computational modelling.

1.8 THE ENGINEERING DOCTORATE RESEARCH APPROACH

An industrial based doctorate has a stronger inclination towards producing research that is beneficial to the relevant industry in which the engineering doctorate (EngD) is taking place. This creates an environment where there is a full and constant interaction with the industrial sponsors, enabling the research to stay focused and not diverting into an area of research that is too specialised for purposeful industrial crossover. The EngD scheme has a core list of examined and coursework subjects to complete: these are listed in the Appendix.

2 THE GENERAL LITERATURE REVIEW

2.1 CONTINUOUS ANNEALING PROCESSING LINE (CAPL)[8, 9]

Introduction

Steel strip hardens after cold rolling due to the dislocation tangling generated by plastic deformation. The annealing process is performed to soften the material from its hard but brittle microstructure. The annealing process comprises of three distinct cycles that being the heating cycle, high temperature soaking cycle, and finally the rapid cooling cycle. Annealing facilitates the movement of iron atoms, thus resulting in the disappearance of tangled dislocations, which cause the brittleness. Annealing is responsible for the growth of new grains known as recrystallisation, with the reversal of the grain structure to a more soften state being referred to as recovery.

In the past batches of coils stacked into a bell-type furnace have been used to anneal the strip. This process is referred to as batch annealing. However, the modern technique for annealing strip is through continuous annealing inside a Continuous Annealing Processing Line or CAPL.

2.1.1 LINE SPECIFICATION

The total length of the strip in the line is as much as 2,000m. Some other facts include:

- A strip travel speed of 200 to 700m/min.
- Run acceleration of +2m/mn/s.
- De-acceleration of -15m/mn/s.
- Emergency de-acceleration -30m/mn/s.
- Speed increase/decrease ±2m/mn/s.
- A capacity of 1 million tonnes per year.
- A maximum line speed of 600m/min.
- A strip gauge of between 0.3 - 2mm.
- A strip width of between 0.85 - 1.8m.

2.1.2 ENTRY SECTION

The entry section at Port Talbot is at the end of the cold rolling mill, with the cold rolled strip storage area right in front on the CAPL, a stock tracking system

operates. The main entry-side equipment comprises payoff reels, a welder, an electrolytic cleaning tank and an entry looper.

2.1.2.1 Un-coilers and Strip Preparation

The coils are moved from the storage area to the un-coilers by an automatic coil car. The un-coilers can handle two coils at any one time. While one is being un-coiled another is being prepared for the same procedure, which keeps the annealing cycle continuous. The various sized coils have their coiling straps broken by an automated machine. The coils are slowly unwound, and a leader of strip is pulled forward ready to be processed after the other coil, which is being annealed at that time, has finished. Once the other coil has finished then the process automatically pulls the leader through and the end is cut off, so that it has a smooth flat undamaged end ready for the next stage.

2.1.2.2 Welder and Notcher

The welder uses an overlapping resistance welding principle and leaves a very small weld seam once complete. This is necessary or the weld would interfere with the processing further down stream, especially when the strip passes around the rollers of the accumulators. The welding process also has to be fast as there is only a limited time that the entry section processing can be stopped; otherwise the entire annealing line will halt. The welder can easily weld together two strips of different gauge and width; however, in practice it will not weld large dimensional differences, as this is a buckle initiator.

2.1.2.3 Cleaning Section

The strip undertakes an intensive brushing; this is to rid the steel of any large particles that may be attached to the strip. The steel then enters an electrolytic cleaning process, which incorporates the use of a bath for soaking; the solution consists of sodium hydroxide (NaOH). The electrolytic solution then has to be removed and dried or it will affect the efficiency of the annealing process. A schematic of the entry section of the CAPL can be seen below *Figure 2.1*.

Entry Section

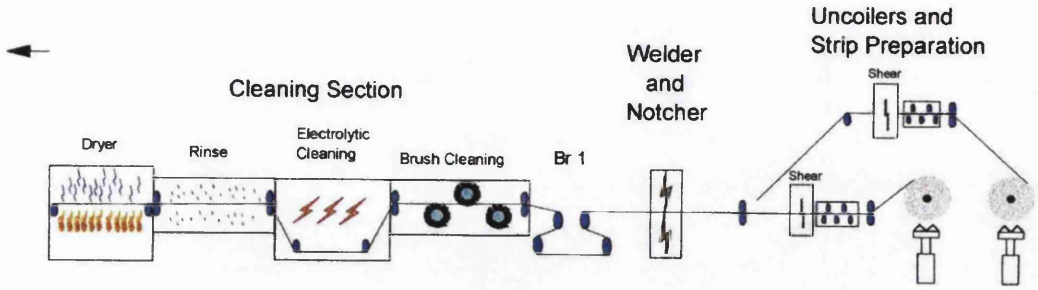

Figure 2.1 The Entry Section

2.1.3 FURNACE SECTION

The heating cycle differs from product to product. For cold-rolled strips in general use, it is normal practice to adopt a heating pattern in which the strip is heated to in excess of 700°C for approximately 1 minute, rapidly cooled, held at 400°C for 1 to 3 minutes to precipitate the solute carbon, and then cooled to room temperature. The furnace section is the largest section of the general layout of the CAPL; it has a total length of 112 metres and can carry up to 2500m of strip. This is where the annealing processing takes place.

2.1.3.1 Entrance Accumulator

The entry accumulator is 28m high and has a processing speed of 350m/min. The accumulator task is to keep the strip moving, either when a new coil is prepared at the beginning of the line (unwound) or packaged at the other end (rewound).

2.1.3.2 Heating Furnace Section (Radiant Tube Furnace: RTF)

The furnace heats the strip from an entrance temperature of around 30°C, to the desired annealing temperature which is dependent on the product being processed e.g. up to 850°C for certain extra deep draw quality (EDDQ) grades of strip steel. Vertical gas fired radiant tubes are used to heat the strip. The furnace is made of a gas tight construction; all heating furnace sections are 'w' shaped radiant tubes, mounted on vertical rows. This provides the most ideal radiative heat flux for the steel, and at the same time maintains a non-oxidising atmosphere. Strip exit temperatures are controlled by pyrometers, which regulate the intensity of gas flow to the burners. The furnace automation system controls the process to

minimise transient conditions, which may affect the strip quality. There are: twenty-four passes in eight zonal areas, which consist of 338 radiant tubes and have a maximum capacity of 58000kW.

2.1.3.3 Soaking Furnace Section (SF)

The soaking furnace section is directly connected to the heating furnace. Its purpose is to maintain the annealing temperature for the 222m of strip so that it has time to fully recover. The soaking furnace is gas tight and relies on wall mounted nickel-chrome (NiCr) electric elements, known as ribbon heaters. The soaking furnace section exit temperature is controlled by an infrared pyrometer, which regulates atmospheric gas temperature in the soaking furnaces two zones. There are ten passes in two zonal areas, using NiCr ribbon type electrical heating elements, with the strip heat loss via radiation - heating only to counteract radiation losses and has typically 1200kw (i.e. 5% of the heat furnace).

2.1.3.4 Conventional Gas Jet Cooling Section (CGJC)

The CGJC, like earlier sections, is gas tight. The strip in this section is slow cooled to its pre-recrystallisation temperature of 675°C, at a rate of 20°C/s. The strip passes between a series of coolers, which blast cold recirculated gas. The cooling system comprises of a recirculating fan coupled to a water cold heat exchanger, which draws atmospheric gases that are cooled to approximately 80°C. The cooled gas is returned to the "Blow Boxes"; where upon a controlled jet of gas is directed evenly across the strip surface. There are three passes in one zonal area and has a maximum capacity of 14560kW.

2.1.3.5 High Gas Jet Cooling Section (HGJC)

In the HGJC the strip undergoes rapid carbon recrystallisation. This part of the process distinguishes the various product categories and as a consequence the demand on accurate cooling control and capability is of extreme importance. The strip is rapidly cooled to 400°C - 270°C accordingly to the desired grade. The cooling rate 84 - 96°C/s. A 50% hydrogen (H_2) atmosphere exists (the other 50% is nitrogen); the gas is blown against the strip via six separate "Blow Boxes". Cooling is monitored by a pyrometer, which regulates gas flow as with the RTF section. Automated dampers in each "Blow Box" adjust blow length to maintain the cooling rate. Each "Blow Box" is subdivided into five zones, with motors enabling the nozzles to go within 50 mm of the surface of the strip. Stabilising rolls are

fitted between the boxes to prevent strip instability. There is one pass in three zonal areas and has a maximum capacity 14560kW.

2.1.3.6 Reheating Over Ageing Furnace Section (ROA)

Certain grades (DQ & DDQ in particular) require rapid cooling to temperatures as low as 270°C in order to optimise nucleation of the fine grain precipitates. So the ROA enables the steel to be reheated to allow rapid precipitation. There is one pass and one zonal area and has a maximum capacity is 3600kW.

2.1.3.7 Over Ageing Furnace Section (OA)

The strip inside the over ageing section is held until the lowest possible amount of carbon is in solution. There is 710m of strip residing in the OA, which equates to 29 passes; the six control zones are regulated by thermocouples, which adjust the current supply to the ribbon heaters accordingly. The strip temperature is held at 400°C for a period of two minutes, alternatively some strip chemistries require the strip temperature to be ramped down from 350°C to 270°C. There are twenty-nine passes and six zonal areas and has a maximum capacity of 3840kW.

2.1.3.8 Secondary Cooling Section (2C)

After ageing the strip is cooled to a temperature of approximately 210°C - 150°C according to the thermal cycle. The cooling unit deployed is a water-cooled heat exchanger atmospheric gas recirculation type "Blow Box. The strip length inside the secondary cooling zone is 170m long. There are seven passes in one zonal area and has a maximum capacity of 2000kW.

2.1.3.9 Final Cooling Section

Strip is cooled to approximately 40°C by means of water sprays and dipping. After wiping by wringer rolls the remaining water film is removed by means of a dryer. The cooling is achieved by the use of a water spray tower and 44 sprays plus two water-quenching tanks and a steam strip dryer. There are two passes in two zonal areas and has a maximum capacity of 3000kW.

2.1.3.10 Exit Accumulator

The exit accumulator is similar to that of the entry accumulator in terms of height and configuration. Both accumulators' top rollers move up and down on a conveyor system. The conveyor system is at its lowest point, when the strip entering is still

running and has not been stopped either for coil preparation or coil packaging. The conveying rollers move longitudinally up the accumulator stack when they have to take up the slack to keep the process running.

The exit accumulator marks the end of the furnace section; by the time the strip leaves this section it should be fully recovered. *Figure 2.2* shows a two-dimensional schematic of the furnace section of the CAPL and shows how the strip can easily move from one area to another in an automated fashion.

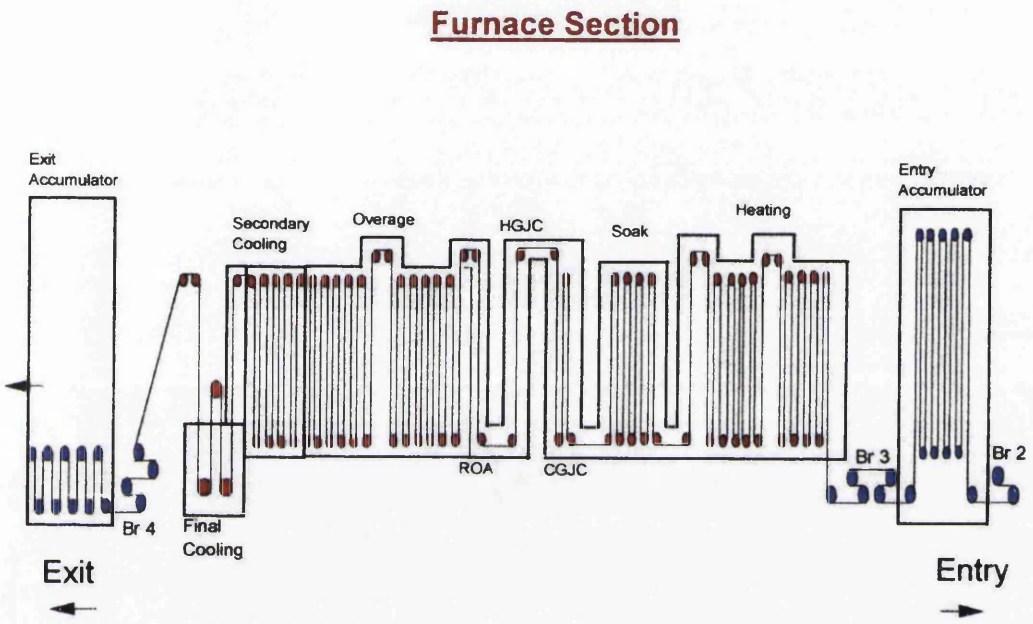

Figure 2.2 The Furnace Section

2.1.4 EXIT SECTION

The main exit-side equipment comprises of the temper mill and shape meter, horizontal accumulator, side trimmer, inspection and finally the recoiler.

2.1.4.1 Temper Mill and Shape Meter

After the annealing process the steel strip is often too soft for the customer. The way this is solved is to slightly cold reduce the surface of the strip; this is called tempering and is done in the temper mill. The temper mill consists of two rollers that exert a force on to the steel and slightly reduce its gauge. In doing so, the strips surface will gain a degree of work hardening through the slight deformation of the fully recrystallised equiaxed surface grains. The temper mill has a shape meter roll. The maximum speed of the strip in this section is 600m/min.

2.1.4.2 Horizontal Accumulator and Side Trimming

The strip leaves a small horizontal accumulator and enters the side-trimming device. Side trimming is required, because the strip is a light gauge product and has very often been damaged in one way or another through either pre-storage or by the actual carriage through the annealing processes itself. Side trimming removes a small amount of strip (Approximately 1 - 2 mm), which makes the delivered product more aesthetically pleasing to the customer.

2.1.4.3 Inspection and Recoil

Inspection involves using rollers arranged so that the strip is inspected on both sides. Inspection is automated and looks for steel deformations, and micro structural irregularities that may have occurred from imperfect recrystallisation. The strip then has a small surface layer of oil applied to prevent surface oxidisation; before finally the strip is recoiled and packaged for the customer. *Figure 2.3* below shows the exit section of the Port Talbot CAPL.

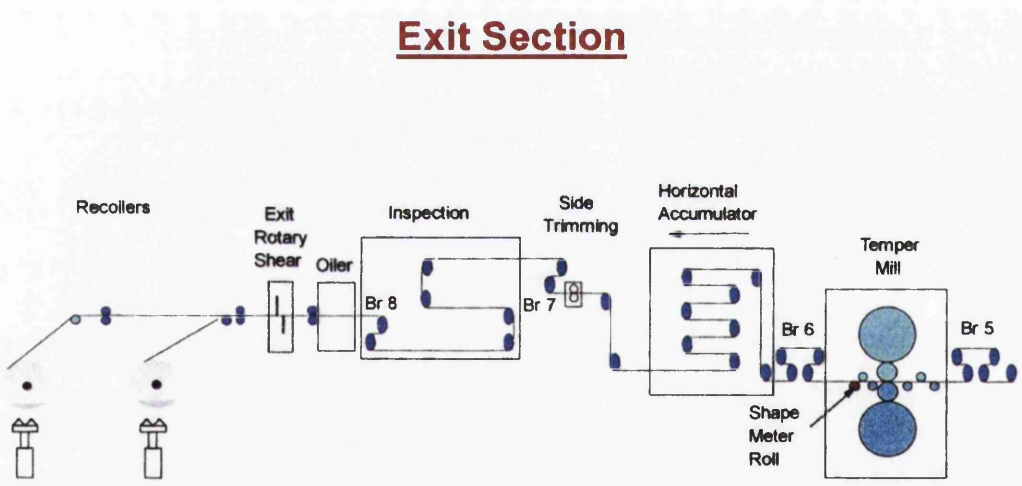

Figure 2.3 The Exit Section

2.1.5 BRIDLES

The bridles, as denoted by the letters Br in *Figure 2.3*, help maintain the inertia of the strip. Transport rolls keep the strip moving and some are driven to prevent strip "snagging" on the roll, however, they do not provide any strip momentum. There are a series of four very closely spaced rollers which the strip moves round under tension, these provide the necessary momentum for the strip to enter the next stage. The two lower bridle rollers are further spaced apart from the top

rollers and their positioning provides a greater surface area for the passing strip to move around and maintain the tension. The speed that the bridle system can create is up to 600m/min.

2.1.6 STEERING UNITS

The steering unit's role is not a separate system of rolls such as the bridles, but is in fact a number of the transport rolls that have the ability to move on their axis to compensate for a strip that moves off centre and thus aiding in its return to the centreline of the roll.

2.2 CONTINUOUS ANNEALING HISTORY

At the beginning of 1970, two Japanese steel producers first started operation of the world's first continuous annealing lines for cold-rolled sheet steels. Both lines included the overaging heat cycle following rapid cooling (the distinction between continuous annealing lines (CAL) and CAPL's). The main products manufactured by both lines were commercial quality (CQ) grade and dual phase high strength steels. In 1980 Kawasaki Steel started operation of annealing lines with accelerated gas jet cooling, the product range increased and included extra deep draw quality (EDDQ) steel. Since then, the continuous annealing line has been widely installed in many steel mills throughout the world. As for cooling techniques, mist cooling and roll cooling methods have been adopted. The initial gas jet and water quenching cooling methods achieved cooling rates of 10 to 30°C/s and approximately 1000°C/s, respectively. Accelerated gas jet cooling and roll cooling techniques have an intermediate cooling rate are currently being used by many steel producers. By 1984 CAPL technology had reached a peak of development with material grades from CQ to EDDQ, including draw quality (DQ) and deep draw quality (DDQ) being able to be annealed at temperatures in excess of 900°C, thus the development of bake-hardenable EDDQ steel was possible[10, 11].

2.3 GENERAL ANNEALING THEORY

Cold rolled sheets have a deformed micro structural matrix due to the temperature being low when the material was being work hardened. The ferrite grain structure has not been able to recover, thus the material is brittle, and with such poor ductility the strip is unable to be sold to customers like those in the automotive industry, on which the strip steel manufacturer is so reliant on.

Annealing must take place within the ferrite phase of the steel and the annealing temperature must stay below the transformation temperature. Otherwise, there is a chance of forming a dual phase steel, which will have a high tensile and yield strength but poor ductility, (dual phase steel has a mixture both face centred cubic austenitic and body centred cubic ferritic grains). *Figure 2.4* shows the structural phase transformation diagram. The phase transformation graph shows that the temperature change from ferrite to austenite is highly dependent on the level of dissolved carbon. The figure shows that when low levels of carbon are used it enables a higher annealing temperature (CAPL region below)[12].

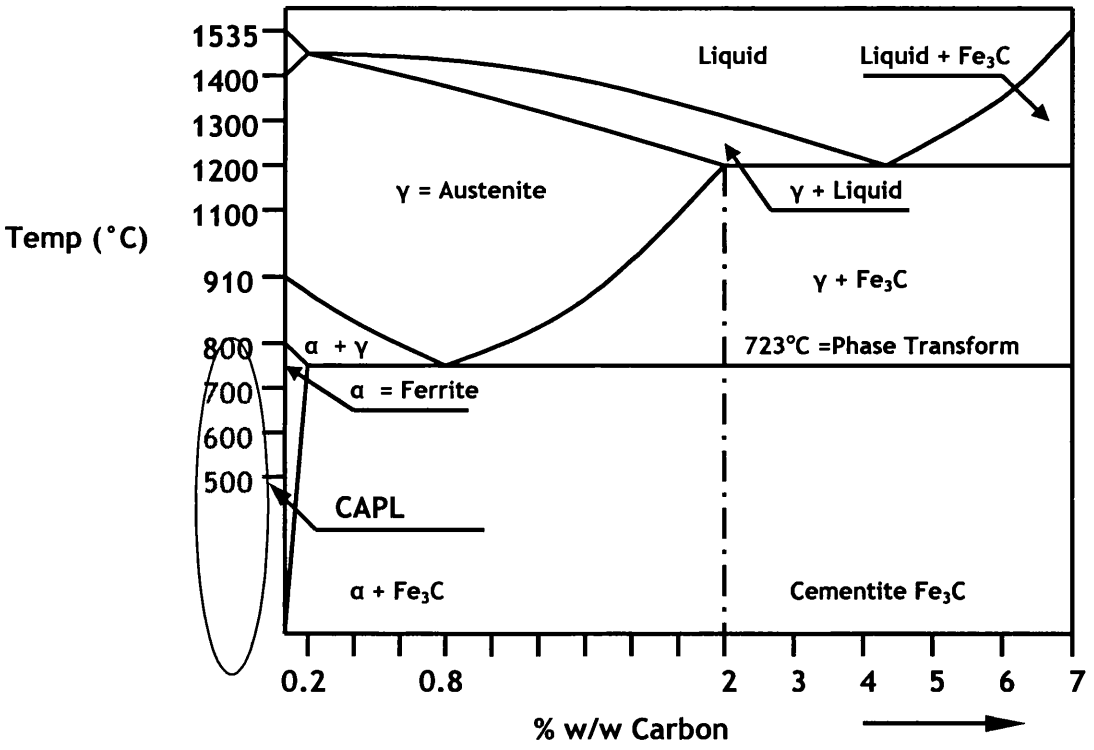

Figure 2.4 The Structural Phase Transformation Diagram

The important factor in continuous annealing is the phase change transformation temperature, of 723°C, this is associated with steels that have a chemistry of above 0.08% parts per million (ppm) of carbon. To achieve a perfect equiaxed grain structure the control of the heating rate and annealing temperature is of critical importance. The soaking temperature can be greater than that of batch annealing, because the steels have a composition chemistry of below 0.08% ppm of carbon, at these levels, phase transformation occurs at much higher temperatures in excess of 800°C. However, the heating and soaking times are

fairly short, yet recrystallisation must grow sufficiently, for the ductility and formability to return.

2.4 COMPARISON OF CONTINUOUS ANNEALING & BATCH ANNEALING

The obvious difference between the continuous and batch process is the size of the unit. Batch annealing utilises a series of small bases, whereas the continuous annealing line requires a considerable enclosed building to house an enormous furnace and accumulator structure, plus entry cleaning and exit inspection sections. However, once the CAPL has been built the advantages soon become clear. *Figure 2.5* shows the batch and continuous annealing cycles. What is evident from this diagram is the length of time it takes to complete batch annealing compared to continuous annealing. When batch annealing is performed the total time for the annealing procedure can be up to 10 days, whereas continuous annealing can be performed in as little as 15 minutes. The continuous annealing process has enhanced the application for steel packaging material [13].

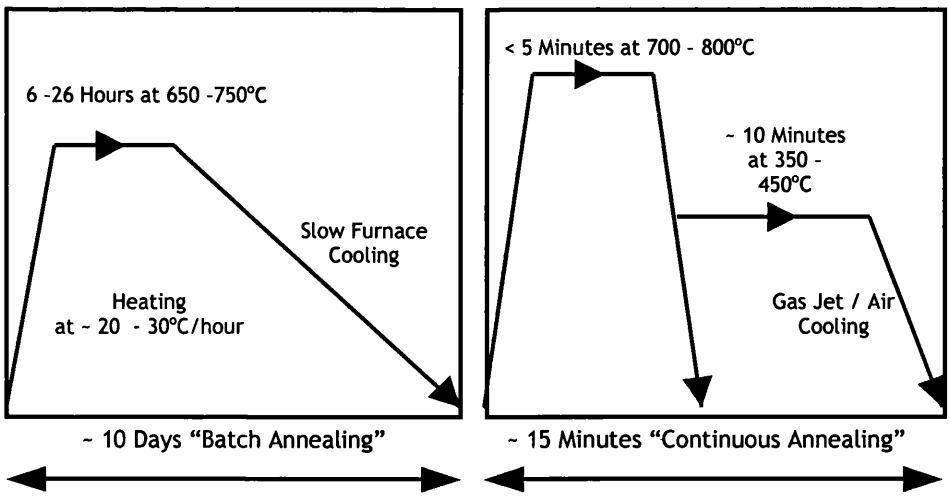

Figure 2.5 The Batch Annealing Cycle Vs The Continuous Annealing Cycle

Continuous annealing produced a number of significant advantages over batch annealing such as

- The CAPL has a design capacity of 1 million tonnes per year. The maximum line speed is 600m/min.
- Improved product quality via more homogenous heating and cooling control.
- Less handling/ crane requirement/ manning - less risk of damage.

- Improved order-delivery to time capability (cycles can be adjusted to sort order book and last minute requirements).
- Greater product range - i.e. multi-temper capability through chemistry and heat cycles.
- Improved "r" values[14].
- Ability to continuously coat after post-annealing.

However, continuous annealing has some major disadvantages. The most important is the financial implication of the initial capital outlay. The continuous annealing process is a much newer technology than that of batch annealing and as would be expected this has provoked many production problems, some of which are quite complex.

2.5 PROCESS CONTROL ISSUES

Introduction

Process Control Issues refer to the operational aspects of the line arising from everyday continuous annealing production. A focus was required on what really affects Corus Port Talbot operations and strip quality? So what type of investigation is required? The furnace has many different operational zones, so where and what specifically inside the furnace is the biggest problem? The answer to all these questions aided in the development of the overall project objective.

2.5.1 QUALITY ISSUES OF INCOMING STRIP

The CAPL handles cold reduced strip that leaves the cold mill, this is extremely hard with a work hardened and jumbled microstructure due to the cold reduction the strip endures due to rolling temperature being below the dynamic recrystallisation temperature. Cold reduction at the Corus Port Talbot works is through a five-stand mill. The hot rolled coils are cold rolled for a 50-70% reduction. The cold rolled strand is 0.7-1.5mm for strip applications, such as for the production of motorcars and domestic appliances. Thinner grades 0.15-0.30mm are processed for tinplate applications such as food/packaging/aerosol containers, however, not all cold mill products are required to be annealed[12].

2.5.1.1 Strip Shape

The definition of strip shape is "strip that is not flat and or is not following the contours of the roll that is transporting it". One of the reasons for a strip

processing line to drift sideways is the existence of asymmetrical shape defects. The strip can be kept within acceptable limits at the centre of a processing line by using pre-shaped and steering rolls and adjustment of the strip speed and tension[15]. Alternatively symmetrical shape defects create the centre and quarter buckle. Therefore, longitudinal straightness of the strip is the most import factor in avoiding poor quality strip[16].

Line data indicates that the very worse case of strip shape height disturbance is no more than 1.5mm. *Figure 2.6* is a brief schematic that shows the array of production problems that have been encountered on the Port Talbot CAPL.

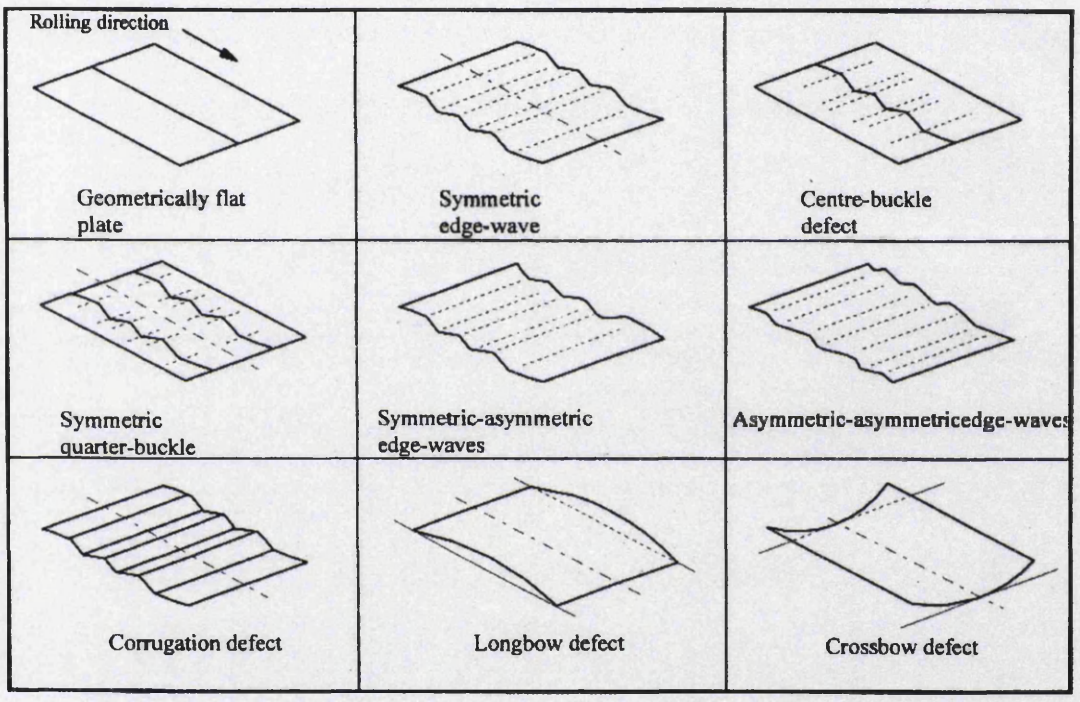

Figure 2.6 The Common Types of Strip Defects

2.5.1.2 Residual Stress

Cold rolling is the preceding manufacturing process. The strip shape entering the CAPL can be compromised even with the strip passing through a tension-levelling device. The built up stress state within the strip at the exit of the cold rolling and tension-levelling process is referred to as residual stress.

Furthermore, according to Roberts[17], strip shape is defined as "relating to the presence or absence of defects in the unstrained work piece which tend to distort its geometrical shape, good shape being ascribed to strip or sheet product which is

essentially free from such distortion". Roberts also states that resultant shape is also dependent on how the residual stress manifest themselves in the material, hence the term residual shape"[17].

Different buckle patterns can be developed from residual stress membranes, from pure twisting to wavy mode and from centre modes to concentration on the edge of the strip. The key factor however, to unleashing residual stress problems is global tension patterns of the strip inside the furnace[18, 19].

2.5.2 QUALITY ISSUES OF STRIP TO ROLL CONTACT

2.5.2.1 Camber

The definition of camber (a specific form of poor strip shape) is strip that is not flat and or is not following the contours of the roll that is transporting it; however, more importantly this strip shape change is not from prior processing. Camber occurs due to the hypothesis that after plastic bending under tension over a roll, at a high temperature, the strip is straightened and the residual elastic longitudinal deformation induces elastic cambering or guttering[5, 20].

2.5.2.2 Air Cushion Affect

Strip quality and efficient strip processing is critically dependent upon the thin lubricating air films that exist between the moving strip and the transport rolls. An inadequate film results in increased friction, web abrasion and resistance to smoothing, where as an excessive film reduces traction[21]. Furthermore, with a sufficient air cushion it acts as a lubricant and minor irregularities are pulled out of the strip; Knox and Sweeney indicated that an air film thickness of 1.0 percent of the strip thickness would have a negligible affect on operational effectiveness[22, 23].

Air cushion philosophy is based on air entrapment and low frictional force; it generally leads to surface scratches. Air Entrapment is defined as [7, 21]

$$\textit{Air Entrapment} = \frac{h}{r} = 0.643\left(6\mu * \left(\frac{Uweb + Uroll}{T}\right)\right)^{2/3} \qquad 2.1$$

h	air film thickness
r	roller radius
T	web tension

μ	dynamic viscosity of lubricating fluid
Uweb	web velocity
Uroll	roller velocity

The air cushion equation is adapted to suit process conditions of the furnace. However, the CAPL is enclosed, thus rendering parts of the equation difficult to interpret. The equation's original development was in the paper transfer industry, employing transportation rolls with tapers similar to that of the CAPL; thus giving the equation some enthusiasm within the strip research fraternity. Even with the author having some reservations on the usefulness of the "Air Cushion Equation" it has been adopted by Corus RD&T department. Lewis et al[24] concluded that the air cushion affect causes localised areas of raised stress on the strips surface due to intermittent contact between the transport roll and the strip. The areas of localised stress increases are due entirely to insufficient process control of the operational conditions. However, even though the air cushion equation is difficult to put into practice, the theory that the lifting of the strip from the rolls' surface causes localised areas of raised stress through intermittent contact is a real problem - the strip tends to be dragged across the rolls surface with varying degrees of severity.

2.5.2.3 Tracking

The definition of tracking is the deviation of the strip from the centreline of the roll that is transporting it. Tracking problems in continuous annealing processing lines generally result in damage and partial rejection of the strip steel. To avoid these strip-guidance problems and to guarantee good strip centre-line tracking, the use of roll crowns (tapered) and steering units (three types: general, tilting and offset pivot guide) has become essential[15]. Overtly flat cold rolled strip (inability to follow roll contour) is one of the major factors that causes strip tracking. Frictional force between the strip and the rolls tends to stop lateral spread of the strip towards the rolls edge[25]. Both the European Coal Science Council (ECSC) and Matoba[6] conclude that transport roll design is behind strip tracking. A commonly held theory dictates that with a large roll crown, the tracking of the strip is going to be small, and vice versa for a completely flat roll; however, buckle incidents increase with large roll crowns - tapers larger than 0.41mm[26]. The strips cross-sectional dimension is an alternative indicator of tracking. The smaller the width to gauge ratio the greater the risk of side tracking

or lateral wandering, whereas a high width to gauge ratio has often been linked to the development of strip folds or strip buckle[25].

Tracking could be associated with the air cushion effect. A type of classic boundary layer contact occurs on the rolls surface, the strip rides on this boundary layer. With the loss of all contact with the transport roll localised areas of frictionless contact can occur. Tracking can also be induced by strip shape effects such as camber. There are several methods to analyse strip tracking. A method developed by Schyns et al[25] looked at the angle of impingement. The angle lies in the plane of the approaching strip, between the perpendicular to the roll and the strip centreline. The strip sidetracks in such a way that the angle of impingement becomes zero, a disturbance, for example camber, as seen *Figure 2.7*[25] can initially cause the angle of impingement to be unequal to zero. The strip sidetracks and a bending line becomes prominent.

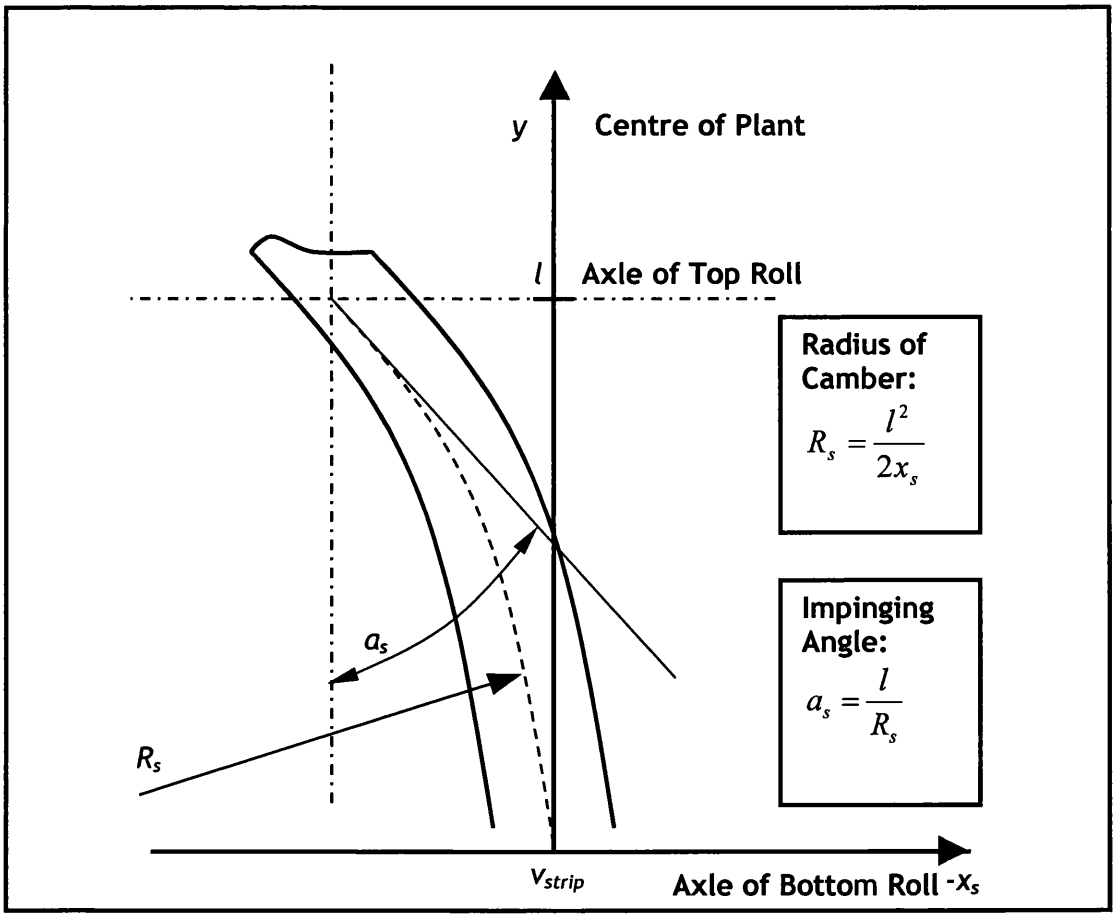

Figure 2.7[25] Strip Camber

2.5.2.4 Effects of Tension

The effects of excessive uniform tension and especially the effects of non-uniform tension have been proven; the issue of tension is fundamental to final strip quality. To take the strip close to its critical recovery level its elastic point when operating at the furnace annealing temperature (>750°C), it is important to keep tight control of the process set points. The point where strip is in most direct contact with the roll is where buckle is most likely to occur (level of highest frictional contact), and thus will produce the most critical region with the highest values of buckle susceptibility[27].

Roll misalignments is the principal cause of non-uniform tension. There is no specific plant specification for roll tolerance, however, the measurements taken from the original rolls when the plant was commissioned have indicated a tolerance of 0.05mm/m i.e. 0.11mm miss-alignment on a 2.2m roll[27].

2.5.3 QUALITY ISSUES RELATED TO STRIP BUCKLE

2.5.3.1 Dimensional Range of Critical Yield Point Limits

Plastic deformation of the steel strip is possible in any location, it can be at the roll contact point or in a transient location between the roll passes. The most significant occurrence is heat or 'snakey' buckle, which can manifest itself during the re-crystallisation stage. *Figure 2.8* below illustrates the typical strip dimensions most susceptible to yield point elongation on CAPL.

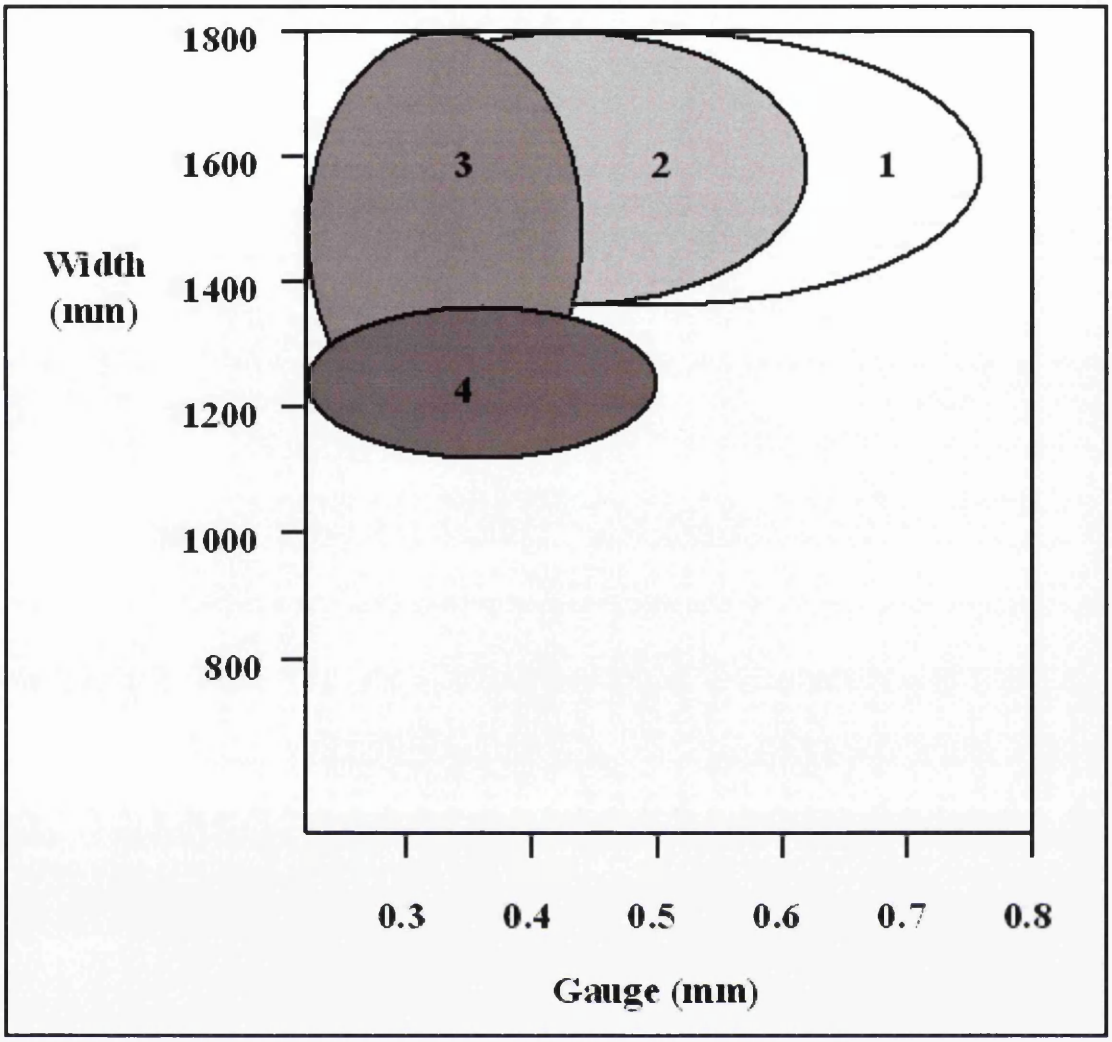

1.	Tension Buckle:	>1400mm Width	<0.8mm Gauge
2.	Heat Buckle:	>1400mm Width	<0.6mm Gauge
3.	Snakey Buckle:	>1200mm Width	<0.5mm Gauge
4.	Cool Buckle:	1100-1300mm Width	<0.5mm Gauge

Figure 2.8 The Four Types of Buckle Reported on CAPL[24, 27-29]

All literature points to similar findings that the extremities of the CAPL product range are where buckle occurs. However, trying to determine where exactly is not an exact science due to buckle being dependent on the grade of steel being processed and the local CAPL operational parameters. An example of this is given by the case of the Armco Ashland Works in Texas; it was observed that furnace buckle occurred in strip with widths in excess of 1140mm, gauges less than 0.76mm and an annealing temperature of 815°C[30]. The Armco Ashland Works suffered from a 76% increase of buckle in the soaking furnace section if the temperature was increased by just 17°C.

2.5.3.2 Locations of Contact Buckle on Strip Steel

There are three principal transport roll to strip contact locations *(Figure 2.9)*. The most common form of buckle (or quality issue) is the centre buckle; this type of strip deformation is associated with the central contact point of the strip and the transport roll. It is at this central contact point that the highest strip compression occurs. The CAPL furnace zones that suffer the most from centre buckle are the end of the heating zone, and the beginning of the soaking zone. Quarter buckle, like centre buckle is also associated with the effects of strip compression. However, it is the contact that the strip has with the roll fillet on the roll crown that is the specific cause of the quarter buckle yield deformation. The third and last form of buckle is edge buckle often referred to as strip edge waviness.

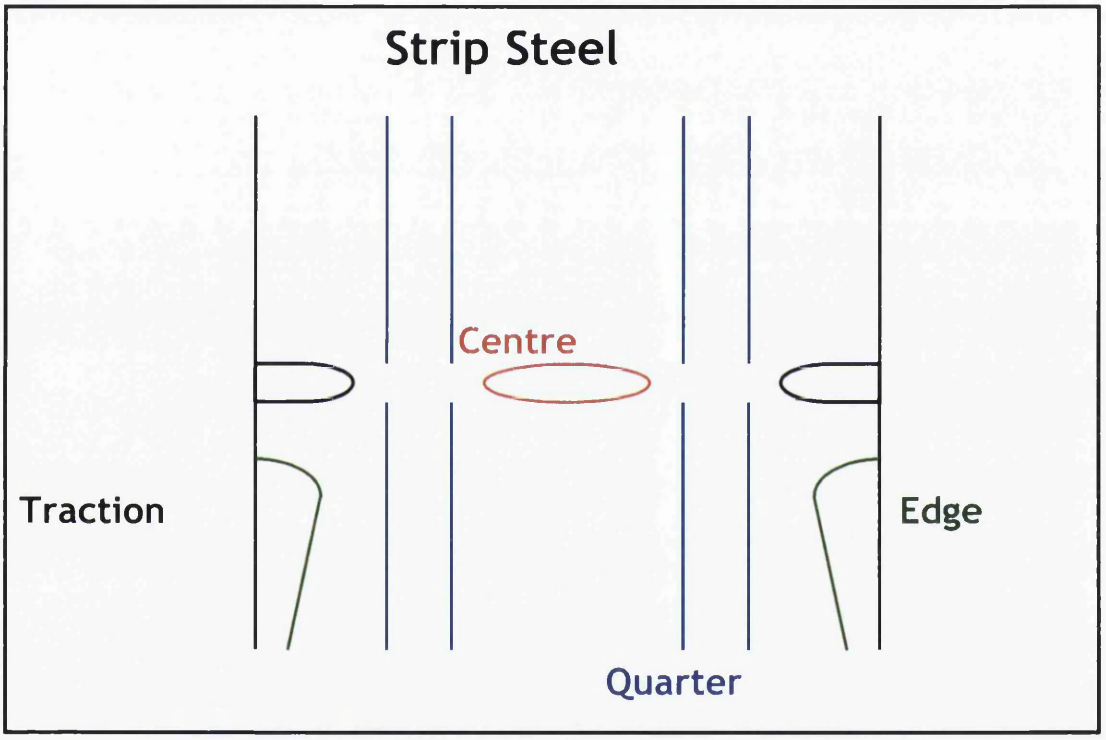

Figure 2.9 The Three-Principle Transport Roll to Strip Contact Locations

2.5.3.3 Tension Buckle

Tension buckle is an intermittent buckle phenomenon that occurs on the exit accumulators of a continuous annealing line. The tension that is induced on the rolls causes the relatively cold annealed strip to sometimes crease in the longitudinal direction and, or at the very least, causes an unsightly blemish on the strip[24].

Corus tension buckle reporting indicates that the material, which is most likely to suffer from this form of buckle, is very thin strip such as the extra deep draw quality (EDDQ) steel. The problem is in general magnified when the strip is at the extremities of the product range, and only forms on the soft wide thin materials (DDQ or EDDQ, > 1400mm, <0.75mm) usually during the rapid acceleration phase of transportation (>12m/pm/sec)[24].

Lewis et al[24] discovered for a large increase in tension, an equally large frictional force is necessary. However, at the same time the compensation that the transport roll drive makes, must remain minimal. Lewis et al[24] concluded that the load on the hanging strip that is in contact with the rolls will generally be of a uniform nature; this is irrespective of roll profile, strip width and tracking conditions. However, as the strip moves down away from the rolls, the strip's non-uniformity grows.

2.5.3.4 Heat and Cool Buckle

Corus has always differentiated between these two types of buckle. However, all literature indicates that the two types of buckle share the same mechanism of failure. Put simply: one occurs when the strip is heated and the other when the strip is cooled. Heat buckle occurs predominately in the heating and soaking section of the furnace and cool buckle, in the case of the Port Talbot works, in the secondary cooling section of the furnace.

Heat and cool buckle differ to tension buckle in one very major operational way - that of thermal loading. This can be the cause of a significant strip quality issue, something that simply was not present when the strip was under tension at ambient temperature conditions within the entry accumulator. A transport roll miss-guidance or a tension control problem emanating from the entry accumulator will have little effect on the strip when the band has its maximum cold iron properties. However, once the strip enters the heating cycle and makes hard contact with a significantly hotter transport roll, a thermal distortion can often take place.

Overheating becomes an issue when the strip has a particularly high yield strength and requires a higher recrystallisation temperature for annealing (permanent deformation to the strip could occur if the temperature within the heating furnace

is raised to quickly to attain the correct recovery temperature for some high yield steels). Overcooling can occur when the strip is under tension at a uniform temperature. If a section of the strip is cooled down, the thermal contraction will be hindered by the surrounding material, thus keeping the same length, but the small section will now be permanently elongated.

Research into overcooling can be credited to Kim et al[31]. Their research gives the most useful insight into methods of stabilising strip shape through controlled cooling.

Kim et al[31] researched in detail rapid cooling technology in continuous annealing lines. Their aim was to set a cooling pattern for the rapid cooling section that would stabilise the strip shape and tracking inside the CAL. An accurate cooling pattern is required because non-uniform tracking inside the CAL occurs readily. Their research highlighted the importance of the temperature gradient between strip centre and the strip edge.

2.5.3.5 Snakey Buckle

Snakey buckle affects the strip steel at Corus in Port Talbot severely. It is a poor surface finish issue rather than an outright buckle issue. The finished strip with snakey buckle has a series of unsightly marks running across the strips width. The automotive industry in particular will not accept strip that has suffered from snakey buckle as it can be seen through even several layers of sprayed paint. Snakey buckle occurs in the heating and soaking zone (incidentally the same zones as heat buckle). However, it is categorised and researched separately. Snakey buckle is most often researched by Corus from a metallurgical standpoint.

Corus RD&T have developed a technique for classifying the different types of snakey buckle in terms of severity. This is important to determine whether the strip should be scraped or reduced to a lower grade product.

Grade	Description
Clear	No snakey buckle visible.

Very, very light	Difficult to see on stationary strip / not picked up by CAPL inspection device.
Very light	Visible on stationary strip / not picked up by CAPL inspection device (CID).
Light	Visible on stationary strip and thread speeds / not picked up on CID.
Medium	Easy to see at stationary and thread speeds, particularly visible at furnace speeds / not picked up by CID effectively.
Heavy	Obvious to stationary strip and visible at furnace speeds / picked up by CID.

The best method to avoid snakey buckle and any other type of buckle generally is tight operational controls. This process is started with an appropriate and well thought out scheduling of the strip steel. However, It must be remembered that when scheduling the strip that any rapid changes in the strip width and gauge destabilises the furnace temperature [32].

2.5.4 FRICTION AND CONTACT PROPERTIES OF TRANSPORT ROLLS

Lewis et al[24] concluded from their research into tension buckle that the extent to which strip tension fluctuates will depend on the levels of roll drive torque deficiency, together with the resistance of rotation. Since resistance increases with acceleration, the more critical situations will occur during rapid accelerations. To prevent slippage, the friction factor between strip and roll must be significantly higher than that necessary during "correct" operation[24].

Figure 2.10 shows a representation of frictional forces between the strip and the roll. The act of roll-strip contact can cause in itself detrimental strain to build up in the strip, even if the strip is perfectly flat, perfectly in contact, and static on the rolls surface - this excessive strain may cause the strip to wander across the rolls surface. This wandering action in itself may relieve some of the lateral strain. However, the band of creep at each edge (assuming symmetry) may be narrow or it may extend intermittently as far as the centre of the strip. A method

in reducing heat generated by contact forces is by the use of water quenching systems[31]. In particular Shelton's[33] research which was performed predominately in the 1960s looked at the issues that surround high speed ultra thin gauge material on rollers, while it is pertinent research, it has not been considered for the Port Talbot CAPL furnace. Shelton's research into lateral web contact, however, does come to conclusions that have long been considered relevant for CAPL research. Especially the areas of research concerned with buckle initiation. Shelton's research highlighted that the areas on the strip, which are most likely to suffer from buckle, are those where the transport rolls geometry alters such as at the roll taper - the point of greatest strip surface load, defined by strip surface area.

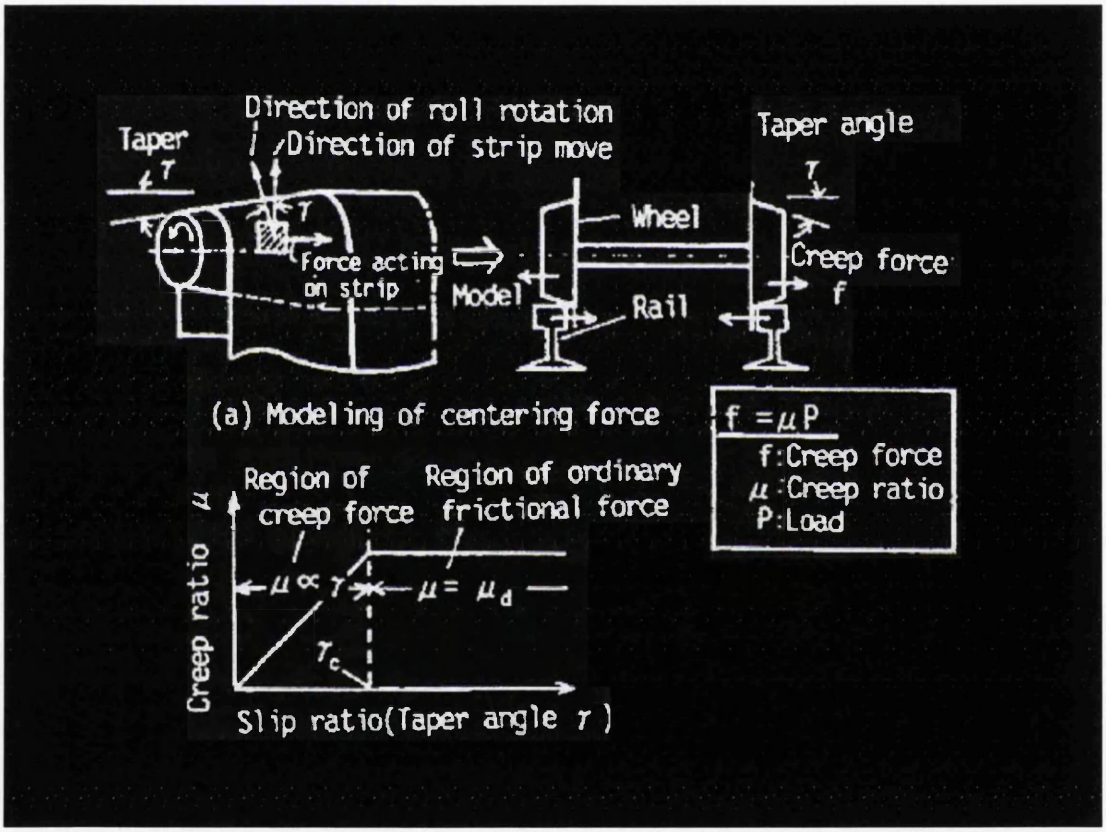

Figure 2.10 The Frictional Forces Between Strip and Roll

2.6 PRODUCT DEVELOPMENT ISSUES

2.6.1 COMMERCIAL QUALITY (CQ)[34]

When a client requests CQ quality it is on the understanding that the tolerances of composition and surface defects are not as tight as the more expensive premium grades. CQ strip has a wide variety of uses, including automotive panels, electrical

home appliances, drums, pipes, farm implements, office supplies, building and civil work materials and as base metal for various coatings. The product normally has a 0.15% maximum carbon content. The recrystallisation temperature is lower than that of other grades especially extra deep draw quality (EDDQ). Therefore, unlike other grades, the strip steel will start to recrystallise in the heating furnace.

2.6.2 EXTRA DEEP DRAW QUALITY (EDDQ)[34]

The high end of the market is a type of steel grade referred to as interstitial free or IF steel. IF steels use solid solution hardening to produce steels with a yield stress (YS) in excess of 300MPa, however, IF steels will still tend to have slightly lower yield strength values than the other deep draw quality steels or the commercial quality strips, due to concessions on formability. The product can have carbon levels as low as 0.02%.

EDDQ steels have a high "R" formability requirement; therefore the steel greatly resists the thinning process. When recrystallisation occurs, if carbon is present, it ruins the deep draw properties of the steel and affects the size of the grain making it coarse. To remove the free carbon the EDDQ steel is overaged, while the CQ is not. However, it could be naturally strain aged by "sitting around", which often occurs to coils that sit in storage for too long.

2.6.2.1 Interstitial Steels (IF)[34, 35]

The most important solid solution strengthening elements are phosphorous (P), silicon (Si), manganese (Mn) and boron (B). *Table 2.1* shows how each element affects the mechanical properties and how, by tailoring the composition, a certain set of properties can be designed. In reality, a combination of the different elements is used for various reasons. For example, too much phosphorous can cause embitterment but boron is added as an antidote.

	Level	YS (MPa)	UTS (MPa)	EL (%)
Mn	/0.1 wt%	+1	+4	-1.0
Si	/0.1 wt%	+10	+12	-1.1
P	/0.01 wt%	+4	+10	-2.0
B	/0.001 wt%	+40	+10	-0.1

Table 2.1 Element Solid Solution Strengthening

2.6.3 EFFECT OF PARTICLE SIZE

When carbides of sufficient diameter (e.g. 0.5 to 10 μm) are present during rolling, they lead to local severely strained regions, which can provide preferential nuclei for recrystallisation[36]. Fine carbide particles may dissolve rapidly during annealing and may contribute, to the development of a poor texture by providing solute carbon during recrystallisation[36].

2.6.4 SURFACE FINISH[35]

Surface finish is an issue that originates in the cold rolling section. The unexposed applications lustre is transferred from cold rolling to continuous annealing. There are three types of surface finish.

Exposed is intended for the most critical exposed applications where painted surface appearance is of primary importance. This surface condition will meet requirements for controlled surface texture, surface quality and flatness.

Unexposed is intended for unexposed applications and may also have special use where improved ductility over a temper rolled product is desired. Unexposed can be produced without temper rolling. This surface condition may be susceptible to exhibit coil breaks, fluting, and stretcher straining. Standard tolerances for flatness and surface texture are not applicable; in addition surface imperfections can be more prevalent and severe than with exposed.

Semi-exposed is intended for non-critical exposed applications. This is typically a hot dip galvanised temper rolled product.

2.6.5 EFFECT OF COLD ROLLING ON THE MICROSTRUCTURE

Finally the general literature review should mention in brief the principal reason for annealing. Recovery is required due to the destructive nature that cold rolling has on the grain structure of the strip steel while reducing. Cold rolling breaks down the equiaxed ferrite grain structure of the hot rolled strip. Equiaxed grains are the ideal grain structure for ductility, they are not tangled and have a uniform pattern, this enables movement to occur easily through inertia, and high forces are associated with brittleness in steel. On an atomic level, the atoms are evenly displaced, with large-scale atomic movement only possible when there is co-operative movement. Slip occurs only when a sufficient inertia force is generated;

in a ductile material the slip is constant due to the uniform grain structure. However, in a brittle material, slip often occurs only when a high inertia force is generated, this is due to the grain structure being non-uniform. Slip in a brittle material often results in catastrophic rapid failure[12, 37].

2.7 THE CLOSING REMARKS OF THE GENERAL LITERATURE REVIEW

In the beginning the research project brief received from Stein Heurtey and Corus was a little vague, it was simply that "the final product quality is poor, please investigate". However, it quickly became apparent, that while the furnace exit quality of the strip is all important, it is entirely of secondary importance to that of in-line strip furnace buckle, the primary cause of poor strip quality. Furthermore, the complete failure of strip inside the furnace has high financial implications to Corus for every hour that the CAPL is not operational. The next question was how to move this forward. Therefore, the initial focus of the literature review was to gain an understanding what exactly the CAPL is and how it performs its duties. Section 2.1 explores all aspects of the Port Talbot CAPL, including the "Entry" and "Exit" sections as well as the "Furnace" section, which is the focus for the rest of the thesis. Section 2.1 details the relevant background information for the entire CAPL; it highlights how the process remains continuous in nature while is passes through these three main sections. Section 2.1 also lays out in detail the entire "Furnace" section, the most relevant CAPL section. It also investigates the operational parameters, which used in the later computational FEA chapter.

Section 2.2 briefly explores the history of continuous annealing, its Japanese routes, and the need to improve on the hugely successful, but ultimately slow, batch annealing process. Section 2.3 briefly looks at the metallurgical theory behind the continuous annealing process. This section defines the fundamental reason for the enablement of such high annealing temperatures. Section 2.4 gives some practical examples of the advantageous nature that continuous annealing has over the historically used batch annealing process.

It was apparent, that once the initial literature review for the thesis was complete, the topic was enormous and complex. An almost impossible job to perform, if all aspects of the CAPL were to be investigated - so a judgement had to be made. The decision taken in association with all the research partners was

to specifically look at strip interaction issues within the "Furnace" section. However, the scale of the research question was still to be defined a little more as no wide-ranging mechanical based CAPL research project had ever been performed by Corus at that time on the CAPL. Even research outside Port Talbot had been limited, most research is confidential to the steel manufacturer and findings are rarely published.

Section 2.5 looks at the process control issues, with a direct emphasis on the transport roll to strip steel interaction. The research is now restricted to just the "Furnace" section where the strip is heated and cooled in the various passes. This is not to say that mechanical deformation does not occur in the other CAPL zones, it is just that this is the focal point of this thesis. To define the focus even further roll-strip interactions within the furnace caused by hard frictional contact are investigated.

The incoming strip shape is a major influence on the final strip quality. However, the annealing process itself often recovers minor incoming strip quality irregularities. Poor shape can still cause a problem once it interacts with the transport rolls within the first few passes of the heating furnace, at this point, the strip is still at its cold rolling temperature and not very ductile. The hard iron strip that enters the CAPL will definitely have detrimental residual stresses from the cold rolling process. Residual stress can increase the likelihood of strip failure if the temperature differential at the start of the annealing cycle is greater than advised by the "scheduling rules".

The purpose of the transport roll is not to deform the strip, like the rolls in the "Cold Mill", but to act as guide while the strip goes through its annealing process. This can be defined more specifically: "the CAPL is designed to return the strips mechanical properties to a pre-cold rolling deformation state while maintaining the strips elastic integrity". All other manufacturing processes include plasticity for band reduction (from the continuous castor all the way to the cold mill). Corus, of course, try to predict if the shape has been compromised at the end of the cold mill. The "I" number used by Corus not only helps to enable the appropriate level of quality control but also directs whether the strip should be re-worked, re-classified or rejected.

Section 2.5 continues with one of the most important sub-sections of the general literature review, that of the "Quality Issues of Strip to Roll Contact". Starting with camber, a form of residual strip shape that causes a quality issue when in contact with the transport roll. Camber can lead to other strip quality issues, in particular tracking. Tracking is not necessarily a quality issue but certainly can be a symptom of poor strip quality. However, camber is most often a symptom of poor operational choices, such as roll type, roll taper and or strip tension. The other important and vastly under researched field is the "Air Cushion" effect. Initial research was performed in the 1960s; however, it was not linked to the continuous annealing process originally, only because CAPL's did not exist. However, the theory based on the use of ultra-thin aluminium foils over a transport roll has direct link to the ultra-thin strip used in modern processing lines. The air cushion effect is thought to occur from the effects of a thin layer of compressible gas existing between the mating surfaces of the transport roll and the strip steel. This author feels that this thin layer is thought to develop through a number of factors such as insignificant strip tension or insufficient surface texture and very possibly from worn roll surfaces, which all aid intermittent contact. This intermittence itself is increased with the use of large roll tapers on type "C" and "D" transport rolls.

The last section of 2.5 refers to the most disruptive quality issue of them all; that of strip buckle. This part of Section 2.5 details Corus continual fight against the three main types of furnace buckle - heating, snakey and cooling buckle. What is apparent from the literature review is even though Corus heavy distinguishes between all of these types of buckle they do have a similar mechanism of failure (temperature, load or frictional contact). The load mechanism of failure can be linked in some places to compressional loads and in others tensional load.

The "General Literature Review" is a look at the broad perspective and nothing more. Section 2.5 is where the mechanical aspects of the research topic are highlighted. This section shows why buckle is such a quality driven issue, it shows why thin and wide gauge are most susceptible; it briefly discusses the frictional and contact properties. The complex issue of fighting in-line buckle in terms of designing appropriate roll crowns and setting correct operational strip tensions is very important. It must be remembered that control of the temperature for metallurgical and strength reasons and advancements in line speed are the

fundamental profit making operational characteristics. Areas of profitability are linked to the grade, which is briefly defined in Section 2.6.

From the start, the sole intention was to move the research along a little more than had already been achieved. So Chapter 2 discusses the major "Process Control" issues that exist today. The chapter highlighted some of the other major areas of research that are being conducted, such as in the "Product Development" field. This field is related purely to metallurgy and is just as extensive and complicated as that of the mechanical one.

3 ELASTICITY & PLASTICITY

Introduction

This chapter principally considers the elasto-plastic constitutive equations that are relevant for the contact between the strip steel and the transport roll.

Unlike most research projects that are performed on transient strip processing techniques that are based upon the operational functions of the Port Talbot Integrated works, the objective of the CAPL is not to reduce the strips cross-sectional area by deformation. The CAPL's sole purpose is to transport the strip steel while it is recovers from prior cold working.

Therefore this section, while it looks into the theory behind strip steel plasticity, it ultimately concentrates on the most pertinent elastic theory, with the exception of the yield criterion according to von Mises, which is the primary identifier of strip yielding in computational finite element models. The yield point is critical to CAPL quality if breached the strip will in all likelihood be scrapped.

3.1 RELATIONSHIP BETWEEN STRESS AND STRAIN[38]

3.1.1 FUNDAMENTALS OF ELASTICITY

3.1.1.1 Hooke's Law

Hooke's Law expresses linear stress-strain relations for small deformations of an elastic homogeneous isotropic solid. These relations are applied to derive expressions of the strain energy for such a solid. In order to determine the load-deformation behaviour of a solid of certain geometry due to a system of loads, the material stress-strain relation must be known. Such relation often termed the material *constitutive law* [39].

Stress-strain relationship is defined as $\sigma = E\varepsilon$. The elastic modulus of an object is defined as the slope of its stress-strain curve in the elastic deformation region. Modulus *(E)* describes tensile elasticity, or the tendency of an object to deform along an axis when opposing forces are applied along that axis; it is defined as the ratio of tensile stress to tensile strain.

3.1.1.2 Stress States

The CAPL's strip stress state is *deviatoric.* The deviatoric stress refers to a state in which the shear stress will distort the solid; however, it will not change its

volume. The alternative stress state is the *hydrostatic*. A hydrostatic stress maintains the original properties of the volume under a load. The hydrostatic stress (σ_h) equation is represented as

$$\sigma_h = (\sigma_{11} + \sigma_{22} + \sigma_{33})/3 \qquad 3.1$$

The deviatoric stress consists simply of the hydrostatic stresses subtracted from the original stress tensor (σ_{ij}). The resulting matrix includes tensile stresses that elongate the volume as well as shear stresses that cause angular distortion. So if the strip distorts in any plane through excessive loading, or localised temperature differential, the elongation will not be uniform across the width.

3.1.2 STRAINS[40, 41]

In two dimensions, the basic problem variable is a vector ***u*** made up of two components, *u* and *v*, the displacements in the x- and y-directions. The concept of strain naturally extends to the two co-ordinate directions, but in addition there is a shearing strain. For a distortion of a body through an applied force only the direct strains would arise

$$\varepsilon_{xx} = \frac{\partial u}{\partial x} \qquad 3.2$$

$$\varepsilon_{yy} = \frac{\partial v}{\partial y} \qquad 3.3$$

However, for general distortion of elements (i.e. rectangular) then shear strain is

$$\gamma_{xy} = \frac{\partial u}{\partial y} + \frac{\partial v}{\partial x} \qquad 3.4$$

Thus there are three strain components, which are given in terms of the displacement vector.

$$\varepsilon = \begin{bmatrix} \varepsilon_{xx} \\ \varepsilon_{yy} \\ \gamma_{xy} \end{bmatrix} = \begin{bmatrix} \frac{\partial u}{\partial x} \\ \frac{\partial v}{\partial y} \\ \frac{\partial u}{\partial y} + \frac{\partial v}{\partial x} \end{bmatrix} = \begin{bmatrix} \frac{\partial}{\partial x} & 0 \\ 0 & \frac{\partial}{\partial y} \\ \frac{\partial}{\partial y} & \frac{\partial}{\partial x} \end{bmatrix} \begin{bmatrix} u \\ v \end{bmatrix} \qquad 3.5$$

The relationship can be written in matrix (Voigt) notation as

$$\varepsilon = \boldsymbol{S}\boldsymbol{u} \qquad 3.6$$

Where $\boldsymbol{S}$ defined by this equation is the matrix operator

$$\boldsymbol{S} = \begin{bmatrix} \frac{\partial}{\partial x} & 0 \\ 0 & \frac{\partial}{\partial y} \\ \frac{\partial}{\partial y} & \frac{\partial}{\partial x} \end{bmatrix} \qquad 3.7$$

3.1.2.1 Compatibility Equations[39]

The strain-displacement relations involve three independent displacement functions for three-dimensions *u(x,y,z)*, *v(x,y,z)* and *w(x,y,z)*. If these functions are known, the six independent strain components are determined by differentiation. If they are given as functions of *(x,y,z)*, then the displacement functions are determined by integration. Thus in both cases, six equations are used to determine three unknown displacement functions. If the strains are arbitrarily described, the six equations are not expected, in general, to yield single valued continuous solution for *u,v,w*. Hence, certain restrictions must be imposed on strains. Strain fields for which a single-valued displacement solution exists are called compatible strain fields. To this end, the additional conditions to be satisfied to limit the arbitrariness of strain fields are known as strain compatibility equations.

Consider first a two-dimensional strain and using *(3.2-3.4)*. Differentiation of theses equations gives (in Cartesian Coordinates)

$$\frac{\partial^2 \varepsilon_{xx}}{\partial y^2} = \frac{\partial^3 u}{\partial x \partial y^2}, \frac{\partial^2 \varepsilon_{yy}}{\partial x^2} = \frac{\partial^3 v}{\partial y \partial x^2}, \frac{\partial^2 \gamma_{xy}}{\partial x \partial y} = \frac{\partial^3 u}{\partial x \partial y^2} + \frac{\partial^3 v}{\partial y \partial x^2} \qquad 3.8$$

This results in a condition to be satisfied by the three strains, namely,

$$\frac{\partial^2 \varepsilon_{xx}}{\partial y^2} + \frac{\partial^2 \varepsilon_{yy}}{\partial x^2} = \frac{\partial^2 \gamma_{xy}}{\partial x \partial y} \qquad 3.9$$

This is the first equation in a set of six compatibility equations for infinitesimal strains. The remaining five which may be derived in a similar way give

$$\frac{\partial^2 \varepsilon_{yy}}{\partial z^2} + \frac{\partial^2 \varepsilon_{zz}}{\partial y^2} = \frac{\partial^2 \gamma_{yz}}{\partial y \partial z} \qquad 3.10$$

$$\frac{\partial^2 \varepsilon_{zz}}{\partial x^2} + \frac{\partial^2 \varepsilon_{xx}}{\partial z^2} = \frac{\partial^2 \gamma_{zx}}{\partial z \partial x} \qquad 3.11$$

$$\frac{\partial}{\partial y}\left(\frac{\partial \gamma_{xy}}{\partial z} + \frac{\partial \gamma_{yz}}{\partial x} - \frac{\partial \gamma_{zx}}{\partial y}\right) = 2\frac{\partial^2 \varepsilon_{yy}}{\partial z \partial x} \qquad 3.12$$

$$\frac{\partial}{\partial z}\left(\frac{\partial \gamma_{yz}}{\partial x} + \frac{\partial \gamma_{zx}}{\partial y} - \frac{\partial \gamma_{xy}}{\partial z}\right) = 2\frac{\partial^2 \varepsilon_{zz}}{\partial x \partial y} \qquad 3.13$$

$$\frac{\partial}{\partial x}\left(\frac{\partial \gamma_{zx}}{\partial y} + \frac{\partial \gamma_{xy}}{\partial z} - \frac{\partial \gamma_{yz}}{\partial x}\right) = 2\frac{\partial^2 \varepsilon_{xx}}{\partial y \partial z} \qquad 3.14$$

However, for a plane stress situation the stresses σ_{xx}, σ_{yy} and τ_{xy} are by definition, functions of *x* and *y* only, therefore from Hooke's Law ε_{xx}, ε_{yy}, ε_{zz} and γ_{xy} are also functions of *x* and *y* only. Therefore the six compatibility equations reduce to

$$\frac{\partial^2 \varepsilon_{xx}}{\partial y^2} + \frac{\partial^2 \varepsilon_{yy}}{\partial x^2} = \frac{\partial^2 \gamma_{xy}}{\partial x \partial y} \qquad 3.15$$

$$\frac{\partial^2 \varepsilon_{zz}}{\partial x^2} = 0 \qquad 3.16$$

$$\frac{\partial^2 \varepsilon_{zz}}{\partial y^2} = 0 \qquad 3.17$$

$$\frac{\partial^2 \varepsilon_{zz}}{\partial x \partial y} = 0 \qquad 3.18$$

3.1.3 STRESSES[40, 41]

In general, the material within the element boundaries may be subjected to initial strains such as those due to temperature changes, shrinkage, crystal growth, and so on. If such strains are denoted by ε_0 then the stresses will be caused by the difference between the actual and initial strains.

In addition it is convenient to assume that at the outset of the analysis the body stressed by some known system of initial residual stresses σ_0 which, for instance, could be measured, but the prediction of which is impossible with out full

knowledge of the material's history. These stresses can simply be added on to the general definition. Thus, assuming linear elastic behaviour, the relationship between stresses and strains will be linear and of the form

$$\boldsymbol{\sigma} = \boldsymbol{D}(\varepsilon - \varepsilon_0) + \boldsymbol{\sigma_0} \qquad 3.19$$

Where ***D*** is the *elasticity matrix of moduli* - defined for isotropic materials in terms of the standard six stress and strain terms, using *Young's modulus of elasticity* and *Poisson's ratio* as the elastic constants. For plane stress three components of stress corresponding to the strains already defined have to be considered, using familiar notation

$$\boldsymbol{\sigma} = \begin{bmatrix} \sigma_{xx} \\ \sigma_{yy} \\ \tau_{xy} \end{bmatrix} \qquad 3.20$$

For an Isotropic material, the ***D*** matrix is obtained from the usual stress-strain relationships

$$\varepsilon_{xx} - \varepsilon_{xx\,0} = \frac{1}{E}(\sigma_{xx} - \sigma_{xx\,0}) - \frac{\nu}{E}(\sigma_{yy} - \sigma_{yy\,0}) \qquad 3.21$$

$$\varepsilon_{yy} - \varepsilon_{yy\,0} = -\frac{\nu}{E}(\sigma_{xx} - \sigma_{xx\,0}) + \frac{1}{E}(\sigma_{yy} - \sigma_{yy\,0}) \qquad 3.22$$

$$\gamma_{xy} - \gamma_{xy\,0} = \frac{2(1+\nu)}{E}(\tau_{xy} - \tau_{xy\,0}) \qquad 3.23$$

On solving

$$\boldsymbol{D} = \frac{E}{1-\nu^2}\begin{bmatrix} 1 & \nu & 0 \\ \nu & 1 & 0 \\ 0 & 0 & \dfrac{(1-\nu)}{2} \end{bmatrix} \qquad 3.24$$

Thus the relationship between stress and strain

$$\begin{bmatrix} \sigma_{xx} \\ \sigma_{yy} \\ \sigma_{xy} \end{bmatrix} = \boldsymbol{D}\begin{bmatrix} \varepsilon_{xx} \\ \varepsilon_{yy} \\ \gamma_{xy} \end{bmatrix} \qquad 3.25$$

3.1.3.1 Equilibrium Equations[40]

Consider the equilibrium of a small rectangle, set in the body, with sides in the direction of the axes. The stresses experienced by the interior of the rectangle are shown in *Figure 3.1*, where allowance has been made for the changes in stress arising from different positions. In addition, we assume that the body is under the action of a distributed force per unit volume, ***b***, with components b_x and b_y.

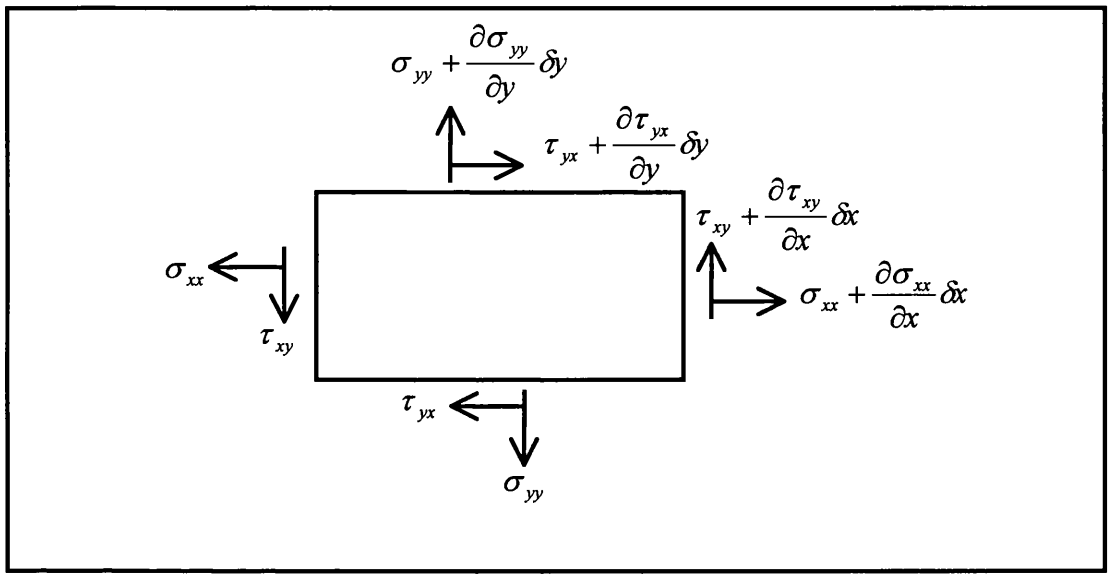

Figure 3.1 Stresses on the Sides of a Small Rectangle

Resolving the forces in the x and y directions gives

$$\left[\frac{\partial \sigma_{xx}}{\partial x}\delta x\right]t\delta y + \left[\frac{\partial \tau_{yx}}{\partial y}\delta y\right]t\delta x + tb_x\delta x\delta y = 0 \qquad 3.26$$

$$\left[\frac{\partial \sigma_{yy}}{\partial y}\delta y\right]t\delta x + \left[\frac{\partial \tau_{xy}}{\partial x}\delta x\right]t\delta y + tb_y\delta x\delta y = 0 \qquad 3.27$$

(t = thickness)

And taking moments about centre

$$\left[\tau_{xy}t\delta y\right]\delta x + \left[\frac{\partial \tau_{xy}}{\partial x}\delta x\right](t\delta y)\frac{\delta x}{2} = \left[\tau_{yx}t\delta x\right]\delta y + \left[\frac{\partial \tau_{yx}}{\partial y}\delta y\right](t\delta x)\frac{\delta y}{2} \qquad 3.28$$

i.e.

$$\tau_{xy} + \frac{1}{2}\frac{\partial \tau_{xy}}{\partial x}\delta x = \tau_{yx} + \frac{1}{2}\frac{\partial \tau_{yx}}{\partial y}\delta y \qquad 3.29$$

Letting $\delta x, \delta y \to 0$ the two shearing stresses τ_{xy} and τ_{yx} are seen to be equal; then *(3.26)* and *(3.27)* become

$$\frac{\partial \sigma_{xx}}{\partial x} + \frac{\partial \tau_{xy}}{\partial y} + b_x = 0 \qquad 3.30$$

$$\frac{\partial \sigma_{yy}}{\partial y} + \frac{\partial \tau_{xy}}{\partial x} + b_y = 0 \qquad 3.31$$

In matrix form

$$\begin{bmatrix} \frac{\partial}{\partial x} & 0 & \frac{\partial}{\partial y} \\ 0 & \frac{\partial}{\partial y} & \frac{\partial}{\partial x} \end{bmatrix} \begin{bmatrix} \sigma_{xx} \\ \sigma_{yy} \\ \tau_{xy} \end{bmatrix} + \begin{bmatrix} b_x \\ b_y \end{bmatrix} = 0 \qquad 3.32$$

Or

$$\boldsymbol{S^T \sigma + b = 0} \qquad 3.33$$

3.1.4 STRESS FUNCTION FORMULATION OF PLANE ELASTIC PROBLEMS[39]

The problem of plane stress can be formulated in terms of a single function called the stress function ϕ, whose appropriate derivates define the stresses $(\sigma_{xx}, \sigma_{yy}, \tau_{xy})$.

To this end the following procedure is adopted

- The compatibility condition is obtained in terms of stress components by substituting the stress-strain relations in the strain compatibility equation. This yields the stress compatibility equation.

- The stress compatibility equation together with the two stress equations of equilibrium will provide three expressions for the three unknown stress components.

- A function in terms of the stress components satisfying the three stress expressions together with the boundary conditions has to be found.

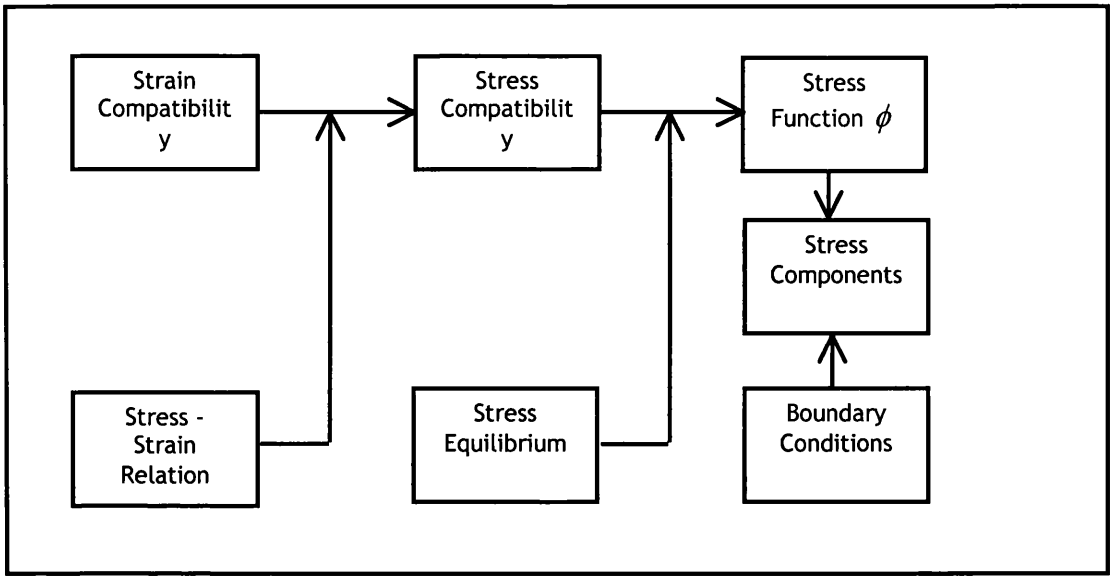

Figure 3.2 Stress Function Formulations of Plane Elastic Problems

3.2 PLASTICITY

Introduction

The mathematical description of plasticity is considerably more complicated than that of the elasticity because when a material is yielding due to plastic strain the relationship between the stress and the strain is now not going to be linear.

The equation used to determine most computational FEA analysis yielding problems is the yield criterion according to von Mises. Therefore the primary output research identifier for CAPL stress state investigations is the "yield stress" or more precisely the "proof stress" due to the difficulty of attaining an exact yield stress value at operating furnace temperatures in excess of 750°C. The proof stress ($\sigma_{0.2}$) with reference to the CAPL computational models incorporates a degree of the strain rate-hardening exponent that may be present in temperatures in excess of 750°C. This use of the proof stress is a common practice with all the CAPL operators that perform this type of high temperature computational investigation. It must be remembered that the research focus is on strip transportation and not strip deformation - therefore the use of a proof stress to represent the yield stress enables the author to use an ABAQUS *"Classic Elastic-Perfect Plasticity Model"*. Furthermore, at high temperatures (above 0.5_{TM}) self-relieving helps to reduce the affects of strain rate hardening. Self-relieving refers to the release of internal stresses within the strip. The internal stresses are released as the strip recrystallises within the soaking section of the furnace.

3.2.1 THE YIELD CRITERION

The measurement of yield is through the yield criterion. There are five key concepts that form the basis of almost all classical theories of plasticity, and they are

- The decomposition of strain into elastic and plastic parts.
- Yield criteria: The prediction on whether the solid responds elastically or plastically.
- Strain hardening rules, which control the way in which resistance to plastic flow increases with plastic straining.
- The plastic flow rule, which determines the relationship between stress and plastic strain under multi-axial loading.
- The elastic unloading criterion, which models the irreversible behaviour of the solid.

The most common method of measuring how ductile materials will behave at the elastic to plastic point is by the use of a yield criterion, these have an empirical relationship - the two generally accepted theories are the maximum-shear-stress theory called "Tresca" and then there is the shear-strain energy (maximum distortion energy) "von Mises" yield criterion. While both forms of the yield criterion are relevant, the von Mises is more established for metal-forming scenarios and states the predicted yield stress, whereas Tresca visualises the maximum shear stress. This makes Tresca less relevant for CAPL research projects, as the author wants to reference when the elastic behaviour within a localised area of the strip will come to an end due to operational permutations - something that a computational von Mises equivalent stress output clearly shows.

3.2.1.1 Yield Criterion According to von Mises[2, 42]

The total strain energy within an element of material consists of energy stored due to change in volume without shape change, in addition to energy stored due to a change in shape without volume change; the latter being distortion or shear. It was proposed that a change in shape could be the only energy component which

causes failure (since materials usually fail due to shear mechanisms) and this could provide a viable criterion for complex yield conditions.

In order to show that the deformation of a material can be separated into change in volume and change in shape consider the element shown below in *Figure 3.3* subject to principal stresses σ_1, σ_2 and σ_3 only (neglecting shear-stress).

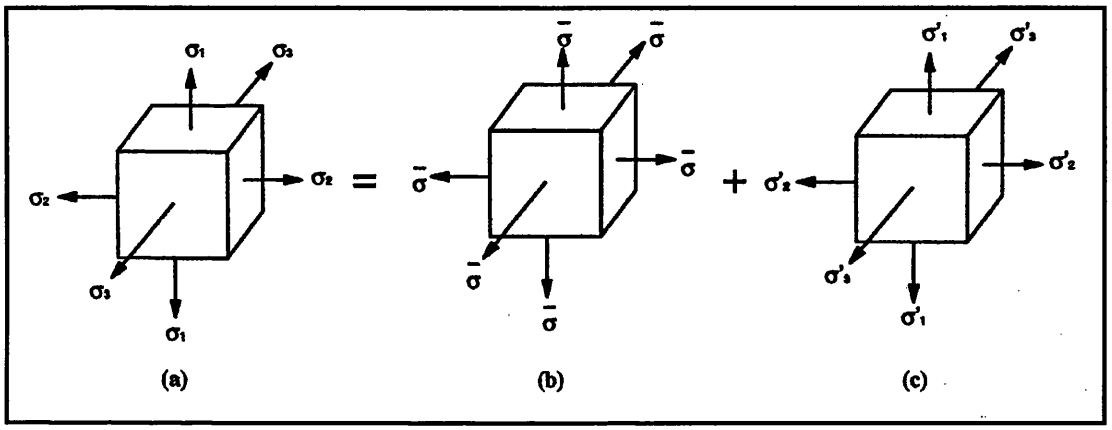

Figure 3.3 The Total Stress at a Point (a) is the Sum of the Hydrostatic (b) and the Deviatoric Stresses (c)[2]

The principal stresses may be written in terms of average stresses

$$\sigma_1 = \bar{\sigma} + \sigma'_1 \qquad 3.34$$

$$\sigma_2 = \bar{\sigma} + \sigma'_2 \qquad 3.35$$

$$\sigma_3 = \bar{\sigma} + \sigma'_3 \qquad 3.36$$

Where

$$\bar{\sigma} = \frac{\sigma_1 + \sigma_2 + \sigma_3}{3} \qquad 3.37$$

Is the hydrostatic, average, or mean stress component with σ'_n representing the deviatoric stresses in the n*th* plane. The total stress on an element is the sum of the hydrostatic and deviatoric components projected on the deviatoric plane.

While summarising *(3.34-3.36)* gives

$$\sigma_1 + \sigma_2 + \sigma_3 = 3\bar{\sigma} + \sigma'_1 + \sigma'_2 + \sigma'_3 \qquad 3.38$$

Hence using *(3.37)*

$$\sigma'_1+\sigma'_2+\sigma'_3=0 \qquad 3.39$$

It can also be shown that from Hooke's generalised equations for stress-strain relationships that

$$\varepsilon_1^{'}+\varepsilon_2^{'}+\varepsilon_3^{'}=e^{'}=\frac{(1-2\nu)}{E}\left(\sigma_1^{'}+\sigma_2^{'}+\sigma_3^{'}\right) \qquad 3.40$$

The sum of three stresses is zero, from equation *(3.39)*, thus

$$\varepsilon'_1+\varepsilon'_2+\varepsilon'_3=e'=0 \qquad 3.41$$

Inspection of *(3.41)* reveals that the deviatoric stress components cause no change in volume but only a change in shape, thus causing potential failure.

Determination of an element's strain energy is obtained by considering the total strain energy

$$\boldsymbol{U_T=U_V+U_S} \qquad 3.42$$

Where $\boldsymbol{U_T}$ is the total strain energy, $\boldsymbol{U_V}$ the volumetric strain energy and $\boldsymbol{U_S}$ the shear or distortion-strain energy. The total strain energy per unit volume is given by the sums of the energy components due to the three principal stresses and principal strains so that

$$\boldsymbol{U_T}=\frac{1}{2}\sigma_1\varepsilon_1+\frac{1}{2}\sigma_2\varepsilon_2+\frac{1}{2}\sigma_3\varepsilon_3 \qquad 3.43$$

The volumetric strain energy can be determined from the hydrostatic component of stress $\bar{\sigma}$

$$\boldsymbol{U_V}=\frac{1}{2}\bar{\sigma}e \qquad 3.44$$

However, $\boldsymbol{U_S=U_T-U_V}$; but before this can be realised *(3.43)* and *(3.44)* are shortened by substituting the principal strains from the stress-strain relationships for $\boldsymbol{U_T}$, and the mean stress from *(3.37)* for $\boldsymbol{U_V}$.

Once that equation has been re-arranged and reduced it finally becomes

$$U_S = \frac{1+\nu}{6E}\left[(\sigma_1 - \sigma_2)^2 + (\sigma_2 - \sigma_3)^2 + (\sigma_3 - \sigma_1)^2\right] \qquad 3.45$$

Finally using the relationship between *E*, *G* and ν for *(3.45)*; U_S becomes

$$U_S = \frac{1}{12G}\left[(\sigma_1 - \sigma_2)^2 + (\sigma_2 - \sigma_3)^2 + (\sigma_3 - \sigma_1)^2\right] = \frac{\sigma_Y^2}{6G} \qquad 3.46$$

or

$$(\sigma_1 - \sigma_2)^2 + (\sigma_2 - \sigma_3)^2 + (\sigma_3 - \sigma_1)^2 = 2\sigma_Y^2 \qquad 3.47$$

For a two-dimensional stress system where $\sigma_3 = 0$

$$\sigma^2_1 + \sigma^2_2 - \sigma_1.\sigma_2 = \sigma_Y^2 \qquad 3.48$$

for yielding to occur.

Equations *(3.47)* and *(3.48)* mathematically describe the von Mises yield criterion in a complex two or three dimensional load system. This criteria states that for yielding to occur the principal stresses must reach a pre-determined value (the yield stress).

Plotting for a two dimensional stress state on axes σ_1/σ_2 and σ_2/σ_Y produces the graph in *Figure 3.4* which shows an ellipse concentrated at 45° to σ_1 and σ_2. The surface of the ellipse represents the transition between elastic and plastic stresses, the elastic stresses are bound inside the ellipse while the surface represents yield, hence the term *yield surface*.

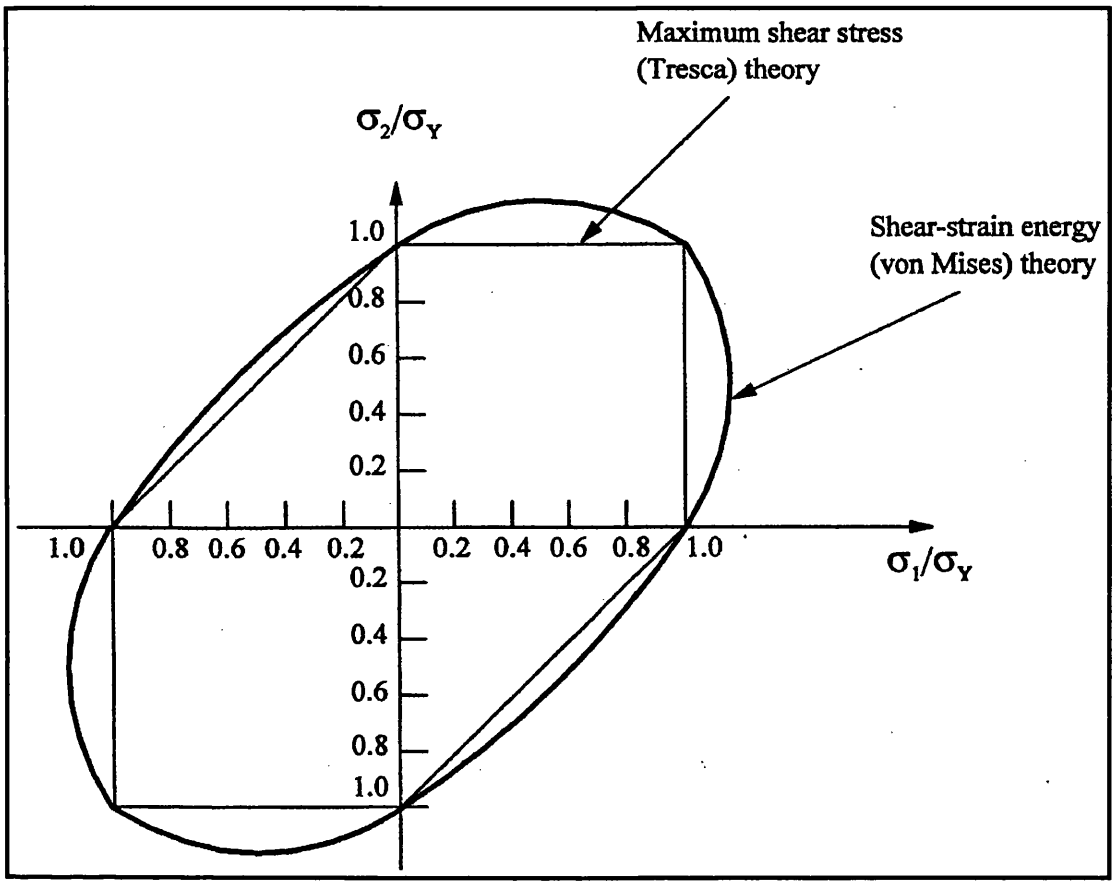

Figure 3.4 Yield Criterion Ellipses (Two Dimensional Case)

Remark - Most computational FEA simulations show their stress model results expressed in terms of the von Mises equivalent stress, as it is a simple method for showing the onset of yield. However, in the case where the yield characteristics are pre-defined such as in this CAPL research project, ABAQUS highlights up to and including the pre-defined yield stress. However, the principal stress values can be greater than the actual yield stress in a single-plane, such as σ_{xx}.

3.3 FRICTIONAL SLIDING

Clearly the CAPL could suffer from frictional sliding. Any inadequacies in the hard contact between the two moving mating surfaces could lead to potential failure in strip quality. The constitutive equation, which defines friction, was developed by Coulomb - adopting an idea of a coefficient of frictional sliding. Coulomb developed the theory that friction (μ) was due to surface roughness and adhesion. The coefficient of friction is determined from the following equation

$$\mu = \frac{F}{P} = \frac{\tau}{p} \qquad 3.49^{[42]}$$

F	force required to move the body
P	normal force
τ	frictional shear stress
p	normal pressure

The Coulomb friction model defines the critical shear stress, τ_{crit} at which sliding of the surface starts ($\tau_{crit} = \mu p$). The standard or constant friction value used for the forthcoming contact models is 0.3 (μ) - this value is used for CAPL computational frictional research models worldwide[24, 27, 29, 43, 44].

The shear stress (τ) is the stress state that is parallel or tangential to the face of the material, and is perhaps the key parameter in frictional sliding.

The frictional coefficient has to be sufficient to maintain uniform contact across the strips surface. In Chapter 7 variations to the frictional coefficient are examined to test the theory on whether 0.3 should be considered a constant.

3.4 CLOSING REMARKS OF ELASTICITY & PLASTICITY

The CAPL presents the author with an elastic problem; or more precisely a yield point problem. It is important to point out straight away that while CAPL research teams world-wide are not generally concerned with the intricacies of plastic yield behaviour, as this tends to make the final product redundant; the researchers are, however, interested in the start of the yield behaviour. At temperatures in excess of 750°C, the material does not clearly show a yield point, this is an important issue; however, it is complicated by two differing factors. The first is that tensile testing at elevated temperatures, where the material may show signs of superplasticity has historically taken many hours to complete due to the constantly applied low strain-rate associated with high temperature tensile testing. The second issue is on the CAPL: the strip is heated, annealed and cooled in a matter of minutes. Therefore, the correlation or association between hot tensile testing and the annealing procedure have always been open to a small degree of conjecture. Thus historically, tensile testing has been used to define a yield point by the use of small 0.2% extension of the original length, which is of

course, universally known as the proof stress. This extension allows for a small but conservative amount of plastic strain to be included into defining the strips yield point, this yield stress can then be "inputted" into an elastic perfectly-plastic computational model. The elastic outputs are the principal stresses and principal logarithmic strains. Similarly the plastic outputs are principally defined by the von Mises equivalent stress, von Mises highlights accumulative elastic behaviour of an element up to and including the defined yield stress or a series of yield stress values if a plastic strain component is included.

It is considered that the roll knuckle contact point is perhaps the most likely starting place for strip deformation to occur according to preliminary computational research.

4 FINITE ELEMENT AND COMMERCIAL COMPUTATION

Introduction

The research project's emphasis is on hard contact between the transport roll and the strip steel. Research of this type has historically been performed by either physical experimentation such as with a CAPL simulator or by the use of the finite element method (FEM).

The most complete method for analysing this relationship and thus gaining a greater appreciation of the unique problems that Corus face now and in the future is by the development of a simplified roll-strip model using a commonly accepted commercial finite element program[2].

4.1 THE FINITE ELEMENT METHOD (FEM)

Introduction

Despite the complex mathematical structure, which has developed around the Finite Element Method, the basic approach can be summarised briefly. Originally proposed separately by Clough, Argyris and Zienkiewicz, the approach starts by discretising the structure in question into a set of small sections, or elements, and these elements are connected at nodes on the element boundaries. Within each element the displacement is assumed to have a known functional dependence on the displacements at the nodes, this functional form being the "Shape Function" of the particular element type. The process then expresses the strain energy of the structure by integrating throughout each element in turn (using either full or reduced integration), followed by a summation over all the elements in the structure. An expression for strain energy is obtained (in terms of nodal displacements) in this way; equilibrium equations are then readily obtained by differentiation. In practice, most of this process is enshrined in the code and the user's main responsibility is in the choice of an appropriate mesh and element type. There is a vast choice of elements in one, two or three dimensions[41, 45, 46].

For a static analysis, the equation of nodal displacement is:

$$[k]\{u\} = \{P\} \qquad 4.1$$

The vector of applied nodal force P is the resultant of the stiffness matrix k and the nodal displacements u[41], which are unknown. The stiffness matrix is the

assembly of two or more elements. In order to find displacements from a given force, *(4.1)* must be inverted to find $\{u\}$, with the solution depending on the initial boundary conditions.

For a dynamic analysis inertia affects are considered, see Section 4.2.2.1 titled "The Central Difference Rule" for details.

4.1.1 THE DISPLACEMENT FUNCTION[41]

In the case of plane stress displacements, ***u*** represents horizontal and vertical movement of a typical point within the element.

$$\boldsymbol{u} = \begin{Bmatrix} u(x,y) \\ v(x,y) \end{Bmatrix} \qquad 4.2$$

The displacement function ***u*** at any point within an element can be approximated as a column vector $\hat{\boldsymbol{u}}$

$$\boldsymbol{u} \approx \hat{\boldsymbol{u}} = \sum_a N_a \tilde{\boldsymbol{u}}_a^e \qquad 4.3$$

Where $\tilde{\boldsymbol{u}}_a = \begin{Bmatrix} \tilde{u}_a \\ \tilde{v}_a \end{Bmatrix}$ 4.4

$\tilde{\boldsymbol{u}}_a$ is the corresponding displacements of a node *a*.

The shape function is defined by (N_a), and must be chosen to give appropriate nodal displacements when coordinates of corresponding nodes are inserted into *(4.3)*.

4.1.2 THE RECTANGULAR ELEMENT[41]

The CAPL computational FEM model uses rectangular shell elements. The rectangular element has side lengths *a* and *b* in the *x* and *y* directions respectively.

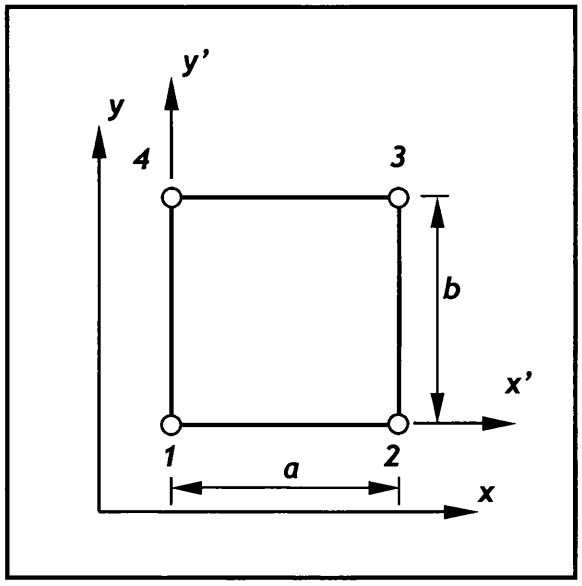

Figure 4.1 Rectangular Element Geometry and Local Node Numbers[41]

The derivation of the shape functions in the Cartesian system is defined by

$$x' = x - x_1$$
$$y' = y - y_1 \qquad 4.5$$

4.2 THE COMMERCIAL COMPUTATIONAL CODE

Introduction

A commercial code was selected as the computational analysis tool. The decision was to use the ABAQUS code developed by Hibbitt, Karlsson and Sorensen (HKS). ABAQUS is widely considered as one of the market leaders in computational finite element analysis (FEA) packages. The decision on which package to utilise was significantly aided by the fact that ABAQUS is the standard commercial FEA computational package that is used throughout Corus RD&T, thus utilising Corus RD&T's existing expertise was a strong consideration[24, 27, 29, 43, 44].

The final version of the finite element analysis package used for this research project was ABAQUS CAE 6.4. The two numerical solution schemes are ABAQUS Standard, used for general-purpose analysis. Standard solves a wide range of linear and non-linear problems, involving the static, dynamic, thermal and electrical response of components. ABAQUS Explicit is used for short, transient dynamic events, such as impact and blast problems. It is a more effective analysis

for highly non-linear problems involving changing contact conditions, such as forming simulations[2].

Numerical solution schemes are often referred to as explicit or implicit. When a direct computation of the dependent variables can be made in terms of known quantities, the computation is *explicit*. In contrast, when the dependent variables are defined by coupled sets of equations, and either a matrix or iterative technique is needed to obtain the solution, the numerical method is *implicit*.

Explicit methods calculate the state of a system at a later time from the state of the system at the current time, while an implicit method finds it by solving an equation involving both the current state of the system and the later one. That said; whether the author should use an explicit or implicit time step method depends upon the nature of the computational problem that is to be solved.

A more detailed explanation is given by the following - "iterations are used to advance a solution through a sequence of steps from a starting state to a final, converged state. This is true whether the solution sought is either one step in a transient problem or a final steady state result. In either case, the iteration steps resemble a time-like process. Of course, the iteration steps usually do not correspond to a realistic time-dependent behaviour. In fact, it is this aspect of an implicit method that makes it attractive for steady state computations, because the number of iterations required for a solution is often much smaller than the number of time steps needed for an accurate transient that asymptotically approaches steady conditions"[47].

However, the principal reason for using implicit numerical solution methods, which are more complex to program and require more computational effort in each solution step, is to allow for large time-steps. A further and some would say more important benefit of the implicit time-step iteration is that the user can directly control the iteration size. The ability to be able to fix an iteration size is crucial for those research cases where an in-model analysis solution is required time after time. Time steps are automatically calculated in the explicit formulation and are therefore often very small and not consistent in time period - i.e. from one iteration to the next.

4.2.1 ABAQUS STANDARD (IMPLICIT)[48, 49]

Provides both linear and non-linear response options. In non-linear problems the objective is to obtain a convergent solution at a minimum cost. Two approaches can be used: direct user control of the incrementation or automatic control, which is more efficient. This type of control is used when time or load increment varies through the step.

ABAQUS Standard determines whether convergence is likely in a reasonable number of iterations. If convergence is deemed unlikely, ABAQUS Standard adjusts the load increment; if convergence is deemed likely, ABAQUS Standard continues with the iteration process. In this way excessive iteration is eliminated in cases where convergence is unlikely, and an increment that appears to be converging is not aborted because it needed a few more iterations. One other ingredient in this algorithm is that a minimum increment size is specified, which prevents excessive computation in cases where buckling, limit load, or some modelling error causes the solution to stall. This control is handled internally, with user override if needed. Several other controls are built into the algorithm; for example, it will cut back the increment size if an element inverts due to excessively large geometry changes.

ABAQUS STANDARD

1. Chapter 5 - Coupled Heat Transfer Analysis
2. Chapter 7 - Static General (Static Roll-Strip Contact)
3. Chapter 7 - Uncoupled Heat Transfer Analysis

4.2.1.1 Uncoupled and Coupled Heat Transfer Analyses[48, 49]

The ABAQUS Standard capability for uncoupled heat transfer analysis is intended to model solid body heat conduction with general, temperature-dependent conductivity; internal energy (including latent heat effects); and quite general convection and radiation boundary conditions. It is assumed that the thermal and mechanical problems are uncoupled in the sense that the heat flux does not depend on the strains or displacements of the body.

The operators are conditionally stable for linear transient heat transfer problems (i.e. CAPL heat transfer model). It is preferred to work with unconditionally stable methods, because ABAQUS is most commonly applied to problems where the

solution is sought over very long time periods. The Euler backward difference method is the preferred operator over the central difference method, which generally provides for greater accuracy but suffers from oscillations in the early time solution.

A fully-coupled thermal-stress analysis is needed when the stress analysis is dependant on the temperature distribution and the temperature distribution depends on the stress solution.

4.2.2 ABAQUS EXPLICIT[49, 50]

The ABAQUS Explicit code formulated to provide a non-linear, transient, dynamic analysis of solids and structures using explicit time integration. Is a general-purpose analysis module that uses an explicit dynamic finite element formulation. The program is suitable for modelling brief, transient dynamic events such as impact and blast problems, and is also very efficient for non-linear problems involving changing contact conditions, such as forming simulations.

ABAQUS EXPLICIT

1. Chapter 7 - Dynamic Explicit (Dynamic Roll-Strip Contact)

4.2.2.1 The Central Difference Rule[51]

ABAQUS Explicit uses a central difference rule to integrate the equations of motion explicitly through time, using the kinematic conditions at one increment to calculate the kinematic conditions at the next increment. At the beginning of the increment the program solves for dynamic equilibrium, which states that the nodal mass matrix, (M), times the nodal accelerations, $(\ddot{u})$, equals the total nodal forces - the difference between the external applied forces, (P), and internal element forces, (I)

$$M\ \ddot{u} = P - I \qquad 4.6$$

The accelerations at the beginning of the current increment (time t) are calculated as (dynamic equilibrium)

$$\ddot{u}\,|_{(t)} = (M)^{-1}.(P - I)\,|_{(t)} \qquad 4.7$$

The accelerations are integrated through time using the central difference rule, which calculates the change in velocity assuming that the acceleration is constant.

This change in velocity is added to the velocity from the middle of the previous increment to determine the velocities at the middle of the current increment (integrate explicitly through time)

$$\dot{\boldsymbol{u}}\,|_{\left(t+\frac{\Delta t}{2}\right)} = \dot{\boldsymbol{u}}\,|_{\left(t-\frac{\Delta t}{2}\right)} + \frac{\left(\Delta t\,|_{(t+\Delta t)} + \Delta t\,|_{(t)}\right)}{2}\ \ddot{\boldsymbol{u}}\,|_{(t)} \qquad 4.8$$

The velocities are integrated through time and added to the displacements at the beginning of the increment to determine the displacements at the end of the increment

$$\boldsymbol{u}\,|_{(t+\Delta t)} = \boldsymbol{u}\,|_{(t)} + \Delta t\,|_{(t+\Delta t)}\ \dot{\boldsymbol{u}}\,|_{\left(t+\frac{\Delta t}{2}\right)} \qquad 4.9$$

"Thus, satisfying dynamic equilibrium at the beginning of the increment provides the accelerations. Knowing the accelerations, the velocities and displacements are advanced "explicitly" through time. The term "explicit" refers to the fact that the state at the end of the increment is based solely on the displacements, velocities, and accelerations at the beginning of the increment. This method integrates constant accelerations exactly. For the method to produce accurate results, the time increments must be quite small so that the accelerations are nearly constant during an increment. Since the time increments must be small, analyses typically require many thousands of increments. Fortunately, each increment is inexpensive because there are no simultaneous equations to solve. Most of the computational expense lies in the element calculations to determine the internal forces of the elements acting on the nodes. The element calculations include determining element strains and applying material constitutive relationships (the element stiffness) to determine element stresses and, consequently, internal forces" [51].

Thus a summary of the explicit dynamics algorithm.

1. Nodal Calculations.
   - Dynamic equilibrium.
   - Integrate explicitly through time
2. Element calculations.
   - Compute element strain increments, from the strain rate.
   - Compute stresses, from constitutive equations.
   - Assembly nodal internal forces
3. Set $t + \Delta t$ and return to Step 1.

4.3 THE CLOSING REMARKS OF FINITE ELEMENT AND COMMERCIAL COMPUTATION

The finite element method's advantages are well documented and accepted. The use of a commercially available computational finite element analysis has also been historically an accepted practice. Both Corus RD&T and world-renowned research organisers have used computational FEM to consider the problems associated with hard contact between CAPL transport rolls and the annealing strip with great success.

The commercial code supplied by ABAQUS was used to help validate the Stein Heurtey experimental programme. A fully-coupled temperature-stress analysis was used to help validate the temperature differential experiments (see Chapter 5). For CAPL contact simulations a multitude of analyses' types was employed. Steady state implicit stress analysis was used for the static models.

5 THE STEIN HEURTEY EXPERIMENTAL PROGRAMME

Opening Remarks

The contact interaction between the strip and transport roll is not for the purpose of strip deformation within the CAPL; however, due to the operational realities of the recovery environment inside the furnace a great deal of deformation can take place inadvertently, a concern, which affects the soaking furnace onwards. The strip quality, which is ultimately affected, is not just the reasonability of operators such as Corus but also is the responsibility of the technology suppliers such as Stein Heurtey.

Stein Heurtey as the principal originator of the research project wanted to have an input into experimental aspect. The best way for them to do this was with the use of their Pilot Test Facility, which acted as a representation of the continuous annealing line. The CAL line that they have at Bar-Le-Duc enables the strip steel to be heated and cooled, and it can also be moved via a transport roll at either end of the pilot line. However, unlike a full-scale CAPL where the strip is kept in a completely homogenous environment the Pilot Test Facility does not have an encasing "Furnace Section". The research into roll-strip interactions is considered a far more commercially beneficial research project, than that of a materials science based research project.

In the beginning, the experimental programmes emphasis was on researching the link between a sudden developing temperature differential between the heat sink and the strip, and then how did this exactly affect strip quality (i.e. This causes the strip to go beyond its elastic limit). Thus, the experimental emphasis would be on how a sudden change in temperature to a small localised area of the strips surface would affect the stress characteristics in the ultra thin strip steel. It has to be noted that the purpose of this experimental work was not to see if the CAPL could be accurately replicated. The issue of representation is a problem; the experimental purpose has to come down to studying how an intermittent temperature differential would behave. Historical studies[29, 32] into strip processing have led the author to understand one important factor about intermittent contact. When the strip is being recovered at a high annealing temperature and at the extreme of the operational load of the steel, the strip's mechanical properties tend to operate close to their yield point; so any non-homogenous cross-sectional temperatures can be a catalyst for strip plasticity.

The aim - to measure the stress and temperature values by the use of strain gauges and thermocouples.

The objective - to increase the overall understanding and knowledge of the localised strip temperature differentials and their effect on strip quality.

The experimental tests where executed at the Stein Heurtey site at Bar-Le-Duc with the author in attendance for these final experiments. The computational FEA simulations were finalised at Corus and Swansea University by the author

5.1 THE STEIN HEURTEY PILOT LINE AT BAR-LE-DUC

The line replicates the three primarily operational aspects of the CAPL, that of a heat and cool zone and a varying line load (tension). The pilot facility is designed to be modular in construction and therefore can be easily altered to consider different research topics; there is also a measuring ability present. The strip is welded laterally to form a continuous band around a pair of rolls at either end of the pilot line.

The original pilot facility set-up is shown in *Figure 5.1*. In this photograph it shows the heating zone in the background with the cooling blow box in the foreground. A roll at the other end of the facility, which is out-of-sight, provides line tension this moves on a rail to exert a load on the strip. An unfortunate complication is the un-natural positioning of the strip in the horizontal position, which means the strip could possibly deform under its own weight. After an initial visit the formulation of an experimental research plan began to develop, the author and Stein Heurtey proceeded to develop ideas on how to modify the pilot line so that a viable heat sink could be incorporated.

An experimental stress analysis relies on the use of strain gauges, these, however, have a finite operating range, which is further complicated if the strip happens to be ultra thin, larger measuring devices, generally used for high temperature analyses, can cause the strip to deform around the strain gauge location points.

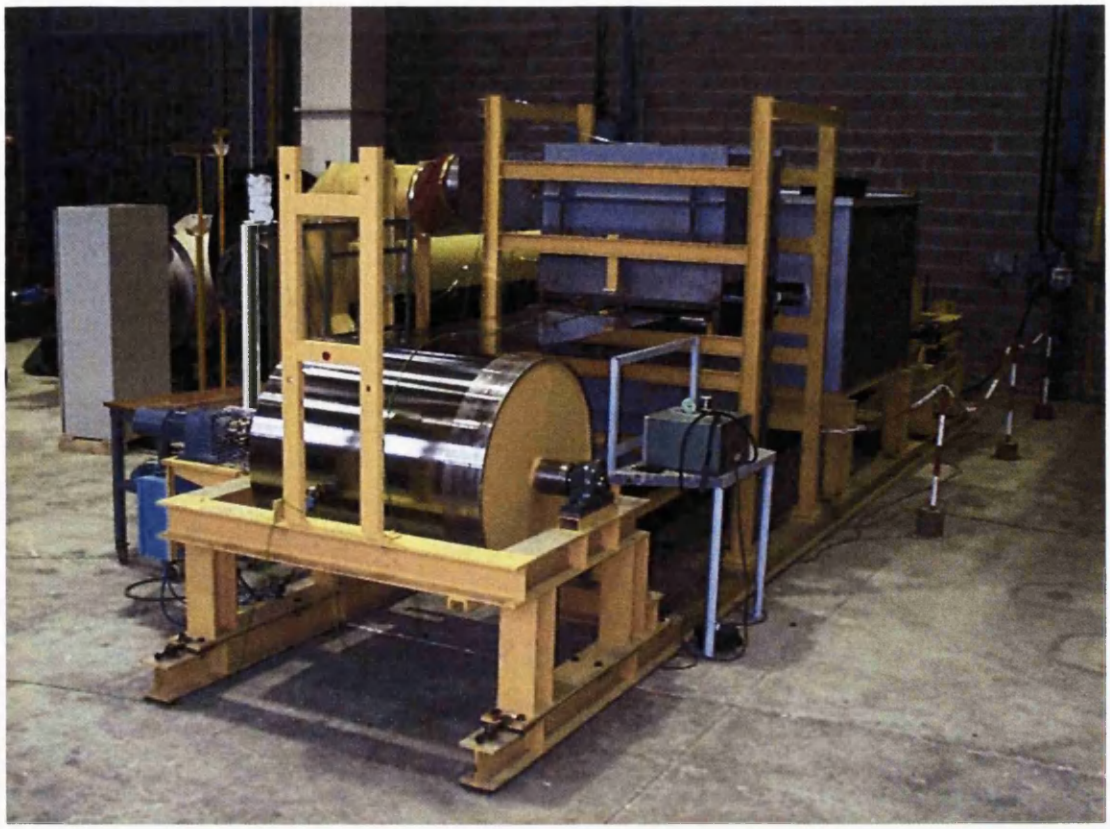

Figure 5.1 The Original Stein Heurtey CAPL Pilot Facility at Bar-Le-Duc, France

5.1.1 THE INITIAL EXPERIMENTAL FOCUS

Before the conclusive experimentation could take place the facilities were assessed. A pre-testing schedule was developed on a wide range of operational aspects to find the best set-up. In particular, testing was performed to research the optimal distance between the opposing support rolls. Roll distance is important when considering horizontal band length. If the span is too great the strip will sag at the roll distance centre point, likewise if the span is too short then the rolls will interfere with the experiment.

There are many operational concerns however; the issue of greatest concern is that of temperature. The extremities of the annealing temperature range create an extremely harsh working environment for even the most advanced measuring devices, which is further made more difficult by the ultra thin nature of the strip gauge. These areas of concern led to an extensive validation exercise being performed by Stein Heurtey, with constant input and discussion from the author. The validation exercise for the most efficient heat sink required the most

experimental effort, in particular maximising the contact conduction between the interfacing surfaces.

5.1.1.1 The Initial Heat Sink Analysis

Computational comparisons were developed to analyse the effects of a variety of conduction contact coefficient scenarios. Using computational models enabled the author to save considerable experimental testing time. The research, while simplistic at this stage, did enable the material and contact loads which created the conductivity values to be analysed in greater detail than by physical experimentation. Researching intrinsically accurate conductivities was virtually impossible to perform in a physical environment such as at the pilot facility set-up in Bar-Le-Duc.

It is known that perfect contact will mean perfect conductivity. The conductivity value of steel is approximately 67W/mK and the conductivity value of copper is approximately 400W/mK at room temperature. Therefore, even though the actual CAPL interaction is steel-steel contact, it was decided at an early stage by the author that copper for a heat sink material was definitely a viable alternative and therefore included in the initial computational research.

The use of a material with a high thermal conductivity for the heat sink enabled the author to identify clearly and precisely where intermittent contact was occurring. A copper heat sink will transfer heat far more efficiently away from the steel strip than a steel heat sink. However, experimentally, copper heat sinks significantly aid in reducing the affects of testing in the open - rapid conductivity nullifies the effects of any other forms of heat transfer.

Thermocouples and strain gauges can cause permanent deformation at annealing temperatures of 850°C. This deformation can be caused by just the weight of the measuring devices alone. Therefore, size was an issue; the market for small measuring devices that can operate at 850°C with any degree of intrinsic accuracy was non-existent.

Because the CAPL moves at such a fast speed, and at such a high temperature, the loss of contact can be both sudden and dramatic - internal stress within the strip can rise very quickly, even when there is only partial contact. Suddenly, there can

be plastic deformation in localised areas of the strip, as the surface stress goes beyond the elastic limit. There are a number of operational reasons for poor contact, with roll geometry among others being the most prevalent. The other parameter essential for conduction is load, which fundamentally determines the area of contact. So the initial research was to look at temperature differentials, which can cause of quality issues in the strip, however, as work progressed, it was shown that temperature differentials were not the worst cause of strip failure.

The temperature differential developed by contact of a CAPL transport roll on the strip substrate is best performed by using commercial finite element analysis (FEA) package such as ANSYS and ABAQUS. There are subtle differences between the programs; however, both have user-friendly visualisation interfaces. Both platforms were considered. However, after careful consideration it was agreed that the commercial ABAQUS program would be used by the author to perform a computational analysis of the experimental results.

(Note: The ABAQUS suite of programmes is supplied by Hibbitt Karlsson and Sorensen[52]).

5.1.1.2 Heating Furnace Exit Temperature Losses - Computational Results

The initial experimentation was to simulate some of the experimental work computationally to allow for a more developed experimental programme at the Bar-Le-Duc test site at a latter date. The first computational result can be seen in *Figure 5.2* below, which was looking at the temperature loss at the pilot facility furnace exit. This particular computational simulation did not include a heat sink, it focused on potential heat losses through natural convection as the strip moved out of the open ended heating furnace into the open air and then onto the point where the experiment would begin some distance from the exit of the furnace. The purpose of this computational run was to discount this form of heat transfer as any anything other than trivial.

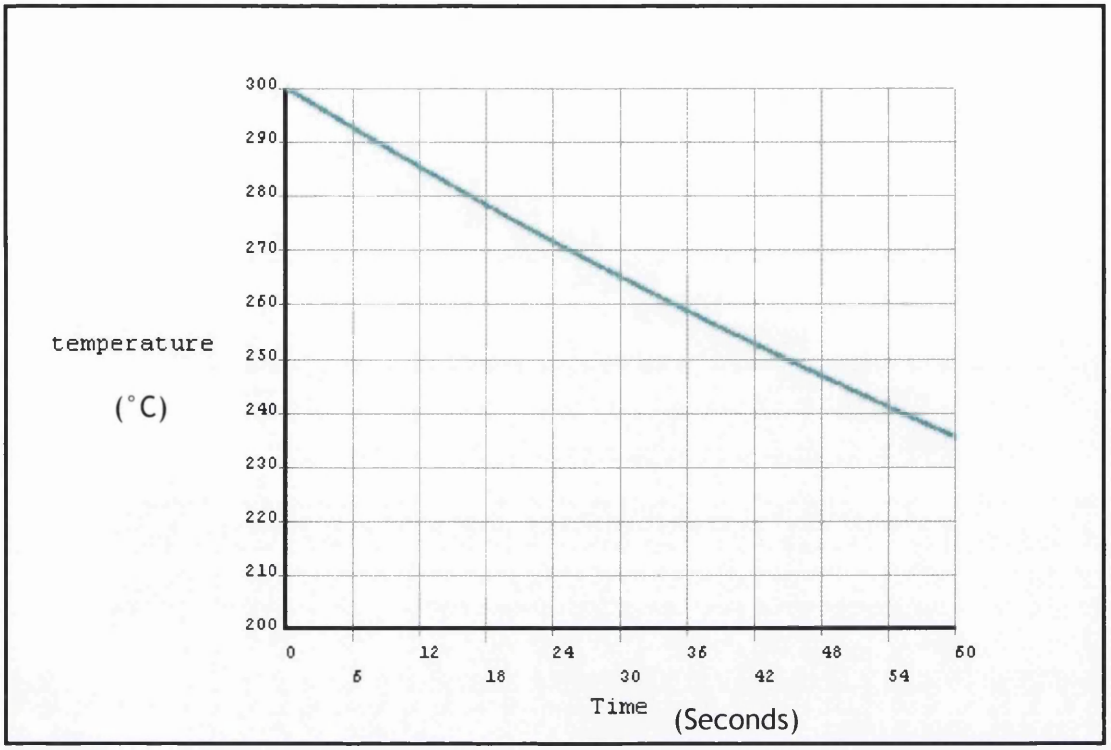

Figure 5.2 The Temperature Loss at Pilot Facility Furnace Exit

The above ANSYS figure (5.2), which was developed in unison with Stein Heurtey's engineers, highlights the importance of rapid strip movement from the furnace exit to the exact testing place over the heat sink.

Anything over seven seconds was likely to cause a heat loss (ΔT) of around 10°C. Seven seconds was thought as fast as the Bar-Le-Duc pilot facility testing team could manage to move the strip with the measuring devices from inside the furnace to the testing position over the heat sink, and then raise the heat sink into a contact position with the strips surface for results capture to begin. This computational experiment, while simple in nature, gave the author a greater understanding of the affects of rapid heat loss in the ultra thin strip due to natural convection. While natural convection could not be eliminated due to the limitations of the experimental facilities, it did allow the author to gain a better understanding of how to accurately vary the furnace temperature. In conclusion, exit temperature analyses gave the author the required temperature compensation for losses due to convection between the exit of the furnace and the point where contact conductance occurred.

Stein Heurtey's pilot facility has the ability to use blow boxes; these force air onto the strip surface for a rapid cooling effect. However, the author's experiments did not require rapid temperature loss through forced convection. Blow boxes have a detrimental effect on the strip temperature and the primary purpose of the author's experiments was the investigation of contact conductance.

5.1.1.3 The ANSYS Contact Model

Once the furnace exit temperature loss were considered, it was time to investigate the contact conductance. Stein Heurtey developed initial contact models in ANSYS. The model was a heat transfer only analysis. The expansion of the shell elements through thermal interaction was then transferred to an isothermal stress analysis. The shell element represented the strip and was ideal for ultra thin strip applications. The thickness or gauge was associated to the shell elements as a material property since shell elements were visualised in two dimensions (2D). A solid or continuum three-dimensional element would be more appropriate if the strip had a considerably larger gauge. However, solid element models required at the very minimum at least four elements in the thickness, thus, a realistic minimum continuum element size of 25mm x 25mm x 0.1mm made solid elements impractical when the strip had dimensions of 722mm x 5000mm (min) x 0.45mm. Furthermore, solid elements had no rotational degrees of freedom, which was essential for strip bending models. The heat sink was a continuum solid element, this was because the heat sink was fixed in position and required no transitional or rotational degrees of movement. Another brief advantage of shell elements was they represented a plane stress situation, which, was the case for all of the CAPL strip steel models.

5.1.1.4 Heat Sink and Material Selection

The first area of concern that required a computational model was the estimation of the thermal conductance, between the contact surfaces of the strip steel and the heat sink (which was representing the transport roll). The problem was that conductance was only ever an estimation, if the contact were perfect then the conductivity between the surfaces would also be perfect. However, in reality the contact and therefore the conductance was never perfect, but was influenced by the materials thermal properties which in itself was highly dependent on the cross-sectional area.

The average value of conductance for a contact of steel (strip) to steel (heat sink) with a low cross sectional pressure being applied was roughly 1000W/m^{2}K[53]. The average value of conductance for a contact of steel (strip) to copper (heat sink) with a low cross-sectional pressure being applied was roughly equal to h_c = 10000W/m^{2}K. The reason for this possible change in heat sink material is that the contact between the strip and a single transport roll pass is as little as 0.1 seconds when the strip is travelling at 600m/s on the actual CAPL, therefore the time for conductance on a single transport roll pass may be very low, even though the accumulated conductance of all the CAPL roll passes is not. However, the experimental procedure for the pilot facility test was only a representation of the CAPL, and was at best considered a single roll pass. The contact time for the physical experiment had to be longer than occurred on the actual CAPL for a single pass, because, the experimental temperature was severely reduced due to the limitations of the pilot facility - the following FEA simulations considered the problem of a series of heat sink materials and conductance conditions at a reduced experimental testing temperature.

The purpose of analysing different contact conditions through FEA was to achieve the best possible experimental set-up for the physical result gathering stage. FEA analyses of different contact conditions not only saved time and expenditure; it gave the author a realistic chance of having the best possible set-up for a successful experimental programme. With that in mind a simplified 2D calculation according to the following contact interaction diagram was performed for different conduction conditions.

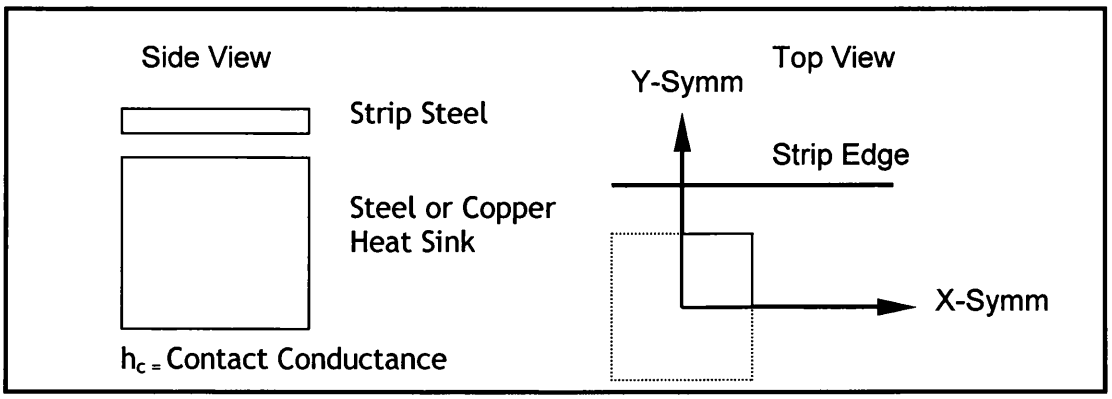

Figure 5.3 Contact Representations of Strip and Heat Sink in 2D

The heat transfers models boundary conditions where: no radiation, no convection, symmetry boundary condition applied to both the X and Y AXES of the strip and heat sink. The application of symmetry boundary conditions enabled the creation of one-quarter strip and one-quarter heat sink geometries within the FEA model (*Figure 5.3*). However, the FEA model will perform a computational analysis as if both the strip and heat sink were whole.

The starting strip temperature was 300°C and the heat sink was at 20°C, this created a considerably larger temperature differential than would normally be acceptable. However, at 300°C the strip is nowhere near its plastic yield point, which is in excess of 700°C. Furthermore, the use of a large temperature differential enabled the author to research temperature differentials - a primary concern of CAPL operators worldwide.

Case 1

If the contact were perfect (i.e. contact conduction = ∞). Then the temperature loss after 0.1 seconds was calculated by the use of ANSYS to be T_c=91°C. This idealised conductance situation never occurred. The steel heat sink was evaluated again with a more realistic contact conduction, and a copper heat sink was added to the investigation for comparison.

Case 2

If the contact were between steel strip and a steel heat sink - the contact conduction would be 1000W/m2K (typical). The heat loss in the strip after 0.1 seconds would be 5°C (T_c) due to the affects of contact conductance.

Case 3

If the contact were between steel strip and a typical copper alloy heat sink - the contact conduction would be 10000W/m2K (typical). The heat loss in the strip after 0.1 seconds would be 42°C (T_c) due to the affects of contact conductance.

The above results showed a greater conduction and therefore control would be possible with a copper heat sink. The three case results also showed the significance of the contact conductance compared to that of the insignificance of the two other heat transfer variables, convection and especially radiation;

reinforcing the comments made in Section 5.1.1.2. - the focus then moved to the size of this heat sink.

To bring these results into perspective - early experiments using steel-to-steel contact had highlighted the difficulty of controlling and therefore calculating the conduction rate between two steel surfaces. Put simply it is because steel to steel contact is often difficult to estimate due to the steels poor conductance values. However, the reality is that the Port Talbot CAPL would not want to operate with a high contact conductance, as this is a cause of plastic deformation due to excessive temperature differentials - this is especially the case within the heating furnace. However, for the pilot facility experiments a large interacting temperature differential was vital, as the measuring devices record more precisely if there is a large transfer of heat. Furthermore, when there was a large temperature differential between the contact surface it was clearer to see where exactly the poor contact occurred (which can be visually apparent). In conclusion a copper heat sink was ideal for the Bar-Le-Duc Stein Heurtey experiments; it enabled visible experimentation as well as a clearer defined localised area of contact conductance for the measuring devices.

5.1.1.5 The FEA Analysis of a Large Copper Heat Sink (400mm^3)

The author and the design team took the decision that the best heat sink material would be copper (Section 5.1.1.4 discusses the decision making process). The next step of the experiment refinement stage was heat sink size and design - through the ANSYS FEA computational program. The temperature differential was to be larger than was often seen on the Port Talbot CAPL to compensate for the lower operating temperature of the pilot facilities heating furnace. The final design consideration was that the strip was to be a thin gauge representing a standard draw quality grade of steel. These operational extremes benefited the author - it enabled a greater understanding of the boundary conditions of the experimentation, and further enhanced the absolute limits of operational possibilities.

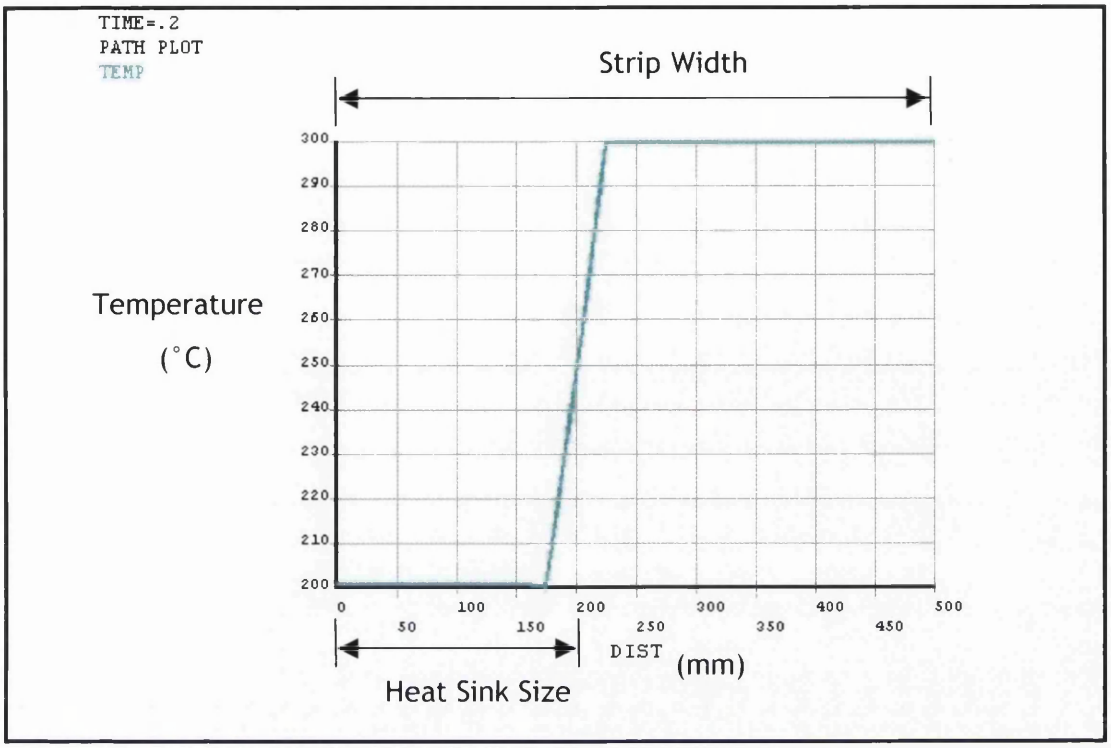

Figure 5.4 The Temperature Profile of the Entire Width of the Strip

The *Figure 5.4* represents the temperature profile across a section of strip with a width of 1000mm. As the computational model used symmetry boundary conditions to limit computational expense, only half the strip width was programmed (into the input deck). Therefore on the X - AXIS the distance 0mm represented the centre of the strip (in a 2D plane only), therefore the edge of the strip was at the X - AXIS distance of 500mm (far right of the axes'). The heat sink was a $400mm^3$ block of copper alloy, which was also modelled with exactly the same symmetry boundary conditions as that of the strip. The width was 400mm, so the centre of the strip was on the X - AXIS at 0mm and the edge of the heat sink was at the X - AXIS distance of 200mm. The strip in this simple case was considered 3D because of the use of continuum elements (grid), thus the symmetry boundary conditions were applied to solid element faces and not just to edges such as in the case of the 2D shell elements (as the depth was defined as material property). The Y - AXIS represents the temperature profile of the strip after 0.2 seconds. If the figure were a representation of the strip profile at 0 seconds then the strip width would be universally at 300°C (the initial boundary condition temperature).

The above computationally processed figure was an indicator of the strip temperature losses due to direct contact with the large heat sink beneath. The

figure shows that between X- AXIS distance values 175 and 225 (a 50mm gap across the strip width) the temperature of the strip surface dropped in 0.2 seconds by as much as 100°C. This 50mm gap was 25mm either side of where the heat sink underneath the strip ended at the X -AXIS 200mm distance value. The temperature loss in the strip was entirely due to conductance (and only conductance) as the base temperature of the steel remains at its initial boundary condition value of 300°C. The non-contact section of the strip will never dissipate heat in this particular FEA example because of the use of only conductance boundary conditions. Furthermore, in this FEA computational simulation the temperature differential generated between the copper heat sink and the steel strip was in excess of 100°C (deformation would be likely if the temperature of the strip was at the CAPL operational annealing temperature); However, the effected area was still only 25mm from where the edge of the heat sink ends, under the strip.

In conclusion the conductance is an issue when the temperature differential is in excess of 100°C. The transfer of heat in 0.2 seconds was aggressive; however, strip steel gauges are only ever a maximum of just 2mm in thickness. Ultra thin gauges under a contact pressure will lose or gain heat instantaneously when in contact with a much thicker heat sink such as a transport roll.

The next three figures indicated the distribution of stress transversely due to longitudinal heat gradient *(Figure 5.5)* then the distribution of stress longitudinally due to transversal heat gradient *(Figure 5.6)*, and finally *(Figure 5.7)*, an explanatory layout of *Figures 5.5* and *5.6* explaining the symmetry and point of contact. The computational model used for this particular experiment was quite simple; the output of a purely heat transfer model was transferred into a model which interpolated the temperature changes from shell element to another and created a stress analysis using expansion coefficients. At the time this was felt to be the quickest solution to getting the desired results - and that a fully-coupled thermo-mechanical model would at this stage have been unnecessary.

As expected the rapid change in temperature affected the stress distribution around the area of contact. The temperature in *Figure 5.4* highlights that the strip area that was affected was roughly 50mm around (either side) the edge of the heat sink contact. However, in *Figure 5.5* and *Figure 5.6* the stress patterns generated from the change in temperature in the strip, caused repercussions considerably further

than 25mm either side of the contact edge. The blue indicates areas of most compression and red areas of most tension (yellow and green are somewhere in the middle of these two maximums). The areas of compression and tension were almost a mirror image of one another; for this type of analysis this was expected - the system must balance, so wherever there was expansion there must be an adjacent contraction. In *Figures 5.5* and *5.6* it can be seen that a rapid change in strip temperature due to contact conductance had created a high tensional stress band. There was a corresponding compressional band developing in the adjacent locale of the strip, but only where it was not in contact with the copper block heat sink.

In conclusion this type of thermal strain occurred in excessive temperature differentials and was not particularly conducive to strip flatness and overall strip quality. A further experimental conclusion that was reached from this particular research analysis was that the size of the heat sink depth was almost irrelevant. The strip can only transfer heat to and from the heat sink at a defined uniform rate under constant pressure. The strip was of course ultra thin, so it appeared the heat transfer was instantaneous. However, the contact time was minimal, so conductance time was limited; furthermore, typical steel is defined by a moderate conductivity value (internal temperature diffusion rate); therefore while excessive temperature differentials will have a detrimental affect, there are scenarios where it could be worse. It is important to note that there are many roll passes within the heating and soaking zones of the furnace. If the furnace temperature were maintained correctly in each zone, then the correct contact temperature differential should be maintained when the strip makes contact with a new roll. However, constant contact conditions increase the likelihood of plasticity.

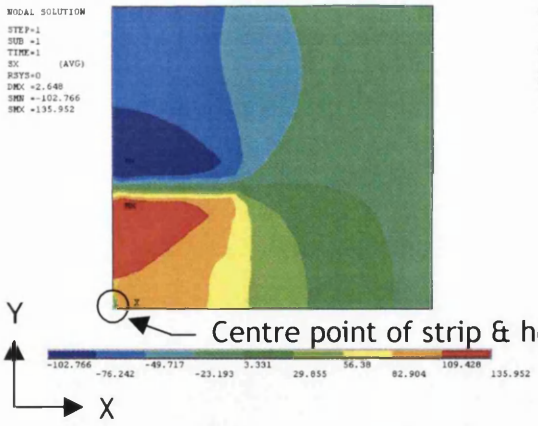

Figure 5.5 Transversal stress (Sxx)

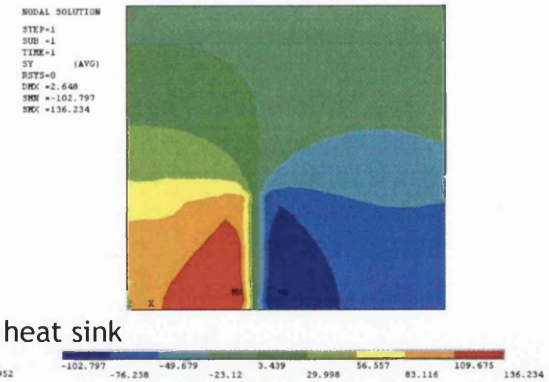

Figure 5.6 Longitudinal stress (Syy)

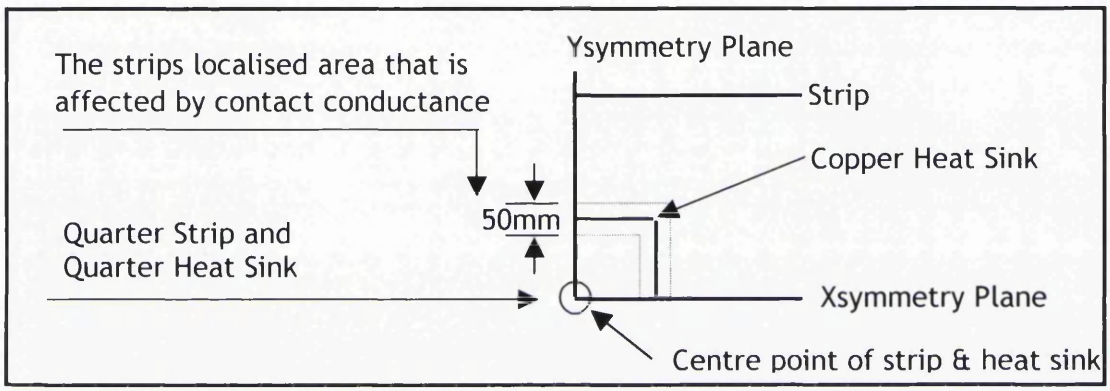

Figure 5.7 Explanatory Layouts of Figure 5.5 and Figure 5.6

5.1.1.6 The FEA Analysis of a Medium Copper Heat Sink (200mm^3)

The FEA simulations so far have shown the restrictive nature of thermal conductance in ultra thin strip steel, which, is not controlled by the heat sink depth, but by the contact cross-sectional area. A large heat sink (400mm^3) would have been extremely heavy (1/4 of a metric tonne), and would therefore be difficult to both manufacture and then support. It would also have proved almost impossible to move rapidly into contact position with the strip without damaging the strip or the measuring devices. The next heat sink examined was a copper block with a dimension of 200mm^3. The results indicated (not shown) that the temperature and stress gradients were almost identical to that of the larger copper heat sink.

In conclusion a smaller heat sink was lighter and therefore cheaper. Smaller heat sinks while having a small surface contact area actually encourage the development of greater stress-strain characteristics in small localised areas of the strip surface.

5.1.1.7 Complications in High Temperature Experimentation

The experiments goal was to mirror as much of the CAPL's operational characteristics as operationally possible. Stein Heurtey performed extensive research on their own into the different measuring devices available. These tests were to analyse the overall experimental performance of the strip and measuring devices at temperatures up to 950°C (possible future CAPL operational temperature). The only types of gauges that can operate at 950°C are very heavy and robust and have to be conventionally welded to the strip. The application of welding heavy gauges to the strip steel substrate causes the strip to severely sag and then deform under just the weight of the measuring devices themselves. Apart from the weight of the measuring devices the strip at 950°C also has a low yield point; therefore any additional sources of load and therefore strain increases the chances of deformation occurring once testing has begun.

A further issue, in reality a more worrying issue, relates to the restrictive and rather basic nature of the Stein Heurtey pilot facility. The strip in the Port Talbot CAPL is supported in a longitudinal direction while being processed: the strip on the pilot facility is tested in the horizontal position and thus has to contend with gravity. This would be fine but as mentioned in the previous paragraph a high operation temperature reduces the yield point - a value which can reduce from 300MPa to as little as 10MPa. This is complicated by the measuring devices, because the measuring devices need to remain tort on the strips upper surface, so a higher than normal CAPL operating tension is required to prevent the horizontally aligned strip from sagging in the centre. The increased tension simply caused the strip to buckle immediately.

In conclusion, the Stein Heurtey temperature testing showed resoundingly that lower furnace temperature testing was the only way forward. This meant that the temperature that the strip steel was subjected to was not to exceed 300°C. At this temperature the yield point of the strip was still sufficiently high for the required tensional load to be applied; to keep the strip from excessively sagging and to allow for non-intrusive strain and temperature gauges to be applied to the strips surface without unduly affecting the experimental results. Low temperature testing in the region of 300°C enabled a large temperature differential to be maintained. Far greater than that would normally be acceptable in normal CAPL

operations, plus more importantly it would enable a certain repeatability of the results, something testing at 950°C could never achieve.

5.1.1.8 The Pilot Facility Modification

The original layout was built with modular construction techniques, which allowed for the removal of unwanted components for a particular experiment (e.g. cooling blow boxes). *Figure 5.1* indicates the original pilot facility, which proved ideal for high temperature tests.

The author's research moved away from the FEA simulations of furnace exit temperature and the unpredictable nature of very high temperature testing. Predictability is important, not just for experimental result validation, but also for operational considerations such as that of the measuring devices, which are highly sensitive.

Figure 5.8 is a schematic of the modified pilot facility. The revamped and smaller pilot facility preserved the 300mm space required each side of the heat sink contact point. This distance was vital; it enabled accurate experimental measurement to take place without interference from either the heating furnace or the supporting roll, which can both interfere with the strain gauge results. The reduction in the distance between the end support rolls, also helped to in-part tension into the strip, this aided in reducing the sagging that the strip was experiencing, this sagging was entirely down to its own weight.

From the *Figure 5.8* it is clear that the significant piece of equipment removed from the original set-up was the cooling section. The cooling section adds unpredictability to the results; blow boxes are difficult to control, and unnecessary at relatively low temperature testing. The Port Talbot CAPL has a sophisticated temperature control system for controlling the strip temperature through heating and cooling. However, the pilot facility was not anywhere near as well developed; the heating of the strip, even to a modest 300°C, took a considerable length of time. The strip then had to be rapidly moved to the testing point (300mm from the furnace exit) so that minimal amount of heat was lost.

The experimental cooling time required in operational conditions was approximately 100s. This time lapse allowed for a full results gathering analysis to

be performed, and more importantly it was considered the minimum time required for a repeatable experimental procedure. Intermittent contact can occur even on the most successful experimental set-up conditions. The problem is that heat transfer is entirely unpredictable when it comes to thin strip. Contraction and expansion of the strip surface will cause a variation in the experimental results; there will always be a small change in operational characteristics from one analysis to the next.

Figure 5.8 shows the final modified pilot facility set-up. The strip passes around the end rolls and joins at the weld point.

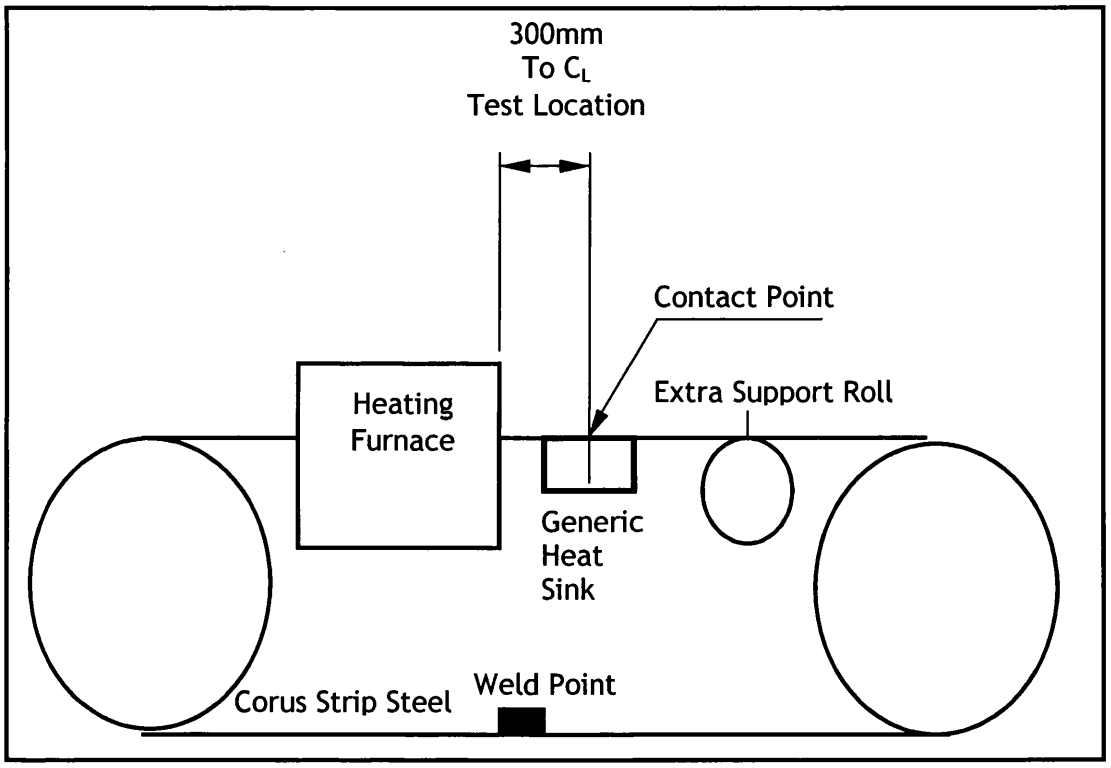

Figure 5.8 The Modified Stein Heurtey Pilot Facility Used for Final Experimentation

The importance of accurate load application was paramount; *Figure 5.9* shows how tension was applied to the strip through a support roll that was on a sliding horizontal runner. The runner was then attached to a set of weights; which can be adjusted to apply the required tensional force.

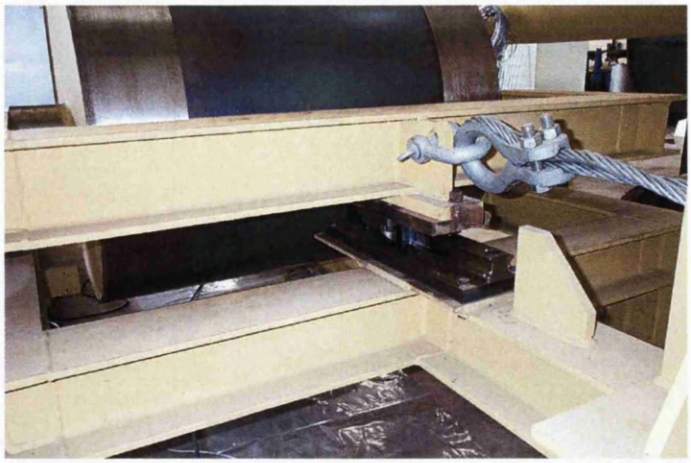

Figure 5.9 The Application of Pilot Facility Strip Tension

5.1.2 THE FINAL EXPERIMENTATION

5.1.2.1 The Final Experimentation Procedure

The final experiment was performed in June 2003 at the Bar-Le-Duc pilot facility and was fully witnessed by author. The experimentation procedure was simplified and consisted of only a few steps:

1. Strip heated to the desired temperature inside furnace (125°C, 175°C, 200°C etc). The only measuring devices attached being the thermocouples and strain gauges. The heating unit consists of an electric furnace with radiant panels: There were 3 heating resistors in the roof and 2 pyrometers. Regulation of the furnace was through electronic means.

2. The heated strip was then moved to the testing place outside of the furnace (300mm from the edge of the heating furnace).

3. The heat sink was rapidly moved into place from underneath the strip to the exact centre point of the measuring devices defined as temperature zero (T_0). The heat sink was not in constant contact with the strip, for two reasons - a) to avoid damage to the soft copper alloy heat sink, and b) so that the heat sink was kept at room temperature.

4. The measuring devices on the surface of the strip transmit the results to the data system for recording.

This simple experimental procedure allowed the focus to switch from an exercise of pure validation to a programme that allowed for a greater understanding of the temperature loss in the strip through localised conduction - this was relevant to the Port Talbot CAPL localised strip quality issue, which comes about from poor contact at the knuckle of the tapered type "C" transport roll.

5.1.2.2 The Measuring Data Systems

The Vishay Measurements Group supplied a data logging system, which has the ability to record 10,000 measurements per second per channel and has an individual input card for strain gauge and thermocouple measurements. The cold mechanical properties such as "Young's Modulus of Elasticity" are necessary for accurate strain gauge measurements. The mechanical property's values used for the experimental programme where:

Modulus of Elasticity: 207.3 GPa @ 300°C.
Poisson's Ration: 0.285 @ 300°C.

(These values represented the cold iron values for the strip supplied by Corus, standard supplied cold iron data for particular steel grade).

5.1.2.3 The Measuring Device Set-Up

The Rosetta strain gauge formation is the most common form of arrangement. The separate gauges are at angles of inclination of 0°, 45° and 90°. Stein Heurtey decided independently that because the strip gauge was ultra thin at 0.45mm, then it would be best to calibrate the two types of strain gauges. The types are the bonded gauge (glued) and the welded gauge, because stress cannot act perpendicular to a free surface, strain-gauge measurements involve a two-dimensional state of strain (linear), thus the measuring equipment must determine shear strains indirectly[38].

The arrangement from the suppliers is shown below (in French) *Figure 5.10*, the gauges on the right represent the bonded gauges (C1, C2, C3); the welded gauges (S1, S2, S3) are on the left. The T_0 represents the centre point of contact with the heat sink, which is on the underside of the strip; T_{25} and T_{50} represent two further thermocouples at 25 and 50mm respectively away from the central contact point.

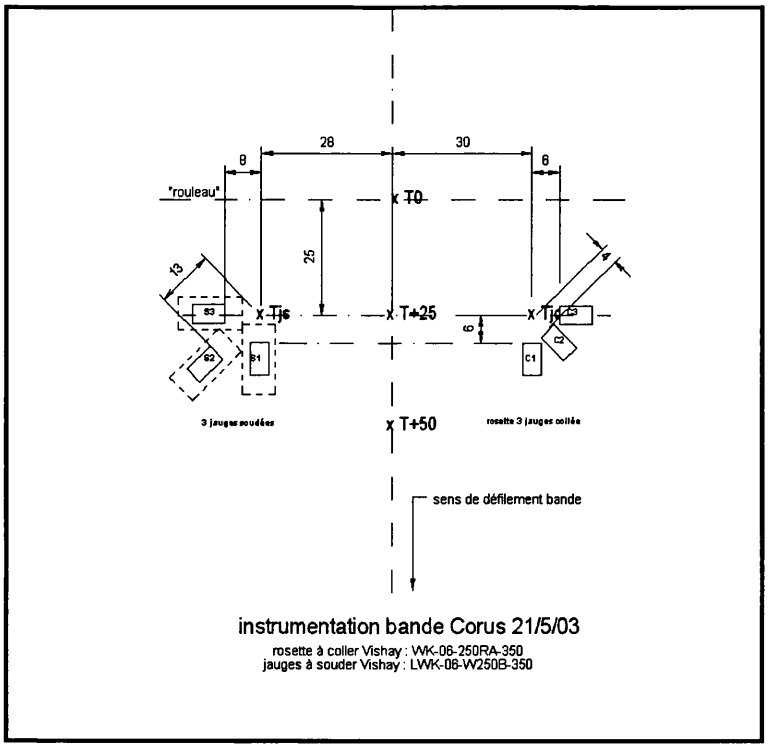

Figure 5.10 The Thermocouple and Strain Gauge Alignment on the Strip Surface

5.1.2.4 The Final Experimental Arrangements and Testing

The initial heat sink decided upon before the pre-testing was a copper block. However, it became clear in the final pre-testing that the contact conditions on a flat heat sink surface were less than ideal. The required repeatability of the experiments results was not possible. Primarily the copper block cut-into and deformed the strip once contact began.

The final heat sink that was chosen had a noticeable crown to give the minimum contact point at initial roll-strip contact. The heat sink was still copper, this was largely due to copper's greater conductance properties over that of mild steel. However, it was also partly due to coppers improved malleability over that of mild steel. The final heat sink design after an incredibly extensive pre-testing programme was considered best that could be achieved with available resources. It had taken 18 months to get to this conclusive stage.

The addition of an internal cooling medium (water) aided in the transfer of heat away from the surface of the heat sink once contact had been made. Thus the heat sink acted as a constant temperature boundary condition - this action meant

that the heat sink required no measuring devices to record the temperature (i.e thermocouples), this further increased the repeatability of the experiment.

The copper water-cooled heat sink was kept at a temperature of approximately 30°C throughout testing by the water acting as forced conduction. The heat sink had a crown of 10mm to minimise as much as possible the contact point and increase as much as possible the repeatability.

It was noted that the strip on the CAPL has been known to contact at just one point, this, however, created excessive temperature differentials in this experiment, which tended to affect the quality of the final product. A simple schematic of the copper water-cooled heat sink can be seen in *Figure 5.11*.

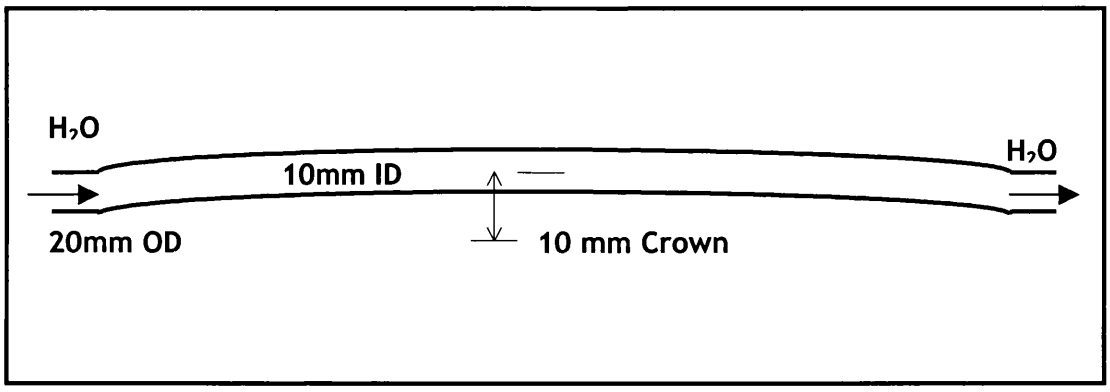

Figure 5.11 The Water-Cooled Copper Heat Sink Specifications

The repeatability of the copper water-cooled heat sink experiments was highlighted in the Stein Heurtey produced *Figure 5.12* below. The figure indicates that the three pre-test temperature values these representing repeated tests are all close to each other. The x-axis shows the time in seconds and the y-axis represents the thermocouple-recorded temperature, thus the figure is a representation of conduction.

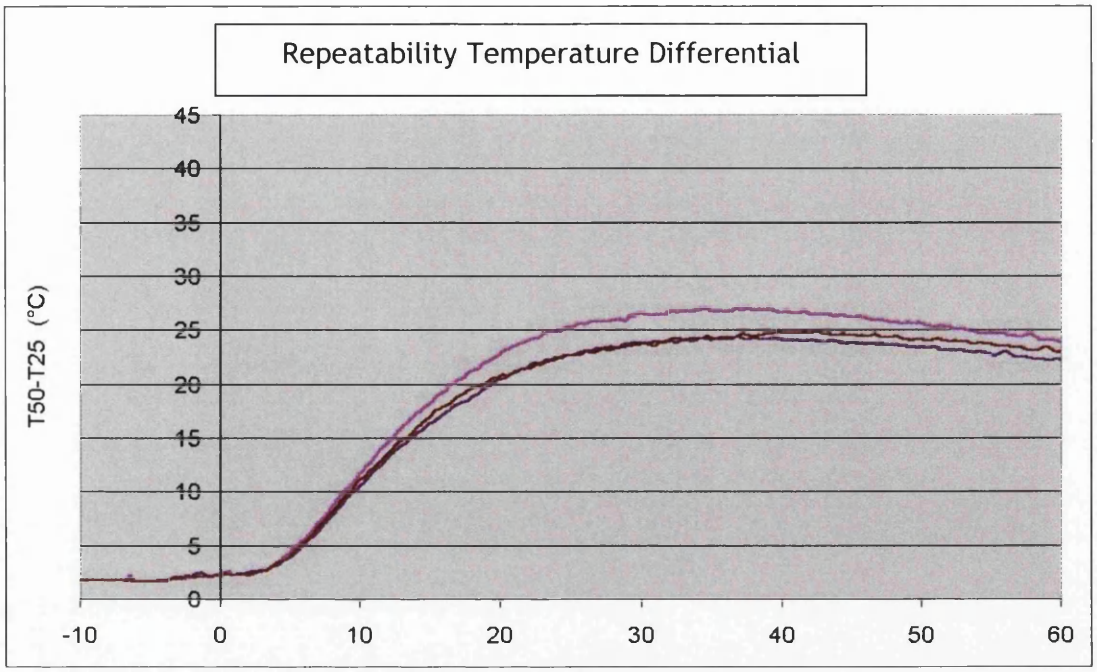

Figure 5.12 The Water Cooled Heat Sink - Repeated Thermocouple Results

An issue that affected the experimental results was the poor strip quality supplied by Corus. It proved extremely difficult for the author to acquire adequate supplies of appropriate gauged CQ material for the experimental testing programme in Bar-Le-Duc. The strip supplied by Corus was an off-cut of the end of one of the coils; and it suffered from a common quality occurrence that occurs particularly at Port Talbot that of wavy edge. Wavy edge on one side of the strip occurs because the slabs are split after continuous casting. *Figure 5.13* below highlights the edge waviness.

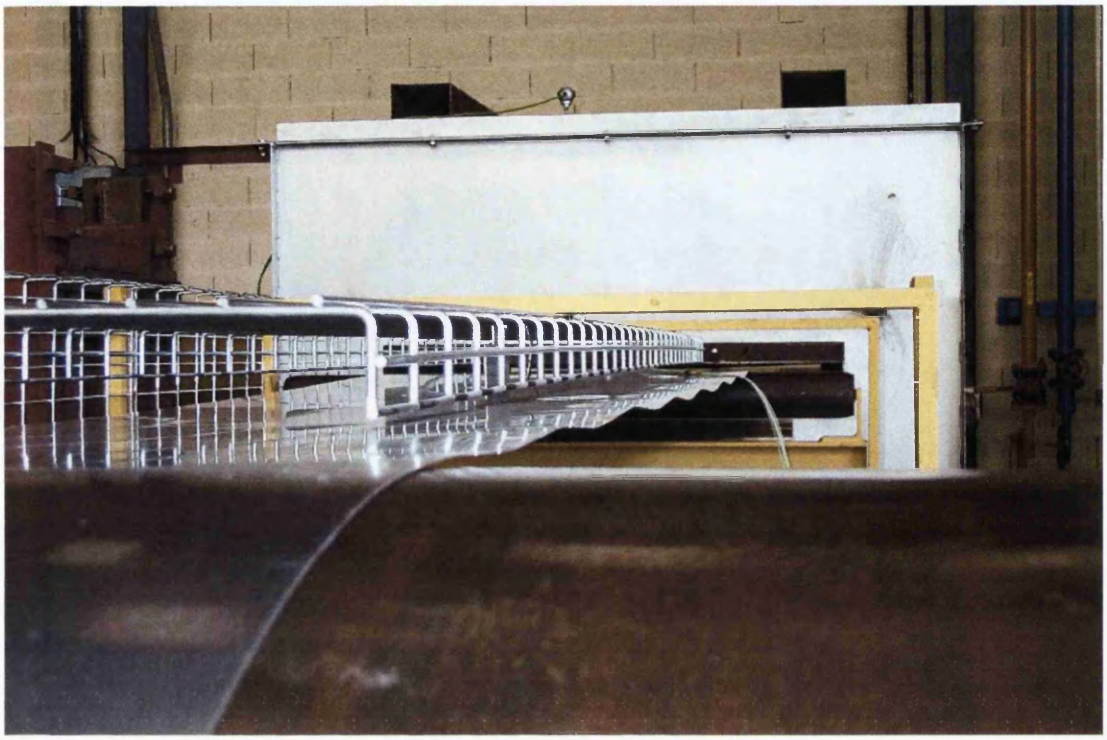

Figure 5.13 The Strip Edge Waviness - Common to Port Talbot Strip Mill

5.1.2.5 The Final Experimental Results

The Corus strip provided was set at 722mm wide with a gauge of 0.45mm. The width appeared to have no effect on the recorded results, because contact only affects the immediate area around the contact point.

The use of two sets of strain gauges enabled values to be compared; the welded gauges were found to provide the most repeatable (reliable) results. However, it was unknown whether they would deform the strip when fitted. Thus this is one of the reasons why the strip could have a gauge no lower than 0.4mm. The focus switched from the strain gauge measurements to the effects of temperature; with the experiments taking place at a maximum of 300°C. At this temperature the steel was certainly nowhere near its recrystallisation temperature. If it were near its recrystallisation temperature then the steel would be softer, with a much lower yield stress value. The strain gauge results were still of some interest because changes in elastic strip surface strain can be linked to behavioural mechanisms that can lead to plastic strain.

There were two distinct discussion topics that came out of the final experimentation, one was the measurements from the measuring devices and the other was the visual observations.

The x-axis represents seconds for the figures on the following pages. The thermocouple and strain gauge measurements both have time represented on the x-axis. Each data line represents 10000 separate recordings, which translates to 100 seconds of thermocouple and strain gauge measurements. The y-axis represents temperature measurements in degrees Celsius.

Each thermocouple measurement had three individual temperature recordings from different locations on the strip surface - these are represented by T0, T25 and T50 and refer to the contact point and then the thermocouples that are 25 and 50mm from the contact point.

The strain gauge values represented in the figures below (*Figure 5.18 - 5.21*) are the more accurate welded gauge results with the three individual data collection streams representing the standard Rosetta arrangement - strain is represented by the dimensionless value dl/l (the change in length divided by the original length). The strain gauge measurements that are presented in the following figures of this section are all compensation strain gauge values.

When the recording device supplied by Vishay Measurements Group was started the measuring devices on the strips surface started to automatically send results, this happens even if the strip is cold and not in contact with the heat sink. The strain gauges primary purpose was to measure the change in stress state that occurs at the strip contact point when conductance begins. Some residual stress (noise) was present and picked up by the measuring devices, this came from a number of sources such as movement, heat and vibration - the measuring devices had to be zeroed before contact was made. It was this zeroing that was referred to as compensation values.

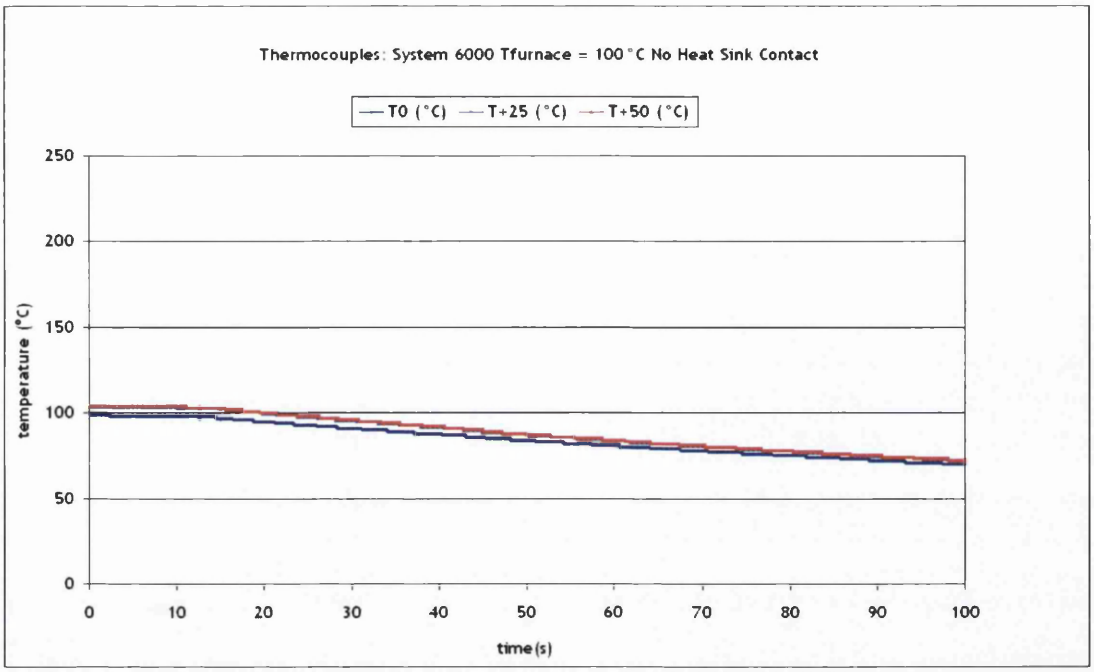

Figure 5.14 Thermocouple Result - 100°C Furnace Exit Temperature - No Contact Result

Figure 5.14 represents the thermocouple results where the strip was heated to 100°C. Once the test area section of the strip had reached 100°C the strip was moved from inside the furnace and was allowed to cool naturally in the open. This gave the author an idea of the effects of natural convection and radiation, and to prove they both were going to be insignificant compared to that of contact conduction. The open air-cooling was still going to affect the three located thermocouples at T+25 and T+50 (25mm and 50mm respectively from the test point - T0 the first thermocouple). This figure will be the only figure that shows the three thermocouples T0, T25 and T50 as having similar strip surface temperature values. Clearly this figure does not represent any contact conductance; which would greatly affect the thermocouple at T0 the heat sink-strip contact point.

This test showed that all three thermocouples were losing heat in unison. The heat loss indicated above was 30°C of convective heat transfer in 100 seconds.

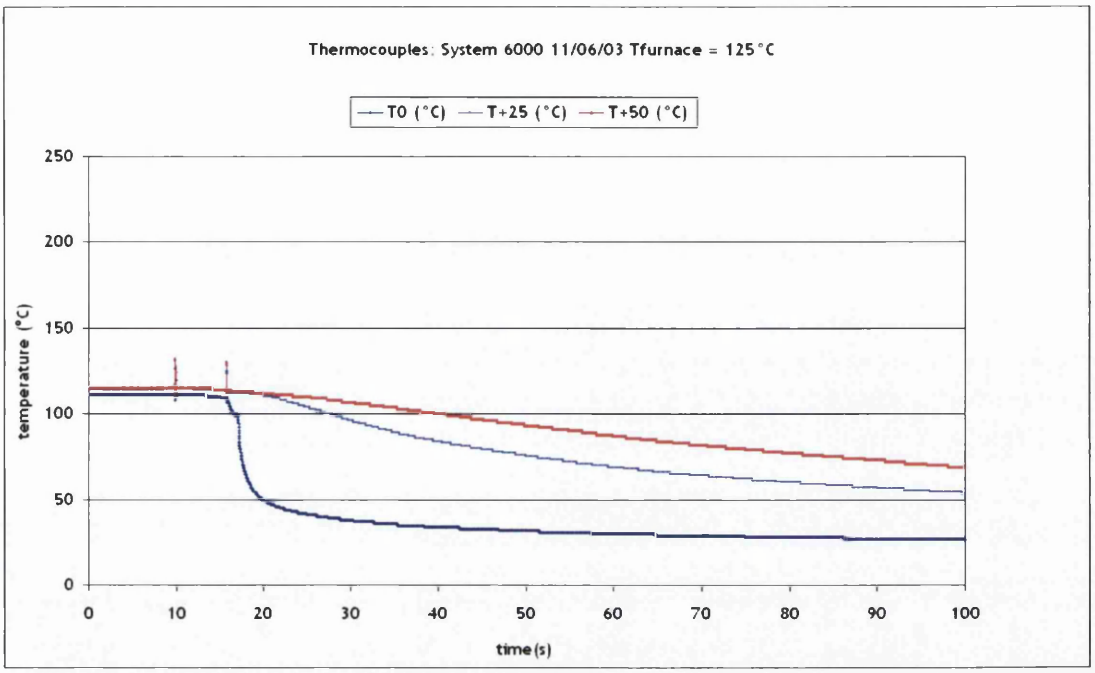

Figure 5.15 Thermocouple Result - 125°C Furnace Exit Temperature - Contact Result

Figure 5.15 represents a furnace exit temperature of 125°C, which then proceeds to full conductance contact. The initial none contact model proved the measuring devices accuracy, the next step was to analyse experiments that include a heat sink contact. The temperature differential, which gave the best results in terms of repeatability were at a furnace exit temperature of 125°C. As mentioned - this was a lower temperature than the Port Talbot CAPL operates at, however, with the heat sink at 30°C this gave a temperature differential of approximately 95°C, this value was roughly 65°C higher than would ever be seen in the worst case temperature differential scenario in the soaking section of the CAPL furnace (where recrystallisation occurs).

The results of this experiment indicate at around 10 seconds all three thermocouples show the same temperature value - the temperature of the strip inside the furnace. *Figure 5.15* show temperature blips occurring when the heat sink first makes contact with the strip at around 20 seconds, this occurs with all experiments that have hard contact. At this time it becomes clear what affect that the massive temperature differential between the contacting surfaces has on the heat transfer rate of the strip. Within a few seconds, the temperature at the

contact point T0 has dropped by some 70°C and continues to drop until it quickly reaches an equilibrium temperature with that of the heat sink.
The other two data lines, which represent the temperatures at 25mm (T+25) and 50 mm (T+50) from the contact point, show a uniform decline in strip temperature. The T+25 and T+50 results are similar to those of *Figure 5.14*, and thus repeat convection as the main heat transfer median. However, the thermocouple at 25mm did show some signs of the presence of the temperature differential generated by the contact, whereas the thermocouple at 50mm did not. It is, however, clear that the two outer thermocouples are not losing excessive temperature from the contact conductance, thus highlighting the very localised effect that contact conduction has on ultra thin strip steel.

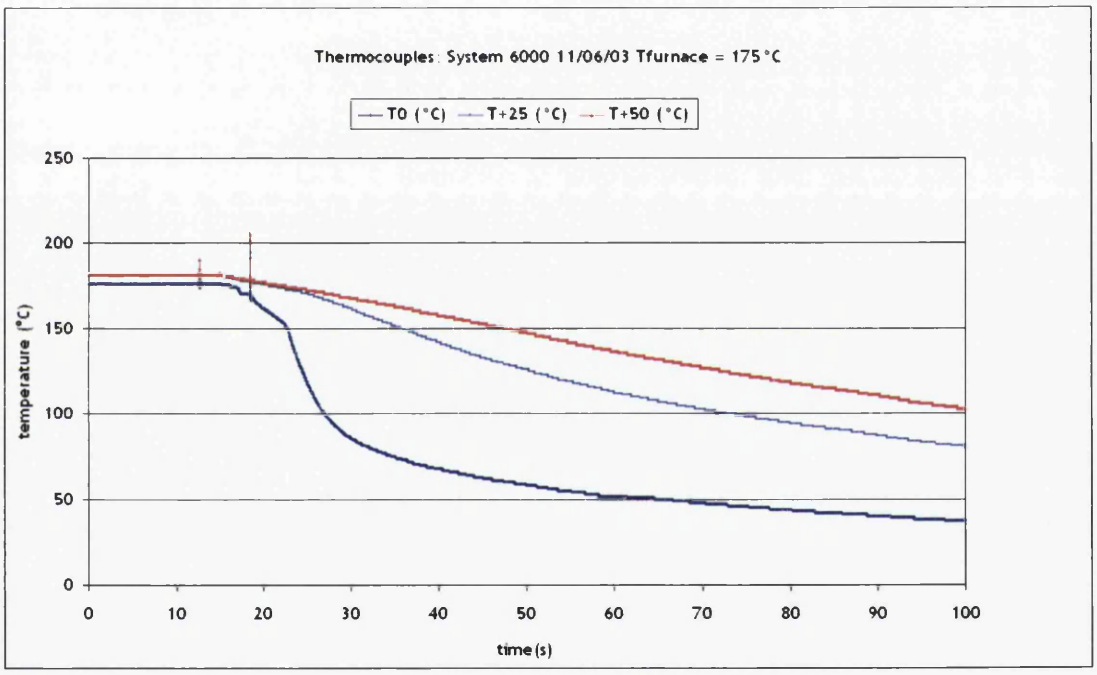

Figure 5.16 Thermocouple Result - 175°C Furnace Exit Temperature - Contact Result

Figure 5.16 represents an increase in the exit furnace temperature, this creates a temperature differential of 145°C. The results show an insignificant difference over that of the 90°C temperature differential. The temperature at thermocouple T+25 cools faster and looses parity with the temperature of the T+50 thermocouple at an even greater rate than in *Figure 5.15*, due to the greater strip surface conductance area of the larger temperature differential.

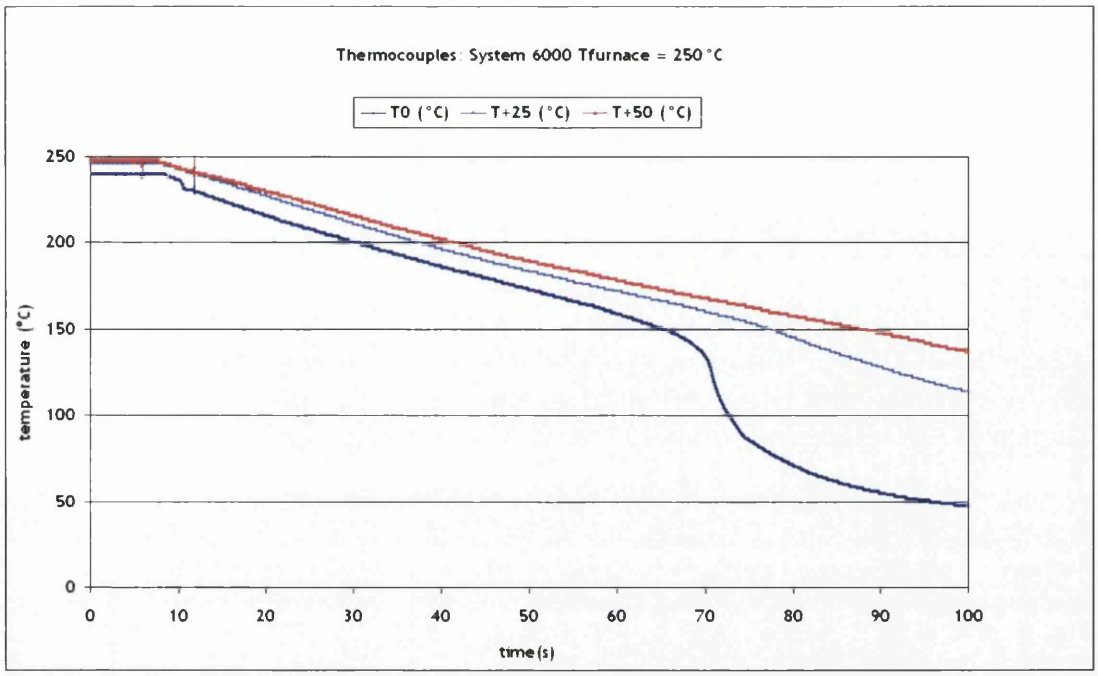

Figure 5.17 Thermocouple Result - 250°C Furnace Exit Temperature - Contact Result

Figure 5.17 represents the highest exit furnace temperature (250°C) experiment that produced reliable results. Once the temperature differential rises above 200°C the results become increasingly incoherent. At first it looks as if all three thermocouples (T0, T25 and T50) are losing temperature simultaneously as in the no heat sink contact experiments - put simply, they are. The temperature differential was so great that the repeatability has completely gone from the experimental results - several experiments performed at this temperature resulted in different results each time. The reason is explained in the next section of this chapter, which discusses the visual observations.

However, briefly what *Figure 5.17* highlights is that excessive temperature differentials cause contraction at the contact point within the strip, however, this has absolutely no affect on the heat sink (the transport roll representation). This effectively causes the strip to lift back off the heat sink after initial contact therefore denying conductance. However, after a fraction of a second, the strip then rests on a couple of new contact points; these are either side of the original contact point. Eventually, temperature throughout the strip equalises and the strip settles back on to the heat sink surface. This initial contact can be briefly seen in *Figure 5.17* at around the 10 seconds mark, just the T0 thermocouple - the

figure briefly shows a slight rapid cooling, this represents the initial point of contact before the strip lifts. Once the strip lifts *Figure 5.17* shows T0 thermocouple continuing to cool in parallel to the other two thermocouples (T25 and T50). However, at around 70 seconds the strip regains contact and thermocouple T0 indicates rapid cooling.

The preceding results concentrate on temperature changes due to contact conductance. The following results continue this investigation into temperature changes; however, they focus on how temperature affects the mechanical properties, in particular the stress characteristics of the strip steel.

The following strain gauge results are a representation of the temperature experiments seen in *Figures 5.14 - Figure 5.17* they should be considered for the purposes of interpretation and that they accompany the thermocouple results.

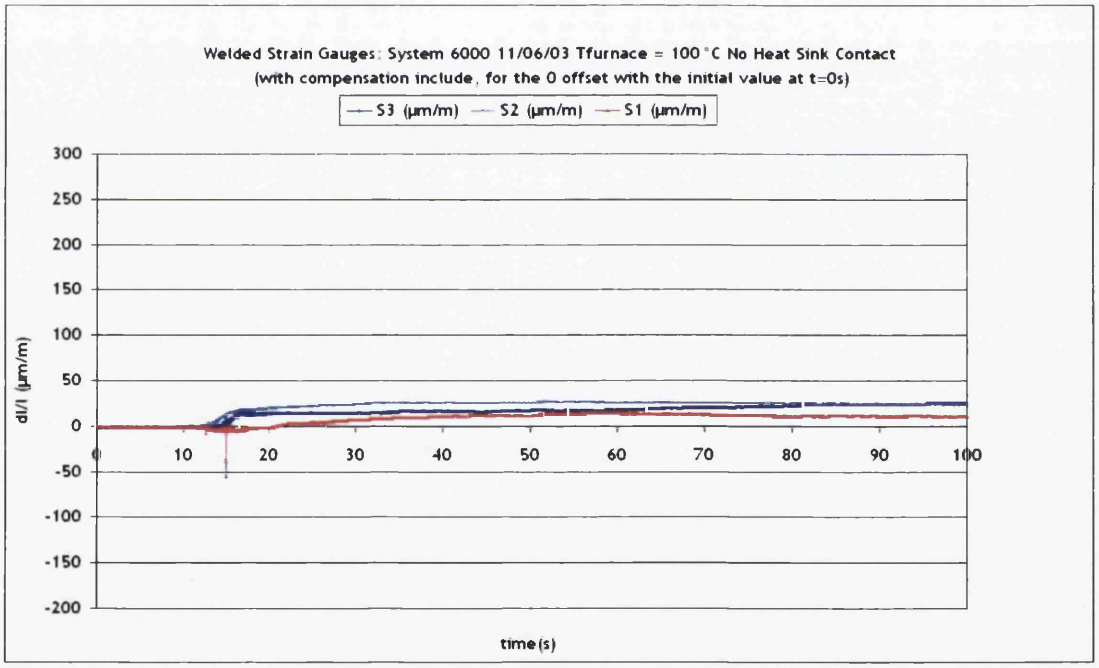

Figure 5.18 Strain Gauge Results - 100°C Furnace Exit Temperature - No Contact Result

Figure 5.18 represents the resultant strain characteristics of the *Figure 5.14.* Thus there is no heat sink and the strip temperature is at 100°C at the furnace exit. The strain gauge measurements for this particular experiment were used to test that the strain gauges were calibrated and working correctly within an acceptable

error tolerance. However, the three strain gauges that make up a Rosetta arrangement are never going to give equal results, as surface strain is dependant on the rolling direction. *Figure 5.10* highlights the strain gauge arrangement.

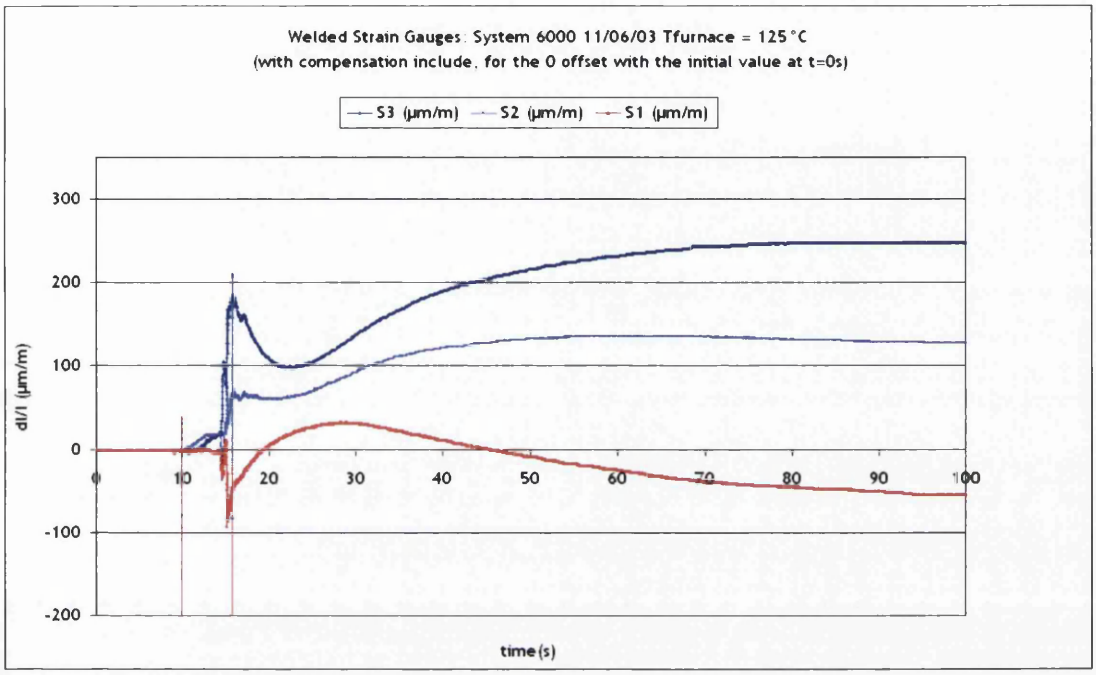

Figure 5.19 Strain Gauge Result - 125°C Furnace Exit Temperature - Contact Result

Figure 5.19 is the strain gauge representation of the thermocouple results from *Figure 5.15*. Once a significant temperature differential is included, the results indicate a loss of parity in the strain gauges (i.e. no parallel strain gauge result). All three different angled strain gauges that make up the Rosetta arrangement have curves that are independent of each other. However, the results in *Figure 5.19* while they do not show straight parallel lines, they do clearly show smooth curves once the three gauges start acting independently (i.e. there are no extreme y-axis blips).

The results indicate that while there was change in local strain within the strip due to the temperature differential created by the presence of the heat sink, the strain gauges that make up the Rosetta arrangement indicate a low level of parity loss. In fact the smooth strain lines of *Figure 5.19* indicate that contact conductance was constant once the initial hard contact had been made. The strain gauge blips at around the 15-second mark are an indication that the heat sink has

made contact with the strip surface. In conclusion, a temperature differential of around 95°C does not create a situation of poor contact at a constant pressure - this experiment can be put into a CAPL context, it is a representation of when the strip is entering the heating furnace at the heating furnaces operating temperature.

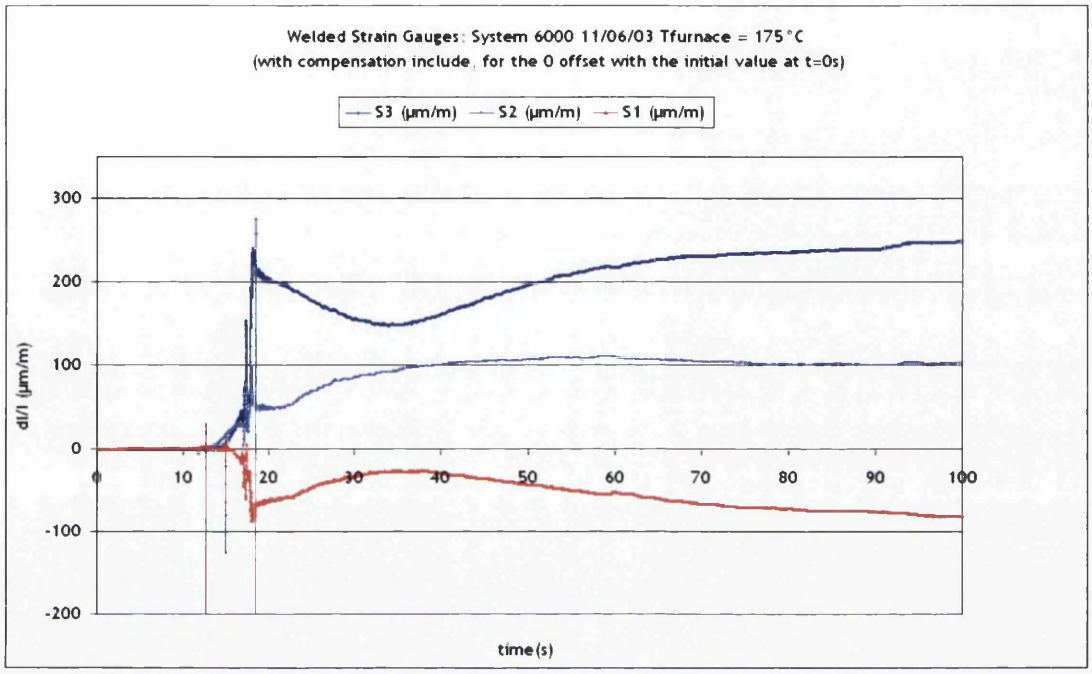

Figure 5.20 Strain Gauge Result - 175°C Furnace Exit Temperature - Contact Result

Figure 5.20 is the strain gauge representation of *Figure 5.16*, a temperature difference of 145°C. As with the temperature increase seen in *Figure 5.19* the variations that are seen when the temperature differential was increased by another 50°C to 145°C show, as would be expected, even less parity in the three strain gauge recordings than when the temperature differential was 95°C. The results in this figure show a contact temperature shock at around 18 seconds (i.e. large y-axis blip), this indicates a far greater reaction to the initial hard contact than was seen in the 95°C temperature differential results of the previous figure. *Figure 5.20* represents a turning point; while the curves do look similar to the 95°C temperature differential seen in *Figure 5.19* they certainly were not as smooth. Thus the temperature differential has got to the point where contact conductance is affected by poor strip shape.

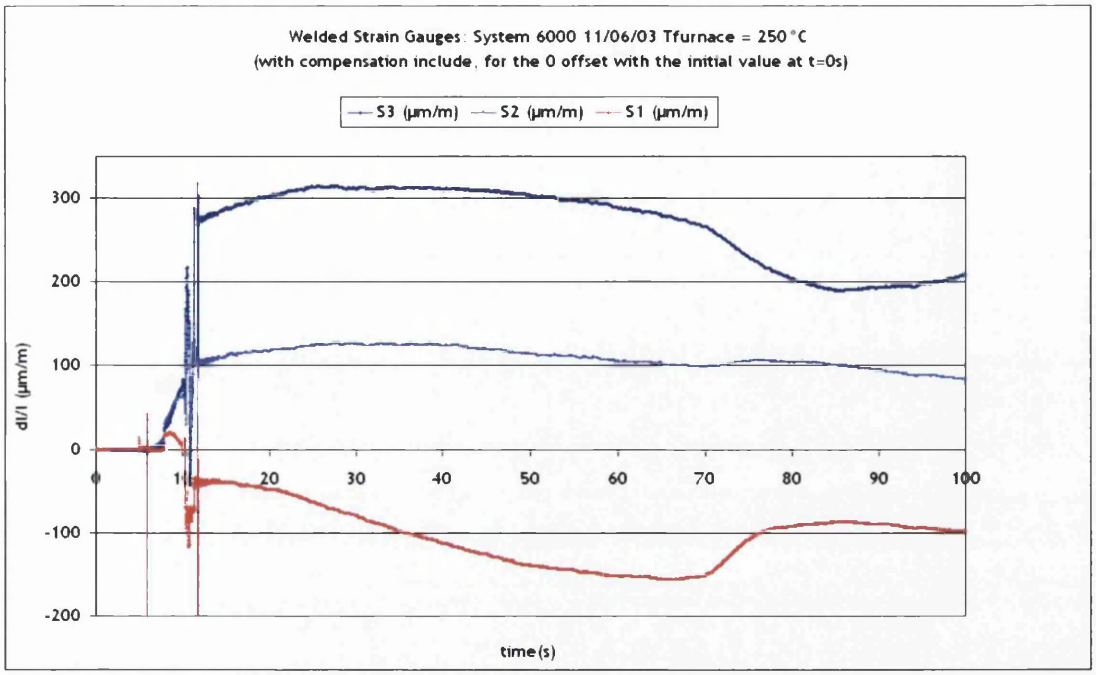

Figure 5.21 Strain Gauge Result - 250°C Furnace Exit Temperature - Contact Result

The above figure (*5.21*), suffers from poor initial contact (even observational examinations indicated poor contact). This was a result of a temperature shock to the strip, far greater than in the previous figure (a contact temperature differential of 220°C exists). The differences in the strain results of the individual gauges of the Rosetta arrangement were now quite pronounced. The curves of the strain gauges were now nowhere near as smooth as in the previous strain gauge results. The initial contact blip in the strain was at just over the 10 second mark, it illustrates the effect that such a large temperature differential has on the stresses within the strip. At the 70 second time mark the strip reaches a homogeneous temperature differential with that of the heat sink, at which time it then proceeds to rest on the heat sinks surface - this change was especially noticeable in the 0° and 90° strain gauges (S1 & S3).

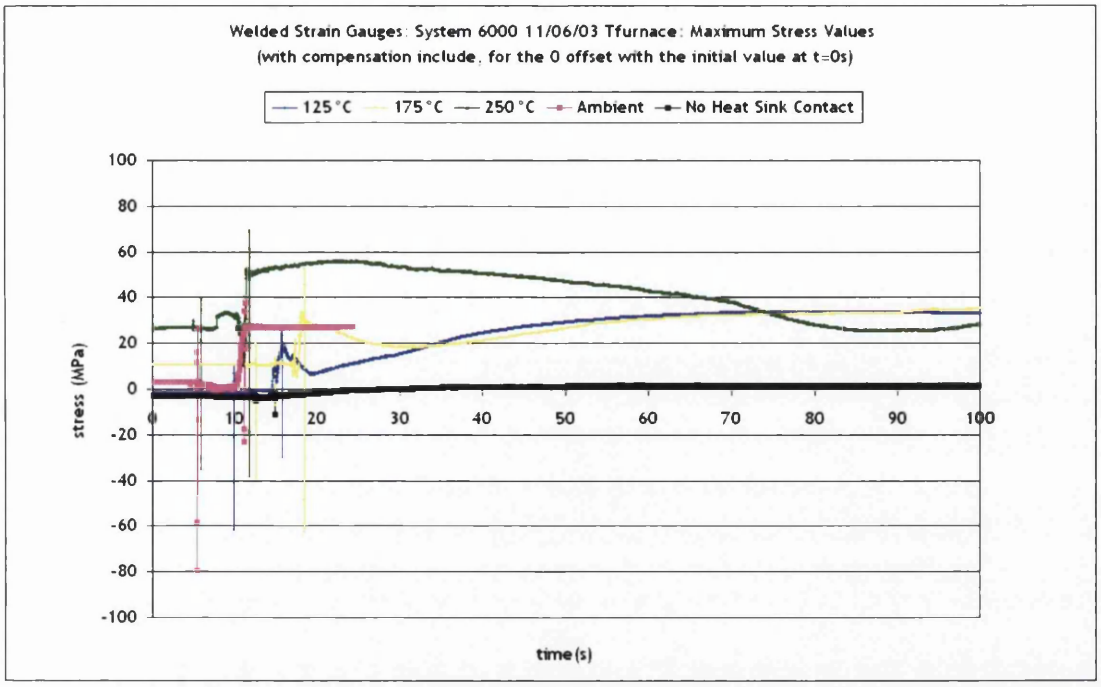

Figure 5.22 Maximum In-Plane Stress Values for Experimental Results

Figure 5.22 represents the maximum in-plane stress values for all operational temperatures. As would be expected the value that represents the 250°C furnace exit temperature has the highest maximum in-plane stress value at the point of contact, with the non-contact model having the lowest in-plane stress value. The ambient contact results show a higher max in-plane stress value at the point of contact than the temperature contact results of 125°C and 175°C; this must be due to increased ductility. Furthermore, this theory on ductility was reinforced by the fact that it can be seen that the ambient condition stress results continue in a linear way once contact has begun, whereas the in-plane stress values that represent the strip at furnace exit temperatures of 125°C and 175°C rapidly increase until they level off at around 80 seconds when strip softness finally affects the stress results.

What is of interest is that both these results, after the initial settling on the roll, are almost identical to each other (i.e. the 125°C and 175°C results). The high temperature differential results of 250°C are poor and the strain gauges continue to read varying results right up to the point of the experimental cut-off, this indicate poor contact between the strip and the heat sink. This fluctuation in temperature differentials would cause poor strip quality, if replicated on the CAPL.

5.1.2.6 Observations of the Contact Between Strip and the Heat Sink

There was good contact between the two surfaces at temperature differentials below 150°C. However, as mentioned in the preceding section (*5.1.2.5*) there are some minor blips in the strain measurements as contact initiates (*Figure 5.19* strain gauge result 125°C furnace exit temperature shows this initial blip at around 15 seconds), this was due to the strip settling down onto the top surface of the heat sink. The contact, however, remains good to the human eye.

There was intermittent bad contact between the two surfaces at temperature differentials from 150°C to 200°C; above 250°C the contact was very intermittent.

The representations below show how high temperatures create intermittent contact conditions.

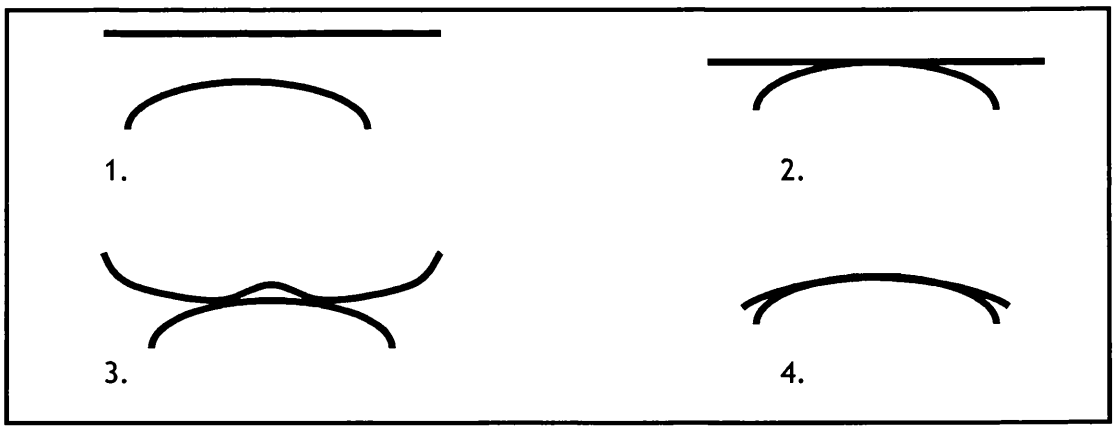

Figure 5.23 Schematic of the Bad Contact

In the first sketch (1.) the strip and the heat sink are apart. In the second sketch (2.) the strip comes into contact with the heat sink. In the third sketch (3.) the strip lifted from the heat sink surface, however, then rapidly drops because of the weight of the strip. It then rests on two points either side of the central contact point until the temperature has equalised throughout the section of the strip that will be in contact with the heat sink. In the fourth sketch (4.) the entire transverse strip temperature had reached a homogenous temperature state with the underlying heat sink (the water cooled copper-heat sink) and the strip settles on the heat sink surface.

In the first of the figures that follow (*5.24*) the contact was fine, however, in the second figure (*5.25*) the strip has lost its shape due to the excessive temperature differential that was present between the strip and the heat sink.

Figure 5.24 The Repeatable Contact at 125°C

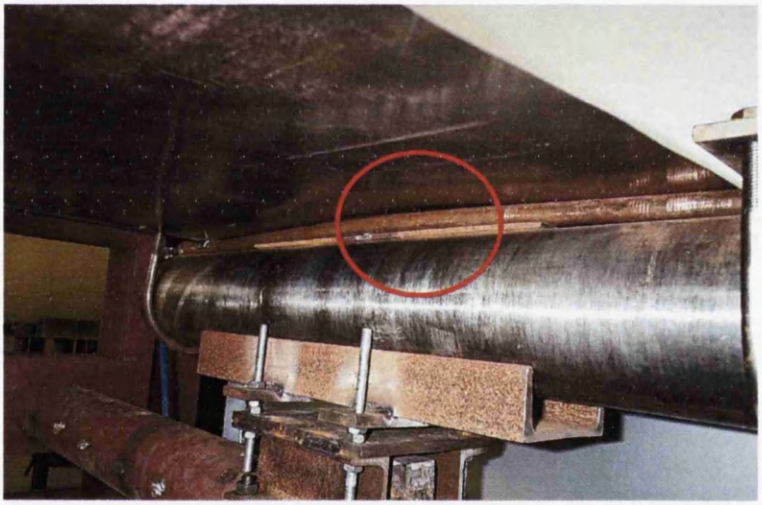

Figure 5.25 The Unrepeatable Contact at 250°C

The above *Figure 5.25* shows the problem (red-circled) that was encountered at the centre point of contact when contraction lifted the strip from the heat sink.

5.1.3 THE FEA COMPUTATIONAL OBSERVATIONS

Opening Remarks

It was decided that a comparable computational experiment should be performed to attempt to check the validity of the observations.

5.1.3.1 The Pilot Facility FEA Computational Model

The commercial ABAQUS FEA programme was used to consider the temperature differential. The model type was a fully-coupled type, which, combines a heat transfer and stress analysis. The advantages of this type of analysis are that any expansion changes within the strip will affect the strain results and displacement values (displacement indicates lift). However, the major disadvantage of this type of model was that it was complex and computationally expensive for anything other than simple geometries and contact simulations. The fully-coupled FEA analysis was a non-contact model.

The model was a series of shell elements representing the strip. A 1mm section (represented by one element width) was assigned boundary conditions to represent a heat sink contact temperature.

The General Code Characteristics:

- Strip shell elements - S8RT (8 nodes, Reduced integration, 3D, Quadratic)

- Strip dimensions - 722mm x 250mm (The dimensions are a replication of the experimental work)

- A 1mm central temperature differential was assigned to a single central element to represent the heat sink. The elements dimensions are 1mm x 10mm. The temperature differential was applied as a temperature boundary condition. The rest of the strip was assigned a field condition temperature of 300°C. The general element size was $10mm^2$

- The thickness of the strip was 0.45mm

- Step - Coupled Temperature-Displacement, deltmx=300
  1e-07, 10, 1e-09, 0.5, nlgeom, inc=1000

- Strip Boundary Conditions -
  - BC-1 Type - Displacement/Rotation - All four edges of the strip, restricted in the x-axis (direction - 1) and the y-axis (direction - 2)

- BC-2 Type - Temperature - Acting upon central 1mm x 722mm section of the shell element(s) thus representing the water-cooled copper heat sink

The Strip Material Properties:

- Density - 7800kg/m^3
- Poisson Ratio: 0.3
- Temperature dependant properties -

Temperature (°C)	Conductivity (W/mK)	Elastic (GPa)
20	51.9	212
100	51.1	206
200	48.6	199
300	44.3	191

Temperature (°C)	Expansion (m/mK)	Specific Heat (j/kgK)
20	1.192E-05	510
100	1.218E-05	519
200	1.266E-05	535
300	1.308E-05	552

Table 5.1 Temperature Dependant Properties

The model was written using ABAQUS Standard, which uses the implicit type solver. The length of the time step is directly related to the maximum size of the increment that is assigned and the total number of increments permitted. Therefore in a Standard model, the time of the run is entirely increment relative.

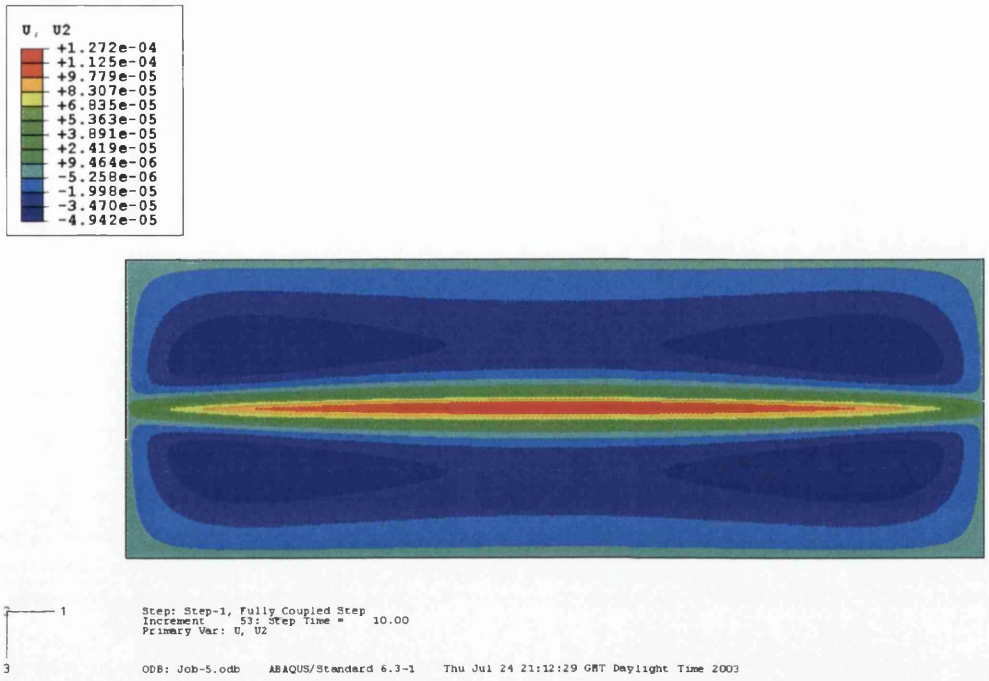

Figure 5.26 The Computational Temperature Profile Showing Variations in Strip Displacement due to Lift (Fully-Coupled Thermo-Stress Model)

The above figure *(5.26)* highlights the central temperature zone that causes the strip lifting effect as seen in the Stein Heurtey Bar-Le-Duc experiments. The displacement was small. However, the strip lifted away from the point of central contact - loss of contact translates to no conductance.

The figure represents translational movement in the y-axis, and is referred to as the U2 value. The red indicates the most extreme upward movement and the blue the most extreme downward movement.

The central boundary condition (the 1mm x 722mm length section) has a temperature of 30°C (ambient). It causes the rest of the strip, which has a 300°C field condition to move downward while it moves in an upward direction. The edges of the strip remain fixed because of the displacement and rotational boundary conditions that have been applied (BC1 & BC2). This representation, while crude, indicates part of the behaviour seen at the pilot facility in Bar-Le-Duc. It highlights the issue of temperature differentials between contacting surfaces, and it is considered by the author as an indicator of the relationship between the CAPL strip and transport roll intermittent contact problem.

Step Time (Seconds)	Strip Lifting (m)
0	0
0.01	4.37-E05
0.1	1.68-E04
1	1.54-E04
10	1.27-E04

Table 5.2 The Strip Lifting: 10 Second Time Period

The above table *(5.2)* indicates that the strip briefly lifts and then starts to settle again once the surrounding strip temperature starts to equalise with the heat sink.

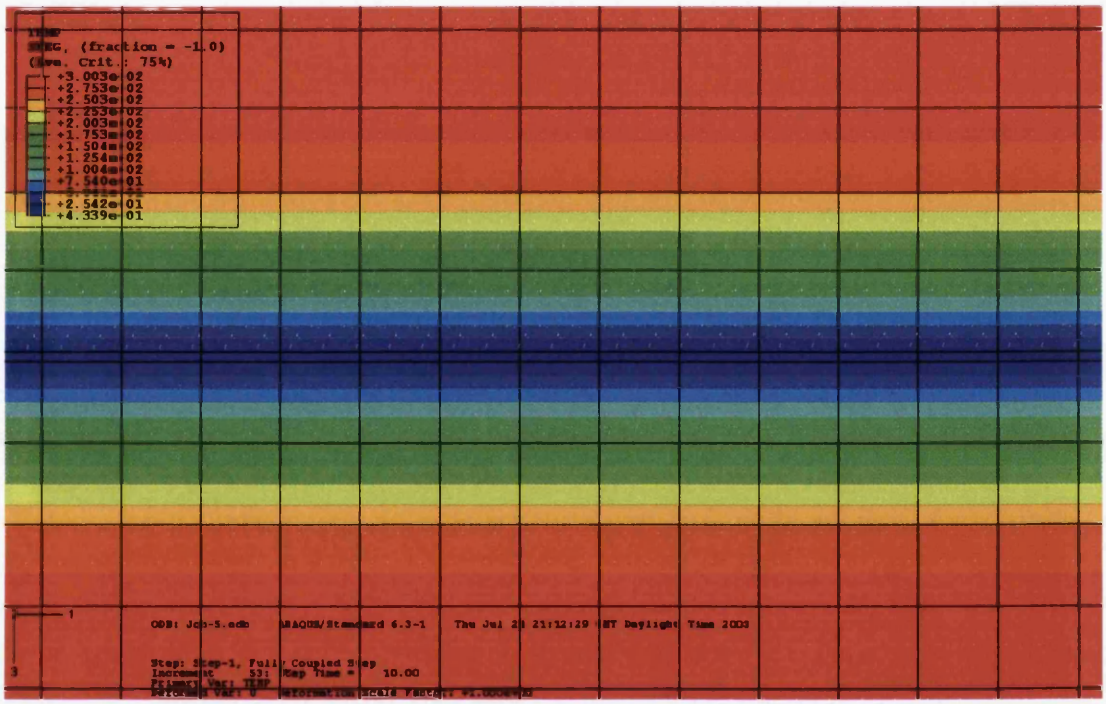

Figure 5.27 The Computational Temperature Gradient in the Strip at Point of Contact (Fully-Coupled Thermo-Stress Model)

The above figure *(5.28)* is a continuation of the previous figure *(5.27)*; it indicates that the strip shape is relative to the temperature gradients across the strips surface. The conductance in such thin strip, as shown in *Figure 5.28*, was very local to the point of central contact. The blue contour colour is at the point of contact and shows rapid conduction has taken place. The small band of green and

yellow contours after this indicate a small area of local heat fluxes; this small band was no more than 50mm from the point of contact, which was similar to the thermocouple readings taken at the pilot facilities. This area was not in contact with the heat sink but was still a temperature-affected area. The last gradients are the red contours; these represent the area of the strip that was not affected by any conduction (300°C).

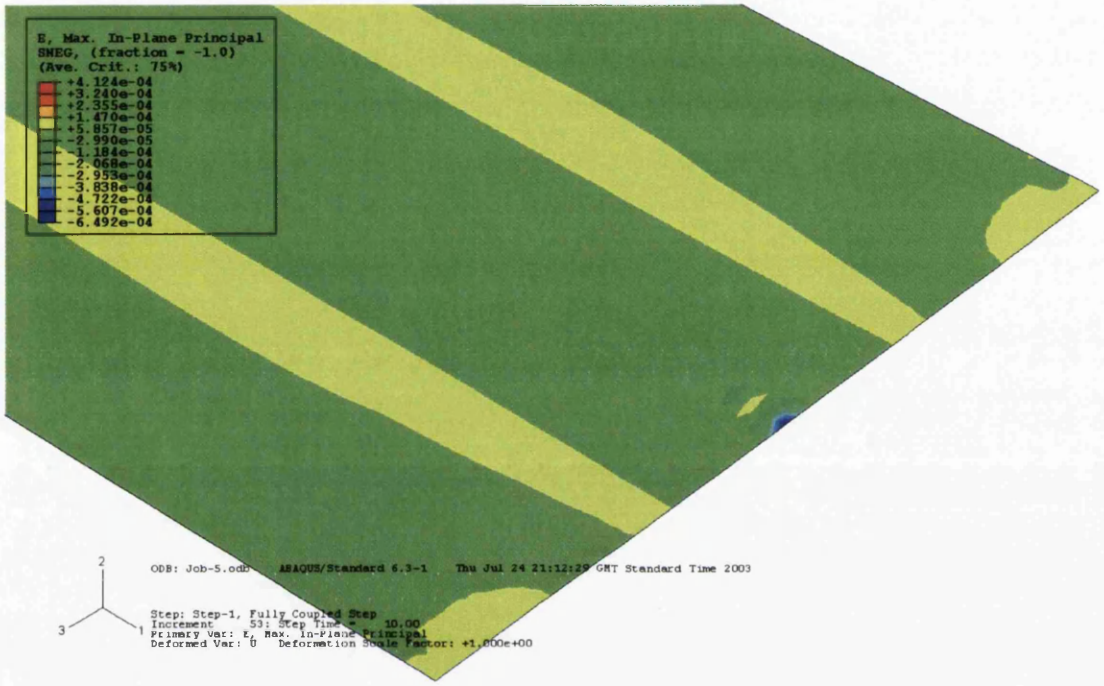

Figure 5.28 The Computational Maximum In-Plane Strain Gradient in the Strip at Point of Contact (Fully-Coupled Thermo-Stress Model)

The strain seen in *Figure 5.28* is the maximum in-plane strain at the end of the experimental run; the figure highlights how the temperature differential affects the strain in the surrounding strip. The figure does not highlight plastic strain because only elastic values were used in this analysis - the case for most CAPL FEM simulations. However, the figure shows that the yellow gradient represents a positive strain (tensile displacement), with the green gradient representing a negative strain (compressive displacement). The affects on the homogenous strain state of the strip come entirely from the central temperature differential. *Figure 5.28* highlights perfectly how temperature differentials across the strips surface change the strains state. In this case it might be considered minor, but the strain was changing either side of the maximum temperature differential.

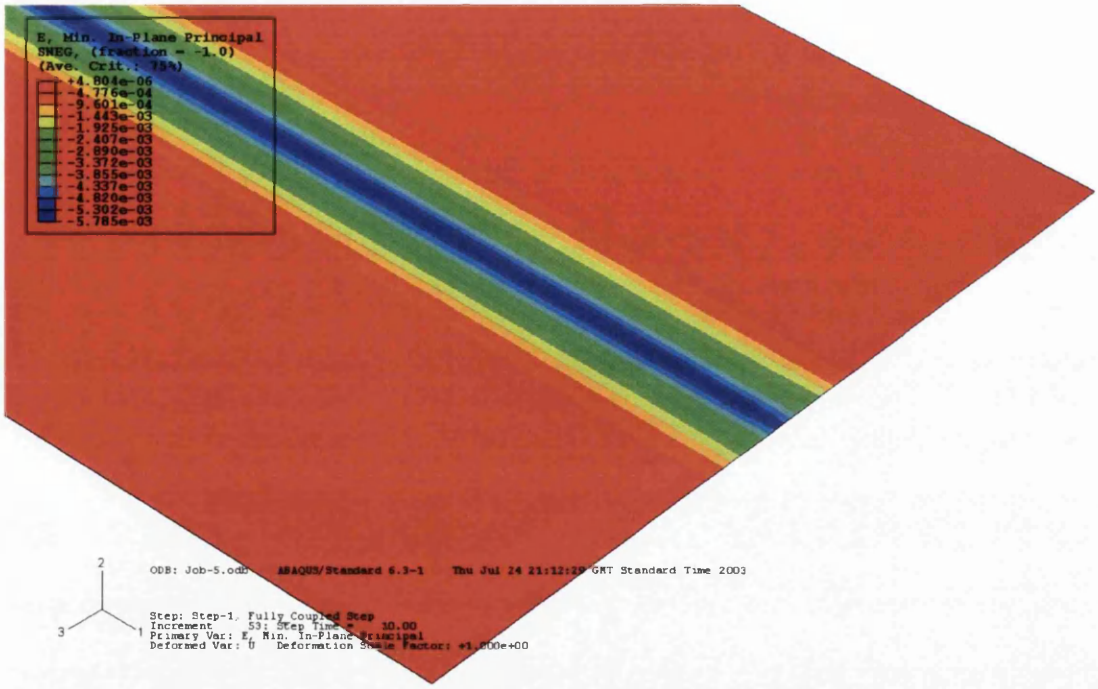

Figure 5.29 The Computational Minimum In-Plane Strain Gradient in the Strip at Point of Contact (Fully-Coupled Thermo-Stress Model)

The above figure represents the minimum in-plane strain gradient and it was clearer than the previous figure on how a temperature differential affects the local strip strain equilibrium. As the heat sink lifts the strip moves into compressive strain at the point of the temperature sink (blue gradient).

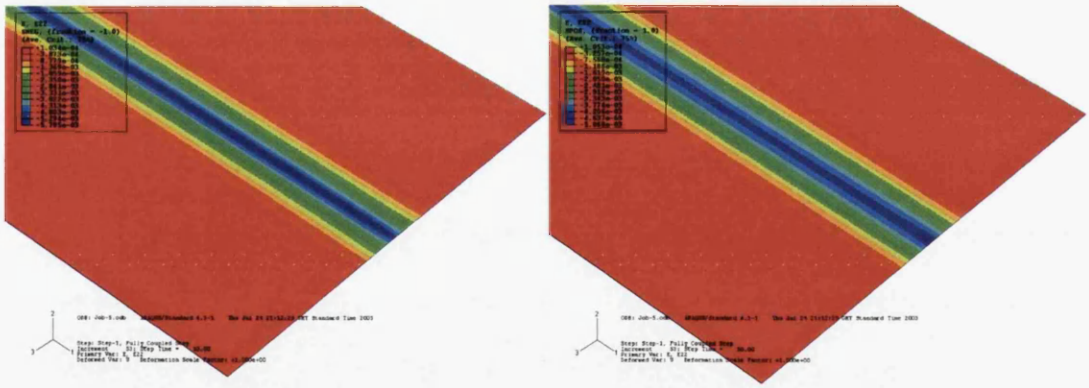

Figure 5.30 The Computational Surface Strain in the Strip at Point of Contact (Fully-Coupled Thermo-Stress Model)

The above figure shows how the temperature differential affects the strain on the strip surfaces. The image on the left indicates how the strain on the underneath of

the strip slightly differs from the strain pattern on the top surface, which is the image on the right. Though the strip was in a plane stress condition ($\sigma 3 = 0$) the strain (ε) was not - thus there will always be some minor variations between the two surfaces strain patterns (SNEG & SPOS). However, this really is a minor issue and somewhat beside the point, because it's the affect on steel quality when the strip is at the recrystallisation temperature under load conditions that is ultimately the most important factor when it comes to temperature differentials.

5.2 CLOSING REMARKS OF THE STEIN HEURTEY EXPERIMENTAL PROGRAMME

The Bar-Le-Duc experimentation was considered a fair indicator of the problems associated with poor strip shape and excessive temperature differentials. Poor contact that comes from localised temperature differentials can lead to preferential heat transfer in some parts of the strip and thus affect the strip quality.

The chapter was made up of three distinct sections. The first was the "Initial Experimentation", the second was the "Final Experimentation" and the last section was the "FEA Computational Observations". The first section was concerned with the thoughts behind the research project with Stein Heurtey, which proceeded into initial experiments and tests to expand theories and thoughts. The second section looks at the actual final stages of testing and then experimentation, results and discussion. The final section looks at the brief FEA computational analysis, which followed the experimental aspect. This was concerned with trying to validate and replicate the Bar-Le-Duc tests.

5.2.1 EXPERIMENTAL REMARKS

The positive experimental results come from the observations of strip lifting. The results indicate an area of concern particularly on rolls with a history of non-uniform temperature distribution, such as sections of the heating and secondary cooling sections of the furnace.

Research and observations have indicated if the temperature contact spots have a temperature difference greater than $\Delta 50^{\circ}C$ it will cause sufficient localised thermal stress to worry operators. This statement was backed up by the cooling buckle team, who in their report indicate that a problem that occurs in the secondary cooling section of the CAPL furnace was a strong variation in local zonal

temperatures, which created significantly cooler areas on the surfaces of the bottom transport rolls than that of the transport rolls at the top of the furnace[27]. Furthermore, Paulus and Laval[5] , who completed extensive analytical and experimental heat buckle modelling, indicated that a temperature difference of greater than Δ 27°C at high temperatures will cause quality issues when the strip is moving at as little as 200m/min (significantly lower than the Port Talbot CAPL). These small temperature differentials have caused Corus and other mass-produced steel manufactures supply problems. Thus the research performed at Bar-Le-Duc was helpful in moving the general understanding of temperature differentials forward.

5.2.1.1 Experimental Failures

The horizontal layout of the strip at Bar Le Duc meant that strip droop was an issue. This was resolved by an increase in line tension. Arbitrary increases in line tension at pre-recrystallisation temperatures are fine, however, in the cases where the strip starts to lose contact on the CAPL transport roll an increase in tension to counter act this may well lead to heat buckle.

The pre-test goals included the estimation of the thermal conductivity value to be used in the CAPL transport roll ABAQUS models. This value was highly dependent on the contact area and pressure. However, calculating this accurately has proved difficult, text books such as Heat Transfer by J.P Holman[53] give only rough estimates for certain grades of steel. The problem was that the strip gauge has proved to have an almost homogenous temperature through its depth, which was especially acute on the thin CAPL gauges (0.5mm). Computational and experimental modelling of the process of heat flow through the strip gauge had further confirmed the difficulties. Thus validation just was not fully possible.

The use of horizontal strip lengths goes against one of the fundamental principles of CAPL design and that was to reduce the unnecessary load points. CAPL's do this by the employing vertical loaded strip and operational parameter controlling devices within enclosed furnaces.

The thermocouple and strain gauge results initially proved slightly disappointing; they were not what the experimental arrangement was originally envisaging, as it was hoped that far higher annealing temperatures would be investigated.

However, while stating this, they did prove useful in understanding how local areas of poor contact generally raise the strain levels to a point that where it translated into considerable higher annealing temperature (which would have a far lower yield point and would be more susceptible to tension fluctuations). It would cause considerable concern to the CAPL operators. Therefore, the emphasis from these experiments was simple: operational parameters have to be carefully controlled, so that extreme temperature differentials are kept in check.

5.2.2 FINAL THOUGHTS AND THE NEXT CHAPTER

The FEA fully-coupled thermo-mechanical model developed for the small scale validation of the Bar-Le-Duc experiments was fine for computational simulations that did not include contact, as long as the discretisation was limited. However, when it came to more complex contact simulations that included roll to strip contact then the computational expense proved to be unworkable.

The forthcoming CAPL computational work (Chapter 7) concentrates on isothermal temperature stress analysis (uncoupled), whereas the earlier Stein Heurtey computational programme concentrated on coupled thermo-mechanical stress analysis. The reason is that a greater understanding of the realities of CAPL furnace stress behaviour had been learnt by the time the latter simulations were being constructed. However, another factor, for using isothermal uncoupled stress analysis models is the computational expense that a fully-coupled contact model demands on any computer system. Finally, it has been proven successfully that the use of temperature dependant mechanical properties is just as accurate (which incidentally is what all previous Corus models and most literature points to using).

While the soaking furnace was where the temperature of the furnace was at its highest, careful control of operational parameters reduces the buckle susceptibility. However, in the heating furnace where the strip starts at room temperature there can be a severe temperature differential generated by the rolls being hotter than the incoming strip steel - a direct link to the experimental work.

In conclusion - The temperature sink must never exceed 150°C even at exceptionally low strip temperatures, or the surface contact simply degenerates. If it degenerates sufficiently then the quality of the strip could possibly be

affected directly from the associated increase in stress. Temperature differentials should be controlled by the process control systems; furthermore, the operators should adhere strictly to the scheduling rules - this does not always happen.

The next step was to look at the CAPL transport roll geometry in detail by the use of computational simulations. The reason - the experimental arrangement was only one part of the strip quality issue problem that affects the Port Talbot CAPL. The major issue is how the roll geometry in different parts of the CAPL furnace in conjunction with variable operational conditions affects CAPL transit strip quality.

6 THE OPERATIONAL AND COMPUTATIONAL EXPERIMENTAL PARAMETERS

Introduction

This chapter discusses the computational models parameters including the mechanical properties. This chapter defines all of the computational parameters and selection criteria for the forthcoming chapter. This chapter discusses the output identifiers and discusses some of the difficult modelling issues that required resolving. This chapter's primary purpose is as a supporting chapter for the forthcoming Chapter 7 "The Computational Modelling of the Transport Roll and Strip Steel Interaction".

6.1 THE PORT TALBOT STRIP

The focal point of the CAPL is the recovery of cold worked steel, however, this depends highly on the steel grade that is being processed, which primarily means formability and secondly the surface quality. The research is based on the commercial quality (CQ) steel and the strip at the other end of the quality spectrum the extra deep draw quality (EDDQ) strip. The EDDQ strip is defined by Corus as the steel with the best formability. However, greater formability translates into a lower yield stress at temperature which makes EDDQ more difficult to anneal successfully[35]. The surface quality requirements of EDDQ are stringent, even the slightest hint of a transport roll scratch are generally not tolerated. The definition of the grade of Corus steel is a reference to the value of formability (r_m)[54].

The formability of the Port Talbot strip is designated as follows

CQ	$r_m = 1$
DQ	$r_m = 1.1\text{-}1.3$
DDQ	$1.5 < r_m < 2$
EDDQ	$r_m > 2$

An isotropic r-value is defined as $r_0=r_{90}=r_{45}=1$, thus the direction of rolling is irrelevant. An anisotropic value of r_m would be greater than 1. The r-value is itself defined as $r = \varepsilon_{width}/\varepsilon_{thickness}$. Shrinkage in the direction of the width is directly proportional to the r-value, the higher the value the less susceptible it is to fracture.

6.1.1 AFFECTS OF HEAT TREATMENT ON GRAIN SIZE [55]

The over-all process of annealing can be divided into three fairly distinct processes, recovery, recrystallisation, and grain growth.

Recovery	The restoration of the physical properties of the cold worked metal without and observable change in the microstructure [38].
Recrystallisation	The density of dislocations decreases considerably on recrystallisation, and all effects of strain hardening are eliminated[38].
Grain Growth	The stored energy of cold work (i.e. the proceeding cold rolling) is the driving force for both recovery and recrystallisation. If the new strain-free grains are heated at a temperature greater than that required to cause recrystallisation, there will be a progressive increase in grain size[38].

6.1.2 THE FUTURE

The furnace temperatures in the soaking section could in the future be sufficient to consider super-plasticity. A metal can be considered super-plastic when its temperature exceeds half of its melting temperature and is referred to as 0.5TM, The melting temperature of carbon steel approximately 1500°C and the current recrystallisation temperature of EDDQ strip being around 750°C.

Looking to the future the CAPL's success will depend somewhat on the more exotic grades of strip that require high annealing temperatures (>850°C). Certain chemistries require a higher recrystallisation temperature than is currently being performed. If the operational restrictions on increasing the temperatures can be overcome them the strip steel could well enter into an area where super-plasticity occurs.

Superplasticity: A fine grain size and a fine dispersion of thermally stable particles which act to pin grain boundaries and maintain the fine grain structure at the high temperature is required for "Superplasticity" deformation.

6.2 THE PORT TALBOT CAPL TRANSPORT ROLL

Introduction

In the modern CAPL there is a mixture of barrelled and tapered rolls. The tapered (hearth) roll is the predominate roll throughout the Port Talbot CAPL; however, it is this type of roll, which is the most complex in design having many geometrical combinations. From the almost near flat to the barrel type roll depending on the size of the taper and central flat section. Furthermore, due to the limited transfer of knowledge between CAPL's around the world it has become clear that no two CAPL's have anywhere near the same roll profile set-ups [25].

6.2.1 DEFINITION OF A TRANSPORT ROLL

The Port Talbot CAPL employs two types of transport roll that of the type "C" - tapered hearth roll, and the type "D" type - barrel roll. *Figure 6.1* shows a two dimensional geometry of the two types of transport roll fitted to the Port Talbot CAPL.

Standard Roll Geometrical Features:

1. The standard radius of curvature machined at the transport rolls fillet point on both the tapered and barrel roll is 20 metres.
2. All the CAPL transport rolls are 2200mm long. This length is fixed by the physical width constraints of the furnace. The strip likewise cannot be wider than 1800mm.

The two principal transport-roll types:

Type "C": (The Conventional Tapered Hearth Roll): Throughout the CAPL, but in many different geometrical set-ups. 750ØD (mm) is the size in the heating and soaking furnaces, and 1200ØD is the size in the secondary cooling section.

Type "D": (Barrel Roll): Limited only to certain top transport rolls within the soaking section of the furnace.

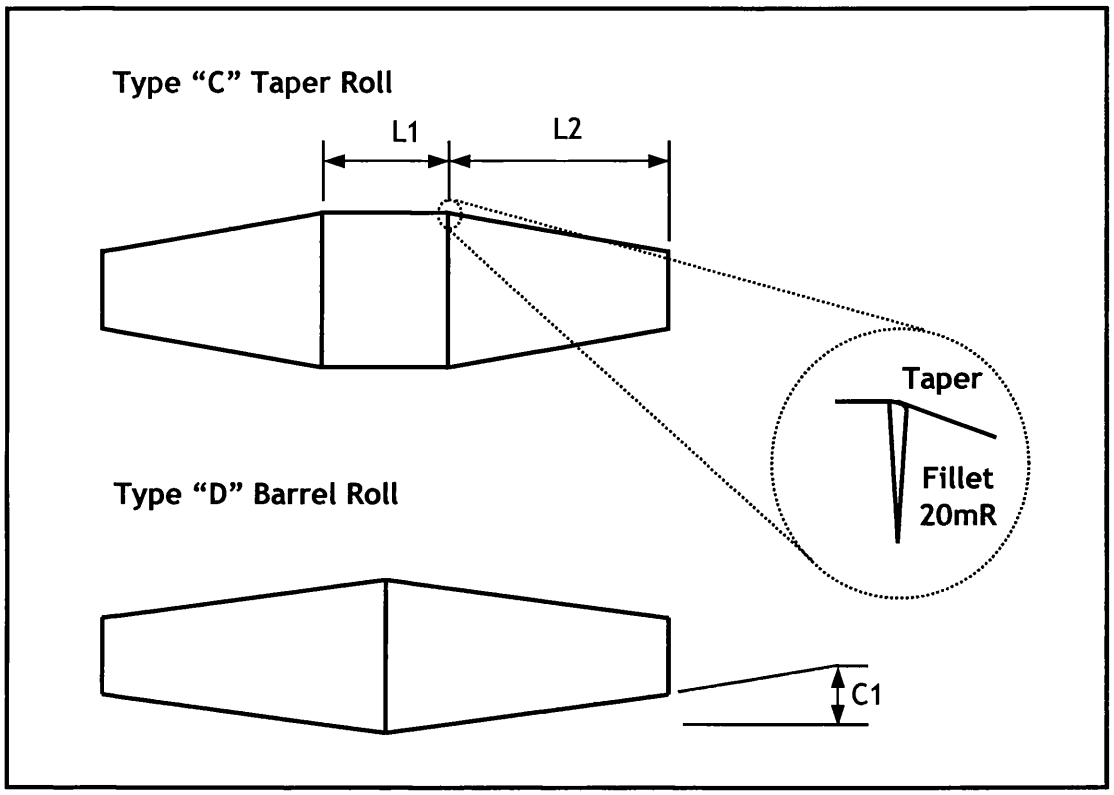

Figure 6.1 The Standard Roll Types of the Port Talbot CAPL

Fillet: Refers to the transition section of the transport roll, and is situated between the central flat section and the taper section.

Taper: Refers to the angled surface section of the rolls; from the roll fillet to the edge of the transport roll.

The simplicity of the geometry of the transport roll is vital. The benefits of the type "C", is the widely accepted theory that the flat section (the "L1" central flat section) helps to reduce buckle susceptibility - the ideal width of this flat section depends entirely on the operational parameters of that section of the furnace and the formability properties of the strip. The taper size ("C1" on length "L2") aids in the prevention of tracking of the strip from the rolls centreline.

Friction is integral to good contact; the CAPL operators know this, and have duly invested in surface texture technology and detailed maintenance schedules to prevent roll wear being an initiator of strip failure. The author considers the transport roll as a constant - the preventative transport roll maintenance schedules employed by Corus prevent uneven roll wear from ever realistically

becoming an operational issue. Corus for their part do not want asymmetrical roll geometries, it simply creates unpredictability.

6.2.2 PORT TALBOT CAPL TRANSPORT ROLL SCHEDULE

Furnace Zone	L1	L2	C1	∅	Length
Heat Furnace	500	850	3.3	750	2200
Soak Furnace	700	750	0.41	750	2200
	-	-	0.35	750	2200
Cool Section	1000	600	0.41	750	2200
Overage Furnace	700	750	1.4	1200	2200
2nd Cool Section	700	750	1.4	1200	2200

Table 6.1 The Standard Transport Rolls Considered (mm)

6.3 HOT TENSILE TESTING OF EDDQ STRIP STEEL

Introduction

For computational model accountability hot tensile test data was analysed for EDDQ graded material. The hot tensile tests were performed at Corus RD&T's Swinden Research Centre (STC) using a "Zwick tensilometer", in accordance to British Standard "BS EN 10002 Part 5". The constantly applied strain rate using the crosshead system was 0.0033per/min, which gives a strain rate to the specimen of 0.002 per/min. The mechanical properties in *Table 6.2* were used in the CAPL roll-strip computational models.

6.3.1 HOT TENSILE TEST RESULTS[28]

Testing Temperature (°C)	0.2% Proof Stress (MPa)	Young's Modulus of Elasticity (GPa)
210	211	191
410	170	172
675	60	95
750	15	70
850	5.5	31

Table 6.2 The Temperature Dependent Mechanical Properties For EDDQ Strip

For confidence purposes the research projects hot tensile test data was compared against confidential Corus reports. The author also consulted with other Corus research engineers[29, 32].

The following communication from the technician that performed the hot tensile tests highlights the difficulties associated with high temperature testing:

- No absolute point of elastic-plastic transformation.
- The limit of proportionality is the only point that can approximately be assessed.
- The standard parameters to quote are the 0.2% proof stress for non-austenitic grades.
- The proof stress is basically a safety factor. Calculated by drawing a line parallel to the elastic portion of the stress-strain graph. This line intersects the x-axis (the strain) at the 0.2% elongation point. The corresponding point it hits on the stress-strain curve is the 0.2% permanent deformation or proof stress, denoted as $\sigma_{0.2}$.

6.3.2 STRESS-STRAIN CURVES OF HOT TENSILE TESTING

For the purposes of showing the difficulties of tensile testing at elevated temperatures the author has given two examples below. (Supplied by CORUS RD&T[28]).

For low temperature (210°C) tensile testing as seen in *Figure 6.2* below, it can be seen that there is a fairly clear point at which the linear behaviour ends and thus the elasticity ends. Generally at a low testing temperature such as this, a proof stress of 0.1% can be used, as the yield point is so clear. A proof stress value of 0.2% is further round the curve and thus represents a small degree more of strain-rate hardening and therefore plasticity. However, in CAPL research there is little requirement for stress-strain analysis of low temperature properties. As mentioned on numerous occasions the CAPL roll-strip contact is about transportation not deformation, therefore strain-rate hardening is of little interest to the author.

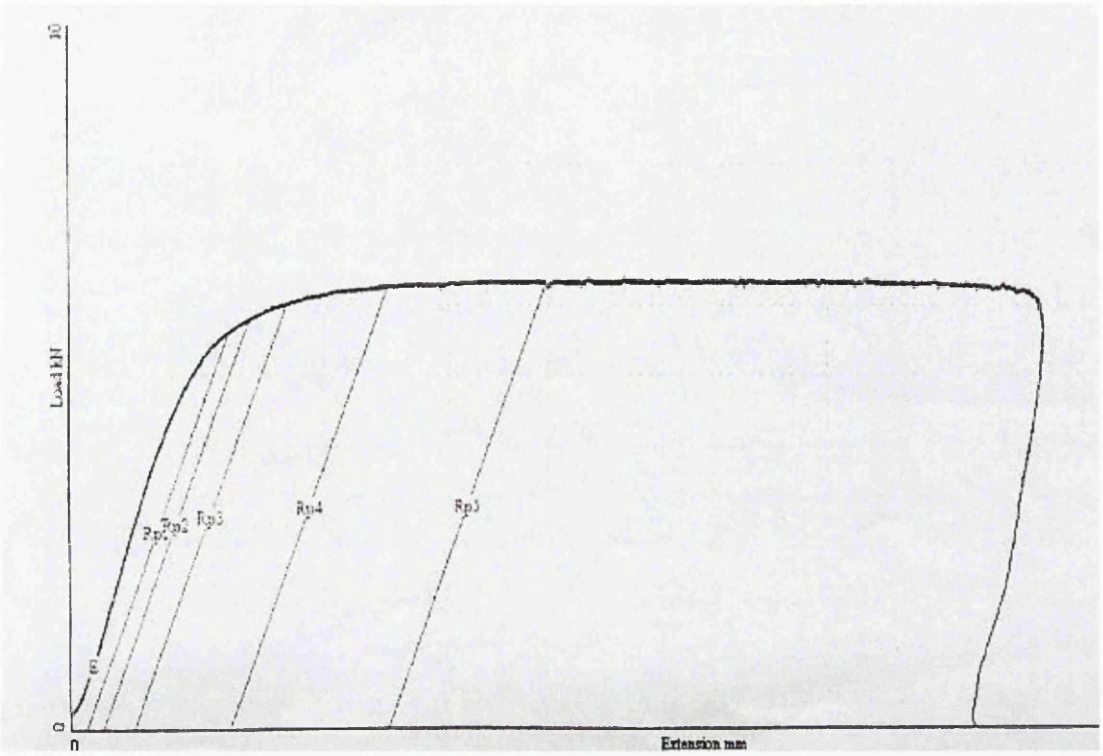

Figure 6.2 Hot Tensile Stress-Strain Graph - 210°C[28]

For high temperature (750°C) tensile testing as seen in *Figure 6.3* below, it can be seen that the experimental results indicate no clear elastic point. A typical high temperature experimental test would last 7 hours at a constant strain rate, where as the CAPL anneals strip in a matter of minutes. Due to the high levels of scatter around the yield point, a proof stress of 0.2% is used to represent the yield stress. The scatter appears to shows areas of strain-rate hardening followed by relief and then strain-rate hardening again etc.

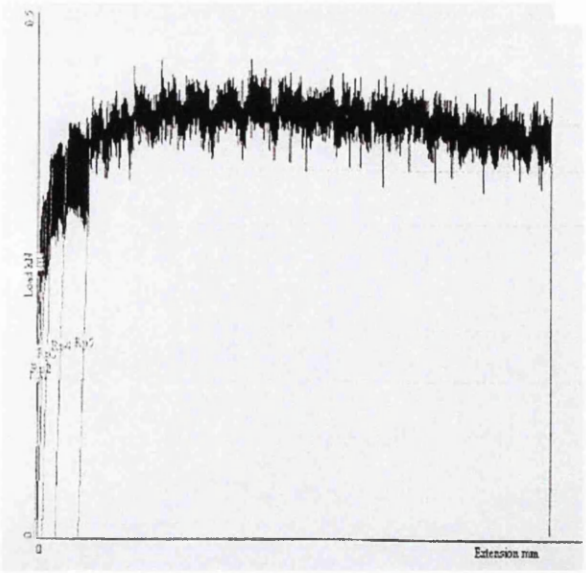

Figure 6.3 Hot Tensile Stress-Strain Graph - 750°C[28]

6.3.3 COMPUTATIONAL MODEL ELASTIC-PLASTIC CHARACTERISTICS

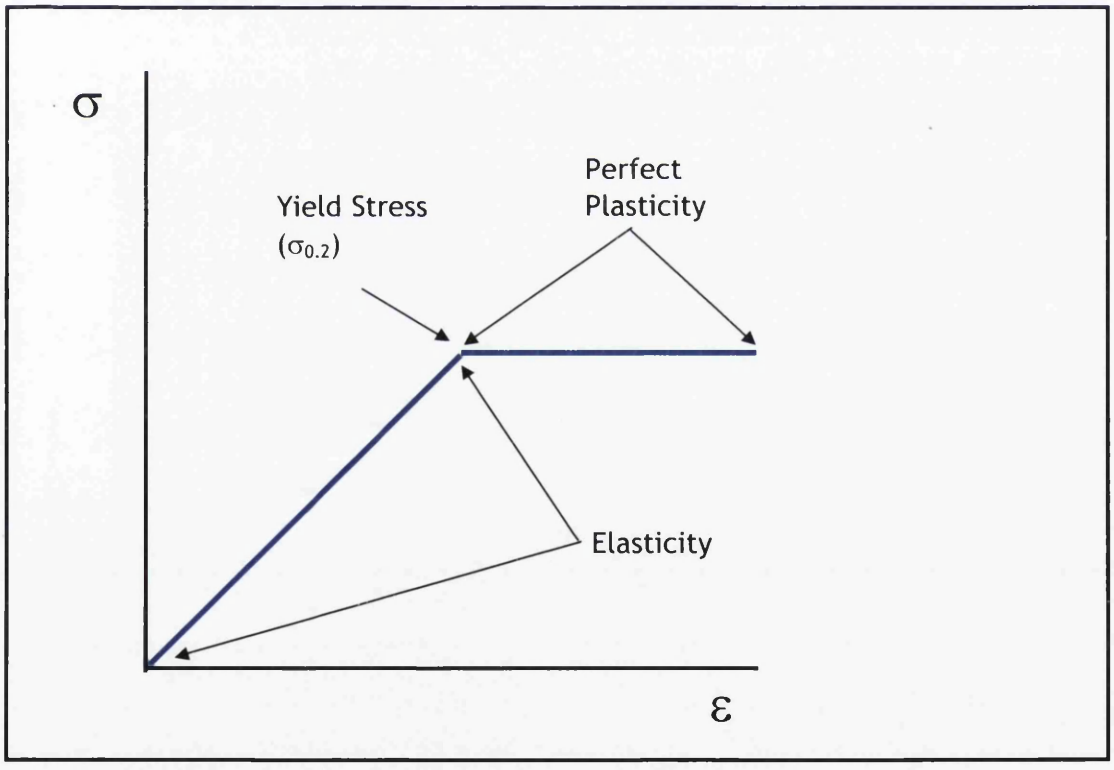

Figure 6.4 Elastic Perfectly-Plastic Stress-Strain Graphs, as Used on CAPL Computational Simulations

As the model is essentially an elastic model, the strip is defined as a set of grouped interlocking shell elements. The FEA inputted values for material

behaviour are limited to Yield Stress (0.2% Proof Stress), Young Modulus of Elasticity and Poisson's Ratio; the model is isothermal. The results from the hot tensile testing are input into separate models to represent the desired furnace temperature.

The stress-strain model does not include rate dependant plastic strain. Thus the yield stress is also the maximum stress accordingly to the von Mises yield criterion. Several papers conclude that elastic perfectly-plastic is the most appropriate method to use for CAPL roll-strip contact research, including the latest paper on CAPL buckle by Jacques N et al[56].

6.4 PRINCIPAL ABAQUS MODEL CONSIDERATIONS

6.4.1 SHELL ELEMENT CONSIDERATIONS

6.4.1.1 Strip Steel

The element choice used for stress displacement analysis is the first-order linear S4R element, which is available to both ABAQUS Standard and ABAQUS Explicit. An S4R is a 4-node, double curved thin or thick shell, reduced integration, hourglass control, finite membrane strains and materials involving non-zero effective Poisson's Ratio. Reduced integration usually provides more accurate results and significantly reduces running time. For first order elements such S4R, hourglass control is required.

The heat transfer shell element is DS4, which stands for heat transfer quadrilateral shell. Hourglass control is recommended for first-order linear elements, because of the occasions of deficiency in the stiffness matrix causing zero energy.

There are several different ways to mesh a model; the most common is through the use of free meshing, which is the most flexible technique. It uses no pre-established mesh patterns and can be applied to almost any model shape. The research here requires partitioning for aiding in uniform tension. However, this has prevented free meshing to be used on the stress displacement model, the alternative meshing technique was structured meshing. This form of meshing gives the most control, because it applies a pre-established mesh pattern to a particular model by forcing it to accept a shape pattern. The Simpson integration scheme is used to calculate the shell cross-sectional behaviour. It has been shown that five

integration points in the shell thickness are sufficient to obtain accurate results[56].

6.4.1.2 Transport Roll

The transport roll is modelled analytically rigid. The term analytically rigid refers to a feature, which is used in a contact situation; it represents a part that is so much stiffer than the rest of the model that its deformation can be considered negligible. The roll is developed as a shell part similar to that as the strip, however, the roll is not meshed and, while it can have a bearing on the strips output identifiers it has none of its own.

6.4.2 CONTACT CONDITIONS

6.4.2.1 The Contact Parameter Formulation[48, 49]

The contact formulation - "finite sliding" or "small sliding" - specifies the expected relative tangential displacement of the two surfaces. "Finite sliding" is the most general, but it is computationally more demanding and can lead to convergence problems if the contacting surfaces are not smooth or one of them has an excessive directional changes in its geometry while interacting. Finite sliding is considered appropriate to serve the low-tension contact conditions that are prevalent with strip transportation. Furthermore, finite sliding while it may be computationally more expensive it gives more accurate results for infinitesimal changes in strain.

The relationship between the contact pressure and initial separation between the contacting surfaces is considered "hard" for both of the authors ABAQUS Standard and ABAQUS Explicit models. The "hard" contact condition is defined in the interaction properties module of ABAQUS CAE, with hard contact being defined as a "normal" frictional formulation. This type of formulation prevents pressure over closure, and thus prevents the interacting master and slave surfaces from inter-penetrating each other - thus "hard" contact helps with convergence as the first time step begins. The normal frictional formulation also employs a default elastic slip value for use with ABAQUS Standard. The use of the "hard" contact can affect results if the model does not allow separation after contact. The use of separation after contact is important, if separation in the model is not permitted after the first increment of the analysis then the contact between the transport roll and the strip steel would be considered perfect. The affect of "no" separation would have

only a small affect on the static model, as this type of model is purely a compression and tension model where the strip is bending around the rolls surface under the load of the line in-line tension applied to the hanging strip. However, if separation were not permitted on a dynamic model the strip would be in perfect contact with the transport roll as it rotates. After much deliberation it was considered that normal friction had to be used for the initial time step increment, it helped with the problems of analysis convergence, which was proving to be an issue with the ABAQUS Standard models. The author's explicit dynamic models employ a two time step approach. The first time step is static with just the application of line tension. The second time step is where the roll velocity is applied. The dynamic nature of this second time step requires a different form of frictional force to maintain roll-strip contact. The other method of introducing frictional forces is the "tangential" friction formulation. When surfaces are in contact they usually transmit shear as well as normal forces across their interface. The tangential friction formulation uses a conventional friction coefficient.

Apart from the consideration given to the friction formulation another important factor of frictional contact are sudden large displacements as the computational model runs. Sudden large displacements can cause the model to fail thus the parameter "NLGEOM" is introduced. The *NLGEOM function is especially useful at model start-up where sudden very large strains can be registered on certain elements, thus "NLGEOM" aids in convergence. The "NLGEOM" parameter does also help to mask poor time step increment settings (implicit models only). The definition of the "NLGEOM" function is given as follows - "This solution automatically introduces pseudo-inertia force at all nodes when instability is detected"[48].

When "NLGEOM" is specified, most elements are formulated in the current configuration using current nodal positions. Elements therefore distort from their original shapes as the deformation increases.

6.4.2.2 Essential Linear Constraints[48, 50, 52]

The linear constraint equation is applied to the edge of the strip steel so that a concentrated force can be applied to represent in-line tension. The ABAQUS model development resulted in shell elements representing the strip (continuum elements are not appropriate for ultra thin applications), which created an instant

problem of how to apply in-line tension? The only sensible way in which to apply line tension is as a concentrated force (*CLOAD) in the "load module". The problem with using shell elements when trying to apply concentrated forces is that they can only realistically be applied to the end nodes at the end of the vertical hanging strip lengths (i.e. the hanging strip lengths either side of the transport roll), thus preventing the tension being applied uniformly across the strips end sections - this is incidentally the same for all previous Corus ABAQUS CAE CAPL models. Previous CAPL researchers have tried to negate this obvious tension inequality issue by modelling the strip length at least 3 times greater than the strip width. The use of long lengths is generally considered fine because on the actual CAPL the rolls are considerably further than 3 times strip width; furthermore, one of the causes of buckle is attributed to the long unsupported distance that ultra-thin strip has to travel between rolls passes. However, unequal line tension is considered alongside poor roll geometry as potentially the most detrimental operational parameter to strip quality, so an alternative end node loading was sought.

The application of a linear constraint to the end of the strip length allows the concentrated force that is then applied to be virtually equal across the strip width. Linear multi-point constraint equations (*EQUATION) are applied in the "interaction module". They effectively combine the whole of the edge of the shell element as one node, however fine the mesh. Thus enabling only one concentrated force load to be applied, which then acts in a normal cross-sectional way like in-line strip tension should do.

The application starts by the formation of four sets (using *SET command), two sets for each end of the hanging strip that circumnavigates the transport roll. One set for the end node (SET- 1 & 3), see figure below.

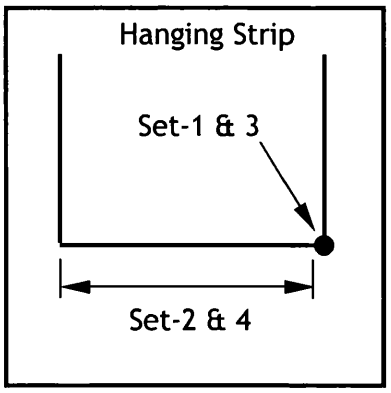

Figure 6.5 Application of *SETS for Interaction and Loads

The other set (SET- 2 & 4) is the rest of the strip width along the same edge as SET 1 (see figure above). The second set involves sectioning all of the strip edge apart from the end node, which makes up the first set. This second set represents more than 99% of the entire edge length. The two sets for one edge are then tied together by the *EQUATION command as a constraint.

SET COMMAND

SET 1	-1	DOF2
SET 2	1	DOF2

The DOF2 refers to the degrees of freedom that have been tied, which, in this case is the y-axis, i.e. vertical strip movement. The (1) and (-1) are required because a linear multi-point constraint requires that a linear combination of nodal variables balance. The only draw back is that even with this technique the tension will not be entirely equal because the section equates to a little over 99% of the strip.

6.4.2.3 Prescribing of Symmetry Boundary Conditions

The primary purpose of the symmetry boundary condition is to reduce the computational time. Symmetry boundary conditions work by turning off nodal degrees of freedom to represent a plane of symmetry.

The symmetry plane is dependant entirely on the orientation of the strip. However, the edge of the half modelled geometry is where the symmetry boundary condition would normally be applied. All dynamic and most static

models have symmetry boundary conditions applied to the edge of the half modelled strip (the edge that represents the centreline).

The orientation of the CAPL models was such that the Z-axis symmetry (ABAQUS variable - *ZSYMM) was assigned to the shell elements that represent the edge of the strip closest to the transport rolls centreline - this *ZSYMM then acts as the strips centreline. The affect of assigning a *ZSYMM is that the computational program doubles the strip width for the axis that the symmetry is applied.

There are six translational and rotational degrees of freedom (DOF). The translational are as follows: X = 1, Y = 2 and Z = 3 and the rotational are as follows X = 4, Y = 5 and Z = 6.

There are three types of symmetry condition that can be applied and a further two more restrictive conditions of which the *ENCASTRE boundary condition is often applied to restrict total movement in the analytically rigid transport roll.

ZSYMM: Symmetry about a plane Z = constant (degrees of freedom 3,4,5 = 0).

The *ZSYMM boundary condition for this research project works as following, the strip at the centreline can move away from the transport roll and lose contact thanks to an active translational DOF1 (x-axis) and translational DOF2 (y-axis). However, the DOF3 (z-axis), which defines the strips width, is restricted to prevent movement, the model cannot move at the strips centreline; the ABAQUS formulation will still affect displacement in the rest of the strip. However, a symmetry condition has now occurred and even though no results are given for the half of the strip which has not been developed, the symmetry condition now treats the other half of the strip from the *ZSYMM edge onwards as half of a whole width strip steel section. This is further reinforced by restrictions to the rotational degree of freedom. The restriction on DOF4 and DOF 5 restricts rotational movement at the centreline of the strip in the x-axis and y-axis. These two axes are restricted while the rotational z-axis (DOF6) is free, if the shell elements on the edge, which represent the strips centreline were capable of rotating at DOF 4 and DOF 5 then they would rotate the strip at its centre (longitudinally in the case of DOF4 and through the gauge if DOF5) this would not be natural if it was the

centreline of a full width strip. Furthermore, a restriction to DOF6 (z-axis) would restrict the strip at the centreline from bending around the transport roll.

6.5 ROLL-STRIP MODEL PARAMETERS

Introduction

The developments of the schedules of work are based firmly on the Corus Port Talbot product range. All models have a fundamental base; only small variations in the computational input parameters are permitted at any one time. This gives the author the opportunity to see how a particular parameter change has affected the output result.

Initial roll strip contact can cause buckle susceptibility right across the contact plane of the strip; however, it is highest at the circumferential knuckle point. To aid in understanding how the stress accumulates the author decided that the roll fillet should be removed on the majority of the CAPL computational models. This cut edge could be significant, however, the worse case angle within the soaking furnace is 0.03°, where buckle susceptibility is at its highest. There are still significant models with fillets for comparisons purposes. Plus it must be remembered that these models are a representation only of contact, and all CAPL computational models differ depending on the research organisation.

Although gravity can easily be considered, it is not included here, because the method of applying gravity to the Port Talbot CAPL varies with the location of the tension meters, which provide line tension values. For simplicity, the top roll is referred to here in all cases. However, the results and discussions apply to the bottom of the rolls as well.

The computational model pre-assumption: Perfect initial flatness, residual stress free and perfect strip alignment.

6.5.1 ABAQUS COMPUTATIONAL PARAMETERS

This section defines all of the model parameters that are used in Chapter 7. The section starts with a list of parameters, which are then defined into models (Section 6.5.2 for static models and Section 6.5.3 for dynamic models) The figure below details the model set-up and defines the four probed element values (contact roll centre, contact roll fillet, top roll centre and top roll fillet).

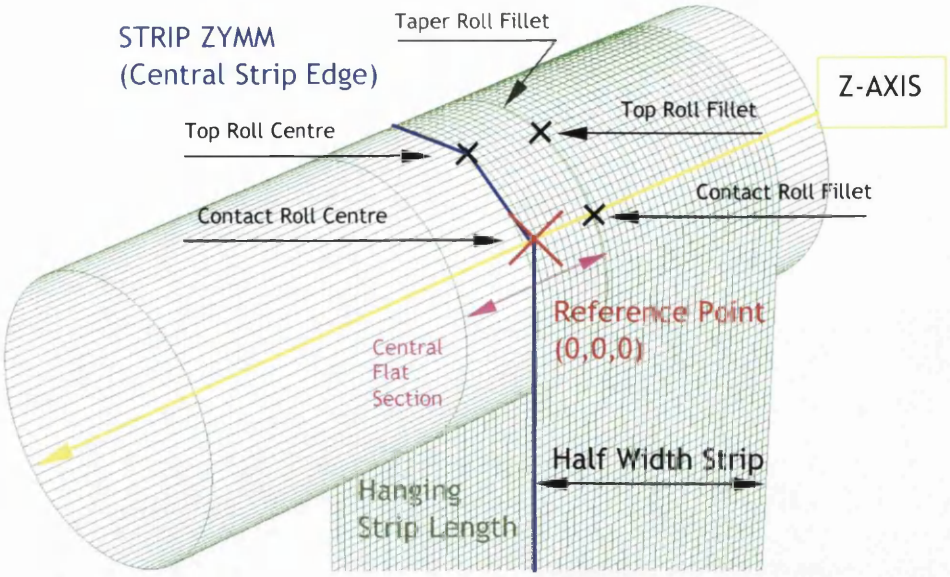

Figure 6.6 3D Illustration of Typical Roll-Strip Contact Assembly for a Half Strip Width

6.5.1.1 Roll Geometries

Roll Geometry: Flat

3D analytical rigid, length 2200mm, central ∅ 750mm

Roll Geometry: Flat_HT

3D deformable, length 2200mm, central ∅ 1200mm

Roll Geometry: Flat_1200

3D analytical rigid, length 2200mm, central ∅ 1200mm

Roll Geometry: C1

3D analytical rigid, length 2200mm, central ∅ 750mm, (L1) 500mm, (L2) 850mm, (C1) 3.3mm

Roll Geometry: C1_0.9

3D analytical rigid, length 2200mm, central ∅ 750mm, (L1) 500mm, (L2) 850mm, (C1) 0.9mm

Roll Geometry: C5

3D analytical rigid, length 2200mm, central ∅ 750mm, (L1) 700mm, (L2) 750mm, (C1) 0.41mm

Roll Geometry: C5_0.05

3D analytical rigid, length 2200mm, central ∅ 750mm, (L1) 700mm, (L2) 750mm, (C1) 0.05mm

Roll Geometry: C5_0.9

3D analytical rigid, length 2200mm, central ∅ 750mm, (L1) 700mm, (L2) 750mm, (C1) 0.9mm

Roll Geometry: C5_1.4

3D analytical rigid, length 2200mm, central ∅ 750mm, (L1) 700mm, (L2) 750mm, (C1) 1.4mm

Roll Geometry: C6

3D analytical rigid, length 2200mm, central ∅ 750mm, (L1) 1000mm, (L2) 600mm, (C1) 0.41mm

Roll Geometry: C6_0.15

3D analytical rigid, length 2200mm, central ∅ 750mm, (L1) 1000mm, (L2) 600mm, (C1) 0.15mm

Roll Geometry: C6_0.9

3D analytical rigid, length 2200mm, central ∅ 750mm, (L1) 1000mm, (L2) 600mm, (C1) 0.9mm

Roll Geometry: C8

3D analytical rigid, length 2200mm, central ∅ 1200mm, (L1) 700mm, (L2) 750mm, (C1) 1.4mm

Roll Geometry: C8_0.9

3D analytical rigid, length 2200mm, central ∅ 1200mm, (L1) 700mm, (L2) 750mm, (C1) 0.9mm

Roll Geometry: D1

3D analytical rigid, length 2200mm, central ∅ 750mm, (C1) 0.35mm

Roll Geometry: D1_0.15

3D analytical rigid, length 2200mm, central ∅ 750mm, (C1) 0.15mm

Roll Geometry: D1_0.9

3D analytical rigid, length 2200mm, central ∅ 750mm, (C1) 0.9mm

Roll Geometry: D1_4.0

3D analytical rigid, length 2200mm, central ∅ 750mm, (C1) 4.0mm

6.5.1.2 Strip Dimensions

Strip Dimensions: F900

3D deformable, full-width 900mm, hanging length 5400mm

Strip Dimensions: F1000

3D deformable, full-width 1000mm, hanging length 1000mm

Strip Dimensions: F1250

3D deformable, full-width 1250mm, hanging length 5400mm

Strip Dimensions: H1800

3D deformable, half-width 900mm, hanging length 5400mm

Strip Dimensions: F1800

3D deformable, full-width 1800mm, hanging length 5400mm

6.5.1.3 Strip Properties

Strip Properties: 10MPa

density 7800kg/m^3, elastic (isotropic) 50GPa, Poisson's Ratio 0.3,

plastic (isotopic) 10MPa, plastic strain 0

Strip Properties: 15MPa
density 7800kg/m^3, elastic (isotropic) 70GPa, Poisson's Ratio 0.3, plastic (isotopic) 15MPa, plastic strain 0

Strip Properties: 60MPa
density 7800kg/m^3, elastic (isotropic) 95GPa, Poisson's Ratio 0.3, plastic (isotopic) 60MPa, plastic strain 0

Strip Properties: 100MPa
density 7800kg/m^3, elastic (isotropic) 95GPa, Poisson's Ratio 0.3, plastic (isotopic) 100MPa, plastic strain 0

Strip Properties: 170MPa
density 7800kg/m^3, elastic (isotropic) 172GPa, Poisson's Ratio 0.3, plastic (isotopic) 170MPa, plastic strain 0

Strip Properties: 211MPa
density 7800kg/m^3, elastic (isotropic) 191GPa, Poisson's Ratio 0.3, plastic (isotopic) 211MPa, plastic strain 0

Strip Properties: Elastic
density 7800kg/m^3, elastic (isotropic) 95GPa, Poisson's Ratio 0.3

Strip Properties: Heat Transfer
conductivity (isotropic) 67W/mK (100°C) 38W/mK (600°C), density 7800kg/m^3, expansion (isotropic) 1.192E-005m/mK (100°C) 1.447E-05m/mK (600°C), specific heat 480j/kgK (100°C) 779j/kgK (600°C).

6.5.1.4 Contact Assembly

Contact Assembly: Half-Width
The roll is positioned along the z-axis with its absolute centre point at co-ordinates (0,0,0). The modelled half-width strip is positioned on the rolls top surface, so that the strips inside edge, lines up with the centreline

Contact Assembly: Full-Width
The roll is positioned along the z-axis with its absolute centre point at co-ordinates (0,0,0). The modelled full-width strip is positioned on the rolls top surface, so that the strips centre, lines up with the centreline

Contact Assembly: Pontardulais
The roll is positioned along the z-axis with its absolute centre point at co-ordinates (0,0,0). The modelled full-width strip is positioned on the rolls top surface, so that the strips centre, lines up with the centreline. The down stream length is positioned so that it is at a 90° angle to that of the upstream length

6.5.1.5 Analysis Step

Step: Static General
Step-1, time period 0.3625, NLGEOM = ON, increment 0.001, 1E-09, 0.02, load = ramp
Step: Heat Transfer
Step-1, transient, time period 2, increment 0.01, 0.01, 0.1, load = instantaneous

Step: Dynamic Explicit
Step-1, time period 0.125, NLGEOM = ON, increment automatic
Step-2, time period 0.6, NLGEOM = ON, increment automatic

6.5.1.6 Interaction Properties

Interaction: Standard
Step-1, master surface = roll, slave surface = strip, finite sliding formulation, adjust only over-closed nodes

Contact Properties: Standard
tangential friction (isotropic) 0.3 (penalty formulation),
normal friction (hard contact), allow separation after contact

Contact Properties: Standard_0.15
tangential friction (isotropic) 0.15 (penalty formulation),
normal friction (hard contact), allow separation after contact

Contact Properties: Standard_0.45
tangential friction (isotropic) 0.45 (penalty formulation),
normal friction (hard contact), allow separation after contact

Strip Constraints: Standard
Constraint-1 (equation) = Coefficient 1, Set-2, DOF2, Coefficient -1,
Set-1, DOF2
Constraint-2 (equation) = Coefficient 1, Set-4, DOF2, Coefficient -1,
Set-3, DOF2
(See Section 6.4.2.2 for details of application)

Strip Constraints: Unequal
Constraint-1 (equation) = Coefficient 1, Set-2, DOF2, Coefficient -1,
Set-1, DOF2
Constraint-2 (equation) = Coefficient 1, Set-4, DOF2, Coefficient -1,
Set-3, DOF2
Constraint-3 (equation) = Coefficient 1, Set-6, DOF2, Coefficient -1,
Set-5, DOF2
Upstream strip end partitioned so that both end nodes at either
edge can be used to specify unequal tension.

6.5.1.7 Load Properties (Full Strip Width 1800mm x 0.4mm Gauge)

In-Line Tension: 3.5MPa
Step-1, CF2 = -1260 (half-strip), CF2= -2520 (full-strip), applied to
Set-1 and Set-3 (See Section 6.4.2.2 for details of application)

In-Line Tension: 5MPa
Step-1, CF2 = -1800 (half-strip), CF2= -3600 (full-strip), applied to
Set-1 and Set-3 (See Section 6.4.2.2 for details of application)

In-Line Tension: 3MPa-7MPa
Step-1, Load-1 = CF2= - 3600 (full-strip), applied to Set-3 (5MPa),
Load-2 = CF2 = -1080 (half-strip), applied to Set-1 (3MPa),
Load-3 = CF2 = -2520 (half-strip), applied to Set-5 (7Mpa)

In-Line Tension: 8MPa
Step-1, CF2 = -2880 (half-strip), CF2= -5760 (full-strip), applied to Set-1 and Set-3 (See Section 6.4.2.2 for details of application)

In-Line Tension: 12.5MPa
Step-1, CF1 = 7031 (90°), CF2 = -7031, applied to Set-1 and Set-3 (See Section 6.4.2.2 for details of application)

Strip Symmetry: ZSYMM
Step-1, Z-SYMM, inside strip edge (See Section 6.4.2.3 for details of application)

Roll Symmetry: Encastre
Step-1, Encastre, roll reference point (0,0,0) (See Section 6.4.2.3 for details of application)

Roll Velocity: 300m/min
Step-1, all components = 0 assigned to roll reference point
Step-2, VR3 = 13.333Radians/Time (all other components = 0)

Roll Velocity: 400m/min
Step-1, all components = 0 assigned to roll reference point
Step-2, VR3 = 17.778Radians/Time (all other components = 0)

Roll Velocity: 500m/min
Step-1, all components = 0 assigned to roll reference point
Step-2, VR3 = 22.222Radians/Time (all other components = 0)

Roll Velocity: 600m/min
Step-1, all components = 0 assigned to roll reference point
Step-2, VR3 = 26.667Radians/Time (all other components = 0)

Strip Velocity: 0.5m/s

Step-1, does not apply

Step-2, V3= -0.5m/s (entire strip instance)

6.5.1.8 Mesh

Mesh: S4R

Size 25 x 25mm, first 2700mm hanging

Size 100 x 25mm, last 2700mm hanging

Mesh: DS4

Size 50 x 50mm, roll & strip

6.5.2 STATIC MODEL PARAMETERS

6.5.2.1 Standard Roll Crowns

Model 1.1 Roll Geometry: Flat, Strip Dimensions: H1800, Strip Properties: 15MPa, Strip Gauge 0.4mm, Contact Assembly: Half-Width, Step: Static General, Interaction: Standard, Contact Properties: Standard, Strip Constraints: Standard, In-Line Tension: 5MPa, Strip Symmetry: ZSYMM, Roll Symmetry: Encastre, Mesh: S4R

Model 1.2 Roll Geometry: C5 (rest *Model 1.1*)

Model 1.3 Roll Geometry: C1 (rest *Model 1.1*)

Model 1.4 Roll Geometry: D1 (rest *Model 1.1*)

Model 1.5 Roll Geometry: C6, Strip Properties: 60MPa (rest *Model 1.1*)

Model 1.6 Roll Geometry: C6, Strip Properties: 170MPa (rest *Model 1.1*)

Model 1.7 Roll Geometry: C8, Strip Properties: 170MPa (rest *Model 1.1*)

Model 1.8 Roll Geometry: C8, Strip Properties: 211MPa, In-Line Tension: 8MPa (rest *Model 1.1*)

6.5.2.2 Variations in Key Operational Parameters

Model 2.1 Roll Geometry: C5_0.9, Strip Dimensions: F1800, Strip Properties: 10MPa, Strip Gauge 0.4mm, Contact Assembly: Full-Width, Step: Static General, Interaction: Standard, Contact Properties: Standard, Strip Constraints: Standard, In-Line Tension: 5MPa, Roll Symmetry: Encastre, Mesh: S4R

Model 2.2 Roll Geometry: C5, Strip Properties: 15MPa (rest *Model 2.1*)

Model 2.3 Roll Geometry: C1_0.9, Strip Properties: 15MPa (rest *Model 2.1*)

Model 2.4 Roll Geometry: C5_0.9, Strip Properties: 15MPa, Strip Gauge 0.2mm (rest *Model 2.1*)

Model 2.5 Roll Geometry: C5_0.9, Strip Properties: 15MPa, In-Line Tension: 3.5MPa (rest *Model 2.1*)

Model 2.6 Roll Geometry: C5_0.9, Strip Properties: 15MPa (rest *Model 2.1*)

Model 2.7 Roll Geometry: C5_0.9, 20mR fillet on roll taper, Strip Properties: 15MPa (rest *Model 2.1*)

Model 2.8 Roll Geometry: C5_0.9, Strip Dimensions: F900, Strip Properties: 15MPa (rest *Model 2.1*)

Model 2.9 Roll Geometry: C5_0.9, Strip Properties: 15MPa, In-Line Tension: 8MPa (rest *Model 2.1*)

Model 2.10 Roll Geometry: C6_0.9, Strip Properties: 15MPa (rest *Model 2.1*)

Model 2.11 Roll Geometry: C5_1.4, Strip Properties: 15MPa (rest *Model 2.1*)

Model 2.12 Roll Geometry: D1_0.9, Strip Properties: 15MPa (rest *Model 2.1*)

Model 2.13 Roll Geometry: C8_0.9, Strip Properties: 15MPa (rest *Model 2.1*)

Model 2.14 Roll Geometry: C5_0.9, Strip Properties: 15MPa, Strip Properties: 60MPa (rest *Model 2.1*)

6.5.2.3 Taper Rolls Influence of Roll Taper Radius

Model 3.1 Roll Geometry: Flat, Strip Dimensions: Width H1800, Strip Properties: 15MPa, Strip Gauge: 0.4mm, Contact Assembly: Half-Width, Step: Static General, Interaction: Standard, Contact Properties: Standard, Strip Constraints: Standard, In-Line Tension: 5MPa, Strip Symmetry: ZSYMM, Roll Symmetry: Encastre, Mesh: S4R

Model 3.2 Roll Geometry: C1 (rest *Model 3.1*)

Model 3.3 Roll Geometry: C1, 20mR fillet on roll taper (rest *Model 3.1*)

Model 3.4 Roll Geometry: C1, 40mR fillet on roll taper (rest *Model 3.1*)

Model 3.5 Roll Geometry: C5 (rest *Model 3.1*)

Model 3.6 Roll Geometry: C5, 20mR fillet on roll taper (rest *Model 3.1*)

Model 3.7 Roll Geometry: D1 (rest *Model 3.1*)

Model 3.8 Roll Geometry: D1, 20mR fillet on roll taper (rest *Model 3.1*)

6.5.2.4 Tension Loading Issues at Corus Pontardulais Works

Model 4.1 Roll Geometry: D1_4.0, 20mR fillet on roll taper, Strip Dimensions: F1250, Strip Properties: 100MPa, Strip Gauge: 0.45mm, Contact Assembly: Pontardulais, Step: Static General, Interaction: Standard, Contact Properties: Standard, Strip Constraints: Standard, In-Line Tension: 12.5MPa, Roll Symmetry: Encastre, Mesh: S4R

6.5.2.5 Heat Transfer Considerations

Model 5.1 Roll Geometry: Flat_HT, Strip Dimensions: F1000, Strip Properties: Heat Transfer, Strip Gauge: 1mm, Roll Gauge: 22mm, Contact Assembly: Full-Width, Step: Heat Transfer, Interaction: Standard, Conductance: 1600W/m^{2}K, Roll Temperature (Field): 200°C, Strip Temperature (Field): 300°C, Mesh: DS4

Model 5.2 Roll Geometry: Flat_HT, Roll Temperature (Field): 400°C, Strip Temperature (Field): 600°C, SFILM 5, SRADIATE 0.25 (rest *Model 5.1*)

Model 5.3 Roll Geometry: Flat_HT, Strip Gauge 0.2mm, Roll Temperature (Field): 400°C, Strip Temperature (Field): 600°C, SFILM 5, SRADIATE 0.25 (rest *Model 5.1*)

Model 5.4 Roll Geometry: Flat_HT, Strip Gauge 0.2mm, Conductance: 1000W/m^{2}K, Roll Temperature (Field): 400°C, Strip Temperature (Field): 600°C (rest *Model 5.1*)

Model 5.5 Roll Geometry: Flat_HT, Strip Gauge 2mm, Roll Temperature (Field): 400°C, Strip Temperature (Field): 600°C (rest *Model 5.1*)

6.5.3 DYNAMIC MODEL PARAMETERS

6.5.3.1 Standard Roll Crowns

Model 6.1 Roll Geometry: Flat, Strip Dimensions: H1800, Strip Properties: 15MPa, Strip Gauge 0.4mm, Contact Assembly: Half-Width, Step: Dynamic Explicit, Interaction: Standard, Contact Properties: Standard, Strip Constraints: Standard, In-Line Tension: 5MPa, Strip Symmetry: ZSYMM, Roll Velocity: 300m/min, Mesh: S4R

Model 6.2 Roll Geometry: C5_0.05 *(rest Model 6.1)*

Model 6.3 Roll Geometry: C5 *(rest Model 6.1)*

Model 6.4 Roll Geometry: D1_0.15 *(rest Model 6.1)*

Model 6.5 Roll Geometry: D1 *(rest Model 6.1)*

Model 6.6 Roll Geometry: C1 *(rest Model 6.1)*

6.5.3.2 Frictional Contact & Strip Tracking

Model 7.1 Roll Geometry: C1, Strip Dimensions: F1800, Strip Properties: 15MPa, Strip Gauge 0.4mm, Contact Assembly: Full-Width, Step: Dynamic Explicit, Interaction: Standard, Contact Properties: Standard_0.15, Strip Constraints: Standard, In-Line Tension: 5MPa, Roll Velocity: 300m/min, Strip Velocity: 0.5m/s, Mesh: S4R

Model 7.2 Roll Geometry: C1, Contact Properties: Standard (rest *Model 7.1*)

Model 7.3 Roll Geometry: C1, Contact Properties: Standard_0.45 (rest *Model 7.1*)

6.5.3.3 Line Velocity

Model 8.1 Roll Geometry: Flat, Strip Dimensions: H1800, Strip Properties: 15MPa, Strip Gauge 0.4mm, Contact Assembly: Half-Width, Step: Dynamic Explicit, Interaction: Standard, Contact Properties: Standard, Strip Constraints: Standard, In-Line Tension: 5MPa, Strip Symmetry: ZSYMM, Roll Velocity: 300m/min, Mesh: S4R

Model 8.2 Roll Geometry: Flat, Roll Velocity: 400m/min (rest *Model 8.1*)

Model 8.3 Roll Geometry: Flat, Roll Velocity: 500m/min (rest *Model 8.1*)

Model 8.4 Roll Geometry: Flat, Roll Velocity: 600m/min (rest *Model 8.1*)

Model 8.5 Roll Geometry: C1 (rest *Model 8.1*)

Model 8.6 Roll Geometry: C1, Roll Velocity: 400m/min (rest *Model 8.1*)

Model 8.7 Roll Geometry: C1, Roll Velocity: 500m/min (rest *Model 8.1*)

Model 8.8 Roll Geometry: C1, Roll Velocity: 600m/min (rest *Model 8.1*)

6.5.3.4 Unequal Tension

Model 9.1 Roll Geometry: C1, Strip Dimensions: F1800, Strip Properties: Elastic, Strip Gauge 0.4mm, Contact Assembly: Full-Width, Step: Dynamic Explicit, Interaction: Standard, Contact Properties: Standard, Strip Constraints: Unequal, In-Line Tension: 3MPa-7MPa, Roll Velocity: 300m/min, Mesh: S4R

6.5.4 MODEL OUTPUT IDENTIFIERS

All results apart from U1 are taken from "integrated element". The value U1 (displacement element) is taken from the nodal displacement.

The graphical interpolations are displayed as SNEG. When the results display SNEG, they represent the strip surface that is adjacent and in contact with the transport rolls surface, they do not represent the top surface of the strip, which would be referred to as SPOS.

There are many ABAQUS CAE output identifiers. However, the author only used the following for the roll-strip contact models

S1 & L1	= σ_{11} & ε_{11}
S2 & L2	= σ_{22} & ε_{22}
L3	= ε_{33}
S12 & L12	= τ_{12} & γ_{12}
S, Mises	= the von Mises equivalent stress
U1	= Displacement component *(x-axis)*

The principal strain (L1, L2, L3) is defined as the logarithmic or natural strain and not normal or engineering strains. Generally logarithmic strain is not required for strip steels that have small changes in strain and largely operate elasticity, however, large deformations can occur, and with that in mind the author chose to include the "NLGEOM" parameter to the step analysis. The use of the *NLGEOM parameter automatically results in the logarithmic strain being used for ABAQUS computational simulations.

7. THE COMPUTATIONAL MODELLING OF THE TRANSPORT ROLL AND STRIP STEEL INTERACTION

Introduction

The history of the CAPL transport roll is one of evolution, from the flat roll to the barrel roll and finally to the tapered roll. However, every time a new design parameter is implemented the chances of strip quality issues rise. The focus of this chapter is to look at the current Port Talbot CAPL, investigate and further the current knowledge and make recommendations for the better.

Initial research considered the area that was thought to cause the greatest increase in localised stress that of the roll-strip contact point (initial point). This contact can cause buckle susceptibility risk (or plastic susceptibility risk) right across the contact plane of the strip and transport roll. However, it is at its highest at the circumferential fillet point where the taper angle and straight section of a type "C" tapered roll meet. Large taper angles increase the risk of buckle susceptibility in the very high temperature environment of the annealing furnace. In particular, the static computational FEA models highlight how the stress gradient in the strip increases towards the elastic limit as tension is applied in a steady state manner.

The operational element, which is not controllable, is the occasion when human interference to the process line has to occur. Overriding the process systems occurs for genuine reasons; the worst case is strip failure, however, every time the line speed is disturbed there is the matter of acceleration, especially start-up acceleration. For a dynamic computational FEA model the start-up is where the major risk to the strip exceeding the elastic limit exists. Start-up failure is linked to a number of parameters including roll geometry, in-line strip tension, strip mechanical properties and the contact friction coefficient.

The investigations into transport-roll contact were broken into two simple analysis types. The first analysis section relates to static, steady state load investigations. The use of steady state loading enabled the author to consider variations, in in-line tension. The second section of this chapter considers strip velocity a computational parameter that has almost been ignored by Corus up to now. The dynamic models developed to analyse strip velocity have a transient loading

system so that all parameters are active in full from the first incrementation of the first step.

This chapter uses a model reference system. Section 6.5 the "Roll-Strip Model Parameters" within Chapter 6 defines all aspects of the computational models that are discussed here. For ease of reference each computational run within this chapter will only be referred to as *"Model 1.1"* etc.

7.1 STATIC ROLL-STRIP CONTACT INVESTIGATION

Opening Remarks

The static models all use ABAQUS Standard (implicit). The implicit time step has highly documented benefits for static analysis. The loads in these models were applied in a steady state manner, except for the heat transfer model; its loads were applied in a transient manner.

ABAQUS CAE's visualisation module enabled the user the ability to present the results visually. Thus, the user has the ability to see how the von Mises equivalent stress, for instance, was developed across the mesh surface. However, these results were difficult to interpret, because, generally the maximum and minimum values are represented, along with a user defined number of intervals, therefore, individual elements or nodes cannot be identified easily. Individually querying the elements or nodes is preferable. Specifically, the elements along the plane or axis of the initial roll contact point, and then along the plane or axis of the top of the roll. The author considers these two points as the location of the greatest concentrations of potential yielding elements, specifically due to the hard contact. The process that went into this decision was as follows. As the strip moves from the pass length between rolls it makes a sudden hard contact with the transport rolls surface at the initial roll contact plane - this massive change in the strips stress state can cause buckle, this concentration point is intensified at the roll's circumferential fillet point, where the taper begins. This change is significant, only under tensioned slack strip between roll passes can cause similar buckle risks. The other focal point was the investigation into buckle risk of the strip across the plane of the top of the roll. Clearly, at the top of the roll the strip has a significantly increased stress state, as it is the strip's central hanging point, either side of the roll at the top there is hanging strip. Furthermore, while the

model does not include gravity, the strip weight was considered due to the inclusion of density.

The static models field outputs are - the two directional stress values, the shear stress, the two directional natural strains, and the spatial displacement value (not all sections of this chapter use all of the field outputs). The final figure of each section considers ideal tension. The ideal tension refers to the correct application of in-line tension to a contact situation so that the strip remains elastic. The variation of in-line tension values to various roll-strip contact scenarios enables a buckle risk index to be developed. The ideal tension was measured by comparing the known yield stress against the von Mises equivalent stress.

7.1.1 STANDARD ROLL CROWNS

This section considers all the main roll profiles that are within the current CAPL. The focus of this chapter considers how the current roll profiles are affecting the strips mechanical behaviour; whether the buckle susceptibility risk is greater than Corus generally believed.

The issues of the past were part of the problem. Historically Stein Heurtey has supplied Corus with CAPL technology under a licence agreement. Corus traditionally have had little control over the roll profiles that were operating on the Port Talbot CAPL. The roll profiles that are in use were historically considered the best available. Limited research into roll profiles had taken place, however, traditionally only when there had been a serious buckle problem that had been continuously reoccurring.

This section will be more detailed than any other in Chapter 7 as it will detail the basis for current roll decision making, which does not need to be repeated in every section. *Figure 7.1* below considers the standard profiles across all zones of the furnace.

7.1.1.1 Directional Stress in the X-Axis

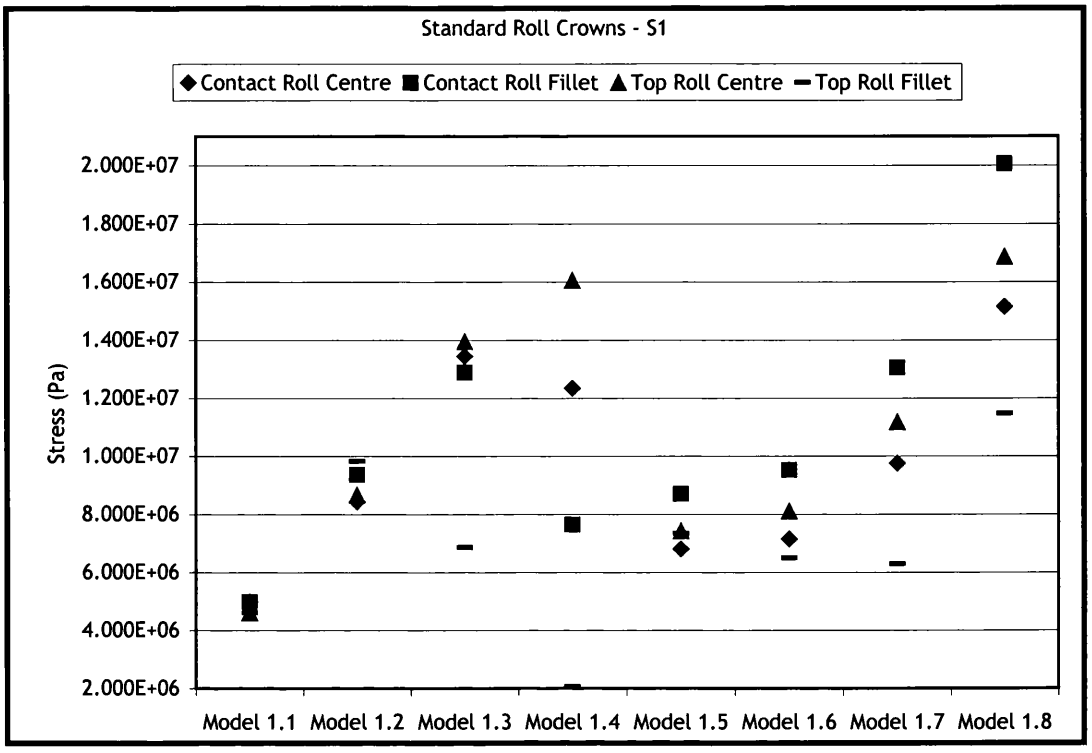

Figure 7.1 Directional Stresses (σ_1) - Standard Roll Crowns

The directional stress value σ_1 will be referred to as (S1) the ABAQUS output identifier. The S1 directional values represent the stress state along the x-axis. Positive stress values indicate the strip in the x-direction is in tension (tensile stress). The application of in-line tension to the end edge of the hanging strip length stretched the strip around the roll's surface.

The critical area of research is the roll-strip contact at the end of the heating furnace that continues into the soaking furnace. Temperatures in the soaking furnace are in excess of 750°C. The author will continue to concentrate on this high temperature environment, as it was critical. However, the thesis will also look at all the roll profiles throughout the CAPL furnace. A full examination of the CAPL roll profiles and operational parameters was required so that a judgement, which had all the facts, could be made on the future of this critical region.

The strip dimensions for the standard roll crowns of *Figure 7.1*, were for a width of 1800mm and a gauge of 0.4mm. These were the standard strip dimensions used throughout this chapter, unless otherwise stated. The mechanical properties for

each model will on occasions only be referring to the yield stress. The Young's modulus will be referred to when it is particularly pertinent to discussing strip stiffness. It was noted from the literature that with an unconstrained uniaxial tension or compression, the Young's modulus of elasticity could be considered as a measure of the stiffness of a material.

Model 1.1 to *Model 1.4* represent a yield stress of 15MPa, which is the yield stress property of strip at the end of the heating section and then throughout the soaking section. This so-called critical zone is where the predominant buckle issues occur, and therefore the in-line tension is currently no higher than 5MPa. While at present no flat roll profiles (*Model 1.1*) exist within the CAPL they have certainly been considered, as Corus tend to see strip failure only on the larger tapered rolls (over 1.4mm). *Model 1.2* refers to a typical tapered transport roll in the soaking section (for reference, the bottom rolls only), with what is considered a low roll taper size of 0.41mm and a flat central section of 700mm. Like all rolls up to the start of the overage section it has a roll diameter of 750mm. *Model 1.2* tends to operate in an environment where the strip temperature and the roll temperature are generally homogenous (750°C). *Model 1.3* refers to a roll that is in the heating section of the furnace, it has a roll profile that is 3.3mm, the largest within the entire furnace, it also had the smallest central flat section of any tapered roll (500mm). *Model 1.3* rolls tend to operate up to the centre of the heating furnace, where temperatures approach 750°C. The strip and the roll in the heating furnace can suffer from temperature variations across their surfaces especially at the strip edges - this is entirely to do with the rapid heating that the strip has to go through when it enters the CAPL furnace. *Model 1.4* refers to a typical barrel roll (no central flat section), which has a taper of 0.35mm. *Model 1.4* barrel rolls are used only at the top of the soaking furnace [29, 43].

Model 1.5 and *Model 1.6* represent roll-strip contacts in the cooling section of the furnace, a low buckle susceptibility risk area. These two models have the same roll taper size to that of the rolls of *Model 1.2*; however, they have a larger central flat section of 1000mm, compared to 500mm. The temperature profile within the cooling sections starts at 675°C and ends at 400°C. The yield stress properties of the strip in this section are 60MPa (@675°C) and 170MPa (@400°C). The cooling of strip in this section relies on "blow boxes" - it has been commented that these themselves can cause the strip to wander. A reference to strip between

passes oscillating backwards and forwards quite visibly. It is important to note that the strip on the rolls will remain stationary, however severe the strip oscillation, due to the roll-strip hard contact. This oscillating affect cannot be taken for granted; it is a buckle risk.

Model 1.7 and *Model 1.8* represent transport rolls with a diameter of 1200mm. These large diameter rolls have a taper size of 1.4mm; and a central flat section of 700mm. However, because of their large diameter, a moderately sized taper has less of an affect on the stress state of a strip being transported at temperatures less than 300°C. The C8 transport roll is used throughout the overage and 2nd cooling sections of the CAPL.

The principal reason for using larger diameter rolls is that the strip is close to the exit of the CAPL furnace and therefore the final quality is paramount. Considerable effort has taken place to get the strip to the final stages of the furnace; therefore the roll diameter that provides the lowest buckle susceptibility risk is to be used. Larger roll diameters reduce the bending load that the strip steel had to endure, because the strip's change of direction is incrementally smaller when the roll circumference increases. Furthermore, at overaging temperatures the strip can have a moderately sized taper (say 1.4mm) because the buckle risk is much reduced compared to the critical region (i.e. the soaking section). It must be noted that a larger taper is always preferential - it reduces the risk of strip tracking.

Discussion Points: Figure 7.1

Model 1.1, the four probed stress values were in close proximity to each other (contact centre, contact fillet, top centre and top fillet). Generally all flat roll profiles for purely static in-line tension models had close results, wherever the S1 values were probed. However, tension had to be applied in a steady state manner. To highlight this point, S1 is 5MPa; this S1 value was the same as the in-line tension. Tracking is the principal reason that has stopped flat profiles rolls from being used throughout the CAPL.

Model 1.2, the four probed stress values were not as close to each other as they were for the flat roll profile. Tracking was not such an issue with this roll profile, as the taper hindered strip movement; it kept the strip on the rolls' centreline.

Furthermore, the taper was sufficiently small that there was a reduced buckle susceptibility risk. The S1 directional stress value was 10MPa; this figure was two-thirds of the yield stress value. However, whether the strip would remain in its elastic region depended on the S2 directional stress value. The two probed element values that were highest, where the contact fillet and top fillet (both are where the flat section of the roll ends and the taper section starts).

Model 1.3, the four probed stress values were close, the exception was the element closest to the top fillet. This element could indicate a very localised reduction in the S1 stress. The maximum stress in the S1 directional plane was 14MPa, which was only 1MPa below the yield stress. This confirmed that large roll tapers, such in this case 3.3mm, are detrimental to the elasticity of the strip. The question of why Corus had continued with this roll was difficult to comprehend. That said, the roll was appropriate in the first few passes of the heating section, where the strip yield stress was at its cold iron maximum. However, it has to be said that Corus do not operate this roll at the end of the heating section where the furnace temperature is at its highest.

The future of the CAPL, which will be mentioned throughout this chapter, is higher throughput, thinner and thicker strip gauges, and higher and lower strip yield strengths. The last point on mechanical properties is perhaps the most pertinent. The current grade, which is most profitable to Corus, is the EDDQ, it is the most formable, the most ductile, and has the most stringent quality requirements in terms of both chemistry and surface finish. However, in the future these stringent formability requirements will be even greater than they are now, so buckle risk needs to be eliminated or certainly better understood.

Unfortunately Corus cannot not rely on commercial quality grades in the future as they do now, because commercial quality grades can be produced cheaper in the developing world. This trend is set to continue with steel companies within the European Union having to contend with even more stringent emission regulations and high running costs.

The author's recommendation is that large roll tapers should eventually be phased out. There are two simple arguments to back up this philosophy. The first is that the recrystallisation temperature is going to be even higher in the future; this

could lead to a soaking section temperature of over 900°C. Thus it can be seen that a large taper size will be even more detrimental in the future. The second argument is based on the simple fact that if the furnace temperature were reduced, from advances in chemistry, then the higher strength mechanical properties would still be transported through the CAPL successfully on a transport roll with a lower taper size.

The highest gradients (or stress variations) occurred along the initial plane of contact and around the circumferential axis of the roll taper fillet. The highest gradients were concentrated within 50mm of the circumferential taper axis (not shown). The stress state can change very quickly across the surface of the strip.

The use of barrel rolls *(Model 1.4)* is historic, it was felt that no central flat section helped to prevent the strip from wandering across the surface of the transport roll. Furthermore, if the strip wandered at the bottom of the furnace where the *Model 1.3* taper rolls exists, then the barrel roll at the top should help to guide the strip back to the centreline of the transport roll at the bottom.

Figure 7.1 highlights the generally poor stress state that barrel rolls induce on the surface of the strip steel. Barrel rolls created by far the greatest levels of buckle risk of all known rolls within the CAPL, even when tension was applied equally. This high buckle susceptibility occurred even though barrel rolls have the smallest taper size, of any of the rolls within the furnace. Referencing *Figure 7.1,* the barrel rolls maximum and minimum probed S1 values were the greatest of all the rolls that operated at 750°C - the author's first instinct was one of unpredictability and then high buckle risk. The two lowest S1 values for *Model 1.4* represent the contact roll fillet and the top roll fillet; these two values do not represent the fillet for a barrel roll, as the barrel roll taper starts at the rolls' centre. They were mid-surface values 250mm from the strips centreline and were included for comparison purposes only. They had S1 values of 7.6 and 2MPa respectively. These values were well below the yield stress; they indicate that the stress state that developed on the strip's open surface remained elastic (for this model), however, the focus must remain on those regions where a plastic stress state is more likely. The highest S1 directional value was at the top of the roll at the strip's centre point, this was the element closest to the start of the taper for a barrel type roll. The S1 value at the top centre was 16MPa, a value greater than

the yield stress, however, this was just in a single plane and therefore does not automatically mean the strip will plastically deform, however, likely. The S1 value for the contact centre point was 12.3MPa, this indicates that the barrel rolls greatest tensile stress was not across the initial contact point like the majority of tapered rolls, but along the plane at the top of the transport roll. This would be considered beneficial if the primary role of the transport roll was to prevent strip from tracking, but it is not.

Considering the high buckle risk that the barrel roll appears to create, then the recommendation would be to replace them with same tapered transport rolls that are present at the bottom of the soaking section (*Model 1.2*). This change would not be as costly, as considering alternative roll tapers or central roll sections that are not currently manufactured. It would be detrimental to the strip's quality to consider any of the roll profiles from the heating section. The cooling section roll profiles are also inappropriate, as will be explained. The roll profiles used in the cooling section are also inappropriate because the central flat section of that roll is 300mm longer, which increases the risk of tracking. The longer the central flat section the closer the transport roll is to a flat profile; and while the buckle risk is reduced the tracking risk is increased.

Model 1.5 and *Model 1.6*, the higher yield stress of both of these models translates into a low buckle susceptibility risk. The yield stress values were 60MPa for *Model 1.5* and 170MPa for *Model 1.6*. The Young's modulus changes from 95GPa *(Model 1.5)* to 172GPa for *Model 1.6*. For reference, the strip in the soaking section had a Young's modulus value of 70GPa; therefore *Model 1.5*, which represents the strip entering the cooling section from the soaking section, had only a slightly higher material stiffness. The highest S1 value for *Model 1.5* was 8.7MPa (60MPa yield stress). Equally the highest S1 value for *Model 1.6* was 9.5MPa (170MPa yield stress), however, this model had a high Young's modulus. Both models highest S1 values were along the contact plane at the rolls' fillet point. The S1 directional values for both models indicated that that the increase in the central flat section (1000mm compared to 700mm) decreased the strip's overall stress state and thus buckle risk was reduced when identical taper sizes were used.

Model 1.7 and *Model 1.8* represent roll profiles and strip operational parameters in the overaging and 2nd cooling section. Both of these sections have relatively low buckle risk. However, there was an exception, cool buckle had been a prominent issue in the last few years within the 2nd cooling section[27]. Cool buckle relates to quality issues as the strip cools. Cool buckle is typical of many buckle related incidents; a parameter or a number of parameters that have exceeded or are not operating at their specified set points. Cool buckle is similar to heat buckle in that the strip and the roll have temperature variations across their surfaces. In the case of cool buckle the strip is hotter than the roll.

Model 1.7 has a maximum S1 directional value (13MPa) at the contact fillet point. This indicates that the strip is no buckle risk when operating at 675°C (dependent on correct in-line tension). Corus should consider keeping the mechanical properties in that range for as long as possible, as they appeared not too soft and not too hard (60MPa yields stress and 95GPa Young's Modulus). Using such large roll profiles (∅1200mm) in the other sections of the CAPL cannot be realistically considered. The primary reason - the overage and 2nd cooling sections are historically the longest sections of the entire CAPL line, where as the soaking furnace only had 10 passes. *Model 1.8* represents strip in the final sections of the CAPL, the strip is now fully recovered. The maximum S1 value for the strip here was 20MPa (211MPa yield stress).

7.1.1.2 Directional Stress in the Y-Axis

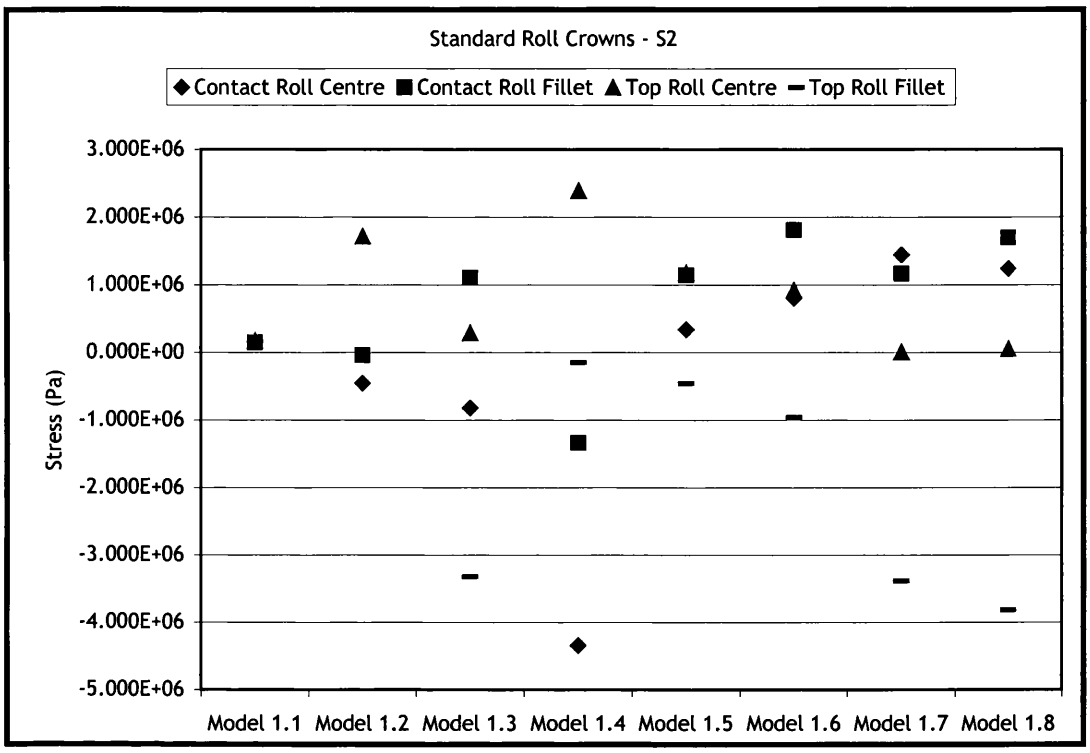

Figure 7.2 Directional Stresses (σ_2) - Standard Roll Crowns

The directional stress value σ_2 will be referred to as (S2) the ABAQUS output identifier. The S1 directional values represent the stress state along the y-axis. *Figure 7.2* indicates the strips stress state is both a mixture of tensile (positive values) and compressive (negative values) stresses (across the strips surface from one edge to the other). Tensile and compressive stresses were considered out-of-plane if the strip did not remain flat on the rolls surface (i.e. ripples are generated).

The author felt, before the analysis into S2 directional stresses began, that they would be lower than the S1 values. It quickly became clear that the focal point is the initial contact plane, which is perhaps better represented by the S1 directional stresses.

The S2 values in theory and in practice predominately represent the stress state of the strip surface as it pressed down onto the rolls' top surface. This is predominately a tensile stress at the centre point and a compressive stress at the fillet point. Unlike the S1 direction there was no initial contact to dramatically

raise the stress state, the strip was already in contact with the rolls surface, however, there was the weight of the hanging strip to increase the load, which, lies in the y-direction.

Compared to the sudden shock to the S1 directional stress in the strip due to the initial roll contact, S2 directional stresses appeared to be less of a risk. Furthermore, several S1 values were high; approaching or exceeding the yield stress value on roll profiles that were not going to plastically deform, so accordingly to the von Mises equivalent stress the stress in the S2 directional plane will have to be either a low tensile stress or possibly a compressive stress value so as not to breach the yield stress. The directional stress in the third plane S3 was zero for a uniaxial plane stress situation as was the case for the ultra thin strip.

The results for S1 and S2 were both integrated from the same element, thus all elements to a degree were under compression and tension. In the case of strip the dominant directional stress plane is the S1 value. While the principal directional stress was the element's stretching tensile stress, it was also the case that there was compressive stress, especially along the top roll plane in the S2 directional plane. The initial contact so often took most of the thoughts concerning buckle, however, the hanging length should always be reviewed in conjunction with the initial contact plane. A sudden rise in tensile stress in the hanging strip often occurred as the strip hits the transport roll, the strip in the pass length now had to deal with both in-line tension and the added load of roll traction.

Discussion Points: Figure 7.2

Model 1.1, the four probed stress values were even closer than they were for S1 the directional stress values. The maximum S1 value was only 1.7MPa (low buckle risk); all values indicate a tensile stress state. Static models were not ideal for investigating flat roll profiles as they always gave a low buckle risk.

Model 1.2 indicates that were S1 the stress state was tensile at all four probed values, there was now a stress state that has some compression stress (negative values). However, the significance had to be called into question, because the minimum stress in compression was just under 40000Pa, compared to an S1 directional value of 9.8MPa (tensile). The highest S2 directional value was 1.7MPa (tensile) at the top roll centre - nearly ten times smaller than the overall yield

stress (15MPa). These low S2 values were expected on a small tapered roll 0.41mm with a medium sized central flat section of 700mm. As this roll was the principal tapered roll within the critical buckle zone the results here showed that this roll profile was in fact ideal for current operational parameters, however, this may not be the case in the future.

Model 1.3 has the greater taper size (3.3mm). *Model 1.3* has high S1 stress (13MPa), but a low S2 stress, at the contact roll fillet 1MPa (tensile stress). This roll typified unpredictability as it had such as range of tensile to compressive stress values across the S1 and S2 directions. A roll that had a high buckle susceptibility risk.

Model 1.4 the barrel roll has S2 directional stress values that are similar to that of the S1 direction. The difference between the top roll centre and the contact roll centre was over 6MPa. The S1 directional stress values reinforce the idea that this transport roll profile should be withdrawn and replaced with the roll profile of *Model 1.2*. This would then mean that all the roll profiles in the soaking section would be identical.

Model 1.5 through to *Model 1.8* required no further discussion they have high yield stresses and minor S2 values.

7.1.1.3 Shear Stress

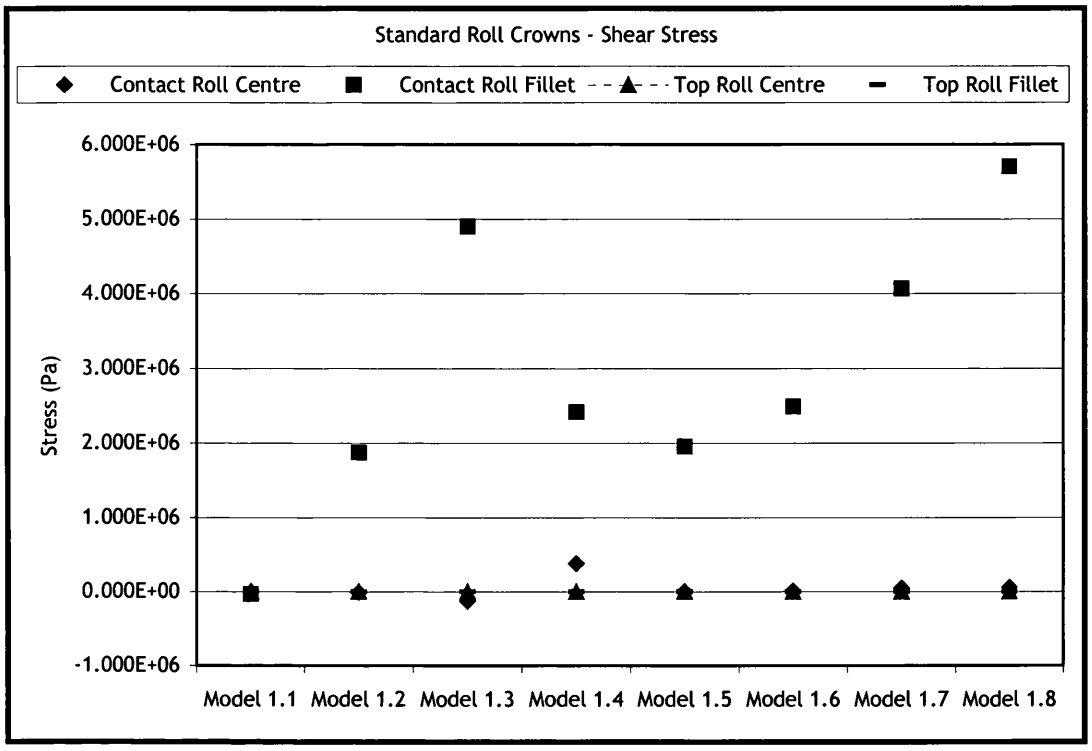

Figure 7.3 Shear Stress (τ_{12}) - Standard Roll Crowns

The principal shear stress value τ_{12} will be referred to as (S12) the ABAQUS output identifier. The S12 directional values represent the stress state along the x-axis. Any element that does not have equal forces acting upon its planes incurs a shear stress.

Discussion Points: Figure 7.3

Figure 7.3 gives a clear indication of the importance of the initial contact plane. The contact roll fillet point where the central flat section ends and the roll tapers starts was the only probed element that showed a significant shear stress value.

Model 1.3 confirms that large roll taper sizes (3.3mm) cause the greatest levels of shear stress. *Model 1.4* the barrel roll (0.35mm taper) and *Model 1.2* the small taper roll (0.41mm taper) have similar shear stress values. While it was not surprising that small taper sized rolls had smaller shear stress values than larger taper sized rolls, it was, however, surprising, that the barrel rolls shear stress value was not considerably higher. The directional stress values of S1 and S2 indicate an exceptionally high buckle risk with this roll type.

The increase in Young's modulus for *Model 1.5* to *Model 1.8* appears to have little or no effect on the strip's shear stress state. However, two points have to be considered here, Model *1.5* and *Model 1.6* represent a taper of 0.41mm and a central flat section of 1000mm, the difference between these two models was the mechanical properties, with the higher values assigned to *Model 1.6* to represent the cooler section that it is transported. However, there was only a slight increase in the shear stress for this model over that of *Model 1.5*, this indicates that the extra stiffness of the strip had little effect on the shear stress. The second point is the difference between *Model 1.5* and *Model 1.2*, the results were similar, they have the same taper size, but of course not the same taper angle as *Model 1.5* has a 1000mm flat central section, while *Model 1.2* has a flat central section of 500mm. The other difference is the mechanical properties for *Model 1.2;* they were for the critical region of the high temperature soaking section where as *Model 1.5's* were not. If *Model 1.2* and *Model 1.5* are compared blindly against each other without taking into account the annealing temperatures and side tracking they indicate that it is both better to have a longer flat section in conjunction with higher mechanical properties.

It is clear from *Figure 7.3*, that directional stress values give a better indicator of high buckle risk roll profiles - shear stress results are only an indicator of large taper size, and as such, other roll profile parameters like the central flat section on a tapered roll are better analysed with directional stresses or the von Mises equivalent stress.

7.1.1.4 Directional Strains in the X and Y-Axes

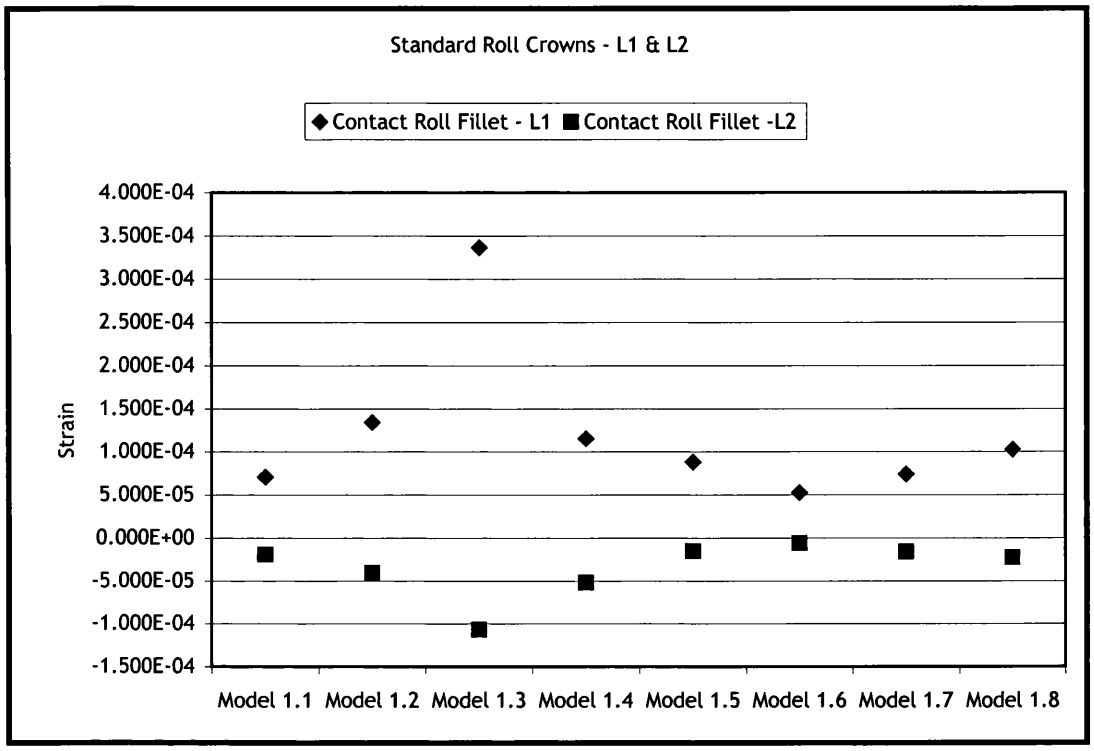

Figure 7.4 Directional Strain(s) $(\varepsilon_1 \& \varepsilon_2)$ - Standard Roll Crowns

The directional strain values $\varepsilon_1 \& \varepsilon_2$ will be referred to as L1 and L2 the ABAQUS output identifiers. They represent the strain state exactly in the same plane as that of S1 and S2. The strain represented in *Figure 7.4* represents only the probed element closest to the fillet point on the contact plane. It was considered that after the investigation into directional stresses had been analysed that this particular element was the most pertinent to investigate strains.

Discussion Points: Figure 7.4

Model 1.3, the large taper (3.3mm) had the highest level of strain. This was to be expected, strain and stress are associated according to Hooke's Law on linear stress-strain relations. The only significant comment that can be made about *Figure 7.4* is that the tensile and compressive strains of directional strains L1 and L2 tend to balance either side of the neutral (zero strain), the exception is *Model 1.3*, where the tensile strain is very high at the initial contact point due to the increased frictional traction generated by the largest roll taper in the CAPL. After careful consideration it was decided that continual investigation into strain was

not warranted. The purpose of the author's computational models is for comparisons, thus the stress results are considered sufficient.

7.1.1.5 Spatial Displacement in the X-Axis

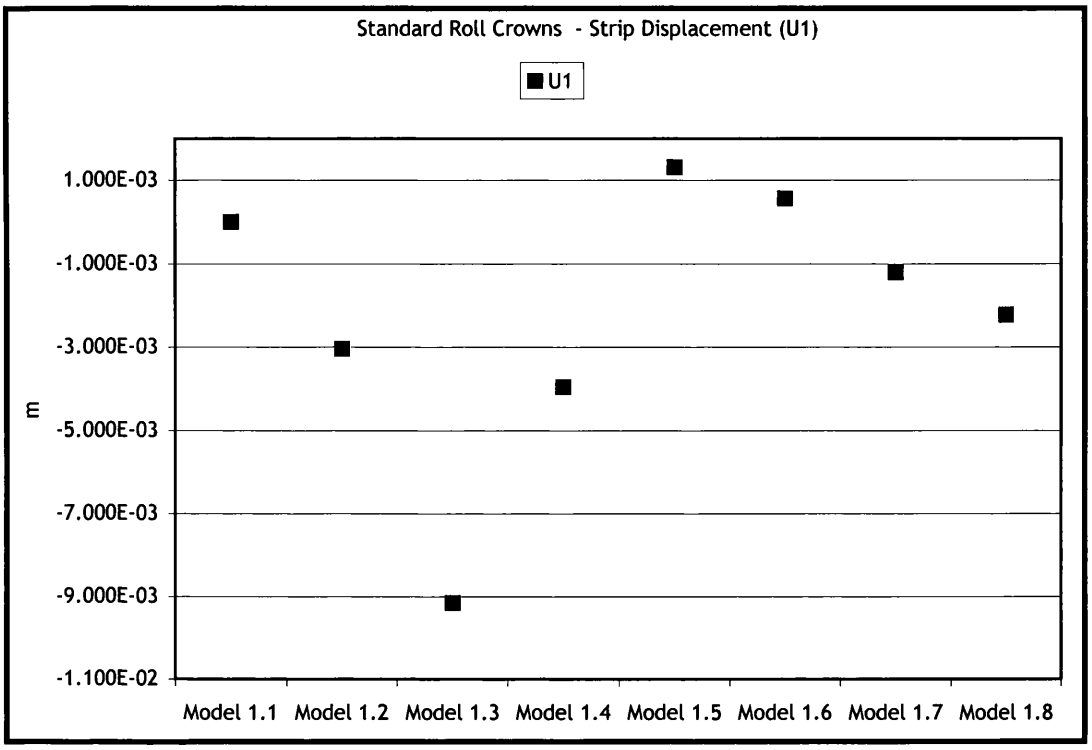

Figure 7.5 Strip Spatial Displacements - Standard Roll Crowns

The focus is the strip steel, its deformable, its wide and ultra thin, and it is in hard contact with an un-deformable transport roll. Due to the computational expense and focus on the initial contact plane the strip length was purposely designed to the minimum length (3x width). However, in reality there was approximately a 21m pass length between the top and bottom rolls on the Port Talbot CAPL, for this distance in-line tension had to be controlled strictly to prevent over tensioning or strip sag.

Considering sag, a reference to the strip moving out-of-plane in the pass length. Sag creates an elastic ripple in the strip upstream of the initial roll contact plane; however, the process is continuous, so the ripple travels up and makes contact with the transport roll at the initial contact plane. Once the elastic ripple hits the roll it turns into a plastic wrinkle due to the compression against the rolls surface. This of course is a worst-case scenario, most often the elastic ripple irons itself

out on contact with the rolls surface. Sag rarely turns plastic within the pass length if no roll contact has been made; this, however, is dependent on the cause and if its unequal tension then plasticity may occur without roll contact. Sag can also be caused by sudden and very localised frictional changes that occur to the strip as it travels around the rolls surface, typically a loss and then a sudden gain of traction can cause not just instance tensile failure but also strip sagging if the in-line tension suddenly slackens.

If normal tension on a flat roll profile is considered, the pass length will be under a tensile stress, because of the in-line tension. However, if the strip has a taper, then the stress state within the strip will be varied. The majority of the strip will still be under a tensile stress, but this will be interrupted with a compressive stress ripple that emanates along the contact plane at the contact fillet point, this ripple travels down the strip's length. Furthermore, a ripple generated at the contact fillet point does not travel straight down the strip; it sweeps diagonally across the strip until it reaches the strip edge, at which point it contributes to edge waviness.

The worst roll profile for this out-of-plane ripple is the large taper sized *Model 1.3;* the strip in the pass length had a tensile stress value of between 5MPa to a maximum of 8MPa, however, the ripple had a maximum compressive stress value of 10MPa. While both of these values were below the yield stress (15MPa), it, however, proved that ripples are a buckle risk, the compressive ripple is localised only a couple hundred millimetres across, and it was often surrounded by strip that has an equally high tensile stress.

The strip between roll passes rotates about its y-axis plane, because the strip in the pass length also hangs in the y-axis (roll lies on the z-axis). The strip resists the rigid transport roll most intensely at the taper's start point; this resistance can cause an angular displacement to originate at the taper start point, which then travels down the strip pass length creating a displacement.

There are several ABAQUS outputs that can be used for considering movement within the pass length. The field output chosen was the directional spatial displacement identifier. The parameter U1 was defined as the spatial displacement at the nodes. The spatial displacement plane was the x-axis,

represented by the number one. The spatial displacement in the x-axis only identified displacement in the hanging strip length. The strip that was in contact with the roll surfaces, not only was unlikely to show any significant out-of-plane displacements, it also changed direction as it followed the curvature of the transport roll thus making it difficult to analyse in a single plane.

While the stress and strain values were taken from the integration point for an element. The displacement values were taken from a nodal position. In this case the node that was closest to the strip's centre, at 2m down from the initial contact point.

Displacement points cannot quantify whether buckle will happen. They can, however, be used to help to identify a risk. Large displacements tend to reiterate the directional stress value.

Discussion Points: Figure 7.5

The spatial displacement values repeat similar conclusions gained in the directional stress results. Both the large taper size and barrel roll models exhibit greater nodal displacements than the rolls with smaller taper sizes. *Model 1.2* the small taper size roll (0.41mm) indicates a 300% improvement over the large taper size roll (3.3mm) *Model 1.3*. This difference further highlights the affect that the roll's initial contact had on the strip's displacement. All models have perfect flatness in the straight between passes as defined in the initial step. However, once the model enters the first step a load is applied to the strip in a steady state manner. The application of in-line tension causes the strip to ripple as it followed the contours of the roll taper. This ripple travels down the strips surface. However, the CAPL is continuously moving, so the out-of-plane displacement travels back up and hits the roll at its initial contact plane, which of course exacerbates the problem. The ripple effect that occurs to the strip's surface is not necessarily plastic, however, rapid compression in the ripple as it hits the rolls surface can cause an elastic ripple to turn into a plastic warp.

Model 1.5 and *Model 1.6* have the same taper size to that of *Model 1.2* (0.41mm); the results from *Figure 7.5* indicate only minor displacements for both models. The principal advantage of the C6 transport roll type is the longer central flat

section (1000mm) - this not only limits increases in the directional stress it also reduces the impact of any strip displacements.

Model 1.7 and *Model 1.8* indicate a greater spatial displacement than *Model 1.5* and *Model 1.6*. Both *Model 1.7* and *Model 1.8* have large tapers sizes (1.4mm). This is known to increase the out-of-plane displacement. The other factor is the large roll diameter (1200mm), this possibly could increase the out-of-plane spatial displacement, but its affects, have to be considered secondary to that of the taper size. The last factors were the mechanical properties; both models have high mechanical properties, considerably greater than that of the soaking section. The conclusion is that high mechanical properties do aid in preventing out-of-plane displacements. However, this was not clear, as *Model 1.8* demonstrates, this particular model has the highest Young's modulus of them all, however, in *Figure 7.5* this extra stiffness can be seen to be detrimental.

7.1.1.6 The Ideal Tension for Standard Roll Crowns According to the von Mises equivalent stress

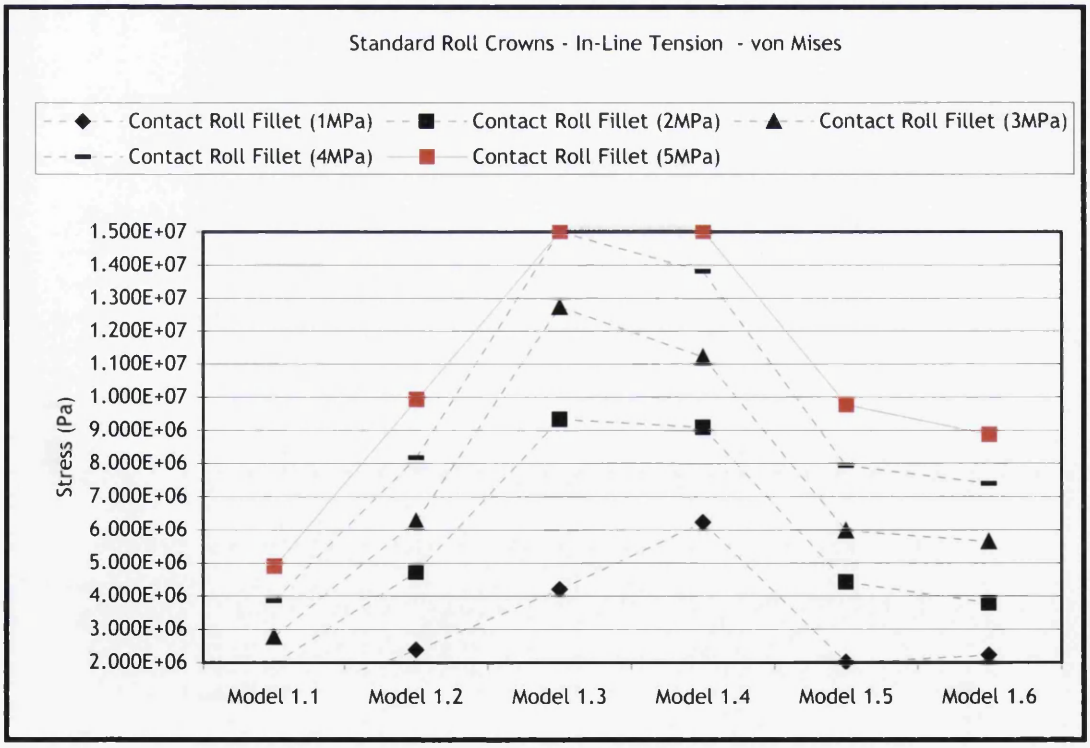

Figure 7.6 von Mises equivalent stress - Variations to In-Line Tension

The principal cause of buckle risk is inherently high in-line tension. The author considered the analysis of in-line tension to be paramount. Thus a study of differing tension levels would be investigated. The von Mises equivalent stress is the principal computational method for interpolating yield.

Only the contact plane fillet was considered, as this was considered the primary roll geometric location for plastic yielding, and the source of the principal out-of-plane displacement in the pass length.

The author considered in-line tension values between an unlikely 1MPa through to the current 5MPa for the very high temperature zones, this gave a clear idea of the ideal in-line tension for individual standard roll geometries. The primary reason for this investigation is the future - high annealing temperatures (+850°C).

Discussion Points: Figure 7.6

Model 1.1 is considered for comparison purposes only; it does have the lowest von Mises equivalent stress values, but flat profiles cannot strop tracking, which will be proved later.

Model 1.2 indicates a maximum von Mises equivalent stress value of approximately 10MPa for a 5MPa in-line tension value, 8MPa for 4MPa in-line tension value and 6MPa for 3MPa in-line tension. These von Mises equivalent stress values were twice that of the flat roll profile results of *Model 1.1*. *Model 1.2* as usual is the best all-round standard roll profile within the CAPL. The profile of the future will have to be in contact with a strip that has a yield stress possibly as low or even lower than 5MPa, which is the in-line tension value associated with furnace temperatures in excess of 850°C[28]. *Model 1.2,* indicates that an in-line tension value of no higher than 2MPa should be used for a strip operating in an environment of 850°C (roll taper: 0.41mm). The Young's modulus value would be in the region of 30GPa (@850°C).

While current tapers in the region of 0.41mm were ideal in reducing the risks associated with current tracking and buckle problems. The future could be somewhat different, if the current progression to pushing the extremities of the yield stress envelope continue then taper sizes will have to be reduced to 0.15mm or even lower. It will not only be the taper size that needs to evolve, the central

flat section may have to be increased over the current 1000mm (a typical C6 roll) to counter oscillations in the strip pass length, especially if the strip gauge becomes thinner than the current minimum gauge thickness of 0.3mm, even though this increases the tracking risk.

The problem with carbon strip steel is that in-line tension can only be reduced so much; there is a point where the strip will buckle with small variations of any of the operational parameters, this can be irrespective of the line tension or roll profiles. An example of this is the transitional weld size that can cause a serious buckle risk when compressed against a transport rolls surface[24].

Model 1.3 yields at 4MPa (tension), however, a reduction to 3MPa immediately reduced the buckle risk and brings the steels von Mises equivalent stress level to a value lower that the 15MPa yield stress.

The barrel roll *(Model 1.4)* in this figure does represent its contact taper point and not a distance along the contact plane like preceding figures, because this figure does not include the contact roll centre. *Figure 7.6* indicates that the barrel roll *(Model 1.4)* yields heavily at a 5MPa in-line tension, this was expected. However, at 4MPa in-line tension, the buckle risk was reduced below that of the yield stress. If the barrel roll was compared to the other roll in the soaking section the small taper size roll *(Model 1.2)*, it compares quite poorly at all in-line tension values from 5MPa to 1MPa.

Model 1.5 as mentioned previously, had the same taper size to that of *Model 1.2*. The central flat section was longer (1000mm compared to 700mm) and the yield stress was 60MPa. However, the results were still comparable, as neither model came close to 15MPa (high temperature yield stress). Furthermore, the extra central flat section length did appear to be somewhat beneficial, even though the strip in *Model 1.5* was somewhat stiffer with a Young's modulus value of 95GPa. *Model 1.6* had identical parameters to that of *Model 1.5;* the exception was the mechanical properties which were based on the EDDQ strip operating at 400°C and not 675°C. However, Model *1.6* really highlighted the limiting effect that high strength mechanical properties had at the initial contact plane, the differences between *Model 1.5* and *Model 1.6* were negligible.

Model 1.7 and *Model 1.8* were ignored for in-line tension analyses, the focus is on models where the roll diameter is 750mm. The large roll diameter was not appropriate for those sections of the furnace where buckle risk was through low yield stress and not other parameters.

Figure 7.6 shows the usefulness of presenting the results as the von Mises equivalent stress. The von Mises equivalent stress interpolates both the directional stress values to come to a definitive stress value.

7.1.2 VARIATIONS IN KEY OPERATIONAL PARAMETERS

The preceding section considered the current roll profiles within the CAPL. This section continues that investigation by concentrating on variations in roll geometries and strip parameters. The idea is to build up a matrix of parameters and how they interact with the strips mechanical properties.

The standard model was a full width version, with a roll taper size of 0.9mm and a central flat section of 700mm. The standard mechanical properties were 15MPa for the yield stress; 70GPa for the Young's modulus and the standard in-line tension was 5MPa. The concentration was now on the so-called critical parameters that were at the end of the heating furnace and then throughout the soaking furnace. The discussion will now be on the increased buckle susceptibility risk for individual parameter changes.

The differences to the standard parameters discussed above are. *Model 2.1* (plastic 10MPa, elastic 50GPa), *Model 2.2* (taper 0.41mm), *Model 2.3* (central flat section 500mm), *Model 2.4* (strip gauge 0.2mm), *Model 2.5* (in-line tension 3.5MPa), *Model 2.6* (standard parameters), *Model 2.7* (20mR fillet), *Model 2.8* (strip width 900mm), *Model 2.9* (in-line tension 8MPa), *Model 2.10* (central flat section 1000mm), *Model 2.11* (taper 1.4mm), *Model 2.12* (barrel roll), *Model 2.13* (roll diameter 1200mm) and *Model 2.14* (plastic 60MPa, elastic 95GPa).

7.1.2.1 Directional Stress in the X-Axis

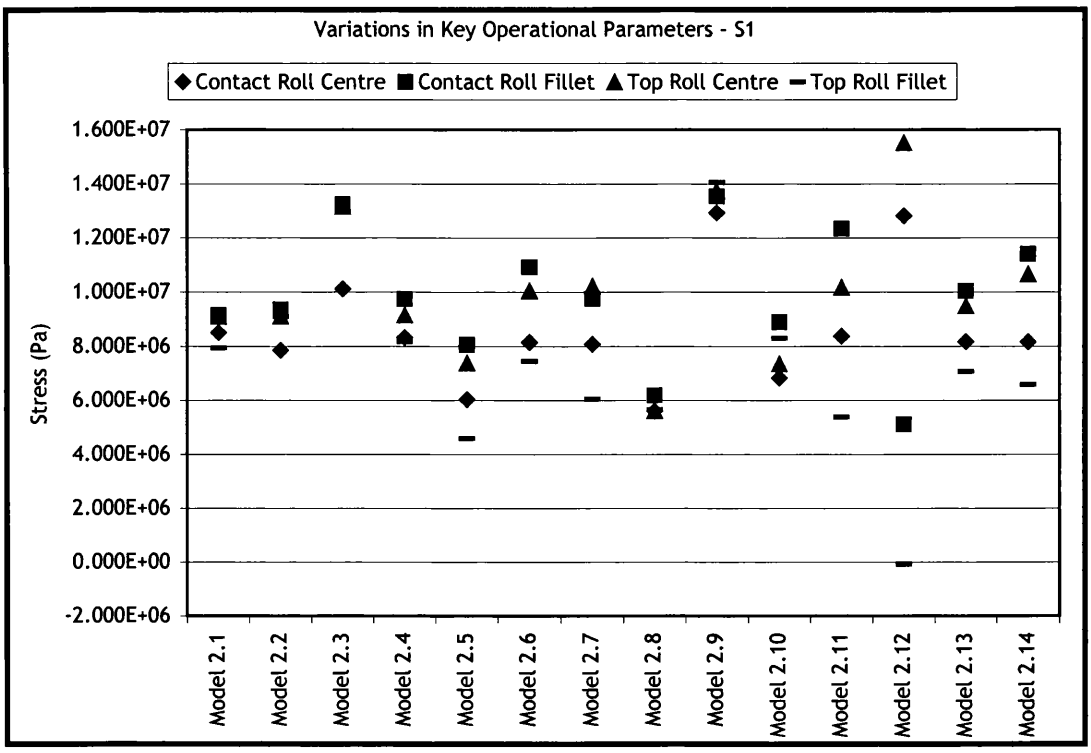

Figure 7.7 Directional Stresses (σ_1) - Variations in Key Operational Parameters

Discussion Points: Figure 7.7

Model 2.12 the barrel roll had an S1 directional value greater than the yield stress value of 15MPa. *Model 2.12* had a taper size of 0.9mm (*Model 1.4* taper size 0.41mm); the results back up the assumption that barrel rolls should be replaced. The S1 difference between the contact and top centre points is 2MPa (barrel rolls fillet point); a value that highlights the importance of transport roll central flat sections. The flat section aids in alleviating and spreading out the stress generated by excessive strip surface loading, this was especially the case with regards to the top plane of the transport roll.

Model 2.8 had the lowest S1 directional values. *Model 2.8* represents a model with a strip width of 900mm. The central flat section was 700mm long so only the last 100mm of the strip width was on the taper section of the roll. The four probed element values of *Model 2.8* were also the closest to each other, a sign of steady state stress. While the results indicate that the strip width is a certain identifiable buckle risk. In the case of *Model 2.8* the central flat section was in contact with a large percentage of the strip, and thus almost acted as a flat roll profile.

Considering S1 the more important directional stress parameter. The following list of roll-contact parameters is listed in order of importance, with the first parameter having the greatest buckle risk.

1. Barrel Roll.
2. 8MPa In-Line Tension.
3. 500mm Central Flat Section.
4. 1.4mm Roll Taper Size.
5. 60MPa Yield Stress, 95GPa Young's Modulus.
6. *The Reference Conditions.*
7. 20mR Fillet.
8. ∅1200mm Roll Diameter.
9. 0.2mm Gauge.
10. 0.41mm Roll Taper Size.
11. 10MPa Yield Stress, 50GPa Young's Modulus.
12. 1000mm Central Flat Section.
13. 3.5MPa In-Line Tension.
14. 900mm Strip Width.

One to four are the principal parameters that have constantly been shown to create the highest buckle risk. Only number two (8MPa tension) was not a typical parameter in the critical buckle region. At 8MPa the strip will buckle instantly within the critical zone - in fact the moment the strip makes contact with the roll; well before compression or tension due to traction could have any effect.

This comparison highlights the risk of small flat sections and large tapers, noted in the previous standard roll profile section. The last four parameters were the typical parameters, which reduce buckle susceptibility (small strip width, low in-line tension, large central flat section and low mechanical properties).

However, number 11 *(Model 2.1)* is interesting, the yield stress for *Model 2.1* is 5MPa less than the reference models yield stress value of 15MPa. The S1 directional value for the element closest to the fillet along the contact plane is 9.1MPa; compared to 10.1MPa for *Model 2.6*. The significant difference is the Young's modulus values; the softer material has a lower S1 value, because the strip is more ductile. However, this is undermined by the fact that the strip is

operating close to its yield stress value, which is 10MPa. The tension that would be required to turn this strips stress state plastic is minimal; therefore number 11 is a high buckle risk and not a low buckle risk.

If the strip velocity and frictional coefficient were treated as constants then the mechanical properties and the cross-sectional area of the strip have the greatest influence on the strip gauge. The strip has a high buckle risk when it is thin (under 0.3mm), wide (1800mm) and thick (over 2mm). Wide strip resists bending; this can cause intermittent contact on the transport rolls surface as the strip changes direction trying to follow the roll surface contour. Thin strip gauges can suffer from intermittent contact due to the air cushion effect. The problem with intermittent contact is the stress state. The strip looses traction and makes fleeting contacts with the roll's surface. The result is areas where the hard contact increases the stress state as the strip is effectively dragged across the roll's surface. Increasing the in-line tension solves the issue of intermittent contact with respect to thicker grades (over 1mm); tension restricts out-of-plane movement.

A large taper size increases the tension along the contact plane, now this would be expected. Large tapers are fine if the mechanical properties are sufficiently high, i.e. 60MPa yield stress and 95GPa Young's modulus. A large taper reduces the risk of tracking and intermittent contact in strip steels that have thicker gauges or higher mechanical properties. However, whereas in-line tension can be altered accordingly when required, roll taper sizes changes require the removal of the transport roll.

Figure 7.7, indicates that the inclusion of a 20m radius of curvature to the fillet at the taper point was a benefit *(Model 2.7)*; it certainly reduces the buckle risk when compared to a roll without a fillet radius *(Model 2.6)*. However, when its affect on the buckle susceptibility index is compared to the other roll geometry and strip parameters it loses its significance. A radius will not alter the maximum S1 directional significantly, however, it will aid in not localising this maximum at the taper points.

7.1.2.2 Directional Stress in the Y-Axis

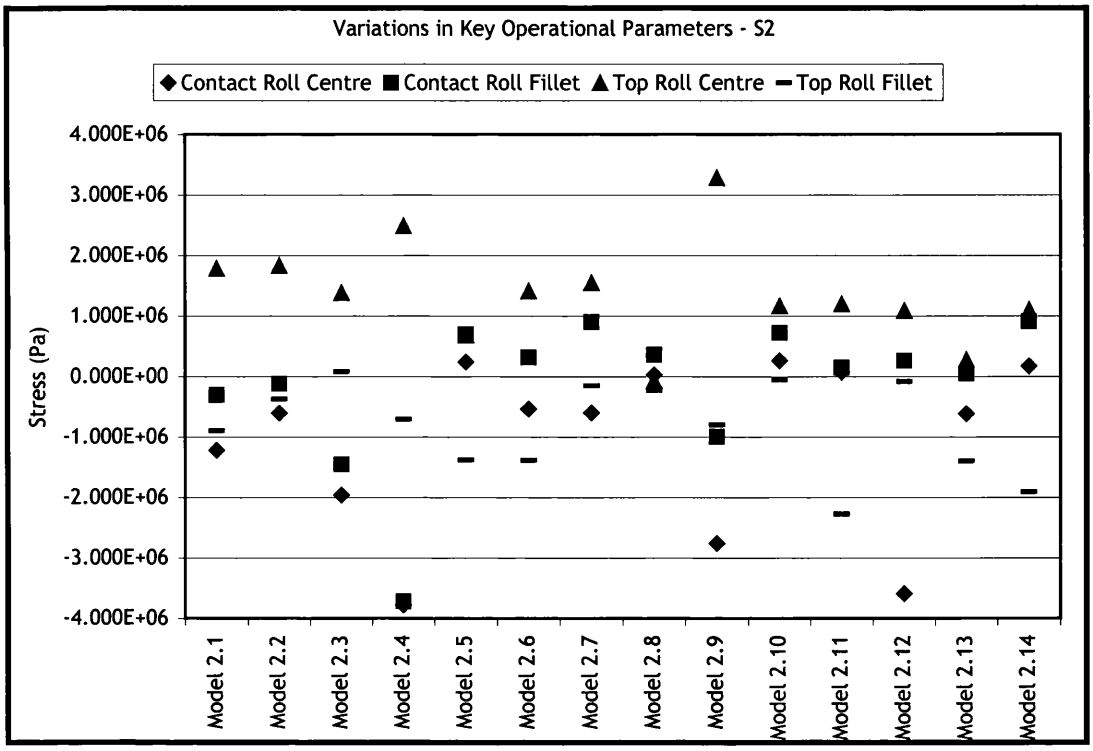

Figure 7.8 Directional Stresses (σ_2) - Variations in Key Operational Parameters

Discussion Points: Figure 7.8

Considering S2 directional stress parameters for the maximum compression values only (compression = negative stress values). The following list has been developed; identical format to that of the S1 direction, the first value (1.) has the greatest buckle risk.

1. 0.2mm Gauge.
2. Barrel Roll.
3. 8MPa In-Line Tension.
4. 1.4mm Roll Taper Size.
5. 500mm Central Flat Section.
6. 60MPa Yield Stress, 95GPa Young's Modulus.
7. ∅1200mm Roll Diameter.
8. 3.5MPa In-Line Tension.
9. The Reference Conditions.
10. 10MPa Yield Stress, 50GPa Young's Modulus.
11. 20mR Fillet.

12. 0.41mm Roll Taper Size.
13. 900mm Strip Width.
14. 1000mm Central Flat Section.

There is a definite pattern developing to buckle risk. The same parameters are constantly highlighted, it also now appears to be irrespective of the stress plane that is being investigated.

The parameters that continue to show minor buckle risk are the small width strip *(Model 2.8)*, large central flat section *(Model 2.10)* and small transport roll taper *(Model 2.2)*. The parameter that changed dramatically in the S2 direction was the 0.2mm gauge strip *(Model 2.4)*. In the S1 direction the ultra thin gauge was a mid table value; now in the S2 direction it suffered the greatest compressive stress of any of the parameters investigated. It appears that the ultra thin strip endured an increase in compressive stress as the strip makes contact with the roll along the initial plane. However, this had to be put into context, the maximum compressive stress value was 3.78MPa, however, the maximum tensional stress value was 9.7MPa (S1) so it was clear that the element will elongate and not fold.

7.1.2.3 Shear Stress

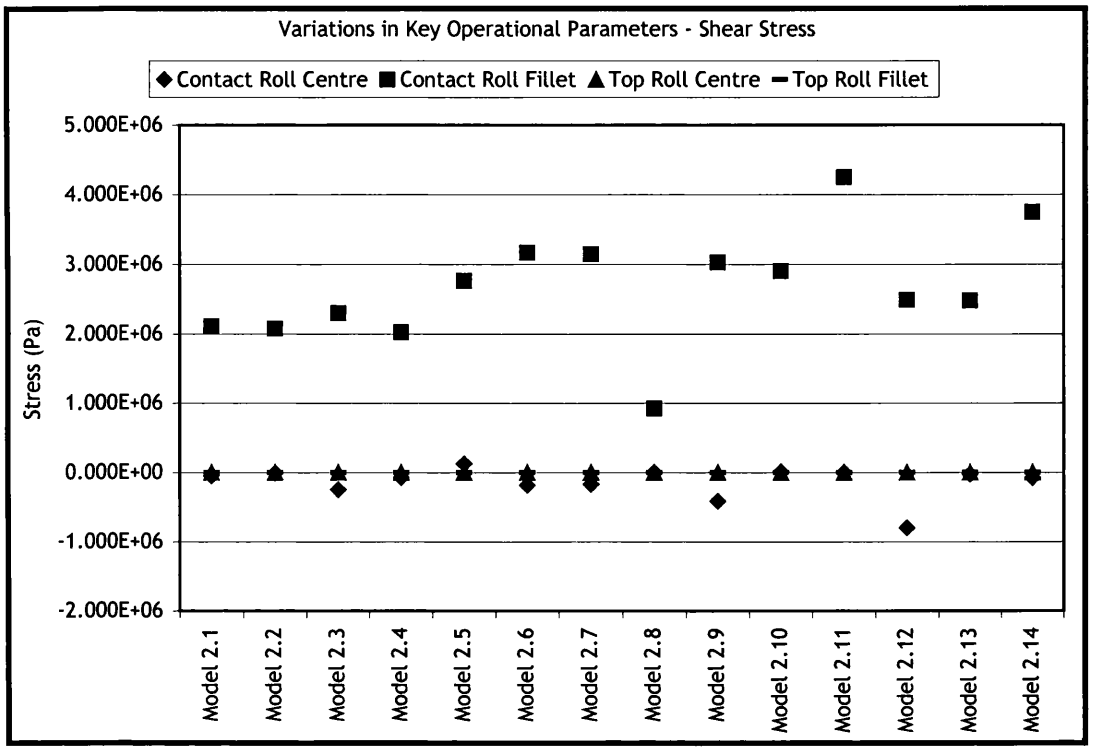

Figure 7.9 Shear Stress (τ_{12}) - Variations in Key Operational Parameters

Discussion Points: Figure 7.9

As with the standard roll crown shear stress results, all the significant shear stress values were along the contact plane at the fillet point. The majority of the values along this contact plane were within a 1MPa band (2MPa to 3MPa). The maximum shear stress value for the large taper size (1.4mm) was just over 4MPa *(Model 2.11)*. For comparison purposes a taper size of 3.3mm the shear stress value was 4.9MPa *(Model 1.3)*, for a taper size of 0.41mm the shear stress value was 2.1MPa *(Model 2.2)*.

The lowest shear stress value was for the 900mm wide strip model *(Model 2.8)*; this had a shear stress value of 1MPa (at the contact plane fillet point), whereas for the same element on the 1800mm wide strip model the shear stress value was 3.2MPa *(Model 2.6)*. While small strip widths had a reduced buckle susceptibility risk over their larger width counterparts, it was, however, the size of the central flat section that was the more important parameters here. Flat profiles do not induce stress state changes like a roll taper; therefore shear stress was kept to a minimum.

7.1.2.4 Spatial Displacement in the X-Axis

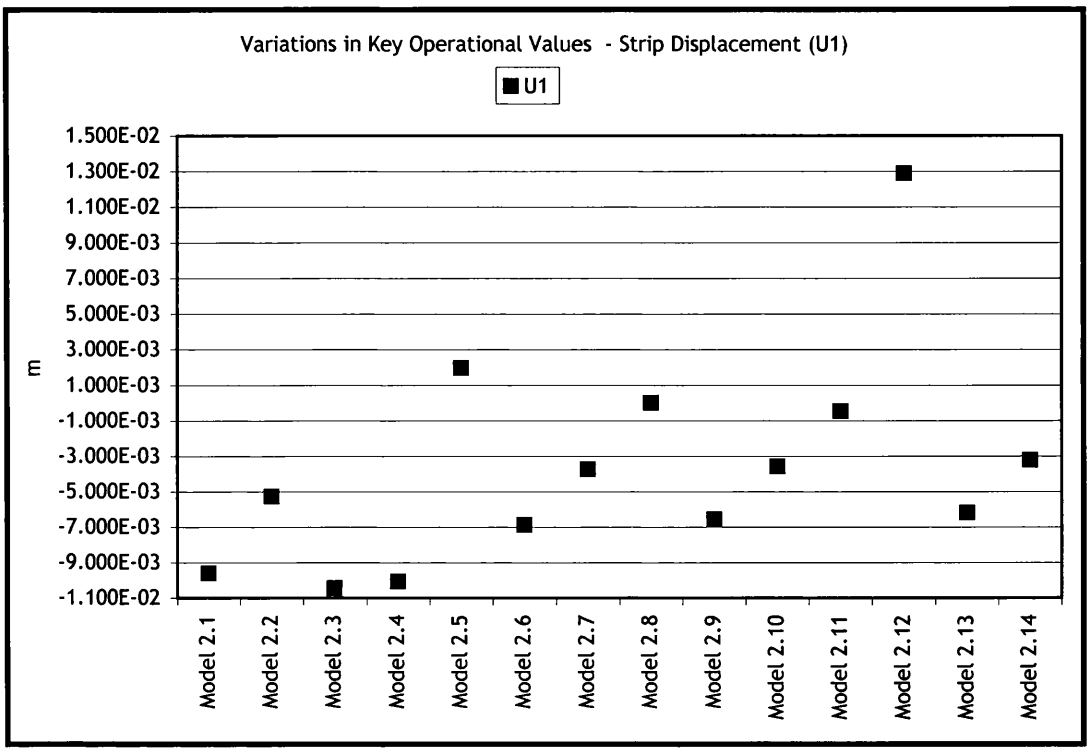

Figure 7.10 Strip Spatial Displacement - Variations in Key Operational Parameters

Discussion Points: Figure 7.10

Model 2.12 had the greatest displacement, 13mm off the centreline of the strips x-axis (nodal position: central strip node 2m upstream from the initial contact plane with the roll). *Model 2.12* is the barrel roll (0.9mm taper size). Part of the reason that the barrel rolls displacement value was higher than any of taper roll models, was that the nodal selection point was exactly on the same y-axis plane as the barrel rolls fillet point (i.e. the centreline of the strip). However, there is little argument that the barrel roll profile is the most detrimental.

Three other models have displacement figures in the region of 10mm; they were the low yield stress model *(Model 2.1)*, the small central flat section model *(Model 2.3)* and the ultra thin gauge strip model *(Model 2.4)*. The small central flat section having a poor U1 value validates the previous paragraphs assumption, because now it was clear that the strip had to spend more time on the taper angle when in contact with the transport roll. Greater contact time on the taper section changes the stress state within the strip for the worse. The strip was forced out-

of-plane closer to its own centreline. The out-of-plane displacement which originates at the strip's contact plane then travelled to the strip's edge from the strip's centreline, thus effectively forcing more of the strips upstream length out-of-plane.

The most neutral and not unexpected U1 displacement value were for *Model 2.8* the small strip width model (900mm width).

7.1.2.5 The Ideal Tension for Variations in Key Operational Parameters According to the von Mises equivalent stress

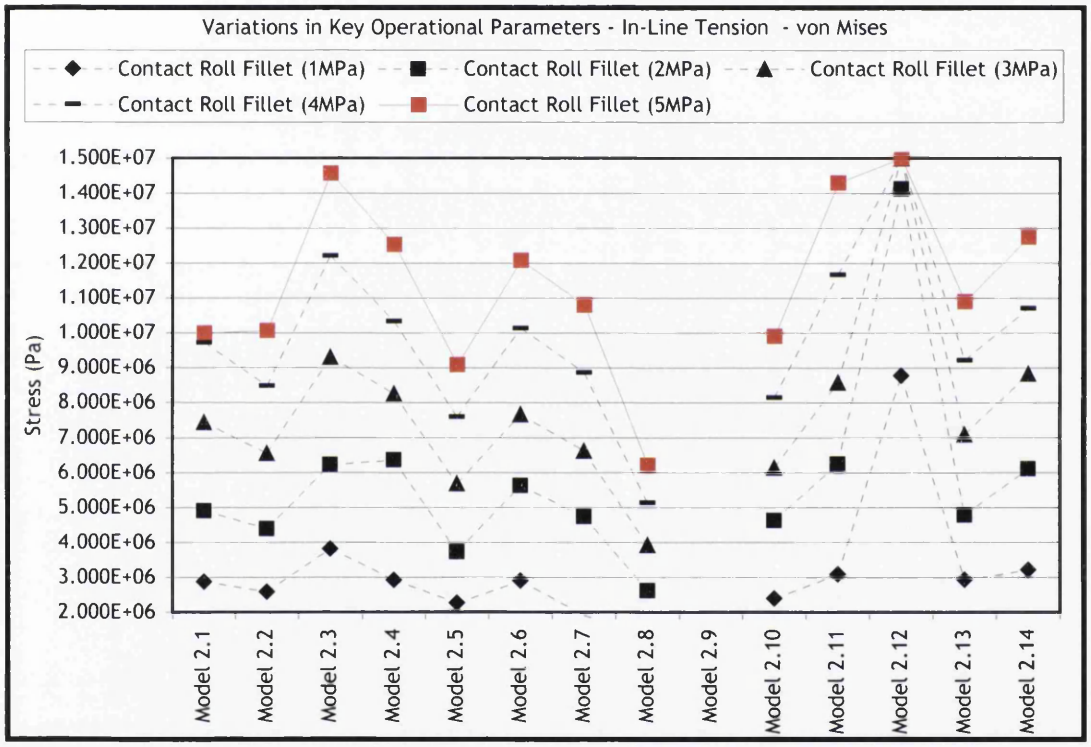

Figure 7.11 von Mises equivalent stress - Variations to In-Line Tension

Discussion Points: Figure 7.11

Model 2.12 the barrel roll had the highest von Mises equivalent stress value. At 5MPa in-line tension the yield stress value of 15MPa was exceeded. However, this barrel roll model had a taper size (0.9mm) that was so detrimental to the strip's stress state that the strip started to yield at 3MPa. While this model did not represent a standard profile on the CAPL the risks associated with barrel rolls were now clear and *Figure 7.11* proved it.

Model 2.3 (small central flat section) was the only other model with a von Mises equivalent stress value above 14MPa (5MPa in-line tension) and thus was a high buckle risk. As with the barrel roll a small central flat section had proven to be detrimental to strip quality. However, the reduction in taper from 3.3mm (*Model 1.3*) to 0.9mm *(Model 2.3)* had helped to reduce the von Mises equivalent stress value from 15MPa down to 12.2MPa for a strip in-line tension of 4MPa.

Model 2.2 (0.41mm taper) was the only model, which, could be used as a direct comparison with a half-width roll model *(Model 1.2)*. At 5MPa of in-line tension both models had a von Mises equivalent stress value of 10MPa. At 4MPa of in-line tension there was a small divergence, with *Model 1.1* recording a von Mises equivalent stress value of 8.2MPa and *Model 2.2* recording a von Mises equivalent stress value of 8.5MPa. This small study proved that unnecessary full width computational simulations were not required.

Model 2.8 continued to show that small width strips were preferable, confirming the findings of the directional stresses analysis. While *Model 2.6* (yield stress 15MPa) and *Model 2.14* (yield stress 60MPa) confirm that while mechanical properties were important, especially in the high temperature critical sections of the soaking furnace their importance was perhaps secondary to roll profile factors. However, if the mechanical properties of *Model 2.14* were to become available for strip steels passing through the soaking section it would most likely be because of changes to the strips chemistry and not the strips annealing temperature. The problem with annealing was that the microstructure requires a stimulus for the steel grains to gain sufficient inertia - this excitation can only be achieved through a high soaking temperature.

Discussion Points: Graphical Interpolation

The distribution figures were the principal method for understanding buckle risk. However, the distribution graphs cannot tell the reader how much of the surface area of the strip was effected by a changed to the local stress state. While it can be argued that a single element yielding was one too many, the focus of the research had to be on prevention. Graphical area graphs allowed the author to analyse how the roll taper affects the surrounding area of the strip while it was still in the elastic region. Graphical area graphs along with the distribution graphs help the author to consider buckle risk more accurately. There was a second

reason for considering graphical area graphs and that was a single element is unfortunately more likely to suffer from a computational irregularity than numerous adjacent elements.

The following is some examples of different taper sizes for a type "C" taper hearth roll and a type "D" barrel roll. The view taken is of the initial contact plane of the strip against the rolls surface. For comparison the author has shown the figures at 3MPa and 5MPa in-line tension.

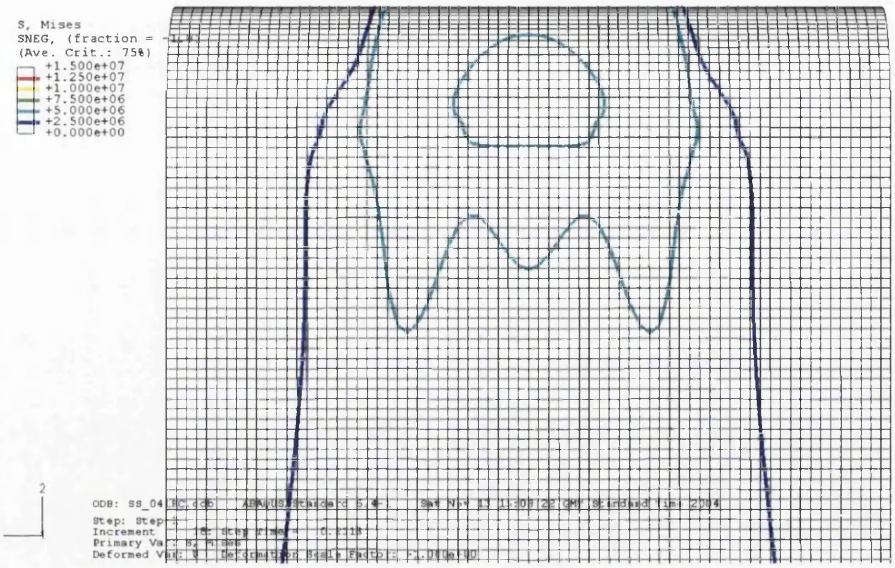

Figure 7.12 Model 2.2 - von Mises equivalent stress - Tension 3MPa

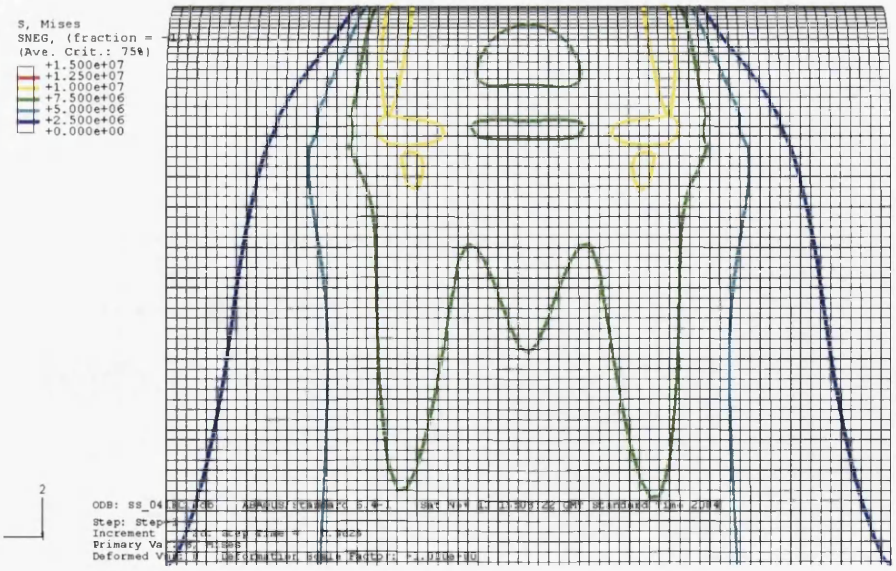

Figure 7.13 Model 2.2 - von Mises equivalent stress - Tension 5MPa

Figure 7.12 represents a case where the strip had an in-line tension is 3MPa (in-line tension for future soaking temperatures), *Figure 7.13* represents a case where the strip had an in-line tension of 5MPa (in-line tension for current soaking temperatures).

Figure 7.12 and *Figure 7.13* represent the von Mises equivalent stress on the strips surface. The transport roll underneath the strip had a taper size of 0.41mm (the CAPL's smallest standard taper size). This roll profile, which includes a 700mm central flat section, had already proven that it only had a minor buckle risk associated with it.

The two figures indicate that increasing the in-line tension increases the von Mises equivalent stress; this was expected. However, the yield criterion value for *Figure 7.13* (5MPa in-line tension) was still lower than the strips designated yield stress (15MPa). *Figure 7.13* highlights the effects of in-line tension and frictional contact perfectly; there was a significant stress state change in the strip located around the central flat section (700mm) of the underlying tapered transport roll. *Figure 7.13* indicates that the majority of the strip had a von Mises equivalent stress value at around the 7.5MPa mark where as for *Figure 7.12* the von Mises equivalent stress majority was around the 5MPa mark - thus lowering the in-line tension by 2MPa decreases the general stress state by a third, relevant for higher soaking temperatures.

The maximum strip von Mises equivalent stress was 10MPa *(Figure 7.13)*. This maximum value is associated with the strip that was directly over the roll fillet circumference and then along the initial contact point where was grown to its widest (approximately 175mm). Strip yielding along the taper (fillet) circumference was referred to as quarter buckle [32].

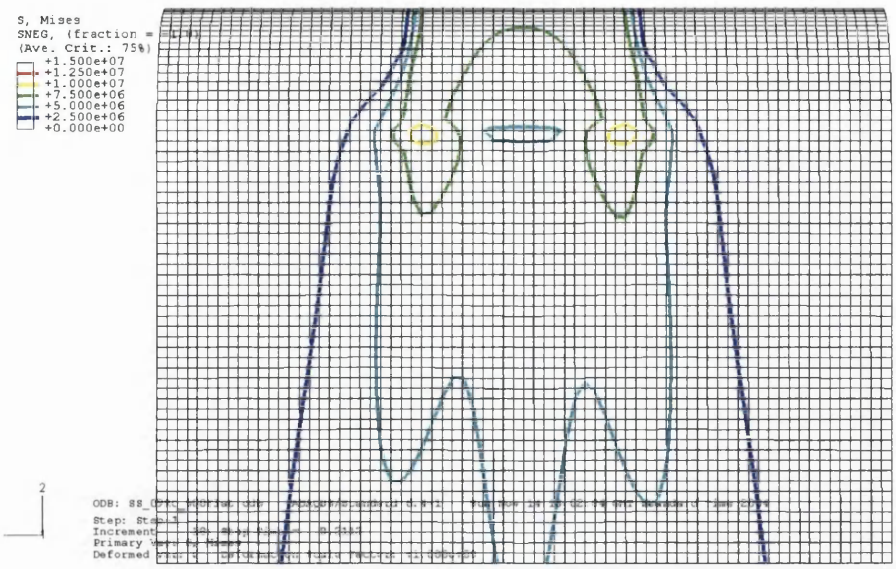

Figure 7.14 Model 2.3 - von Mises equivalent stress - Tension 3MPa

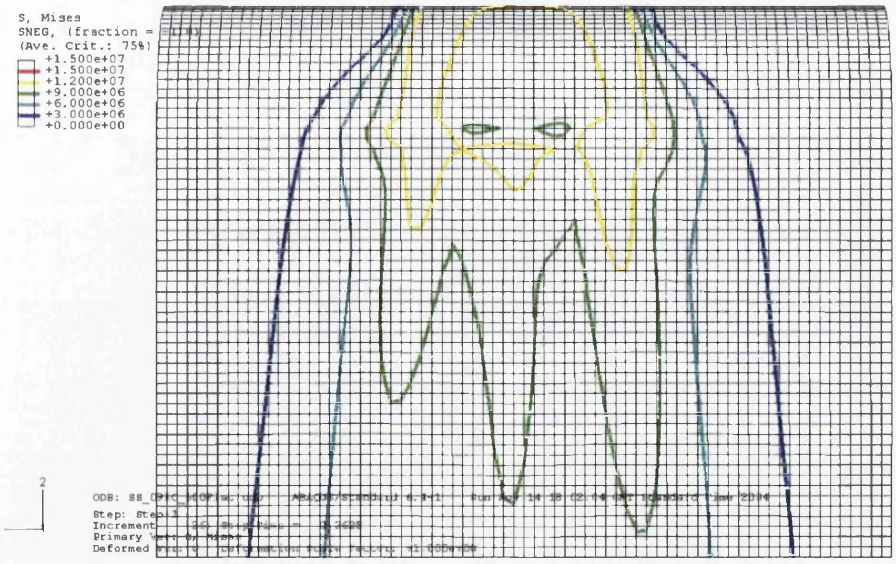

Figure 7.15 Model 2.3 - von Mises equivalent stress - Tension 5MPa

Figure 7.14 and *Figure 7.15* represent different in-line tension values when the strip was in contact with a roll profile that had a small central flat section of 500mm.

Throughout this chapter the author has commented on the buckle risk that this small central section poses. *Figure 7.14* represents 3MPa of in-line tension, it can be seen that the area of concern (the yellow lines represent the highest von Mises equivalent stress condition) was along the initial contact plane with the roll, more specifically at the location of the fillet points where the roll tapers began either side of the central flat section.

Figure 7.15 represents the strip at 5MPa of in-line tension, at this point the yellow line did not represent 10MPa anymore, it now represents 12.5MPa, which is a value far closer to the yield stress. The high stress designated by the yellow line (12.5MPa) was now starting to travel down the incoming strip; the wrinkles, which develop, were areas of compression on a generally tensile stress surface. Wrinkles that develop on the strips upstream surface can turn plastic when they make contact with the roll.

Figure 7.16 Model 2.6 - von Mises equivalent stress - Tension 3MPa

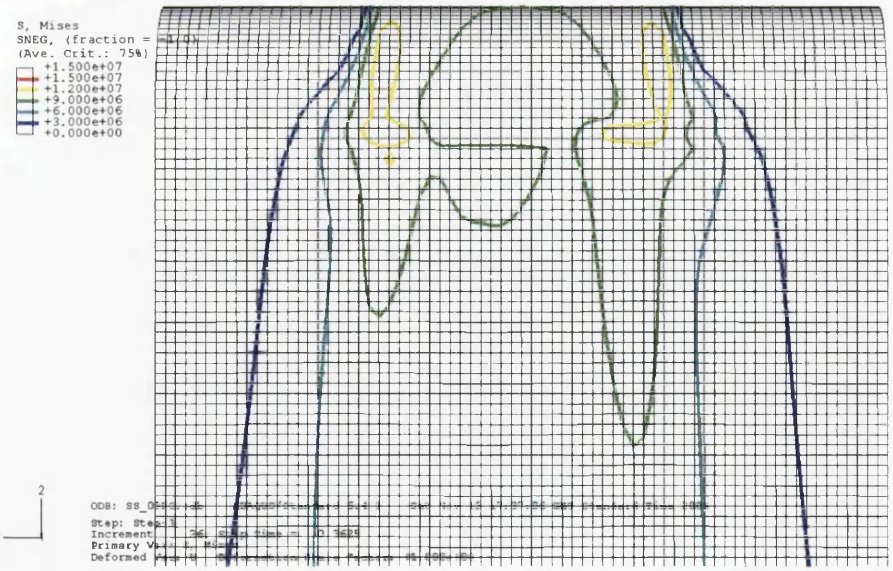

Figure 7.17 Model 2.6 - von Mises equivalent stress - Tension 5MPa

The two figures *Figure 7.16* and *Figure 7.17* represent the reference conditions for the variations in key operational parameters (taper size: 0.9mm, central flat section of the roll: 700mm). When compared with the two previous figures, which represented a central flat section of 500mm (0.9mm taper size), they compared favourably *(Figure 7.14* and *Figure 7.15)*, while for the 5MPa in-line tension value *(Figure 7.17)* the 12.5MPa von Mises equivalent stress value travels around the circumferential fillet point as it did in *Figure 7.15*, however, the 200mm increase in the central flat section (500mm to 700mm) restricts the incoming or preferably the upstream strips out-of-plane displacement, this helped to prevent potentially plastic compressive stresses originating from the initial contact plane.

Figure 7.18 Model 2.11 - von Mises equivalent stress - Tension 3MPa

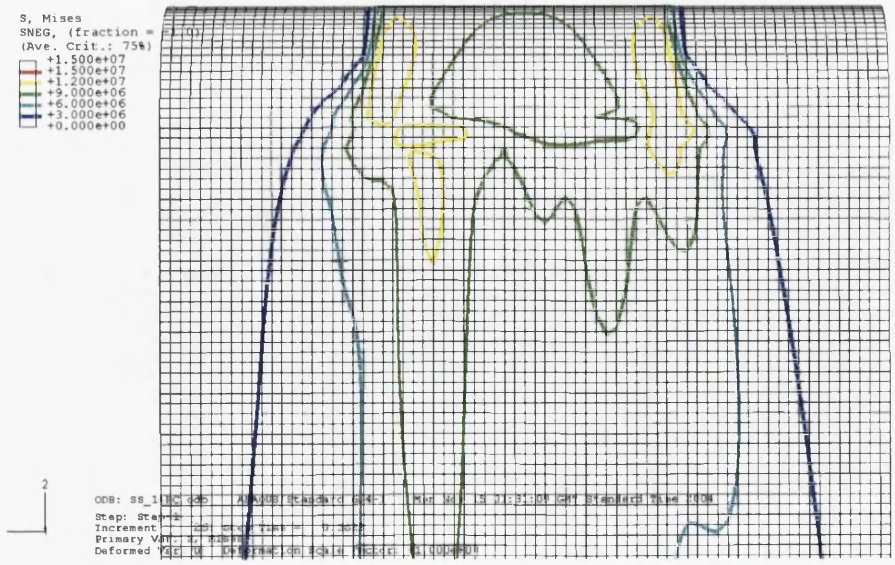

Figure 7.19 Model 2.11 - von Mises equivalent stress - Tension 5MPa

The two figures *Figure 7.18* and *Figure 7.19* represent a roll profile with a mid-range taper size of 1.4mm (central flat section: 700mm). The 12MPa von Mises equivalent stress area affected by an in-line tension of 5MPa was greater than for a roll taper size of 0.9mm - the high von Mises equivalent stress value (12MPa) was starting to travel down the strip, however, not to the same extent as that of the small flat section of *Model 2.3*.

Closing Remarks: Graphical Interpolation

The issue was that the roll profiles represented in *Model 2.3* and *Model 2.11* have had their place within the CAPL in the past. This was because strip wandering was best prevented by the use of large taper sizes and small central flat sections. However, the future commercial success of the CAPL depends on the strip having improved formability at thinner gauges. Thus as the strips soaking temperature increases its yield stress decreases. The result was that the roll profile will have to evolve across the entire soaking section; this starts with the removal of all the barrel rolls. The central flat section of the type "C" taper roll will have to be wider - minimum of 700mm, however, preferably 1000mm. The taper size will also have to change to no more than a maximum of 0.41mm.

7.1.3 INFLUENCE OF TAPER ROLL RADIUS

While much literature already exists on the effect of a varying roll taper on buckle risk, most notably that provided by the "Matoba" equation[6, 26], relatively little is noted on the stress fields generated at the taper itself.

Traditionally the CAPL rolls had utilised a radius of curvature of 20 metres *(Figure 7.20)*. The radius was added at the end of the central flat section of the roll profile. The greatest transport roll taper size was 3.3mm over a taper length of 850mm *(Model 1.3 and Model 3.2)*. While the radius was not visible to the naked eye it had proven benefits. The radius of curvature helped to prevent the development of intense localised stress states around the circumferential fillet point of the roll profile.

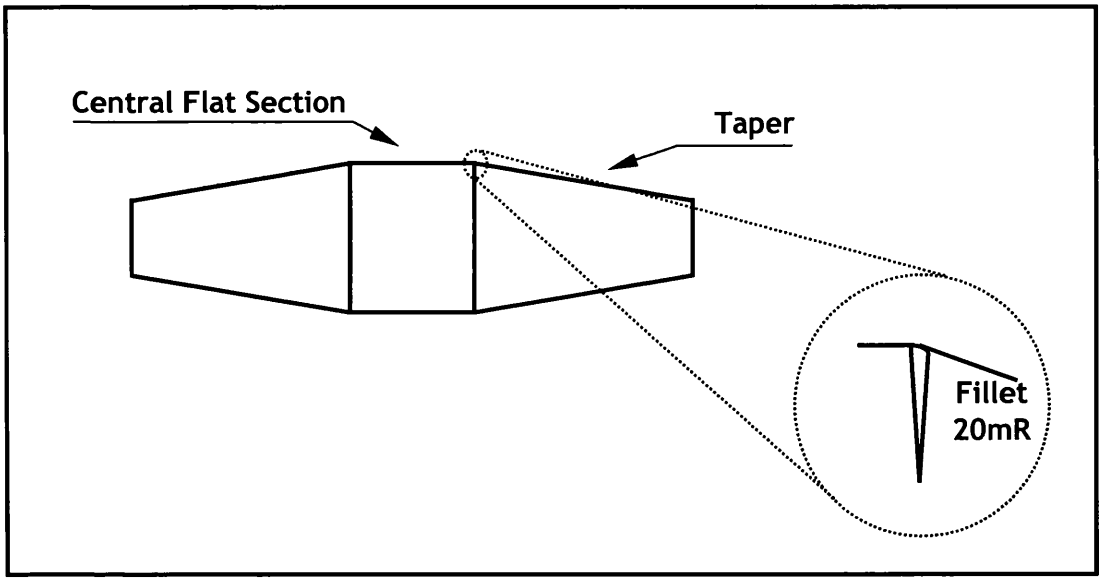

Figure 7.20 Typical Type "C" Taper Hearth Roll, Highlighting The Radius Point at the Taper Fillet

The author has shown in this chapter the importance of applying a 20 metre radius of curvature to the fillet point. It helped to reduce the buckle risk by 8% for an in-line tension value of 5MPa *(Model 2.6* compared to *Model 2.7).* However, compared to other roll profile variables its ability to significantly reduce the overall buckle risk has to be put into some sort of perspective.

Corus Group drove this section; the operators wanted to know if an increase in the curvature of the radius would help to reduce the buckle risk within the soaking section of the furnace. Analyses were performed comparing a roll profile with no radius of curvature, another with a 20 metre radius of curvature and finally a roll profile with a new, never used 40 metres radius of curvature.

7.1.3.1 The Ideal Tension for Variations in the Taper Roll Radius

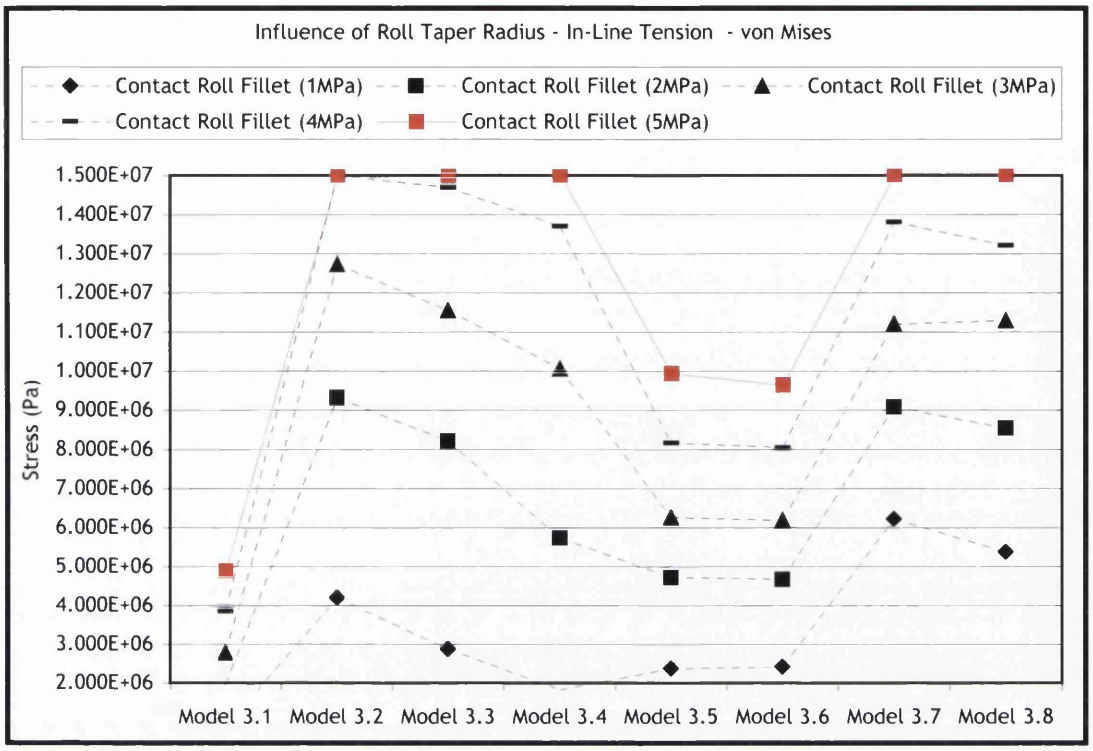

Figure 7.21 von Mises equivalent stress - Variations to In-Line Tension - Influence of Taper Roll Radius

Discussion Points: Figure 7.21

The above *Figure 7.21* is the von Mises equivalent stress for a number of rolls profiles. The author chose to investigate two known buckle risk roll profiles, because an improvement in buckle risk would then be clear. Corus will only consider changes in terms of a measured economical benefit, because changing the roll profiles curvature of radius would be both costly and time consuming. Furthermore, a change can only be performed at a designated maintenance interval or summer stop. A third low buckle risk roll profile was included for comparison purposes.

Model 3.1 represents a flat profile. *Model 3.2* represents a roll profile with a 3.3mm taper size and flat central section of 500mm. *Model 3.3* represents the same profile as *Model 3.2*, however, includes a 20mR. *Model 3.4* represents the same profile as *Model 3.2*, however, includes a 40mR. *Model 3.5* represents a roll profile with a 0.41mm taper size and a flat central section of 700mm. *Model 3.6* represents the same profile as *Model 3.5*, however, includes a 20mR. *Model 3.7*

represents a barrel roll with a taper size of 0.35mm. *Model 3.8* represents the same profile as *Model 3.7,* however, includes a 20mR.

Model 3.1 the flat roll profile is used as a reference profile - the von Mises equivalent stress closely follows the in-line tension values.

Model 3.2 - *Model 3.4* considers the large taper size of 3.3mm in conjunction with the small central flat section of 500mm. This roll type was designated "C1" by Corus and is operational in the heating section of the furnace. At 5MPa in-line tension the von Mises equivalent stress was at its maximum, a yield stress value of 15MPa for all three models. Thus for *Model 3.2* to *Model 3.4* the radius of curvature is irrelevant the strip will plastically deform at the standard in-line tension value of 5MPa.

With respect to in-line tension values that were applied to the strip 5MPa was the maximum tensile value that can be realistically be used on ultra thin strip gauges that were operating at velocities in excess of 180m/min. The author understands, that strip chemistry enhancements which have been considered, do not allow for a significant increase in the in-line tension load within the soaking section of the furnace, because the strips gauge is so thin and the operating temperature is so high that the strip is still going to have a relatively low yield stress. High tension (5MPa) is often used to keep the strip tort on the roll to prevent sideways wandering (tracking), and in the straights between the roll passes to prevent strip sagging - both of which were highly detrimental to strip quality.

Once the in-line tension is reduced to 4MPa, the results become more interesting. *Model 3.2* the no radius of curvature model is indicating strip yielding. However, *Model 3.3* the model with a 20 metre radius of curvature at the roll fillet is indicating a von Mises equivalent stress that is just below the strips yield stress of 15MPa. *Model 3.4* the model with a 40 metre radius of curvature indicates a von Mises equivalent stress of 13.7MPa, which is a reduction of 9% over the no radius of curvature model and 7% over the 20 metre radius of curvature model. For reference, *Model 3.3* (20mR), had only a 2% improvement in its von Mises equivalent stress when it was compared to *Model 3.2*, a no radius of curvature model.

When the in-line tension was reduced further to 3MPa the percentage reduction in the von Mises equivalent stress for the 40 metre radius of curvature model becomes even greater. *Model 3.4* has a von Mises equivalent stress value of 10MPa, a reduction of 13% over *Model 3.3* (a 20m radius of curvature model).

The computational models *(Figure 7.21)* clearly show that as the in-line tension reduces even further (2MPa and 1MPa) then the percentage difference between the 40 metre radius of curvature model (3.4) and the 20 metre radius of curvature model (3.3) grows further. For an inline tension value of 2MPa the reduction in the von Mises equivalent stress was 30% and at 1MPa of in-line tension the reduction was 36%. The application of a 40 metre radius of curvature to the roll fillet had to be classified as an immediate financial benefit to Corus if it were implemented. Furthermore, results indicate that if the change to the radius of curvature were achieved in conjunction with a reduction in the in-line tension then even greater benefits can be achieved. In this particular case benefits refer to better strip quality and a reduction in buckle incidents.

Model 3.5 and *Model 3.6* considers the small taper size of 0.41mm in conjunction with the medium central flat section of 700mm. This roll type was designated "C5" by Corus and is operational in the soaking section of the furnace where the strip undergoes recrystallisation at annealing temperatures in excess of 750°C. There is no 40 metre radius of curvature model, because it was deemed that under current operational conditions a 40 metre radius of curvature would not be required for a profile that already exhibits limited buckle susceptibility, however, a 20 metre radius of curvature model and a no radius of curvature model were investigated. *Model 3.5* represents the no radius of curvature model and *Model 3.6* represents the 20 metre radius of curvature model. Neither model had a von Mises equivalent stress value greater than 10MPa at an in-line tension value of 5MPa (yield stress: 15MPa). The model with the 20 metre radius of curvature *(Model 3.6)*, exhibits at every tension level a reduction in the von Mises equivalent stress over the model with no radius of curvature *(Model 3.5)*. However, the difference is almost insignificant, a 1.5% reduction in von Mises equivalent stress at 4MPa of in-line tension.

For comparison purposes the barrel roll was included. *Model 3.7* represents a roll with no radius of curvature and *Model 3.8* represents a barrel roll with a 20 metre

radius of curvature. At 4MPa of in-line tension the reduction in the von Mises equivalent stress was 4%, this was fairly significant considering the roll taper size was only 0.35mm. However, the roll still exhibits a high buckle risk and should in the author's opinion be replaced.

Concluding, for large taper sizes (over 1.4mm) increasing the radius of curvature from 20mR to 40mR would certainly be beneficial in reducing the overall stress state of the strip, especially at the fillet point of the roll profile. However, for all other roll profiles, this small benefit is unlikely to be greater than the financial cost of implementing such a maintenance change.

Discussion Points: Graphical Interpolation

Figure 7.21 clearly shows the benefits of using a 40 metre curvature of radius. The issue was that "scatter" graphs define a result of a single element, for a true picture of the area effected, it is appropriate to use a graphical representation showing all the affected elements.

Figure 7.22 to *Figure 7.24* are models with three different radiuses of curvature (at 3MPa of in-line tension). The figures represent a side on view (x-axis) of the strip (the roll has been removed), this is the view, which best shows the initial contact plane. *Figure 7.22* represents *Model 3.2* (no radius of curvature). *Figure 7.23* represents *Model 3.3* (20 metre radius of curvature). *Figure 7.24* represents *Model 3.4* (40 metre radius of curvature).

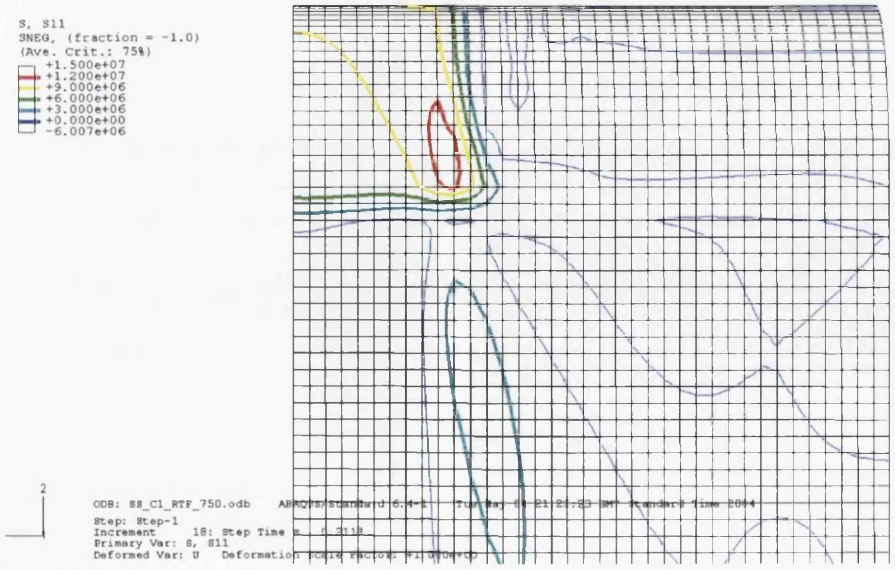

Figure 7.22 Model 3.2 - S1 Directional Stress - Tension 3MPa

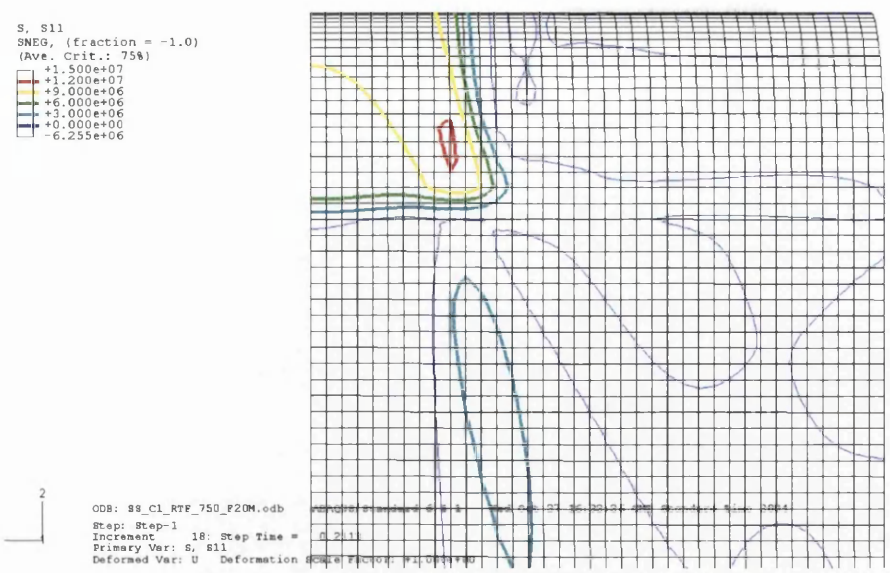

Figure 7.23 Model 3.3 - S1 Directional Stress - Tension 3MPa

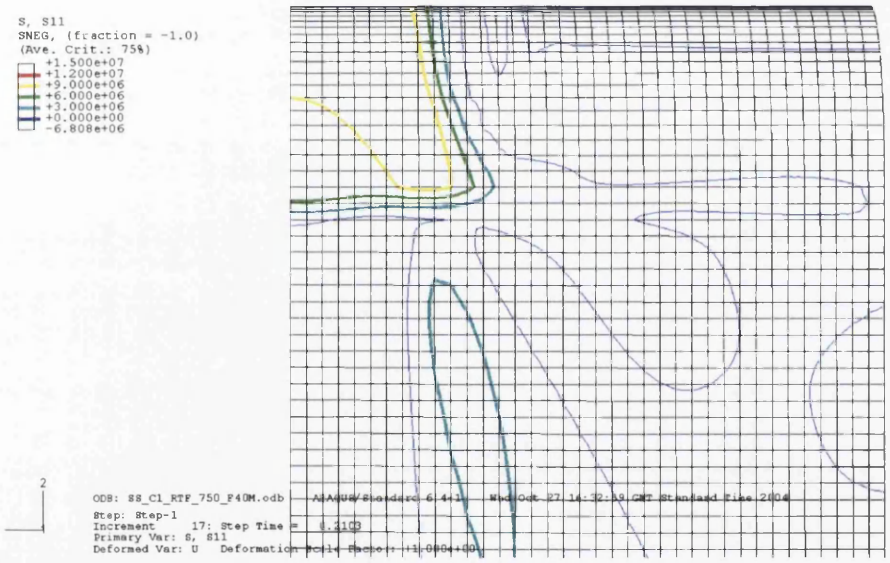

Figure 7.24 Model 3.4 - S1 Directional Stress - Tension 3MPa

What is clear from the figures above *(7.22 - 7.24)* is that as the radius of curvature increases the buckle risk reduces. *Model 3.2* indicates an area of approximately 125mm^2 that was under a S1 directional stress of greater than 12MPa (15MPa YS). *Model 3.3* indicates an area of approximately 50mm^2 that was under a S1 directional stress of greater than 12MPa. *Model 3.4:* there is no S1 directional stress greater than 12MPa. However, this was not the same story at a S1 directional value of10MPa. Each figure indicates a greater area covered by the 10MPa S1 directional stress than the figure that was immediately proceeding. Thus the radius of curvature not only reduced the maximum stress value at the fillet

point, it also helped to spread the stress out across the strips surface, thus limiting areas of high stress concentration.

7.1.4 TENSION LOADING ISSUES AT CORUS PONTARDULAIS WORKS

Corus operate several different plants in South Wales. At Pontardulais there was concerns over the 90° wrap angle of the strip passing around the deflector roll, which has a barrel roll profile. This transport roll has a 4mm crown and a 20 metre radius of curvature at the rolls central fillet point. The aluminium coated product line is used for transportation and not deformation in a similar way to that of the CAPL at Port Talbot.

The mechanical properties of the strip were a yield stress of 100MPa and an elastic modulus of 95GPa. Due to the increase in mechanical properties the strip can withstand an in-line tension value of 12.5MPa.

The strip travelling at 90° around a transport roll translates into a reduced contact time between the strip and said transport roll. Therefore the roll taper size has to be more aggressive than that on the Port Talbot CAPL to prevent the strip from wandering (tracking).

Corus's request was simple: what can the 12.5MPa in-line tension be reduced to. For a satisfactory reduction in the buckle risk while not jeopardising the ability of the roll crown to prevent strip tracking?

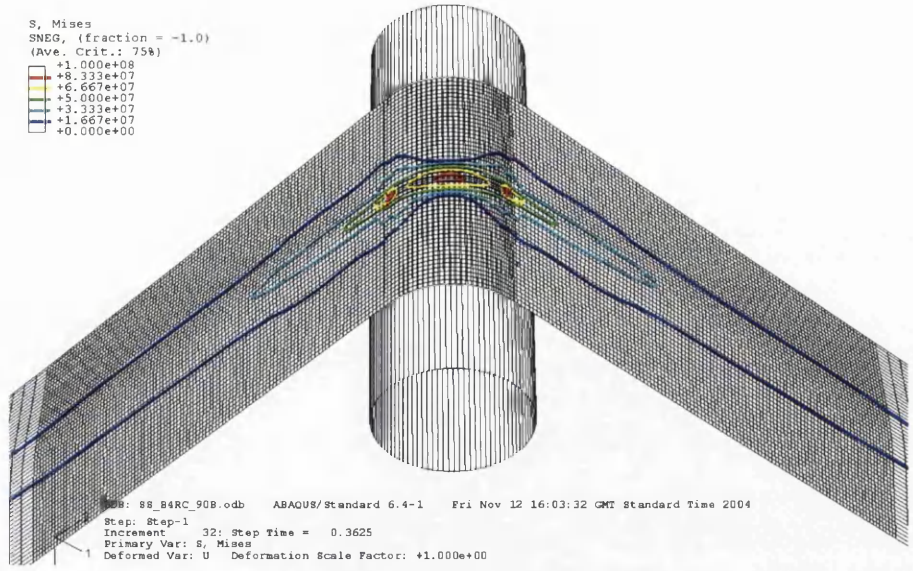

Figure 7.25 von Mises equivalent stress - Pontardulais Barrel Roll Profile - In-Line Tension 12.5MPa

The above figure *(7.25)* indicates that while the strip never reaches a 100MPa von Mises equivalent stress value, which would indicate yielding. It did, however, have two distinct if not small localised areas of high stress, these two concentrations of 83MPa could be considered an indication of an in-line tension that could create a buckle risk. The first was at the initial point of contact (along the contact plane) and second was at the exit point, in both cases this was along the central roll profile fillet.

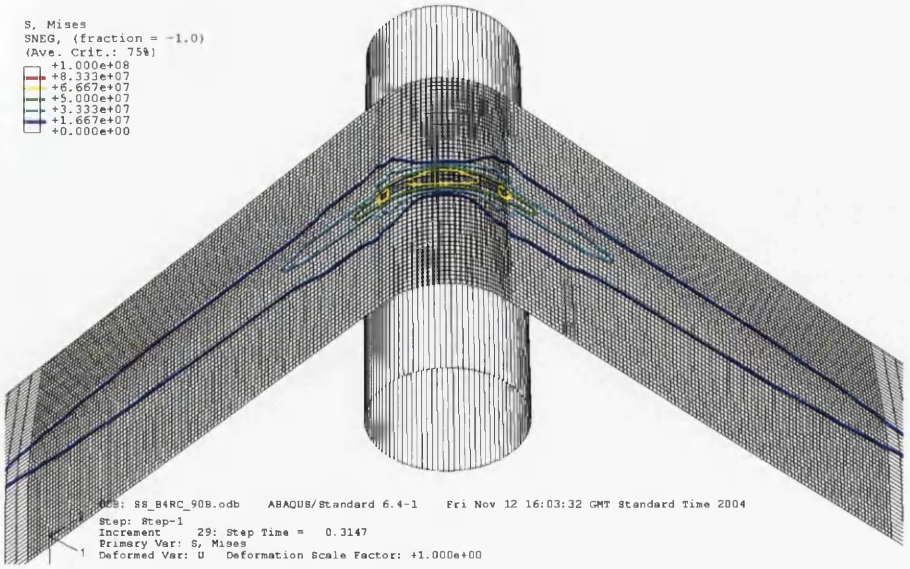

Figure 7.26 von Mises equivalent stress - Pontardulais Barrel Roll Profile - In-Line Tension 10.85MPa

The above figure *(7.26)* indicates that an in-line tension value of 10.85MPa will remove the stress concentrations at the transport rolls upstream and downstream contact points. Thus a reduction of at least 10% to the in-line tension value would be beneficial. However, while this had to be considered an immediate benefit to Corus operations there was another consideration. Reducing the in-line tension increases the risk of tracking and other buckle risks associated with strip slacking or sagging between passes.

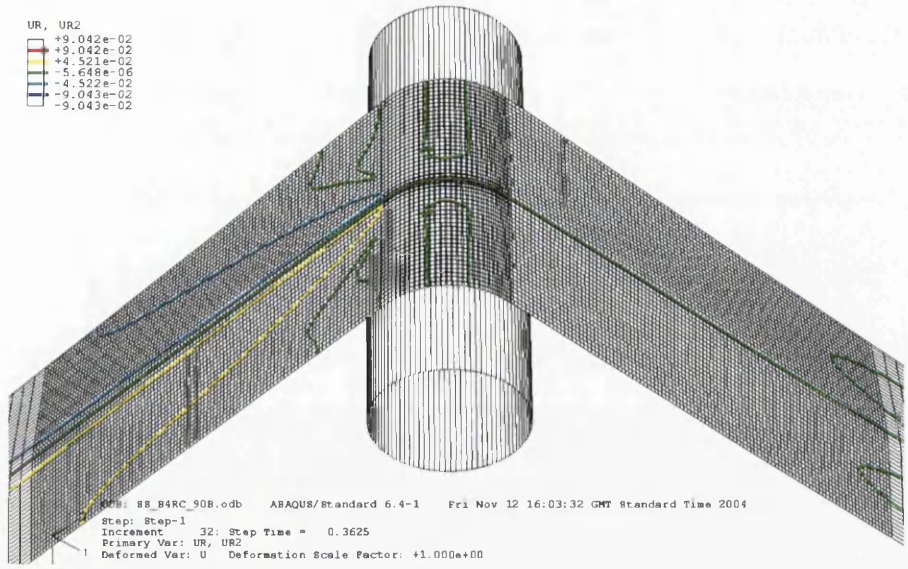

Figure 7.27 Strip Displacement - Pontardulais Barrel Roll Profile - In-Line Tension 12.5MPa

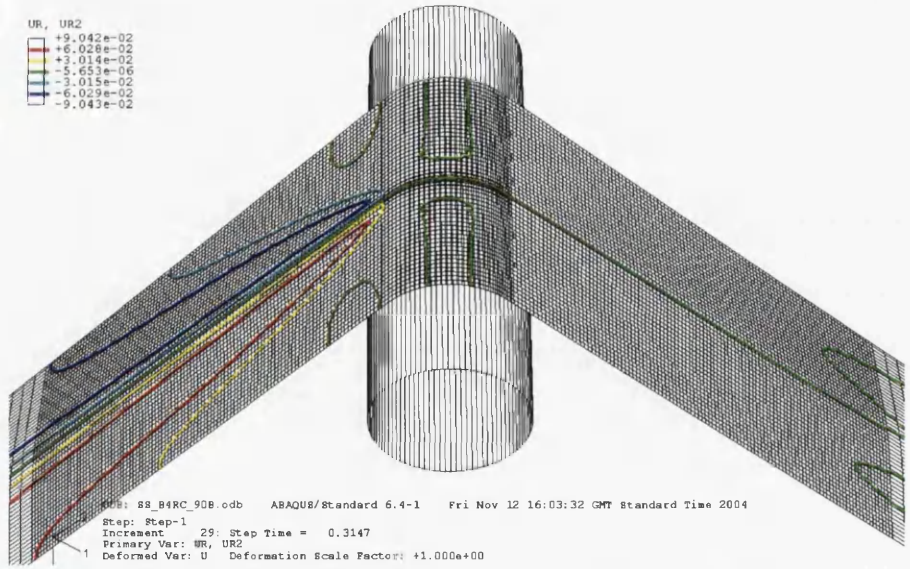

Figure 7.28 Strip Displacement - Pontardulais Barrel Roll Profile - In-Line Tension 10.85MPa

The rotational displacement about the y-axis is considered a good indicator of strip slackness between the roll passes. *Figure 7.27* indicates the rotational displacement is restricted to +/- 4.5cm upstream of the contact. Whereas, for *Figure 7.28* the displacement is +/- 6cm upstream of the contact. The author cannot say for sure whether this would lead to high buckle susceptibility, because displacement cannot easily be quantified in those terms, certainly not as easily as stress with its defined yield point. However, if the strip had a greater out-of-plane displacement in the band between passes then in all likelihood the chances of tracking occurring have, at the very least, increased. In consideration, the author can suggest that a decrease in stress from a reduction of the in-line tension could be beneficial in reducing the chances of strip buckle, however, there should be an element of caution.

7.1.5 HEAT TRANSFER CONSIDERATIONS

The roll-strip temperature differential was investigated in some detail in the experimental programme chapter. The conclusion from that section indicated that small temperature differentials would have only a minor effect on strip shape. However, a large temperature differential between the transport roll and the strip will increase the strips susceptibility to plasticity. The two CAPL parameters, which reduce high temperature differentials, are ultra thin strip gauge, so that the temperature change is instantaneous and contact time. However, neither is particularly satisfactory, ultra thin gauge will certainly increase the likelihood of buckle risk and the contact time is a fraction of a second because this is a continuous annealing line and not a batch annealing process. The best way to assure temperature differentials are maintained at appropriate levels is by the use of the CAPL's process control systems. If the parameters are set appropriately the temperature difference between the strip and the transport roll can hopefully maintained at the minimum for as long as operationally possible. The process control systems can control a number of factors to maintain the correct temperature differential. This includes the furnace ambient gaseous temperature, the in-line strip speed and the in-line strip tension, in some instances the roll temperature can also be controlled. Again there are issues here, the temperature of the furnace is fundamentally important for the recrystallisation process of the strip inside the soaking furnace, so changes can only be finite. The in-line speed of the furnace has two majors issues associated with it. Increasing in-line speed will of course increase throughput, something Corus desperately wants, however, it

will also decrease contact time so temperature differentials will, in all likelihood, increase. The line speed also affects the annealing time that the strip spends inside the soaking furnace and, perhaps most importantly, in-line speed directly increases the strips buckle susceptibility risk. Furthermore, the fundamentals of heat transfer, as well as the experimental research performed in this thesis, tell us that convection and radiation while both relevant are overwhelmed when conductance is present. This lowers the importance of the gaseous atmosphere in particular unless the temperature of the gas, the roll and the strip are all homogenous, then the gas maintains the strip and roll temperature between contact passes.

Observations on the CAPL itself have shown that large temperature differentials between the roll and the strip still do occur very rarely. The cooling buckle team[27] have reported that large temperature differentials can occur between the bottom and top rolls in the secondary cooling section, which while this was not considered normal it did highlight possible process control system failures or more likely problems with the cooling system. The blow boxes purpose in the secondary cooling section is to cool the strip as it passed through the zone, however, in this case the predominant heat transfer parameter was convection, this in its self was not as effective as conduction in distributing or removing heat, thus any ineffectual blow box discharge will affect the strip zonal temperature. However, this did not matter, if cooling buckle occurs even intermittently then the fact that there had been any buckle will cause the strip to fail inspection.

While the Stein Heurtey experimental work was conclusive with respect to the affects of conductive heat transfer, it was felt necessary to analyse a typical CAPL roll-strip contact scenario using a static uncoupled heat transfer computational FEA analysis. The individual model parameters can be seen in Section 6.5 the "Roll-Strip Model Parameters"

7.1.5.1 The Results

The following highlights some typical CAPL scenarios involving varying degrees of conditions of contact. The roll width of 1200mm ∅ is associated with rolls in the overaging section onwards, where strip temperatures in this section onwards would rarely be over 300°C, However, the context of the effects of heat transfer holds true for all sections of the CAPL.

Model No	Strip Gauge (mm)	Temperature Differential	Conductance (W/m^2K)	Convection (W/mK)	Radiation	Temperature Loss (°C)
5.1	1	100	1600	0	0	24.5
5.2	1	200	1600	5	0.25	33
5.3	0.2	200	1600	5	0.25	90
5.4	0.2	200	1000	0	0	76
5.5	2	200	1600	0	0	20

Table 7.1 The Effects of Different Heat Transfer Components

7.1.5.2 Heat Transfer Discussion Points

The temperature differentials created at elevated temperatures such as seen in *Table 7.1* highlight the importance of minimising such affects.

The temperature difference between *Model 5.1* and *Model 5.2* is approximately 7°C. *Model 5.2*, represents a further 100°C temperature differential at the roll-strip contact (total temperature differential of 200°C). *Model 5.2* includes the effects of convection and radiation, where as *Model 5.1* does not. These results highlight that once the gauge was greater than 1mm the strip thickness was of sufficient depth to prevent instantaneous conductance. The reason is simple - the short contact time that occurs on each pass does not allow for a perfect transfer of heat, this is an issue in all sections of the furnace except the soaking furnace where the temperature should be fairly homogenous.

The operating conditions of *Model 5.3* are the same as *Model 5.2*, however, it is clear that the ultra thin nature of the strip in *Model 5.3* (0.2mm) gauge, will loss heat very quickly to a much cooler transport roll. This rapid transit of heat, which was 57°C, was far higher than in the case of *Model 5.2*, which had a gauge that was 5 times thicker at 1mm. This would cause a great deal of concern if the strip were operating close to its yield stress (15MPa for the soaking furnace) the rapid transit of heat would in all probability cause the strip to instantly buckle (plastically). However, the chances of both a high temperature differential and perfect conductance conditions is, in the authors' opinion, limited. Primarily because the high temperature differential would cause the strip to lift from the surface of the roll the moment contact was made - Chapter 5 "The Stein Heurtey Experimental Programme", discusses such an effect.

Model 5.4 uses the same operational parameters as that of *Model 5.3*. The difference is the reduced contact conductance value (1000W/m^{2}K). *Model 5.4* highlights that a reduction in conductance from the perfect contact conditions reduces the temperature loss within the strip by 14°C from 90°C to 76°C (contact period 0.65 seconds). However, the reduction in conductance conditions tends to be linked with poorer contact conditions generally.

The 2mm thick strip *(Model 5.5)* highlights the issue surrounding processing thicker grades (over 1mm). In an isothermal stress-strain model, thicker gauges have been shown to actually increase the risk of buckle susceptibility, because of the increased resistance to bending (around the roll as the strip travels). Deformation of thicker grades occurred more readily if the in-line tension spikes, which often occurred because of poor contact conditions. However, this creates a vicious circle, because as the tension spikes the following uneven in-line tension then creates even poorer contact conditions than the previous poor contact conditions, which in turn obviously increases the buckle risk even further than before. The temperature loss of 20°C in 0.65 seconds was low considering the temperature differential was 200°C and had absolutely perfect contact conditions.

7.1.5.3 Heat Transfer Conclusions

As far as temperature considerations are concerned the thicker the strip gauge the smaller the temperature loss due to contact conductance. This automatically makes thicker gauges better at withstanding higher contact temperature differentials than the thinner more conventional CAPL gauges run at present (below 1mm). However, the computational models indicated that the temperature losses were not uniform across the surface. The edge of the strip appeared to be a little more resistant to conducting heat than the centre of the strip, which created an uneven stress state. An uneven surface stress is only really an issue when the strip is operating close to its yield stress; which of course is possible in the heating section of the furnace moving through to the soaking section of the furnace where the contact temperature differential was at its greatest. Port Talbot CAPL transport rolls generally will have cooler roll edges then at the rolls centre (particularly the flat section of a taper roll, which was always in contact with the strip that is passing). However, because the strip width can change from one coil to the next, intermittent conductivity can occur. The use of thicker strip is the responsibility of the operator, it is a risk, but the rewards could be high.

Traditionally batch annealing is the only way to anneal product with a large strip gauge (over 2mm).

The heat transfer models were run for 0.65 seconds to put this into context, the contact time for a roll with a diameter of 750 was less than half a second even for a moderate strip velocity of 300m/min. Corus want to increase the throughput rate, the increased strip velocity will lead to a reduced contact time, this could be a problem in the heating and cooling sections where contact conductance plays a part in heating and cooling the strip.

The uncoupled heat transfer model has some drawbacks compared to the fully-coupled model that was used in Chapter 5 "The Stein Heurtey Experimental Programme". Principally, the thermal effects were not translated into stress-strain effects, and this could be a significant, as mechanical outputs determine if the strip will plastically deform. Furthermore, friction and line tension cannot be included into the models design parameters. Thus the un-coupled model was used just to analyse the effects of contact conductance, with temperature dependent properties used for the isothermal stress -strain models.

For these results and in general for contact models, convection and radiation effects can be considered constant. They have little overall effect on the heat transfer that was taking place between the transport roll and the strip steel, furthermore, research (not shown here), backed up by literature has indicated that contact conductance can be as little as $160W/m^2K$[7] and can still be effective. The values used in these contact models, even the $1000W/m^2K$ conductance value are close to perfect conductance. Typically, however, contact and therefore the conductance values were disrupted by a series of operational inadequacies.

These results, while simple, do help to validate and move the discussion topics along that were initially being raised in the Stein Heurtey experimental chapter, that of the importance of roll-strip contact temperature differentials.

7.2 DYNAMIC ROLL-STRIP CONTACT INVESTIGATION

Opening Remarks

The authors' static models concentrated on the effects of in-line tension on strip steel (EDDQ) in hard contact with a stationary transport roll. Static models are ideal for investigating individual operational parameters and how they will affect the strips yield stress, strip quality or buckle susceptibility.

The author can analyse most operational parameters with the use of static models. Static models are ideal because they are inherently linear in nature. Non-linear parameters, such as the frictional coefficient and strip velocity, can be kept as constants. However, strip velocity is integral, as the purpose of the CAPL is continuous annealing. The use of a dynamic model enables investigations into strip velocity, frictional coefficients, strip tracking and unequal tension, all which cannot be appreciated when using a static model.

The dynamic models used throughout this chapter have similar properties to those of the static models of the previous section. However, the distinct difference is strip velocity, applied in the form of an angular rotational velocity boundary condition to the central reference point of the transport roll. The standard velocity value used throughout the dynamic section of this chapter is 13.333 radians/time - 300m/min for a 750mm diameter transport roll.

Section 6.5 the "Roll-Strip Model Parameters" within Chapter 6 defines all aspects of the computational models that are discussed here

The dynamic analysis must run for 0.6 seconds before steady state results can be recorded. Prior to 0.6 seconds, the strip is under high roll contact stress start-up conditions, due to the instantaneous nature of how in-line tension is applied in the first increment.

7.2.1 STANDARD ROLL CROWNS

The static section *(7.1)* investigates individual parameters in detail. The dynamic section will not revisit such areas but will concentrate on the parameters that cannot be explained in a static computational model. However, the one exception is roll profiles, as the author investigated roll profiles that were smaller than the standard CAPL roll profiles (0.41mm taper size). Furthermore, it is useful to gain

some idea of how velocity effects standard roll profiles that are considered a low buckle risk under static conditions.

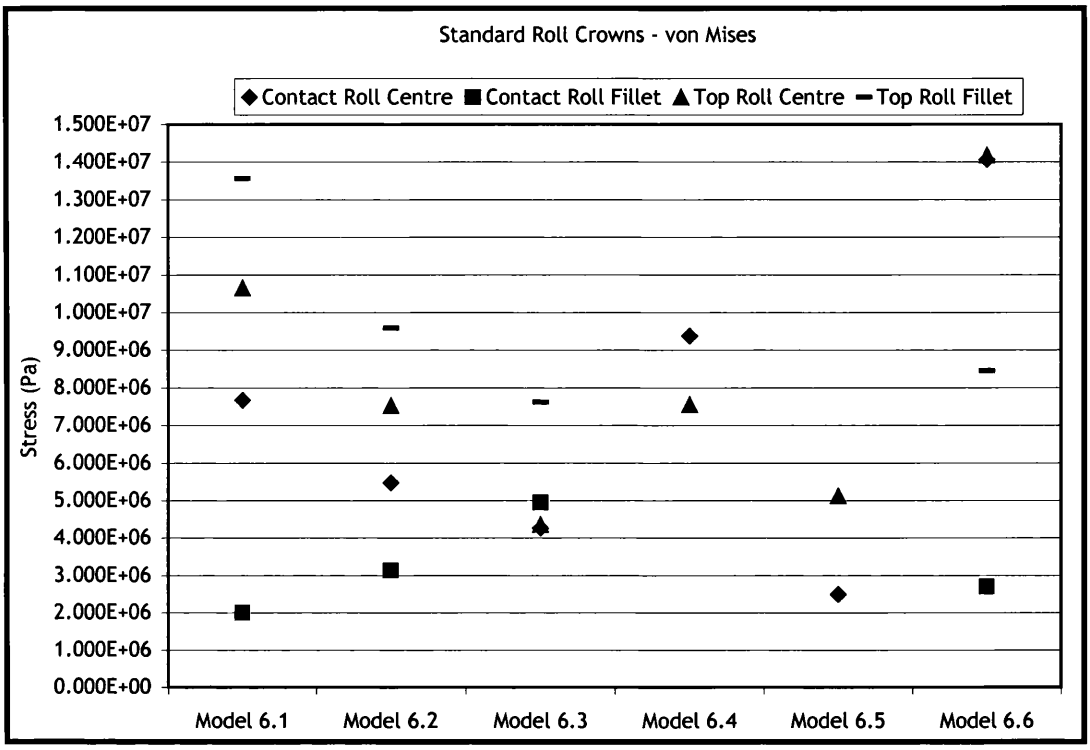

Figure 7.29 von Mises equivalent stress - Standard Roll Crowns

The above figure *(7.29)* represents results where the yield stress is 15MPa. The mechanical properties representative of the strip passing through the critical buckle risk region.

Figure 7.29 considers the three standard roll types: *Model 6.1* represents a flat roll profile. *Model 6.2* represents a taper roll with a taper size of 0.05mm and a central flat section of 700mm. *Model 6.3* represents a taper roll with a taper size of 0.41mm and a central flat section of 700mm (current profile). *Model 6.4* represents a barrel roll with a taper size of 0.15mm. *Model 6.5* represents a barrel roll with a taper size of 0.35mm (current profile). *Model 6.6* represents a taper roll with a taper size of 3.3mm and a central flat section of 500mm (current profile).

The flat roll profile *(Model 6.1)*, which has an exceptionally low buckle risk in the static models, now in the dynamic models shows its complete inappropriateness. The maximum von Mises equivalent stress value of 13.5MPa is considerably higher than the von Mises equivalent stress value of 5MPa for the static model *(Model 1.1)*. The issue with flat profiles is that the frictional coefficient is incredibly important. If the value is not maintained appropriately then traction difficulties can occur, high stress could be generated across the surface of the roll. Associated with poor traction is the roll profile, a small taper creates a resistance to sideways movement. If as in this case there is no taper for the strip to grip, then the strip starts to wander, which can be made worse because of unequal tension or air entrapment (air cushion effect).

In a computational model unequal tension is fairly easy to control. However, the mesh is not always perfect across the strip surface. This is made more complicated because the in-line tension is applied as a concentrated force at the end nodes of the hanging strip. This can lead to a small discrepancy in the tension distribution across the strip's cross-sectional area. Therefore, even a computational model will have a small degree of unequal tension, which would not show on a static model. However, compared to the actual CAPL, the tension will always be perfect.

Model 6.3 represents a typical soaking section taper roll; the von Mises equivalent stress value was 7.6MPa, which is considerable less than the for the flat profile of *Model 6.1* (13.5MPa), thus introducing a taper (0.41mm) to a flat roll profile helped to reduce the maximum in-plane stress, which in turn reduced the buckle risk. Furthermore, all four probed values, along both contact planes, have close von Mises equivalent stress values; this suggests that this roll profile helped to prevent high stress intensities developing solely around the circumferential fillet point (at the start of the taper). Interestingly, however, the von Mises equivalent stress value for a similar static model was 9.8MPa *(Model 1.2)*. However, the author considers that after 0.6 seconds of rotating hard contact, which included constant tensile and compressive stress state changes, the von Mises equivalent stress values would differ. Furthermore, there was a fundamental difference in how the time step was considered between the two models. The dynamic model used automatic incrementation; the static models used user-defined incrementation. Automatic incrementation is particularly useful for non-linear

problems; it helps convergence and cuts the computational expense. Finally, element probing on the static model was straightforward because the element never moved; they stretched or shrunk depending on whether the prevailing stress state was tensile or compressive. However, for dynamic models the same element will definitely have moved, and not always to the exact same new location, as the roll profile can interfere with the distance the strip travels each new increment.

Model 6.2 has a taper size of 0.05mm and has a von Mises equivalent stress value of 9.5MPa, compared to 7.6MPa for *Model 6.3* (0.41mm taper size) and 13.5MPa for *Model 6.1*(flat profile). What was clear was that a small taper size was beneficial, however, only to a certain point. When the taper size was smaller than 0.41mm then the benefit was reversed and buckle susceptibility increases. The maximum von Mises equivalent stress value for all three models was located at the top of the roll; this was considered good, as this translated into lower stress values along the initial contact plane. Lower less buckle susceptible stresses along the initial contact plane translates into a reduced buckle risk in the strip length between the roll passes, as out-of-plane behaviour in the strip was unlikely to originate along the transport rolls initial contact plane. As mention previously in this chapter, when potentially plastic inducing high levers of stress occurred along the initial contact plane, it could travel down the incoming strip from its point of origin, and thus exasperating the original problem.

Model 6.4 represents a barrel roll with a reduced taper size of 0.15mm. *Model 6.5* represents a barrel roll with a taper size of 0.35mm (standard soaking section barrel roll). Considering just the probed element values at the contact roll centre point and top roll centre point, i.e. the starting points for the taper angle on a barrel roll (there is no central flat section). The small taper size (0.15mm) again proved detrimental to the overall stress state of the strip, when compared to a large taper size (0.35mm). For *Model 6.4* the maximum von Mises equivalent stress was at the contact centre point, a value of 9.3MPa (yield stress: 15MPa). However, the stress at the contact centre point was only 2.5MPa for *Model 6.5*, its maximum von Mises equivalent stress value was 5MPa and that was at the top roll centre point. Again as with the taper roll models discussed prior, the results reinforced the idea that there should be a minimum taper size in the same way as there should be a maximum. Certainly a barrel roll with a taper size of 0.35mm will be far better suited in preventing tracking than a barrel roll with a taper size of

0.15mm. However, as mentioned within this chapter, the author feels that barrel rolls should be discontinued. Dynamic results, not shown here, indicated that barrel rolls were not as efficient as taper rolls in dispersing the high localised stress intensification that occurred at the roll's circumferential fillet point, even if the fillet incorporated a radius of curvature greater than 20 metres, this still will not be as beneficial as central flat section of at least 700mm. The high stress intensification tended to manifest itself in high tensile stress at the circumferential fillet (the centre of a barrel roll), followed by an equally high compressive stress immediately adjacent. Furthermore, the barrel roll has a far greater negative effect on the strip - this is both upstream and downstream of the initial contact. On a barrel roll high stress is concentrated at just one point, whereas on a taper roll there is a circumferential fillet either side of the strip's centre so the stress had effectively three points to disperse any high stress intensification that may be generated.

Model 6.6 represents a roll profile within the heating furnace, a roll taper size of 3.3mm and a central flat section of 500mm. Like the rest of the dynamic models which have reached a degree of steady state equilibrium, the maximum von Mises equivalent stress value had not yet reached the yield point. However, the value was still significant at 14.2MPa and was the roll profile with the highest buckle risk. The highest von Mises equivalent stress values were associated with the contact roll centre and the top roll centre, two points, which indicated that any failure in the strip would be through, what is known as, the centre buckle[43]. What appeared to be happening was that the small central flat section and large taper size was causing the strip to lift off the transport roll at the strip's centreline, this was severely affecting the strips stress state at that point.

7.2.1.1 The Affects of CAPL Start-Up

The best and perhaps only way of seeing how start-up conditions affect the initial strip quality was through the use of a dynamic model. The following series of figures (see below) represented the start-up conditions between a section of strip with a width of 1800mm (half-width model) and a taper hearth roll that had a taper size of 3.3mm, and a central flat section of 500mm *(Model 6.6)*. However, Corus understood that at start-up the strip quality was going to be compromised, therefore all parts of the coil that were affected by the start-up conditions were scrapped.

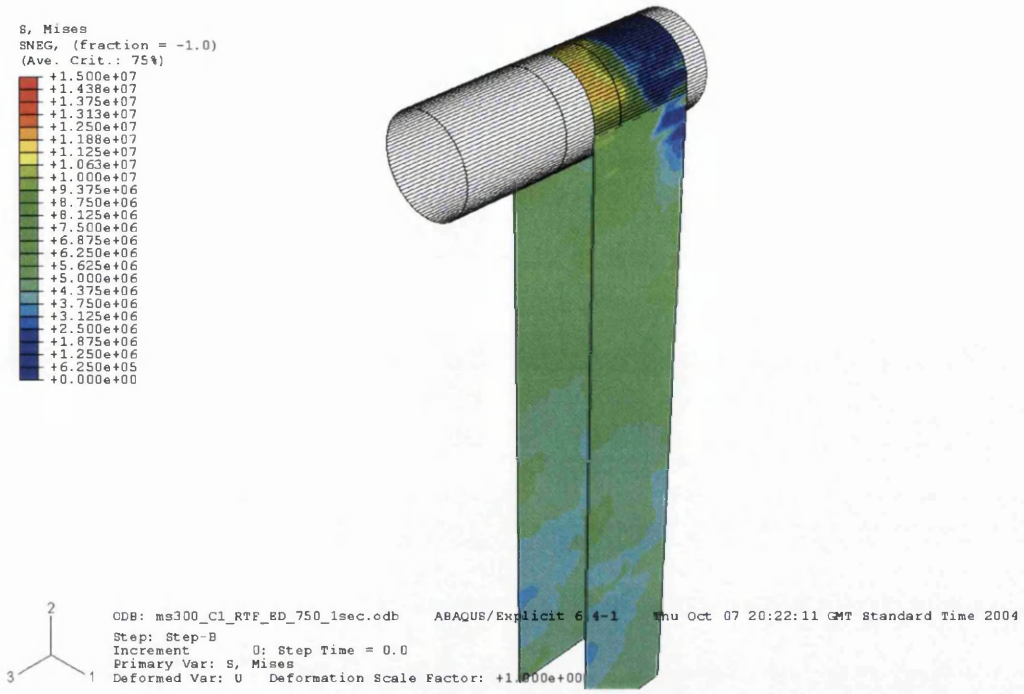

Figure 7.30 von Mises equivalent stress - Model 6.6 - Step Time 0

The above figure (7.30) represents in-line tension (5MPa) only. It can be seen that the highest stress values were associated with the strip on the central flat section of the roll only. The strip that was situated on the taper angle had an almost negligible von Mises equivalent stress value. This figure in particular showed the disadvantages of using roll profiles with large taper sizes and small central flat sections - the stress was not adequately dispersed across the strips surface; it accumulated at the strip's centre point.

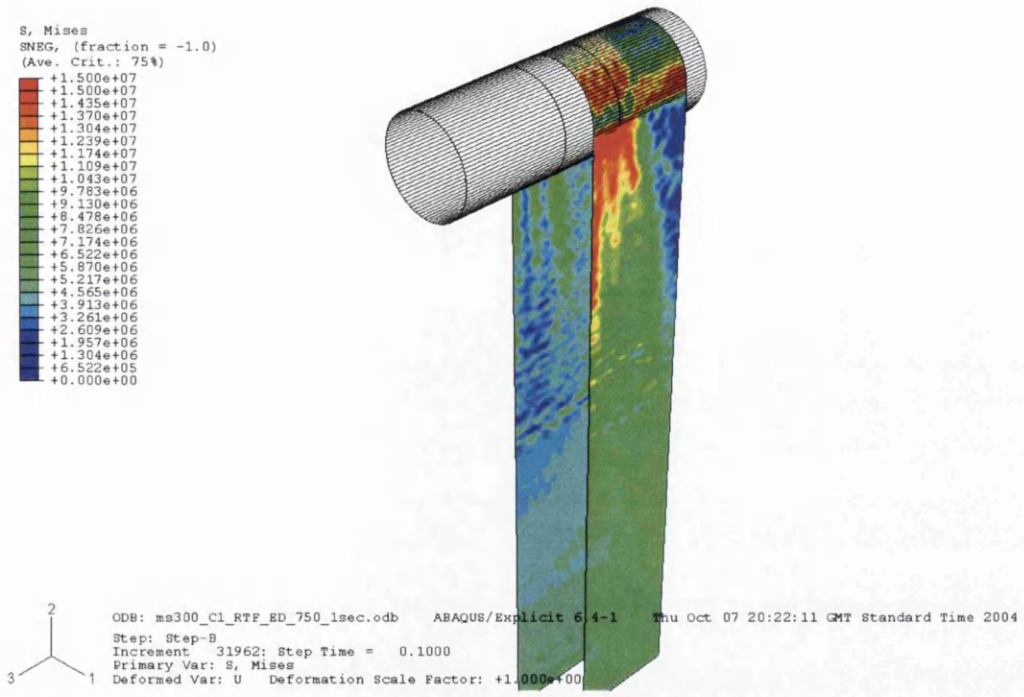

Figure 7.31 von Mises equivalent stress - Model 6.6 - Step Time 0.1

After 0.1 seconds of analysis time, the von Mises equivalent stress was indicating that the strip was yielding right across the entire initial contact plane, furthermore, it can be seen that the yielding was starting to travel down the strip's incoming length. These initial start-up conditions, which occurred in the first few fractions of the very first second, indicated that the frictional coefficient and in-line tension were sufficient for continual traction as the line speed picked-up.

Figure 7.32 von Mises equivalent stress - Model 6.6 - Step Time 0.3

The figure above *(7.32)* represents the von Mises equivalent stress values after 0.3 seconds. The yielding here was even more severe than that of the previous figure, however, what was of interest was the contact yielding has now started to travel back down the upstream strip in the form of an out-of-plane wrinkle. In the case of the upstream strip the wrinkle was clearly plastic, however, in the downstream strip the story was somewhat different, there was a staggered and broken "blue" line that represented elastic ripples starting at the roll's exit fillet point. These ripples, however, while elastic have to be considered a buckle risk, because anything that is out-of-plane increases susceptibility (the exit fillet point refers to the fillet point along the exit plane, this plane refers to the point where the strip ceases to be in contact with the transport roll and starts to travel downstream).

The dynamic model did not start to exhibit steady state non-yielding stress values until the computational run had been moving for 0.65 seconds (for 300m/min velocity).

Figure 7.32, includes all three types of buckle. Centre buckle, where the strip in the centre of the strip buckles. Quarter buckle where the strip at the fillet point buckles and edge buckle where the yielding has reached the strip edge. The edge

buckle originates along the strips initial contact plane and then travels to reach the strip's edge.

7.2.1.2 The Affects of Strip Sagging in the Hanging Strip

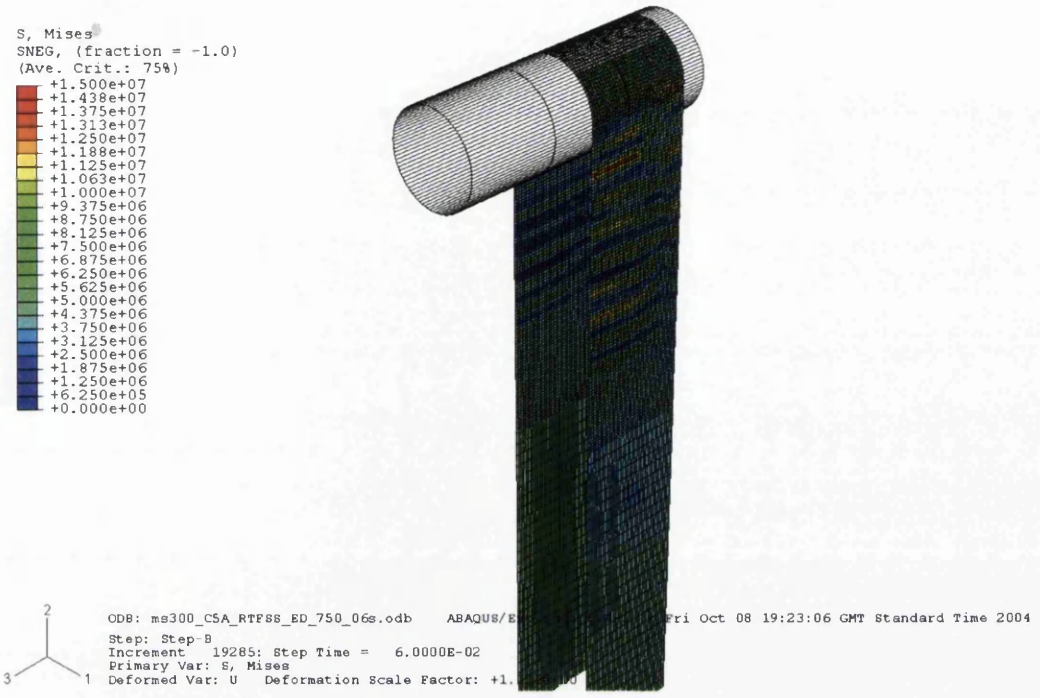

Figure 7.33 von Mises equivalent stress - Model 6.3 - 2nd Increment

The above figure *(7.33)*, represents the contact between strip and a tapered transport roll with what is considered the best roll profile within the CAPL - a taper size of 0.41mm and a central flat section 700mm. The analysis result is from the second increment where momentum in the strip is starting. This figure *(7.33)* shows that the in-line tension (5MPa) was simply not tort enough for the strip; the lines that crossed the hanging strip's upstream face indicate areas of high von Mises equivalent stress followed by areas of low von Mises equivalent stress. This can be solved by increasing the in-line tension, which will either decrease the strips sagging or have the opposite effect and cause the strip to plastically deform where the von Mises equivalent stress is already close to the yield stress (15MPa). This problem tended to only affect strip at start-up and or when the strip loses contact with the roll for some reason or another. Primarily, sagging only affected strip that was both wide (1800mm) and ultra thin (0.4mm).

7.2.2 FRICTIONAL CONTACT AND TRACKING

The frictional coefficient was considered a constant in all computational models that analyse roll-strip contact within a continuous annealing processing line. The research performed by Corus and research institutes' worldwide all use the coefficient value 0.3. To prevent excessive roll wear Corus has implemented extensive maintenance schedules to maintain the correct frictional coefficient and roll taper angle at all times. However, because of the frictional resistance generated by a roll's surface is of the up most importance the author decided to investigate a lower (0.15) and higher frictional coefficient value (0.45) to see if Corus should stop considering the frictional coefficient value as a constant.

An initial thought, adequate traction between the strip and roll could prevent the air cushion effect from developing. The air cushion effect is where the strip loses frictional contact with the spinning roll trying to transport it[33].

The following series of figures briefly look at several different frictional coefficient values. *Figure 7.34* represents a roll profile where the taper size is 3.3mm and the central flat section is 500mm, the frictional coefficient is 0.15 *(Model 7.1)*. *Figure 7.35* represents the same operational set-up apart from the strip having a frictional coefficient of 0.3 *(Model 7.2)*. *Figure 7.36* also represents the same operational set-up apart from the strip having a frictional coefficient of 0.45 *(Figure 7.3)*.

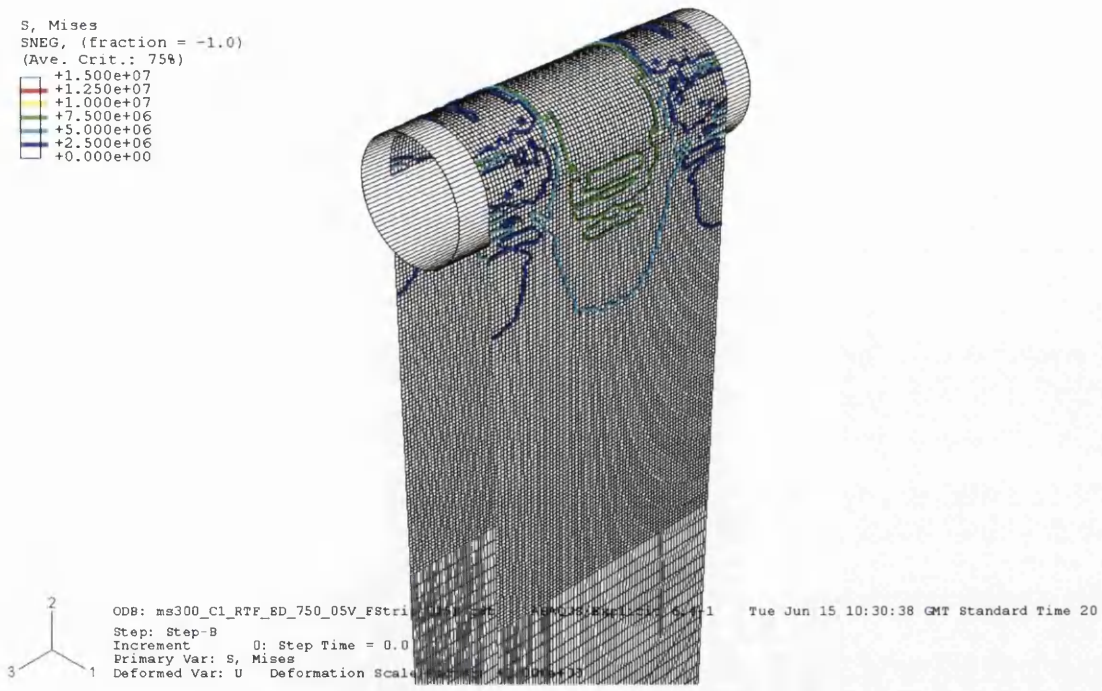

Figure 7.34 von Mises equivalent stress - Model 7.1 - Friction Coefficient 0.15

The above figure represents a reduced frictional coefficient value of 0.15 *(Model 7.1)*. The strips maximum von Mises equivalent stress value across the central flat section of the roll is 7.5MPa. The majority of the upstream and downstream strip has a very low von Mises equivalent stress value. The strips von Mises equivalent stress value on the rolls taper is a much reduced value of 2.5MPa, this is even though the in-line tension is keeping the strip in hard contact with the roll's surface.

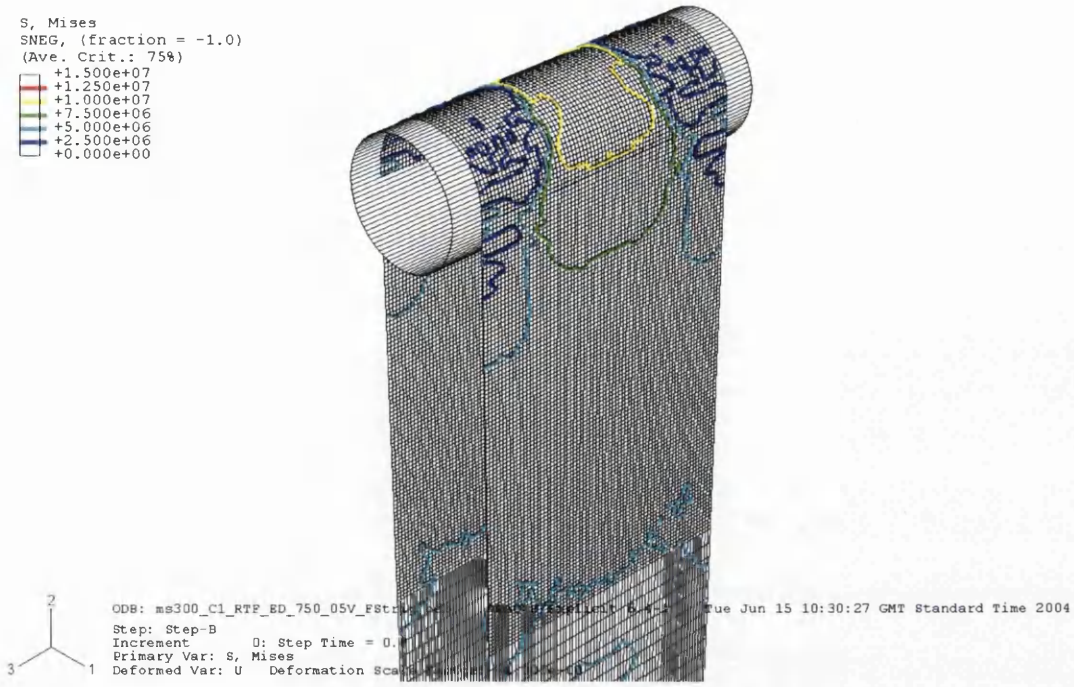

Figure 7.35 von Mises equivalent stress - Model 7.2 - Friction Coefficient 0.3

The above figure represents the standard frictional coefficient value of 0.3 *(Model 7.2)*. The strips maximum von Mises equivalent stress value across the central flat section of the roll is 10MPa. This figure indicates that applying a frictional coefficient of 0.3 to the roll's surface significantly increased the von Mises equivalent stress at both the roll-strip contact and in the upstream and downstream strip lengths (hanging lengths). Again as with the low frictional coefficient (0.15) model, the majority of the strip in contact with the taper angle either side of the central flat section has a low von Mises equivalent stress value. However, the higher frictional forces that have developed between the transport roll and the strip steel now affect a large area of the strip below the initial contact plane (von Mises equivalent stress: 7.5MPa).

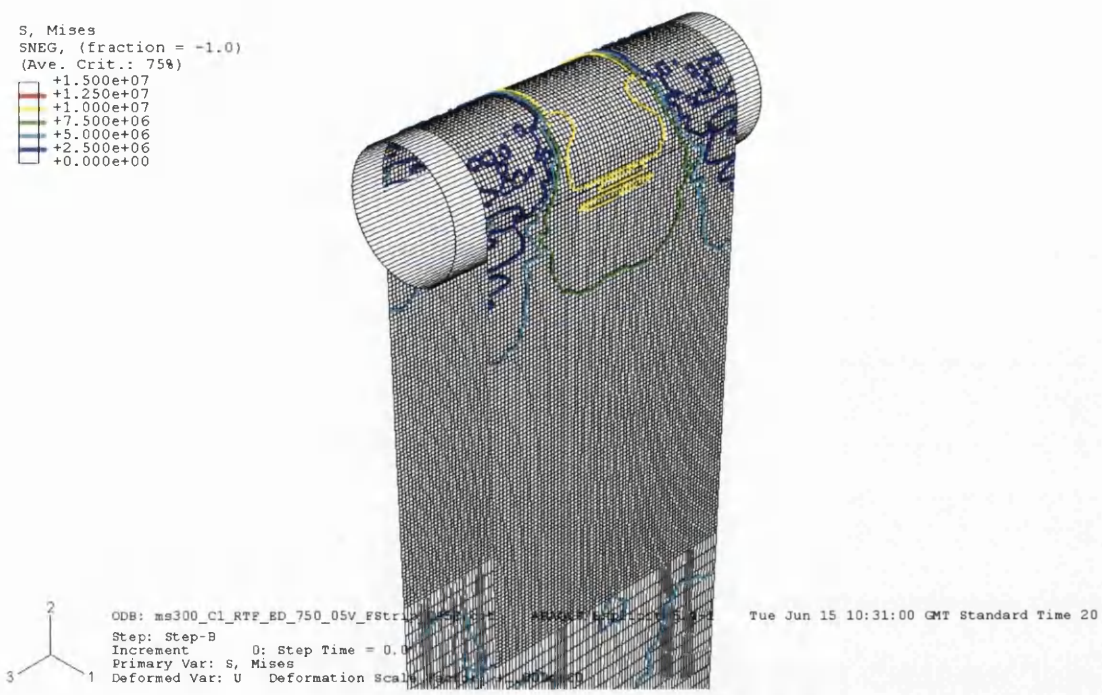

Figure 7.36 von Mises equivalent stress - Model 7.3 - Friction Coefficient 0.45

The above figure represents an increased frictional coefficient value of 0.45 *(Model 7.3)*. The strips maximum von Mises equivalent stress value across the central flat section of the roll is 10MPa. However, the area of the strip covered by this 10MPa von Mises equivalent stress is greater than the area covered by the 10MPa von Mises equivalent stress for the proceeding model *(7.2)*. Furthermore, the high von Mises equivalent stress has started to move down the incoming strip, which is a definite buckle risk. In conclusion, the standard frictional coefficient value of 0.3 is clearly appropriate and should remain as a constant. The author has shown that low frictional coefficients and high frictional coefficients both increase the buckle susceptibility risk, but in entirely different ways.

1. Low frictional coefficient: Poor traction creating areas of high stress on roll re-contact, strip surface scratching, tracking, strip sagging in pass length.
2. High frictional coefficient: Heavy traction causing strip failure, heavy scratching of the strip's surface, strip yielding both upstream and downstream of the initial and exit contact planes.

These results were performed on a dynamic explicit model just prior to the start of the application of angular velocity. These three figures are essentially a snapshot of how the strip will behave when the in-line tension is applied

instantaneously. They are effectively governed by the mechanical properties and frictional coefficients only.

Figures (7.34 - 7.36) indicate the area of the roll profile, which has the greatest effect on the frictional coefficient - the central flat section. However, to put these results into their proper context they have to be compared to a computational model that is simulating sideways tracking.

7.2.2.1 Strip Tracking

Clearly previous results indicate that a frictional coefficient of 0.15 would be a poor choice. Low frictional coefficients provided limited resistance to sideways movements, even when the roll profile had a large and quite obstructing taper size (i.e. such as 3.3mm). The problem with a low frictional coefficient is simple; if the strip starts to wander off the transport rolls centre-line then a low frictional coefficient will only likely encourage this further.

The two models investigated for sideways movement were *(Model 7.2)* with a frictional coefficient of 0.3 and *(Model 7.3)* with a frictional coefficient 0.45.

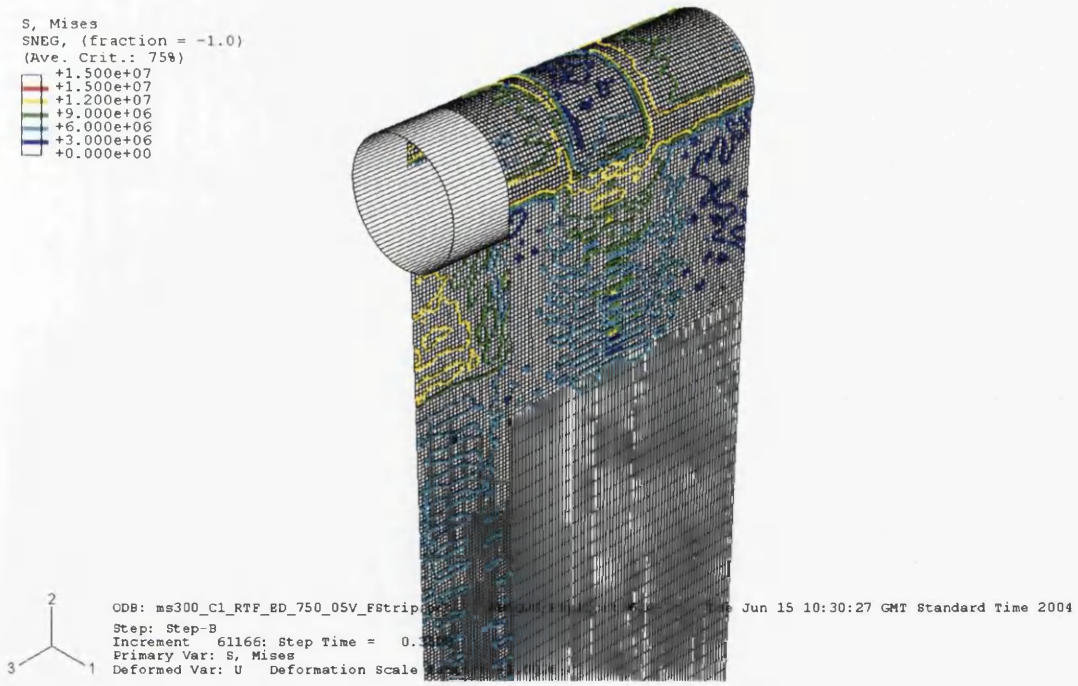

Figure 7.37 von Mises equivalent stress - Model 7.2 - Friction Coefficient 0.3 - Strip Tracking

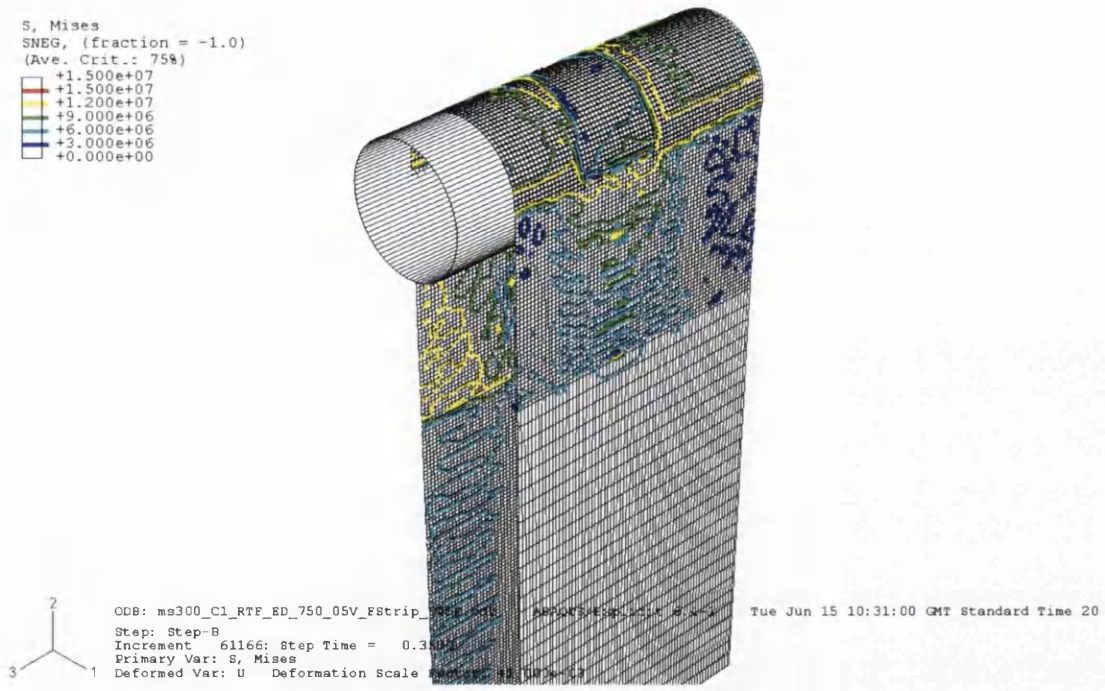

Figure 7.38 von Mises equivalent stress - Model 7.3 - Friction Coefficient 0.45 - Strip Tracking

The purpose of this section is to analyse whether the standard frictional coefficient value of 0.3, which is known to be sufficient for traction when the strip is on the transport rolls centreline is adequate when sideways motion occurred. Sideways motion can cause the strip to lose traction and travel across the transport roll's surface and hit the side of the furnace that is why there is a limit of 1800mm on the strip's width. However, perhaps more importantly sideways motion will cause the strip to move out-of-plane in the pass length.

Figure 7.37 and *Figure 7.38* indicate that a frictional coefficient of 0.3 was sufficient to maintain adequate frictional contact. The large roll taper is especially obstructing with the maximum von Mises equivalent stress value close to the yield stress (15MPa). The results indicate that for both models the von Mises equivalent stress value around the circumferential fillet either side of the central flat section was approximately 12MPa. However, the one area where a frictional coefficient of 0.3 appears to have some negative effect was in the stress state of the incoming strip. For *Model 7.2* there was some areas of von Mises equivalent stress in the 12MPa yield criterion category, these high stress intensifications were located around the centre point of the strip and travelled down the upstream strip. A high von Mises equivalent stress was most often an

indication of in-line tension that was set incorrectly. However, in this case the strip showed signs of being out-of-plane due to a degree of failure in the traction at the roll's face - the strip was slipping due to the excessive sideways motion. The problem is simple, if Corus increase the frictional coefficient it will reduce tracking and increase the contact traction; it would also keep the strip tort in the pass length. However, the strip operates at 750°C currently and has a yield stress of only 15MPa. The future could be 850°C and the yield stress could be 5MPa, the fear is that the strip could then fail on the roll's surface from traction alone. Furthermore, the results indicated that the quality of the final product appeared to be compromised when the frictional coefficient was above 0.3. In conclusion keeping the frictional coefficient at 0.3 for all computational models is not entirely without merit or reason.

7.2.3 LINE VELOCITY

The CAPL was designed to achieve a line velocity in the region of 700m/min, however, this has never been realised for a number of reasons. However, Corus are keen to use the CAPL to its full potential.

Considering a flat roll profile and a tapered roll profile the author considered the velocities of 300m/min, 400m/min, 500m/min and 600m/min. The yield stress was 15MPa; therefore the models represented results from the critical buckle region only.

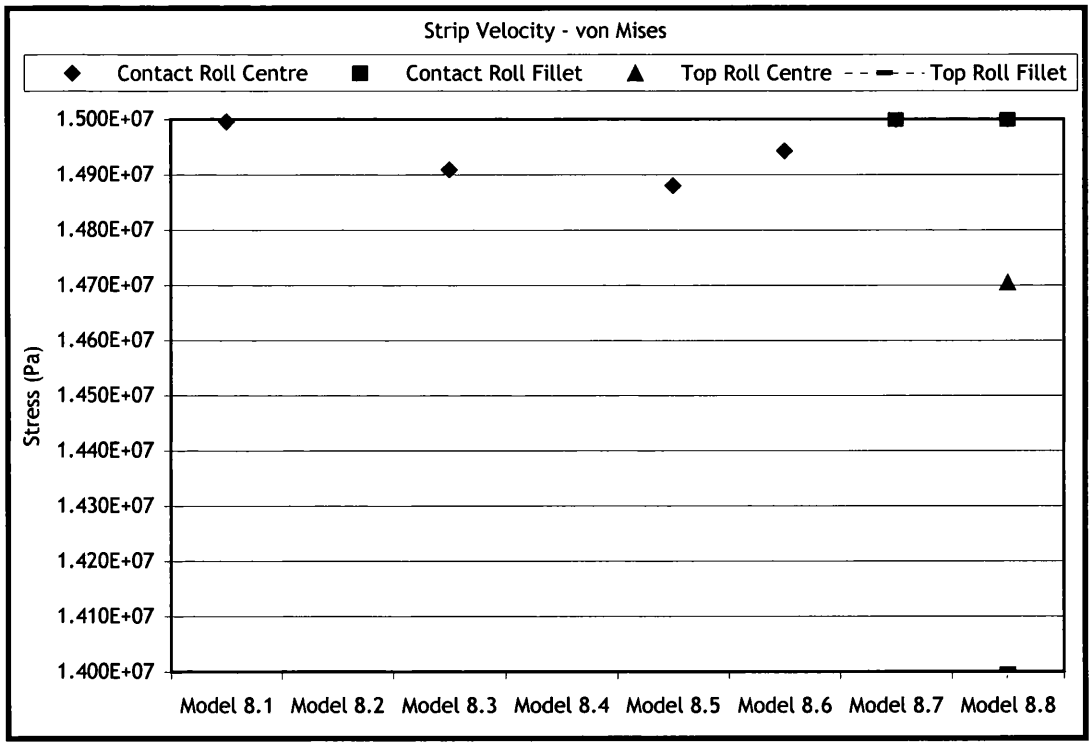

Figure 7.39 von Mises equivalent stress - Strip Velocity

The results shown above *(Figure 7.39)* indicate only the critical results where the von Mises equivalent stress was within 1MPa of the yield stress. *Model 8.1* to *Model 8.4* represent flat roll profiles at line velocities of 300m/min - 600m/min in increments of 100m/min. *Model 8.5* to *Model 8.8* represent tapered roll profiles (3.3mm taper size and 500mm central flat section) at line velocities of 300m/min - 600m/min in increments of 100m/min.

The issue with dynamic models is the unpredictability of an entirely non-linear process; certainly as far as computational modelling was concerned. The results

are not recorded until the models have reached a steady state equilibrium, which is not until after 0.65 seconds. The majority of the results at the four probed elements did not pose a significant buckle risk. However, it was clear that the stress state at the contact roll centre, across all the models, at almost any velocity, will be the location at which the strip will almost certainly buckle first.

Model 8.8 perhaps is the model, which shows the most extreme operational conditions of any of the models in this thesis. *Model 8.8* represents roll profile with a taper size of 3.3mm and a central flat section of 500mm, a strip width of 1800mm, a strip gauge of 0.4mm, an in-line tension of 5MPa and a strip velocity of 600m/min. *Figure 7.39*, indicates that all four probed element values indicate a von Mises equivalent stress close to the strips yield stress. If *Model 8.8* represented a roll with a small taper size, then the maximum von Mises equivalent stress value would be lower. However, at very high line velocities a large taper or high in-line tension (over 5MPa) would be required to keep the strip on the transport rolls centreline. So the buckle risk is reduced by operational changes to the roll profile and in-line tension, but the risk of buckle is still there, the strip's yield stress is still only 15MPa and the strip gauge is still going to be less than 1mm. In conclusion it will be difficult for Corus to eliminate buckle risk, they can only manage it, with sensible operational conditions.

7.2.4 UNEQUAL TENSION

The following figure represents unequal tension in a full-width model. An unequal amount of in-line tension was applied only to the upstream strip length in the form of differing concentrated forces. *Model 9.1* does not include any plastic properties but does include a Young's Modulus of elasticity of 95GPa. The purpose of this computational run was to show how a wrinkle emanating on the upstream strip length can pass around the roll and then continue on downstream without particularly showing any untoward effect on the roll's surface, where contact pressures flatten out-of-plane wrinkles.

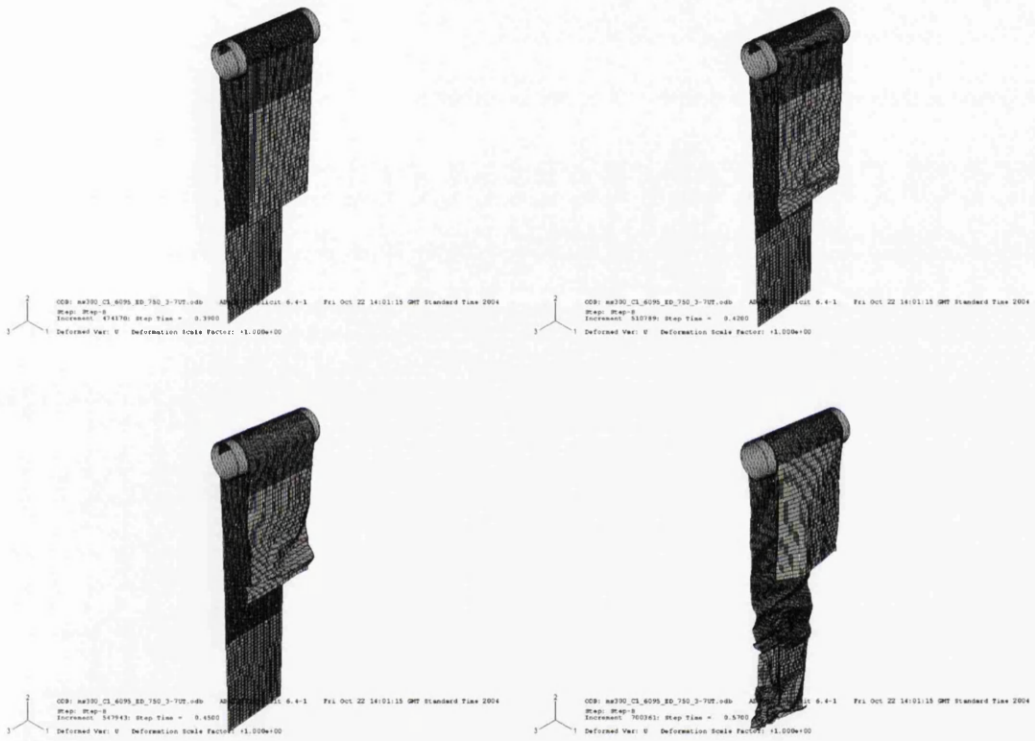

Figure 7.40 Development of a Wrinkle

Clearly the above figure would represent massive strip failure. However, it is interesting to see even in such a ludicrous case as shown here that the strip on the contact surface of the roll remains in hard contact with the rolls surface and shows only limited sign of moving off the transport rolls surface.

Figure 7.40 the top left hand corner shows strip running on the transport rolls centreline. The top right hand corner shows that the strip in the upstream length is now starting to move a little out-of-plane because of the unequal tension. The bottom left hand corner sometime latter in the analysis now shows a distinct

wrinkle, if the model included plasticity then the strip would almost certainly buckle the moment it hit the initial contact plane of the transport roll. The bottom right hand corner figure shows that the wrinkle has travelled around the roll, and has now moved downstream of the exit roll contact. The in-line tension in the downstream strip remained equal, however, once an out-of-plane wrinkle developed it grew until strip failure was almost assured.

7.3 VALIDATION COMPLICATIONS AND THE USE OF MATOBA THEORY[6]

Introduction

Performing meaningful research on the Port Talbot CAPL itself is just not possible for a variety of reasons; therefore researchers worldwide use computational FEA to perform contact scenario investigations, to which comparisons are then made against a well regarded formula such as in the Matoba equation [6, 26].

7.3.1 REFERENCES TO PRIOR VALIDATION

Previous Corus research and some literature have used the Matoba equations to draw comparisons. Therefore, some brief conclusions can be drawn. The reports that are most relevant are those of the cooling buckle team[27] that tackled buckle incidents in the 2nd cooling zone of the Port Talbot CAPL, and those of snakey buckle team[29] whose focus was on buckle within the soaking furnace. Finally, a brief summary from Steve Hill on how the author's computational simulations compare to that of the work performed by Corus RD&T at their Swinden laboratories.

The cool buckle report validates its findings by using a variation of the Matoba equation. The cool buckle team refer to the length of the strip between roll passes as a constant. The thinking behind this is that the Matoba equation takes into consideration the pass length. However, most computational models employ the minimum length of hanging strip required to accurately portrayal in-line tension, because of the computational expense of thin, but very wide meshes of shell elements that represent the hanging strip. The cooling buckle team consider that the Matoba question should only be interested in the actual point of initial contact between the strip and the transport roll. The snakey buckle team use the full Matoba equation. However, they do comment on the difficulty of using an equation where so many unknown actual CAPL operations can be present, referring to the enclosed nature of the Port Talbot CAPL furnaces. Wang et al[29]

indicated that initial progress in applying the Matoba equation was promising, however, difficulties arose with respect to the correlation between the friction coefficient and the roll surface roughness. The comparison of friction effects is based on the averaged values of the roll surface specification, assuming that friction is directly proportional to the square root of roughness.

Corus RD&T compared the author's simulations to those models that have been developed by Corus RD&T research staff at the Swinden laboratories in Rotherham. The conclusions were detailed in a private technical report, however, they can be summarised below.

The conclusions reached showed that the static results were not expected to be significantly different to those of the roll bending models that STC currently use. However, Corus RD&T commented that the author's dynamic model had a clear advantage over the static model that Corus RD&T currently used. The dynamic model enabled the author to analyse not just the upstream stress state, but also the down stream stress state because of the addition of line velocity. The primary and significant difference is that a static model is considered linear; the upstream and downstream hanging strip lengths behave identically. A dynamic model includes strip velocity; therefore the downstream strip will include the effects of hard roll contact (a source of non-linearity in the strip). Dynamic models truly come into their own as such when detail investigations into tracking are required, as the sideways motion across the roll cannot be considered on static models. The one area where the author's models, whether they where static or dynamic, had a clear advantage, was in the application of in-line tension.

The author believes for accurate analysis of roll geometries then static implicit models are superior to explicit. The explicit models used for the dynamic analyses of Section 7.2 where primarily employed because of convergence concerns. These concerns focus on instability, instability because of the in conclusion of angular velocity. However, ABAQUS Standard is quite suitable for dynamic analyses and was considered, however, both convergence and computational expense was proving too costly.

7.3.2 STEIN HEURTEY EXPERIMENTAL VALIDATION

The sole initial purpose of the Stein Heurtey experimentation was validation. However, while it ultimately did not work out like that some interesting results did come about.

Research and observations have indicated if the contact temperature difference is greater than Δ50°C it will cause sufficient localised thermal stress to worry operators. This statement was backed up by the cooling buckle team, who in their report indicate that a problem that occurs in the secondary cooling section of the CAPL furnace was a strong variation in local temperatures, with significantly cooler areas on the bottom transport rolls to the top rolls[27].

7.3.3 MATOBA THEORY FOR MAXIMUM CRITICAL TENSION[6, 26]

Due to the difficulties of validating a completely enclosed furnace that works 24 hours a day researchers worldwide consider the Matoba equation as the closest thing to a universally accepted validation tool.

The Matoba Equation *(7.1)*, was developed by NSC Nagoya R&DT using their in-house experimental CAPL set-up and aluminium foil.

The parameter that was being assessed is the critical line tension ($\sigma_{t\text{-}crit}$). The critical line tension is the point at which elasticity within the strip could be compromised and plastic yielding could start. The equation to determine the critical tension is as follows

$$\sigma_{t-crit} = \left(\frac{k.R^2}{a^2}\right).\left(\frac{{\sigma_e}^2}{E}\right)\left(\frac{h}{\gamma.\mu(w-c)}\right)^2 \qquad 7.1$$

Where:

$\sigma_{t\text{-}crit}$	critical line tension
k	experimentally determined constant
σ_e	yield stress
E	young's modulus
R	roll radius
h	strip gauge

a	pass length
b	strip width
c	flat length on roll profile
γ	roll taper angle (crown)
μ	contact friction coefficient

The absolute values of critical tension are difficult to determine, because some of the required input parameters are either difficult to determine or are unknown. Essentially, the equation implies that the risk of buckle decreases with increase in the square of the following parameters:

- Strip steel yield stress
- Strip gauge
- Roll diameter

and increases with the increase in square of the following parameters:

- Pass length
- Roll taper angle
- Friction coefficient

Since the variations are in squared terms, relatively small changes in parameters would result in large decreases or increases in the critical line tension value for buckling[29, 32].

7.3.3.1 Analysis of the Matoba Equation with Port Talbot CAPL Parameters

The Matoba equation in the author's opinion can be compared to a single roll strip contact computational static model. The following list of parameters was based on *Model 1.3;* variations will be performed around this

The following parameters are constants

k	3.9×10^6 (Experimentally determined and provided by Matoba)
σ_e	15MPa
E	70GPa
R	0.375m
a	5.4m

The following parameters can be adjusted, however, the following are the primary values

h	0.4mm
b	1800mm
c	500mm
y	0.00388° (3.3mm taper size and 750mm long taper).
μ	0.3

The critical in-line tension value for the above parameters using equation *(7.1)* was calculated to be

$\sigma_{t\text{-}crit}$ = **4.22MPa.**

According to the computational simulation results for *Model 1.3 (Figure 7.6)* the in-line tension value where the strip is just starting to yield is around the 4MPa of in-line tension. Therefore for Matoba to calculate the maximum in-line tension value to be in the region of 4.22MPa is encouraging, especially since there are a number of unknowns associated with the Matoba equation and the computational models are somewhat ideal.

The following table *(Table 7.2)* is a selection of the parameters where the critical in-line tension value has been assessed using the Matoba equation.

Strip Width	σt-crit
1.6m	5.89MPa
1.4m	8.8MPa
1.2m	14.6MPa
1m	28.5MPa

Strip Gauge	σt-crit
0.2mm	1MPa
0.8mm	16.9MPa
1mm	26.4MPa
2mm	100MPa

Central Flat Section	σt-crit
700mm	4.59MPa
1000mm	5.55MPa

Frictional Coefficient	σt-crit
0.15	16.9MPa
0.25	6.08MPa
0.35	3.1MPa
0.45	1.8MPa

Table 7.2 Critical Tension Values of Variations in Operational Properties of Model 1.3

The above results indicate that the Matoba equation has to be used with a degree of scepticism. If a certain selection of parameters is inputted into the equation then a result can be obtained, which can be compared against another Matoba equation result with slightly different parameters. Often the result is going to be obvious before any parameter change is inputted, especially if it is a minor change from the current operational profile. For instance increasing just the strip gauge obviously means that the in-line tension value can in all certainty be increased, however, when there is an entire new selection of parameters that need considering then Matoba is useful. Matoba enables the user to determine if certain values would create a buckle risk without considering complex computational model or experimental testing.

Considering *Table 7.2* the value, which appears to be the most susceptible, is the strip gauge. The differences in in-line tension values are significant. The Matoba equation calculated a value of 4.22MPa for a gauge of 0.4mm, 1MPa for a gauge of 0.2mm and a massive in-line tension value of 16.9MPa for a strip gauge of 0.8mm, which is not likely as the yield stress is 15MPa. However, the author believes the Matoba equation can be used to say that the chances of failure when compared to the current strip gauge of 0.4mm is approximately four times less, whereas with a gauge of 0.2 the chances of failure are approximately four times greater.

The author considered a strip width of 1000mm and a strip gauge of 0.2mm. The critical in-line tension value was 7MPa compare to 1MPa for the same gauge but a strip width of 1800mm. This proves that wide gauge strip creates a high buckle risk; it also proves that if ultra thin EDDQ gauge was used then it had to be in-conjunction with a reduction in the strip width. It simply is not possible to have throughput that was both large in width and ultra thin in gauge when the yield stress is 15MPa.

The other notable values were the variations in the central flat section of the tapered transport roll. At 500mm the critical tension value was 4.22MPa, at 700mm the critical tension value was 4.59MPa and at 1000mm the critical tension value was 5.55MPa. These values all for rolls with a taper size of 3.3mm and thus represent variations in *Model 1.3,* which has an original central flat section of 500mm. Unlike the strip gauge, changes to the central flat section were not as sensitive, with only quite small changes in critical tension present. The results however, do follow the computational research in that 1000mm central flat section are considered less of a buckle risk than 700mm central flat sections, which in turn are considered less of a buckle risk than central flat section of 500mm.

The one significant parameter that was missing from *Table 7.2* was how the Matoba equation interprets variations in the roll taper size and thus the roll taper angle. After some time performing analysis the author came to the conclusion that the equation was simply not suitable unless the taper angle was large. The Matoba literature[6] points to a roll taper size of in the region of 0.004mili radians when testing, which is considerably higher than the majority of CAPL roll taper sizes.

Therefore for a taper size of 3.3mm the Matoba equation is fine, however, at small taper sizes the results would have to be considered carefully.

7.3.3.2 Further Considerations

- Corus research into the Matoba equation for the cooling buckle[27] report was limited. The report made a bold assumption that the strip length was not required at all, not even as a constant.

- Matoba relies on several assumptions including the usual such as the incoming strip was residual stress free and had no out-of-plane ripples.

- The Matoba equation is based on ultra thin aluminium foil.

- There is one assumption that could be important and that is with respect to the constant value that is *K*, which is experimentally derived using aluminium.

- The experimental programme set out by Matoba was based entirely on work performed at local room temperature. At local temperature the strip behaves far more linearly than it would do if it where operating at 750°C.

- All papers and all Corus research quote Matoba. However, in a similar fashion to the author's research thesis all authors struggle to validate Matoba's work and thus treat the Matoba equation as a tool for comparative studies.

- The dynamic model is impossible to compare to Matoba.

- Plans for line trials on the Port Talbot CAPL were abandoned due to cost and available downtime.

- Corus RD&T validated the author's static and dynamic models against the current strip bending models that Corus RD&T employ. The conclusion was that the static models were very similar in terms of their input conditions and gave similar output results. However, the dynamic model was something that Corus RD&T had not considered before.

- Matoba did not directly discuss gravity, however, the pass length was included so the weight of the strip is considered.

7.4 CLOSING REMARKS OF THE COMPUTATIONAL MODELLING OF THE TRANSPORT ROLL AND STRIP STEEL INTERACTION

The author considered the standard roll profiles, standard strip dimensions, and standard operational conditions in the critical region of the soaking furnace. The soaking furnace operates at 750°C that translates into a critical yield stress of only 15MPa for Corus EDDQ strip. The goal was to further current knowledge of the Port Talbot CAPL set-up, and then considers the problems of the future. Chapter 7 had been split into three primary sections. The first section *(7.1)* considered variations in all the principle parameters associated with the roll-strip contact. The first section was the primary focus of the computational work performed by the author. The second section *(7.2)* considered parameters associated only with strip velocity, such as tracking and frictional coefficients. The third section *(7.3)* considered validation attempts.

The computational section had come to some considered opinions on current and future CAPL operational set-ups surrounding roll-strip contact. Theses are discussed in detail in throughout this chapter and are summarised in Chapter 8 "The Conclusions".

8 THE CONCLUSIONS

Introduction

The question could be asked why even consider plasticity? The answer is simply that even though the computational FEA models highlight the yield stress (the end of elasticity), the point where supposedly linear behaviour stops, most if not all stress analysis reports present their results in the form of the von Mises equivalent stress, which is related to plasticity theory. Put simply, the von Mises equivalent stress investigates the point where yielding will occur by interpolating the two principal stresses for a plane stress state, such a state exists within the Port Talbot CAPL.

The next perhaps most important question is why even worry when the purpose of the CAPL is not deformation. The strip should most definitely be operating inside the elastic zone; if it enters into permanent elongation then the strip is scrap. The answer to any question about plasticity and the CAPL is, however, two fold. First it is important to understand the limits of the strip so that these limits can be pushed further, and secondly the CAPL's future. It must be remembered that the CAPL's and Corus fortunes in South Wales depend on diversifying, and that means wider and thinner strip steels, but most essentially it means greater throughput.

Paramount importance to this will be the understanding of contact conditions. In this thesis the author has tried to address the contact conditions from two standpoints. First by considering the temperature differentials that occur between the strip and the transport roll and how the affects of excessive temperature differentials affect the stress state. These experiments were performed by the use of an experimental programme that the author witnessed in the French town of Bar-Le-Duc, the research home of co-project sponsors Stein Heurtey the suppliers of furnace technology to Corus. The second aspect of the research project was to investigate the standard roll geometries that currently being used within the different zones of the CAPL furnace. Corus had never completed a full-scale study, and have arguably never fully understood how different roll geometries behave within the different zones of the furnace section of the Port Talbot CAPL. Stein Heurtey supplied the furnace roll geometries, theses geometries represented the continual good working practices of other preceding CAPL's that are operating worldwide. The trouble is that no two CAPL's ever behave the same; they are very large and complex installations that require years of research for the local roll

geometry and operational parameters to be fully optimised. This second aspect was developed even further. It was to take the standard roll geometries and look at how variations to the roll geometries and other operational parameters would impact on the strip steels stress state and therefore its final quality, this is with an eye on the future. The second aspect of research also allowed for two current issues to be considered that had immediate benefits to Corus. An increase in size to transport rolls taper fillets within the soaking furnace of the CAPL and to consider the in-line tension requirements to an issue of continual but sporadic buckle that had been developing at the Corus Pontardulais works. This second aspect was entirely researched by the use of the commercially available computational finite element method (FEM) program ABAQUS Standard for the static and heat transfer simulations and ABAQUS Explicit for the dynamic simulations.

8.1 INCOMING STRIP QUALITY ISSUES

The CAPL predominately handles cold reduced strip that leaves the cold mill. The incoming cold milled strip is extremely hard; due to being extensively work hardened. The strip that leaves the cold mill also has a jumbled microstructure because the cold rolling temperature is below the dynamic recrystallisation temperature. Therefore strip recovery is not achievable in the cold mill, and is why the strip is sent to the CAPL for annealing. Apart from the effect that cold rolling has on the microstructure its other significant effect is to the strip shape. The cold rolling process, which is a deformation process, can add surface defects to the cold rolled product that hinder the transportation process through the CAPL. Strip camber is one of these defects that is a severe problem, it creates strip tracking. A tension-levelling device is used to counter most of the effects of cold rolling. However, the build up of stress within the strip at the exit of the cold rolling process is referred to as residual stress.

Tracking is the deviation of the strip from the centreline of the process roll that is transporting it. Tracking occurs even if the strip exiting the cold rolling mill has been adequately tension-levelled. To avoid these strip-guiding problems and to guarantee good strip tracking, the use of steering units is essential.

8.1.1 EXTRA DEEP DRAW QUALITY (EDDQ)

EDDQ steels have a high "R" formability requirement; therefore the steel greatly resists the thinning process. When recrystallisation occurs, if carbon is present, it ruins the deep draw properties of the steel and affects the size of the grain making it coarse. To remove the free carbon the EDDQ steel is overaged.

8.2 ELASTIC-PLASTIC CONSIDERATIONS

Strain-rate hardening can influence the mechanical properties once the strip steel has reached its elastic yield point. At the yield point the linearity ends and plasticity starts. The results become unpredictable, especially at recrystallisation temperatures. The cold rolled strip is at ambient temperature it has a high and fairly pronounced yield stress, at this point the strip is considered brittle and the strain-rate hardening exponent is often clearly visible - this is the state of the strip entering the CAPL. However, once the strip has been transported through the soaking zone for it to be annealed at a temperature in excess of upwards to 750°C, the elasticity of the strip steel depending on line tension can be as little as 5MPa. The strip is therefore extremely soft at this temperature; its strain-rate hardening component is difficult to distinguish from the rest of the oscillating scatter that is prevalent in high temperature hot tensile tests. Even at very low loading levels, both the elastic yield point and the ultimatum tensile strength are virtually at the same point on the stress-strain graph. This indicates that any plastic strain hardening that is present at CAPL annealing temperatures would have a minimal impact on the work hardening exponent. The research into the CAPL requires the author to know the yield stress, for this research project and all Corus RD&T research projects this value has been taken from the "Proof Stress" ($\sigma_{0.2\%}$). The Proof Stress includes a small degree of plasticity due to its conservative nature. However, Corus do not want the computational results to hit the strips yield stress value, for that would include a degree of plastic deformation, and that is unacceptable. Furthermore, using the proof stress for the yield stress enables elastic perfectly-plastic stress-strain characteristics to be used within the computational simulations.

The fundamental observations

1. For modest stresses (and strains) the strip responds elastically. Stress is proportional to the strain, and the deformation is reversible.

2. If the stress exceeds a critical magnitude, the stress-strain curve ceases to be linear. It is often difficult to identify the critical stress accurately, because the stress strain curve starts to curve rather gradually.

3. If the critical stress is exceeded, the specimen is permanently changed in length on unloading.

8.3 COMPUTATIONAL CONSIDERATIONS

Computational work has indicated that the unconditionally stable implicit method, will encounter some difficulties when a complicated dynamic three-dimensional model is considered. The reason for this is: as the reduction of the time increment proceeds, the computational cost to the tangent stiffness matrix increases and even causes divergence. The explicit techniques are thus introduced to overcome the disadvantage of the implicit method for dynamic research; the CPU cost is approximately proportional to the size of the finite element model and does not change as dramatically as in the case of the implicit method. The drawback of the explicit method is that it is conditionally stable, which makes definitive analysis through step incrementation impossible between two different model runs. For the static models the implicit time step formulation (ABAQUS STANDARD) is employed and utilises a steady state loading system, where as, for the dynamic models explicit time step formulation (ABAQUS EXPLICIT) would be used employing a transient loading system.

8.4 EXPERIMENTAL PROGRAMME

Introduction

The experimental results from Bar-Le-Duc, which while proved interesting and moved thinking along on the subject of temperature differentials, were not as detailed as originally intended. The area, which most concerned Corus, were roll geometries in the Port Talbot CAPL, and how they directly affected the strip quality, especially the future grades, which would be annealed faster, thinner and at higher recrystallisation temperatures. As a validation exercise the Bar-Le-Duc experiments were a failure. It was hoped that they could be used to validate the CAPL computational model at a strip annealing temperature of 750°C. However, operating temperature restrictions with the testing equipment meant that only relatively low temperature investigations could be considered. At 300°C the strip

still has the majority of its cold iron properties, which is systematic of the problems of validating CAPL research. For instance Stein Heurtey, the supplier of CAPL technology to Corus, had a pilot facility that represented a heating furnace and cooling unit, but it was not enclosed in a hydrogen rich atmosphere, so that raised the issue of strip oxidisation.

8.4.1 TEMPERATURE DIFFERENTIAL RESULTS

The strip was removed from the pilot facilities heating furnace. It was then rapidly moved into contact with a copper heat sink, which was representing a transport roll. The goal was to analyse temperature differentials to gain an understanding of how they affect both the temperature profile and stress state of the strip.

At a furnace exit temperature of 150°C were the results with the most repeatability, even with a contact temperature differential of approximately 95°C. This temperature differential was roughly 65°C higher than would ever be seen in the worst case Port Talbot CAPL scenario. The strain gauge results indicated that at this furnace exit temperature the strip had a fairly steady stress state and therefore was considered a low buckle risk.

At a temperature differential of 145°C the results showed only a small difference in temperature loss compare to the experiment with a 95°C temperature differential. However, the strip was now starting to cool quicker in the surrounding strip. Previously, the contact point was the only point on the strips surface where the strip cooled rapidly, however, that is only limited by the strip's conductivity and thickness. The stress-strain results indicate a temperature shock to the strip now that the temperature differential was 145°C. The temperature differential had now reached a point where the conductance was so rapid that poor strip shape was inevitable. This rapid transfer of heat caused a dramatic change to the stress state, which led to poor strip shape purely because the strip could not transfer heat fast enough.

Once the temperature differential rose above 200°C the results became increasingly incoherent. The temperature differential was so great that the repeatability had completely gone - several experiments performed at this temperature gave different results each time. The strain gauge results became

incoherent and indicated that the transfer of heat from the strip to the heat sink was now so rapid that strip buckle would be assured if the strip temperature were closer to the annealing temperature.

At temperature differentials above 200°C the author could physically see that the strip shape was compromised the instant it made contact with the heat sink, which incidentally was at an ambient temperature. The strip lifted instantly off the surface of the heat sink when contact was first made; it then only rested on the heat sink's surface because the weight of the strip forced it to. Only once the strip temperature had cooled sufficiently from both conduction to the heat sink and possibly a little convection to the open-air environment did it fully rest on the heat sink's surface.

A fully-coupled computational model was used to validate the experimental results from Bar-Le-Duc. The successful results indicated that the strip did indeed move out-of-plane when a much cooler heat sink was applied to a small localised area to create a significant temperature differential.

Ultimately the results were a little disappointing. They gave some valuable insight into temperature differentials. However, the fundamental problem was that the experiments were performed at 300°C. Even Stein Heurtey, who are the furnace suppliers to the Port Talbot CAPL, struggled to perform temperature differential experiments at the correct soaking section temperature of 750°C.

8.5 ROLL-STRIP CONTACT MODELS

Introduction

A computational programme was developed to assess all the different parameters that make up the roll-strip contact scenario. Every principal parameter was assessed to both develop the current understanding and make suggestions for improvements to the future operational set-up. The goal was simple: to improve and maximise throughput while not risking the strip quality.

8.5.1 STATIC MODEL CONCLUSIONS

8.5.1.1 Standard Roll Profiles

The standard roll profiles were considered against a number of output identifiers all, which can be seen in Chapter 7, the results and discussion chapter for the roll-strip contact models.

For this chapter only the principal stress in the x-direction (S1) and the von Mises equivalent stress are considered. The reason is that it became clear that the S1 direction gave the more interesting results when compared to the S2 direction. The S1 direction represented the plane of the initial contact, this the author considers to be the principal direction for analysing the sensitivity of different parameter changes.

Roll Taper Size 0.41mm and Central Flat Section 700mm

The maximum S1 directional stress value was 10MPa, two-thirds the yield stress (15MPa) for a strip operating at 750°C within the soaking or heating section of the furnace. Considered the ideal roll profile in terms of both taper size and central flat section. The buckle risk was kept to an acceptable level and the profile created enough resistance to prevent sideways tracking.

The von Mises equivalent stress values confirmed that this roll profile was not considered a buckle risk. The strip had perfectly acceptable von Mises equivalent stress values for in-line tension values up to and including 5MPa.

Roll Taper Size 3.3mm and Central Flat Section 500mm

The maximum S1 directional stress value was 14MPa, very close to the yield stress (15MPa) for a strip operating at 750°C within the soaking or heating section of the furnace. Large tapers sizes are used in cooler sections of the furnace such as at the start of the heating furnace. Large tapers, however, are extremely detrimental to the strip's stress state; however, they were also excellent at stopping sideways tracking. The author's opinion is that all large tapered rolls except those in the first few passes of the heating section where the strip still had its cold iron properties should be removed and replaced with rolls with smaller taper sizes (i.e. 0.41mm). Furthermore, a small central flat section intensifies the effect of the large taper size. If the central flat section is small then the force

generated by contact is concentrated in a smaller central area; again this helps to prevent tracking but increases the buckle risk.

The von Mises equivalent stress values confirm that at 5MPa in-line tension this model is a buckle risk. The risk of buckle becomes acceptable when the in-line tension is reduced to below 3MPa.

Roll Taper Size 0.35mm, Barrel Roll

The maximum S1 directional stress value was 16MPa, a stress value greater than the yield stress (15MPa) for a strip operating at 750°C within the soaking or heating section of the furnace. The author's opinion is that the barrel roll should be replace. Corus use the barrel roll in the top roll passes only of the soaking section, to help to keep the strip on the roll's centreline. The author believes that the barrel rolls should be replaced with the taper rolls used for the bottom roll passes. These taper rolls have a roll taper size of 0.41mm and a central flat section of 700mm and are considered a low buckle risk.

The von Mises equivalent stress values confirm that at 5MPa the strip yields heavily. The risk of buckle becomes acceptable when the in-line tension was reduced to below 4MPa.

Roll Taper Size 0.41mm and Central Flat Section 1000mm

The maximum S1 directional stress value was 8.7MPa, a stress value considerably lower than the yield stress (60MPa) for a strip operating at 675°C within the cooling section of the furnace. This model proves that a large central section is beneficial in reducing buckle risk, however, the closer the roll profile gets to a flat profile the higher the risk of tracking, as the strip struggles for traction.

The von Mises equivalent stress values confirmed that this roll profile was not considered a buckle risk. The strip had perfectly acceptable von Mises equivalent stress values for in-line tension values up to and including 5MPa.

8.5.1.2 Variations in Key Operational Parameters

The author considered many variations of the roll-strip parameters to highlight the principle buckle risk initiators and of course those, which are safe. Some of the parameters on the list are not currently standard and could be used in the future.

The list below starts with the parameter, which is the highest buckle risk. The list represents only the S1 directional stress and is presented in full in Chapter 7. While the list does not represent the von Mises equivalent stress or the stress in the S2 direction, it does highlight those parameters that persist in being a buckle risk, whatever output identifier is considered.

1. Barrel Roll.
2. 8MPa In-Line Tension.
3. 500mm Central Flat Section.
4. 1.4mm Roll Taper Size.
5. 60MPa Yield Stress, 95GPa Young's Modulus.
6. 700 mm Central Flat Section
7. 20mR Fillet.
8. ∅1200mm Roll Diameter.
9. 0.2mm Gauge.
10. 0.41mm Roll Taper Size.
11. 10MPa Yield Stress, 50GPa Young's Modulus.
12. 1000mm Central Flat Section.
13. 3.5MPa In-Line Tension.
14. 900mm Strip Width.

One to four are the principal parameters that have constantly been shown to create the highest buckle risk. Only number two (8MPa tension) is not a typical parameter in the critical buckle region. This comparison highlights the risk of small flat sections and large tapers, noted in the previous standard roll profile section. The last four parameters are the typical parameters, which have a low buckle risk (small strip width, low in-line tension, large central flat section and low mechanical properties).

8.5.1.3 Influence of Taper Roll Radius

The standard radius of curvature for roll profiles is 20 metres. Corus asked the author to consider whether this value could be increased to 40 metres to elevate some of the buckle risk associated with high temperature annealing.

Increasing the radius of curvature for a large taper size does not significantly decrease its strip buckle risk when 5MPa of in-line tension is applied. However,

once the in-line tension is reduced to 4MPa the 40 metre curvature of radius improves the strips susceptibility to buckle by 7% compared to that of the model with a 20 metre radius of curvature. This trend continues as the in-line tension decreases even further. The research has proven that there is an immediate benefit to Corus by increasing the radius of curvature from 20 metres to 40 metres. However, the results indicated that increasing the radius of curvature for a roll profile with a small taper size (0.41m) is not cost effective; the reduction in buckle risk was insignificant.

Concluding, for large taper sizes (over 1.4mm) increasing the radius of curvature from 20mR to 40mR would certainly be beneficial in reducing the overall stress state of the strip, especially at the fillet point. However, for all other roll profiles, this small benefit is unlikely to be greater than the financial cost of implementing such a maintenance change.

8.5.1.4 Tension Loading Issues At Corus Pontardulais Works

At Pontardulais there was concerns over the 90o wrap angle of the strip passing around the deflector roll, which has a barrel roll profile. This transport roll has a 4mm crown and a 20 metre radius of curvature at the rolls central fillet point. The mechanical properties of the strip were high with a yield stress of 100MPa and an in-line tension value of 12.5MPa.

The author approached this request by considering what would be an appropriate in-line tension value, to satisfactorily reduce the buckle risk associated with a 90° strip bend and a very high roll taper size.

The results concluded that reducing the in-line tension value by 10% from 12.5MPa to 10.85MPa would remove the stress concentrations points in both the up and downstream roll-strip contact points and thus satisfactorily reduce the buckle risk without significantly increasing the potential for tracking.

8.5.2 DYNAMIC MODEL CONCLUSIONS

8.5.2.1 Frictional Coefficient

The level of frictional contact can clearly have an adverse effect on the contact conditions that develop between the strip and the transport roll. These adverse effects could result in strip failure and line stoppages, or at the very least, strip

surface scratching. The frictional coefficient is often quoted as a constant with a value of 0.3.

In practice a constant frictional coefficient along with initial perfect strip flatness are the two principal assumptions of all roll-strip contact analyses. In the author's opinion frictional contact, while a major issue for all roll-strip contact models, is a parameter that can hurt operators even more when its effects are accumulate over a number of roll passes.

The computational models developed indicate that the frictional coefficient is certainly important at the contact face as it determines the strip surface quality. However, the frictional coefficient also has a say in the out-of-plane movement of the strip in the pass length between transport rolls, something not considered by Corus RD&T before.

In conclusion: The standard frictional coefficient value of 0.3 is appropriate and should remain as the constant. The author has shown in this thesis that low frictional coefficients and high frictional coefficients both increase the buckle susceptibility risk, however, in entirely different ways.

1. Low frictional coefficient: Poor traction creating areas of high stress on roll re-contact, strip surface scratching, tracking, strip sagging in pass length.
2. High frictional coefficient: Heavy traction causing strip failure, heavy scratching of the strips surface, strip yielding both upstream and downstream of the initial and exit contact planes.

8.5.2.2 Sudden Line Stoppages

It has been the case that serious buckle can occur after long stops. During a prolonged stop sagging of the strip can result in tension oscillations on start-up. Apart from start-up being a concern, line acceleration is also a significant concern. Acceleration can create an oscillation across the strips surface, which, will, gradually diminish as the strip reaches a constant speed (i.e. steady state velocity). The dynamic models developed by the author show how sudden acceleration at line start up can seriously affect the strips stress state. The dynamic model naturally simulates sudden acceleration within the CAPL, because within the first step the in-line tension is fully applied or ramped. The results

generally show that sudden increases in acceleration cause the stress state within the strip, especially that part of the strip, which is in contact with the transport roll to reach its critical elastic limit almost instantly (@750°C). Sudden acceleration and deceleration must be considered a serious buckle susceptibility risk. Furthermore, this risk is magnified on rolls with larger tapers; these rolls tend to be the ones with the greatest roll-strip contact temperature differential - a very serious buckle risk in its own right.

8.5.2.3 Line Velocity

The CAPL does not run at full velocity, the fear is that if the line speed exceeds 300m/min then the buckle risk becomes too great. However, Corus are pushing for greater throughput rates, which can only be achieved by increasing the strip velocity. The results indicate that increasing the velocity on roll profiles that have small taper sizes is fine for strip speeds up to 400m/min. However, after 400m/min the buckle risk increases significantly. The problem is even greater on large taper size transport rolls, which already have a high buckle risk on line velocities at the current 300m/min.

To increase throughput and achieve line velocities of 600m/min - Corus realistically will only be able to achieve this with greater strip gauges and thinner strip widths. The alternative is to change all the roll profiles, something that cautious steel manufacturers never consider lightly.

8.5.3 MODEL DEVELOPMENT ISSUES

For the models to be truly representative of the Port Talbot CAPL they would have to run for a considerable length of time - certainly more than the current model time of 0.6 seconds for the dynamic model. The strip lengths would have to be the full pass length of 20.6m instead of the current maximum of 6m. The mesh for the strip would also have to be a very fine around the roll-strip contact, perhaps $10mm^2$ instead of the current $25mm^2$. Furthermore the strip would have to have multiple roll passes, so that accumulative effects could be studied. However, the problem is computational expense - the dynamic model weighed in at 135Mb per run and that is with modelling half-width strip and analytically rigid transport rolls. The current time for the dynamic models was based on the minimum length of time that the model needed to run before the results were considered settled and therefore steady state. The current strip length was the recommended length

so that concentrated forces applied to the end of the strip length did not interfere with the contact results (minimum x 3 strip width). Similarly, for static models the length of time that the model was in contact with the roll for an in-line strip velocity of 300m/min was just 0.365 seconds.

8.6 ROLL-STRIP CONTACT CONSIDERATIONS

8.6.1 ISSUES RELATED TO GENERAL CONTACT

8.6.1.1 In-Line Tension

The application of longitudinal tension results in tensional stresses being induced into the transverse plane of the strip's surface. If such forces are not uniform across the width of the strip they can result in the strip pulling, and creasing elastically, or if the force exceeded the yield stress, creasing plastically. A stress state develops within or on the surface of the strip from the application of line tension (i.e. before hard contact). Once the strip starts to travel around the roll any out-of-plane elastic elongation can easily lead to permanent deformation once hard contact is realised.

Correct furnace tension is important to maintain strip quality. Tension that has a high set point will lead to plastic deformation, whereas tension set low will cause the strip to wander across the roll's surface. Furthermore, if the tension is not uniform the strip is often pulled across the roll surface causing small areas of localised stress intensification as traction comes and goes - associated most promently with cases of Snakey Buckle. Poor Tension can cause minor surface scratching or full-blown buckle incidences where the CAPL had to be stopped. Tension trims can help to reduce the effects of unequal tension. The use of tension trims signifies that tension can be treated as a process control issue.

8.6.1.2 Air Cushion Affect

Air cushions are a problem associated with roll crown geometry, tension, and contact friction and are considered by the author to act in the same way as a "classic" fluid boundary condition. Air cushions have been known on the Port Talbot CAPL to cause the roll to rotate at a completely different angular velocity to that of the strip that it is transporting. In that case the air cushion did not cause strip to buckle or even scratch the surface of the strip, however, at some point the strip has to make hard contact. The air cushion affect seems to be more prevalent in the secondary cooling section of the CAPL, where the cooling method

is "blow boxes". The strip in the secondary cooling section is post annealed and therefore fully recovered, however, it is softer. The secondary cooling section operates typically at only 210°C so the yield stress is considerable higher than that of the soaking furnace where the air cushion effect could increase buckle susceptibility. The reasons why air cushions develop is not fully understood, however, the following tend to be linked to the development

- Air or gas films generated were permanent and cannot be completely dissipated.
- As the film becomes thicker it caused a decreasing level of asperity contact between strip and roll, up to a level at which no asperity contact remains.
- Film thickness increases with temperature, the coefficient of traction increased by 10% for every 100°C drop in gas temperature.

The air cushion affect could affect the future of the CAPL in two ways. First, the CAPL goes thicker; this will eliminate most issues of the air cushion affect. However, thicker grades lead to other buckle susceptibility issues. Secondly, the CAPL goes ultra thin, and this could lead to the air cushion becoming more common.

8.6.2 ISSUES RELATED TO CONTACT TEMPERATURE

Introduction

The roll-strip temperature is not always uniform, in some zones, the roll is hotter than the strip and in others it is the reverse. However, the affect to the strip quality is always the same, if a sufficiently big enough temperature differential is developed between the strip and the roll then the strip shape will be affected due the effects of expansion and contraction, which can lead to buckle. An added complication is that often the temperature distribution is not that equal across the rolls surface; homogenous temperature across the strip is never an issue unless there is poor contact. The most important controlling factors, are operational parameters such as line tension and roll taper size; these variables are controllable and therefore the risks associated with buckle sensitivity can be addressed with changes to either of these, whereas the high operating temperatures required for the recrystallisation process are essential.

8.6.2.1 Strip Temperature Conductivity

Due to the strip being ultra thin (a gauge that is as little as 0.3mm), conductivity within the strip is considered homogeneous throughout the gauge when the strip is in contact with the transport roll at normal operating speeds (i.e. the bottom and top of the strip are considered the same temperature). However, computational simulations completed as part of this research degree has shown that on-start-up there can be temperature differentials between the initial roll contact point and an area of the strip just a few centimetres or less away from this interaction, due to differences in contact conductance. (i.e. some of the strip is contact with the roll and some is not). This can induce variations in the local thermal strain in the strip with either hot or cold spots depending on the nature of the roll contact. Of course this is dependent on the furnace section in which it occurs. Heating section rolls are generally hotter than the strip whereas the situation is reversed in the cooling section.

8.6.2.2 Reduction in Strip Temperature

From a mechanical point of view reducing the strip temperature in the heating section and soaking section of the furnace will reduce buckle susceptibility because the yield point of the strip will increase. However, from a metallurgical point of view the problem with decreasing or even on occasions increasing the temperature inside the soaking furnace is the effect on the microstructure of the strip steel. The annealing cycle and the strip chemistry is in its self is complex, so much so that it could be regarded as entirely different research topic on its own. Therefore, while suggesting increasing the materials yield stress may help to solve some of the problems of buckle susceptibility, it will likely have a non-specific effect on the chemistry and grain size of the strip steel. This could manifest itself in poor recrystallisation and thus leaving the strip in a poor homogenous state, where the strip is still brittle.

8.6.2.3 The Affects of Thermal Distortion on Roll Geometries

Research performed by the author and others has shown that a change in the roll's diameters due to thermal expansion has a limited impact on the stress state of the travelling strip. Generally, increases are only an issue if the taper angle significantly increases when thermal expansion occurs. Initial research by the author considered the use of uneven tapers, to see if the change to the stress state of the strip would be significant. Unfortunately the results were

inconclusive and are not shown in the thesis. The problem is that thermal roll crown is generally dependent on a number of underlying factors. These include the ambient atmospheric temperature inside the furnace, i.e. if the roll has a homogenous temperature then thermal distortion is less likely. A second factor involved the strip; while a single ultra thin strip pass will have little or no impact on the roll's thermal distortion, the entire passing coil if not at the appropriate zonal temperature will have some effect, either effectively heating or cooling the roll and thus increase or decreasing the roll tapers sizing depending on the section of the furnace that the strip is in. N Jacques *et al*[56] in a recently published paper confirm that inhomogeneous temperature led to changes to the roll geometry.

8.7 RECOMMENDATIONS FOR FUTURE WORK

This is the first research project to look at process control issues within the Port Talbot CAPL. The project has advanced roll-strip interaction understanding, however, there are several areas where research needs to be further continued.

- Research into the air cushion effect.
- Research into the impact of increasing the annealing temperature. How will this affect the strip's chemistry and mechanical properties?
- Development of a pilot facility that has a fully enclosed furnace section, so that a proper validation study can be performed on the computational results.
- Continual development of the computational models so that they encompass the entire critical buckle region of the CAPL. I.e. multi-roll model.
- Development of a fully-coupled computational model of a roll-strip contact.

APPENDIX A: RECORD OF TRAINING

EPSRC ENGINEERING DOCTORATE PROGRAMME IN STEEL TECHNOLOGY RECORD OF TRAINING - PAUL SAUNDERS

"Examination of the Factors Affecting Quality on Continuous Annealing Processing Lines"

Summary

The above titled project has focused on aspects of strip quality associated with continuous annealing. In particular focusing on the transport roll-strip interaction within the heating and soaking zones of the Continuous Annealing Processing Line (CAPL) situated at the Port Talbot integrated works of Corus Group PLC. The initial brief of the research project was to investigate all aspects of strip quality throughout the CAPL. This was to include both thermo-mechanical and metallurgical considerations, however, apart from the required need to focus the research project on a particular research objective the industrial partners were ultimately only interested in the transport roll-strip interaction. Furthermore from literature, internal and external to Corus Group PLC this area of research is perhaps the most critical to overall strip quality.

Although many finite element (FE) simulations were developed through the course of the research project, the main objective remained: to develop a series of simulations that would enable a greater understanding of the roll-strip contact interaction.

Finally a series of recommendations were put forward, which built on the current knowledge.

The issues addressed where:

- Evaluation of current CAPL transport rolls, by "Type".
- Evaluation of different roll geometries for both current and future use.
- Evaluation of strip size.
- Investigation of the effects of high and low strength strip.
- Investigation into the effects of current and future operational conditions, such as in-line tension and transport roll velocity.

Coupled with the finite element analysis work in roll-strip interactions was the experimental work completed with industrial partners Stein Heurtey. The experimental work was completed in the spring and summer of 2003, and represents a valuable incite into how the strip behaves when there is a considerable temperature differential.

PLATFORM PRESENTATIONS

Annual Engineering Doctorate Conference, Swansea University, Taliesin.

PROFESSIONAL DEVELOPMENT

Institute of Mechanical Engineers (IMechE)

EngD TRAINING

Core training courses are aimed at developing the research engineer's knowledge and skills, attributes required for a successful career as a professional engineer and manager.

The course aim is to comprehensively cover two areas:

- Technical Expertise: process of steelmaking and its environmental impact.
- Professional Competence: communication skills, team working, leadership and management skills.

Most courses were followed by a formal examination, which required the research engineer to pass before an EngD degree could be awarded.

Year One

- Communication Skills, Professional Development, Process Evolution in the Steel Industries, Project Planning, Steel Processing, Coated Steel Products, Engineering Applications, Environmental Applications, Environmental Issues, Personal Development for Research Engineers, Innovation and Exploitation (St Pierre), Investment Appraisal in Engineering, Numerical Analysis Techniques, Practical Finite Element Computing, Design and Analysis of Engineering Experiments and UK Tour of Customer Supplier Company Facilities.

Year Two

- Business Processing Engineering, Management Science Techniques, Financial Issues for Management, Aluminium and its Alloys, Stainless Steel, Business and Quality Awareness and European Visit to Corus Operations on the Continent (Year2/3)

Year Four

- Effective Management, Financial Awareness, Employee Relations Awareness and Health and Safety Awareness.

PROGRESS MONITORING

Formal procedures are in place in the engineering doctorate regarding the monitoring of progress throughout the scheme. These include:

- Quarterly presentations at theme group meetings, chaired by a senior Corus representative, designated theme champion. Meeting forums attended by theme leader, academic supervisor, industrial supervisor, EngD co-ordinator and client representatives.
- Regular consultations and meetings throughout the scheme with academic and industrial supervisors.
- Monthly progress meetings with theme leader, who is a Corus representative and the research engineers link to the theme champion.
- Presentations of "Posters" at the annual EngD seminar 2001, 2002 and 2003.
- Formal platform presentation at the EngD seminar, 2004.

REFERENCES

1. Hochon, B., *User Experience and Demands of Continuously Annealed Steels.* Scandinavian Journal of Metallurgy 13 - Proceedings of the International Symposium Held in Stockholm, June18-20th, 1984: p. 352-358.

2. Morris, J.W., *Analysis of Product Shape in Tension Levelling and Plate Stretching Processes, Department of Mechanical Engineering.* 2001, University of Wales Swansea.

3. Obara, T., et al., *Control of Steel Chemistry for Producing Deep Drawing Cold Rolled Steel Sheets by Continuous Annealing.* Scandinavian Journal of Metallurgy 13 - Proceedings of the International Symposium Held in Stockholm, June18-20th, 1984: p. 201-213.

4. Seter, B., U. Bergström, and W.B. Hutchinson, *Extra Deep-Drawing Quality Steels by Continuous Annealing.* Scandinavian Journal of Metallurgy 13 - Proceedings of the International Symposium Held in Stockholm, June18-20th, 1984: p. 214-219.

5. Paulus, P. and P. Laval, *Study of the Heat Buckling and Shape Problems in Continuous Heat Treating Lines and Discussion of Proposed Solutions.* The Metallurgical Society / AIME, 1985: p. 420-439.

6. Matoba, T., et al., *Effect of Roll Crown on Heat Buckling in Continuous Annealing Lines.* Tetsu to Hagane, Vol.80, No.8, 1994: p. 641-646.

7. Elias, E., et al., *Improvement of Strip Guidance and Investigation of the Mechanics of Wrinkling of Strip during Continuous Annealing.* 1999, European Commission. p. 52.

8. Lewis, D.W., *CAPL Technical Information,* P. Saunders, Editor. 2001.

9. Mignard, F., *Manual No1: Furnace Description Manual* 1997, Stein Heurtey.

10. Abe, H. and S. Satoh, *Progress of Continuous Annealing Technology for Cold-Rolled Sheet Steels and Associated Product Development.* Kawasaki Steel Technical Report, No.22, 1990.

11. Williams, J.S., *Tinnopolis History of Tin Mill Products in Llanelli.* 1999: Llanelli Star Publications.

12. Dasarathy, C., *Processing of Uncoated Sheet Steels.* 2000.

13. Jab, S., *Comparison of Continuous Annealing and Batch Annealing for Tinplate.* Review of Annealing Technology, 1986: p. 65-85.

14. Mendoza, R., et al., *Mechanical Properties of a Recrystallized Low Carbon Steel.* Scripta Materialia 48, 2002: p. 391-395.

15. Limpens, C.H.L., *Impact of Strip Shape on Strip Tracking in a Processing Line.* 1998, European Commission.

16. Masui, T., Y. Kaseda, and K. Isaka, *Basic Examination on Strip Wandering in Processing Plants.* ISIJ International, Vol.40, No.10, 2000: p. 1019-1023.

17. Roberts, W.L., *Cold Rolling of Steel Manufacturing and Materials Processing.* Marcel Dekker INC, 1975: p. 655.

18. Rammerstorfer, F.G., F.D. Fischer, and N. Friedl, *Buckling of Infinite Strips Under Residual Stresses and Global Tension.* Journal of Applied Mechanics, Vol.68, 2001: p. 403.

19. Orban, A., D. Steinier, and C. Counhaye, *Shape Control in Cold Rolling.* 2nd Continuous Casting Conference, 6th International Rolling Conference, Düsseldorf, Hune 20-22, 1994.

20. Nguyen, D., *On-Line Sensing of Sheet Flutter Using Infrared Light.* AMD, Vol.29. Web Handling, ASME, 1992.

21. King, S., B. Funk, and F. Chambers, *Air Films Between a Moving Tensioned Web and a Stationary Support Cylinder.* Proceedings of the Second International Conference on Web Handling, June 6-9, 1993: p. 286-301.

22. Knox, K. and L. Sweeney, *Fluid Effects Associated with Web Handling.* Ind. Eng. Chem. Process Des. Develop, Vol.10, No.2, 1971: p. 201-207.

23. Blok, H. and J. vanRossum, *The Foil Bearing - A New Departure in Hydrodynamic Lubrication.* Lubrication Engineering, 1953: p. 316-319.

24. Lewis, D.W., J.C. Duggan, and C.J. Wallis, *Control of Tension Buckle in the Exit Accumulator of CAPL - Port Talbot (Confidential Technical Note).* 2001, Corus UK Limited: WTC - Welsh Technology Centre.

25. Schyns, M., et al., *Improved Strip Shape in High Speed Continuous Annealing Lines.* 1999: p. 1-87.

26. Matoba, T. and M. Ataka, *Effect of Roller Crown on the Occurrence of Buckling and Walk of Strip in Continuous Annealing Line.* Transactions ISIJ, Vol.27, 1987.

27. Watts, K., et al., *Cooling Buckle (Confidential Internal Report).* 2002, Corus UK Limited.

28. Sotheran, S., *Hot Tensile Test Results (Confidential),* Corus UK Limited: STC - Swinden Technology Centre

29. Wang, N., R.J. Walsh, and Z. Husain, *Modelling of Snakey Buckle on the Port Talbot CAPL (Confidential Internal Report).* 2000, Corus UK Limited: TTC - Teesside Technology Centre.

30. Ljo, H., W. Dunbar, and J. Moore, *Buckling of Analysis of Heated Steel Strip in a Continuous Annealing Furnace.* ASME, 1999.

31. Kim, J.Y., J.K. Kim, and S.Y. Kim, *Rapid Cooling Technology in Continuous Annealing Line.* Review of Annealing Technology 1986: p. 37-49.

32. Caycik, M., et al., *Snakey Buckle on EDDQ Strip (Confidential Internal Report)*. 2000, Corus UK Limited: WTC - Welsh Technology Centre. p. 1-17.

33. Shelton, J., *Buckling of Web from Lateral Compressive Forces*. Proceedings of the Second International Conference on Web Handling, June 6-9, 1993.

34. Evans, P., *Port Talbot CAPL Facts and Figures*, P. Saunders, Editor. 2004.

35. *Hot Rolled and Cold Rolled Steels (Section 2.4-1)*. Automotive Steel Design Manual 2002: American Iron and Steel Institute. 16.

36. Hudd, R.C., *Chapter 6. Processing - Cold Rolling and Annealing*. Materials Science and Technology, A Comprehensive Treatment, Vol.7, Constitution and Properties of Steel, 1992.

37. Kumar, A., R. Sengupta, and A. Chatterjee, *Annealing Technologies for Cold Rolled Flat Steel Product: A Technical Assessment*. Steel World, 1997: p. 29-38.

38. Dieter Jr, G.E., *Mechanical Metallurgy*. 1961: McGraw-Hill Book Company. 615.

39. Ragab, A.-R. and S.E. Bayoumi, *Engineering Solid Mechanics - Fundamentals and Applications*. 1999: CRC Press. 921.

40. Henwood, D. and J. Bonet, *Finite Elements - A Gentle Introduction*. 1996: MacMillan. 205.

41. Zienkiewicz, O.C. and R.L. Taylor, *The Finite Element Method, The Basis, Vol.1*. 5 ed. 2000: Butterworth Heinemann. 689.

42. Benham, P.P., R.J. Crawford, and C.G. Armstrong, *Mechanics of Engineering Materials*. 2 ed. 1996: Longman Group Limited. 627.

43. Wang, N., *Description of the TTC FE Models of Strip Heat Buckle Analysis for Continuous Annealing Lines (Confidential Internal Report)*. 2002, Corus UK Limited: TTC - Teesside Technology Centre.

44. Bird, D.W., et al., *Examination of Heat Buckling on Trostre CAPL (Confidential Technical Note)*. 1990, British Steel Tinplate: Welsh Laboratories - Port Talbot.

45. Turner, M., et al., *Stiffness and Deflection Analysis of Complex Structures*. Journal of Aeronautical Science, Vol.23, 1956: p. 805-824.

46. Lees, A., *Personal Communication*. 2007.

47. *Flow Science Inc*. 2007.

48. Hibbitt, Karlsson, and Sorensen, *ABAQUS Standard User's Manual, Version 6.3*. 2002.

49. Hibbitt, Karlsson, and Sorensen, *ABAQUS Theory Manual, Version 5.8.* 1998.

50. Hibbitt, Karlsson, and Sorensen, *ABAQUS Explicit User's Manual, Version 6.3.* 2002.

51. Hibbitt, Karlsson, and Sorensen, *Getting Started with ABAQUS Explicit, Interactive Version, Version 6.3.* 2002.

52. Hibbitt, Karlsson, and Sorensen, *ABAQUS CAE User's Manual.* 2002.

53. Holman, J.P., *Heat Transfer (in SI units).* Seventh ed. 1992. 53-56.

54. Asensio, J., et al., *Ferritic Steels Optimization of Hot-Rolled Textures through Cold Rolling and Annealing.* Materials Characterization, Vol.47, 2001: p. 120.

55. Schey, J.A., *Introduction to Manufacturing Processes.* Second Edition ed. 1987: McGraw Hill International Editions.

56. Jacques, N., et al., *Buckling and Wrinkling During Strip Conveying in Processing Lines.* Journal of Materials Processing Technology, Vol.190, Issues 1-3, 2007: p. 33-40.

32. Caycik, M., et al., *Snakey Buckle on EDDQ Strip (Confidential Internal Report)*. 2000, Corus UK Limited: WTC - Welsh Technology Centre. p. 1-17.

33. Shelton, J., *Buckling of Web from Lateral Compressive Forces*. Proceedings of the Second International Conference on Web Handling, June 6-9, 1993.

34. Evans, P., *Port Talbot CAPL Facts and Figures*, P. Saunders, Editor. 2004.

35. *Hot Rolled and Cold Rolled Steels (Section 2.4-1)*. Automotive Steel Design Manual 2002: American Iron and Steel Institute. 16.

36. Hudd, R.C., *Chapter 6. Processing - Cold Rolling and Annealing*. Materials Science and Technology, A Comprehensive Treatment, Vol.7, Constitution and Properties of Steel, 1992.

37. Kumar, A., R. Sengupta, and A. Chatterjee, *Annealing Technologies for Cold Rolled Flat Steel Product: A Technical Assessment*. Steel World, 1997: p. 29-38.

38. Dieter Jr, G.E., *Mechanical Metallurgy*. 1961: McGraw-Hill Book Company. 615.

39. Ragab, A.-R. and S.E. Bayoumi, *Engineering Solid Mechanics - Fundamentals and Applications*. 1999: CRC Press. 921.

40. Henwood, D. and J. Bonet, *Finite Elements - A Gentle Introduction*. 1996: MacMillan. 205.

41. Zienkiewicz, O.C. and R.L. Taylor, *The Finite Element Method, The Basis, Vol.1*. 5 ed. 2000: Butterworth Heinemann. 689.

42. Benham, P.P., R.J. Crawford, and C.G. Armstrong, *Mechanics of Engineering Materials*. 2 ed. 1996: Longman Group Limited. 627.

43. Wang, N., *Description of the TTC FE Models of Strip Heat Buckle Analysis for Continuous Annealing Lines (Confidential Internal Report)*. 2002, Corus UK Limited: TTC - Teesside Technology Centre.

44. Bird, D.W., et al., *Examination of Heat Buckling on Trostre CAPL (Confidential Technical Note)*. 1990, British Steel Tinplate: Welsh Laboratories - Port Talbot.

45. Turner, M., et al., *Stiffness and Deflection Analysis of Complex Structures*. Journal of Aeronautical Science, Vol.23, 1956: p. 805-824.

46. Lees, A., *Personal Communication*. 2007.

47. *Flow Science Inc*. 2007.

48. Hibbitt, Karlsson, and Sorensen, *ABAQUS Standard User's Manual, Version 6.3*. 2002.

49. Hibbitt, Karlsson, and Sorensen, *ABAQUS Theory Manual, Version 5.8.* 1998.

50. Hibbitt, Karlsson, and Sorensen, *ABAQUS Explicit User's Manual, Version 6.3.* 2002.

51. Hibbitt, Karlsson, and Sorensen, *Getting Started with ABAQUS Explicit, Interactive Version, Version 6.3.* 2002.

52. Hibbitt, Karlsson, and Sorensen, *ABAQUS CAE User's Manual.* 2002.

53. Holman, J.P., *Heat Transfer (in SI units).* Seventh ed. 1992. 53-56.

54. Asensio, J., et al., *Ferritic Steels Optimization of Hot-Rolled Textures through Cold Rolling and Annealing.* Materials Characterization, Vol.47, 2001: p. 120.

55. Schey, J.A., *Introduction to Manufacturing Processes.* Second Edition ed. 1987: McGraw Hill International Editions.

56. Jacques, N., et al., *Buckling and Wrinkling During Strip Conveying in Processing Lines.* Journal of Materials Processing Technology, Vol.190, Issues 1-3, 2007: p. 33-40.